

TOPICAL REVIEW • OPEN ACCESS

Key properties of inorganic thermoelectric materials—tables (version 1)

To cite this article: Robert Freer *et al* 2022 *J. Phys. Energy* 4 022002

View the [article online](#) for updates and enhancements.

You may also like

- [Millimeter Light Curves of Sagittarius A* Observed during the 2017 Event Horizon Telescope Campaign](#)
Maciek Wielgus, Nicola Marchili, Iván Martí-Vidal *et al.*
- [A Universal Power-law Prescription for Variability from Synthetic Images of Black Hole Accretion Flows](#)
Boris Georgiev, Dominic W. Pesce, Avery E. Broderick *et al.*
- [Broadband Multi-wavelength Properties of M87 during the 2017 Event Horizon Telescope Campaign](#)
The EHT MWL Science Working Group, J. C. Algaba, J. Anzarski *et al.*



ROADMAP

OPEN ACCESS

RECEIVED

21 July 2021

REVISED

22 December 2021

ACCEPTED FOR PUBLICATION

10 January 2022

PUBLISHED

22 March 2022

Original content from this work may be used under the terms of the [Creative Commons Attribution 4.0 licence](#).

Any further distribution of this work must maintain attribution to the author(s) and the title of the work, journal citation and DOI.



Key properties of inorganic thermoelectric materials—tables (version 1)

Robert Freer^{1,*}, Dursun Ekren², Tanmoy Ghosh³, Kanishka Biswas^{3,4,5}, Pengfei Qiu⁶, Shun Wan⁷, Lidong Chen^{6,8}, Shen Han⁹, Chenguang Fu⁹, Tiejun Zhu⁹, A K M Ashiquzzaman Shawon¹⁰, Alexandra Zevalkink¹⁰, Kazuki Imasato^{11,12}, G. Jeffrey Snyder¹¹, Melis Ozen^{13,14}, Kivanc Saglik^{13,14}, Umut Aydemir^{13,15}, Raúl Cardoso-Gil¹⁶, E Svanidze¹⁶, Ryoji Funahashi¹⁷, Anthony V Powell¹⁸, Shriparna Mukherjee¹⁸, Sahil Tippireddy¹⁸, Paz Vaqueiro¹⁸, Franck Gascoin¹⁹, Theodora Kyratsi²⁰, Philipp Sauerschnig^{12,21} and Takao Mori^{21,22}

- ¹ Department of Materials, University of Manchester, Manchester M13 9PL, United Kingdom
 - ² Department of Metallurgy and Materials Engineering, Iskenderun Technical University, Iskenderun 31200, Hatay, Turkey
 - ³ New Chemistry Unit, Jawaharlal Nehru Centre for Advanced Scientific Research (JNCASR), Jakkur PO, Bangalore 560064, India
 - ⁴ School of Advanced Materials, Jawaharlal Nehru Centre for Advanced Scientific Research (JNCASR), Jakkur PO, Bangalore 560064, India
 - ⁵ International Centre for Materials Science, Jawaharlal Nehru Centre for Advanced Scientific Research (JNCASR), Jakkur PO, Bangalore 560064, India
 - ⁶ State Key Laboratory of High Performance Ceramics and Superfine Microstructure, Shanghai Institute of Ceramics, Chinese Academy of Sciences, Shanghai 200050, People's Republic of China
 - ⁷ Center for High Pressure Science and Technology Advanced Research (HPSTAR), Shanghai 201203, People's Republic of China
 - ⁸ Center of Materials Science and Optoelectronics Engineering, University of Chinese Academy of Sciences, Beijing 100049, People's Republic of China
 - ⁹ State Key Laboratory of Silicon Materials, and School of Materials Science and Engineering, Zhejiang University, Hangzhou 310027, People's Republic of China
 - ¹⁰ Chemical Engineering and Materials Science Department, Michigan State University, East Lansing, MI 48824, United States of America
 - ¹¹ Department of Materials Science and Engineering, Northwestern University, Evanston, IL, United States of America
 - ¹² Global Zero Emission Research Center, National Institute of Advanced Industrial Science and Technology (AIST), Tsukuba, Japan
 - ¹³ Koç University Boron and Advanced Materials Application and Research Center (KUBAM), Istanbul 34450, Turkey
 - ¹⁴ Graduate School of Sciences and Engineering, Koç University, Istanbul 34450, Turkey
 - ¹⁵ Department of Chemistry, Koç University, Istanbul 34450, Turkey
 - ¹⁶ Max-Planck-Institut für Chemische Physik fester Stoffe, Nöthnitzer Straße 40, 01187 Dresden, Germany
 - ¹⁷ National Institute of Advanced Industrial Science and Technology, 1-8-31 Midorigaoka, Ikeda, Osaka 563-8577, Japan
 - ¹⁸ Department of Chemistry, University of Reading, RG6 6DX Reading, United Kingdom
 - ¹⁹ Laboratoire CRISMAT UMR 6508 CNRS ENSICAEN, 14050 Caen Cedex 04, Caen, France
 - ²⁰ Department of Mechanical and Manufacturing Engineering, University of Cyprus, Nicosia 2109, Cyprus
 - ²¹ International Center for Materials Nanoarchitectonics (WPI-MANA), National Institute for Materials Science (NIMS), Tsukuba, Ibaraki 305-0044, Japan
 - ²² Graduate School of Pure and Applied Science, University of Tsukuba, Tsukuba, Ibaraki 305-8671, Japan
- * Author to whom any correspondence should be addressed.

E-mail: Robert.Freer@manchester.ac.uk

Keywords: thermoelectric, data, compilation

Abstract

This paper presents tables of key thermoelectric properties, which define thermoelectric conversion efficiency, for a wide range of inorganic materials. The twelve families of materials included in these tables are primarily selected on the basis of well established, internationally-recognized performance and promise for current and future applications: tellurides, skutterudites, half Heuslers, Zintl, Mg–Sb antimonides, clathrates, FeGa₃-type materials, actinides and lanthanides, oxides, sulfides, selenides, silicides, borides and carbides. As thermoelectric properties vary with temperature, data are presented at room temperature to enable ready comparison, and also at a higher temperature appropriate to peak performance. An individual table of data and commentary are provided for each family of materials plus source references for all the data.

Contents

1. Introduction	3
2. New entries	6
3. Data tables and commentaries	7
3.1. Tellurides	9
3.2. Skutterudites	20
3.3. Half Heuslers	33
3.4. Zintl	39
3.5. Mg ₃ Sb ₂	44
3.6. Clathrates	48
3.7. FeGa ₃ -type	64
3.8. Actinides and lanthanides	70
3.9. Oxides	81
3.10. Sulfides and selenides	89
3.11. Silicides	102
3.12. Borides and carbides	109
4. Challenges and future perspectives	115
References	116

1. Introduction

Scope and organization

This compilation is concerned with the properties of inorganic thermoelectric materials which are being explored to provide fundamental understanding and for a wide variety of thermoelectric applications. We begin with a brief introduction defining the thermoelectric figure of merit, which specifies conversion efficiency, then define the thermoelectric-related parameters in the data tables and provide an overview of the twelve families of materials forming the basis of the compilation. This is followed by individual sections which comprise, for each family of materials, a table of data plus a commentary on the data for that section, with source references for the data in the table and any additional references cited in the commentary. In the final section we summarize challenges and future perspectives for inorganic thermoelectric materials.

The rationale for the selection of materials is outlined in section 1.3. The twelve sections and their authors are:

1. Tellurides (Tanmoy Ghosh and Kanishka Biswas)
2. Skutterudites (Pengfei Qiu, Shun Wan and Lidong Chen)
3. Half Heuslers (Shen Han, Chenguang Fu, Tiejun Zhu)
4. Zintl (A K M Ashiquzzaman Shawon and Alexandra Zevalkink)
5. Antimonides (Mg_3Sb_2) (Kazuki Imasato and G Jeffrey Snyder)
6. Clathrates (Melis Ozen, Kivanc Saglik and Umut Aydemir)
7. FeGa_3 -type materials (Raúl Cardoso-Gil)
8. Actinides and lanthanides (Eteri Svanidze)
9. Oxides (Dursun Ekren, Robert Freer and Ryoji Funahashi)
10. Sulfides and selenides (Anthony V Powell, Shriparna Mukherjee, Sahil Tippireddy and Paz Vaqueiro)
11. Silicides (Franck Gascoin and Theodora Kyratsi)
12. Borides and carbides (Philipp Sauerschnig and Takao Mori)

Thermoelectric figure of merit

Thermoelectrics can be used to generate power, when the material is located in a temperature gradient, or enable cooling when a current is passed through the material. The thermoelectric performance (for either mode of operation) depends on the efficiency of the material for converting heat into electricity. The efficiency of a thermoelectric material depends primarily on the thermoelectric materials figure-of-merit, known as zT or ZT [1, 2]. Whilst both versions are found in the literature, we will employ zT when referring to the figure of merit of a material, and ZT for a device or module. In its simplest form zT is described by:

$$zT = (S^2\sigma)T/\kappa \text{ or } zT = (\alpha^2)T/\rho\kappa \quad (1)$$

where the voltage generated is defined by the Seebeck coefficient (denoted by S or α). In order to maximize efficiency at a particular temperature (T), a high electrical conductivity σ (or low electrical resistivity ρ) is required along with low thermal conductivity κ . The latter parameter (κ) is made up of two components, lattice thermal conductivity (κ_L) and electronic thermal conductivity (κ_e). As the electrical transport and the electronic contribution to thermal transport are directly linked through the Wiedemann–Franz law [3], there have been considerable efforts to modify σ and κ independently in order to maximize zT [1, 2, 4].

To achieve sufficient power, a thermoelectric generator must be used efficiently across a large temperature difference $\Delta T = T_h - T_c$ and so the material zT must be high across this temperature range. The *Device* ZT is a weighted average of the thermoelectric material zT that gives the maximum efficiency η across this finite ΔT , where the maximum efficiency is given by:

$$\eta_{\max} = \frac{\Delta T}{T_h} \cdot \frac{\sqrt{(1+ZT)} - 1}{\sqrt{(1+ZT)} + T_c/T_h}. \quad (2)$$

Thermoelectric materials and the tables

The thermoelectric performance of most materials varies widely with temperature, thereby defining an effective temperature range of operation or ‘thermal window’ (see section 3 and figure 1). Thus, it is important that peak zT occurs in the range of temperatures appropriate to a specific application, and indeed the average zT over that range may be more important than maximum zT . For convenience, thermoelectric materials are broadly divided into families suitable for low temperature (273–500 K), medium temperature (500–900 K) and high temperature (900–1300 K) applications [2, 4], although some materials, or combination of materials, can be exploited in more than one range. Traditionally, telluride materials (such as

Bi_2Te_3) were established as the first commercial thermoelectric materials and are still employed widely today. However, because of their limited thermal window, restricting operation to low temperatures (peak performance ~ 380 K), and increasing environmental and sustainability concerns, there is active interest in a wide range of alternative materials. This compilation presents data for 12 families of inorganic thermoelectrics (listed in section 1.1) which are candidates for a wide range of applications. These inorganic materials have been selected primarily on the basis of well established, internationally-recognized performance (some for up to 60 years) and their promise for current and future applications. This applies to the tellurides, skutterudites, half Heuslers, Zintl, Mg–Sb antimonides, clathrates, oxides, sulfides, selenides, and silicides. With growing interest in ultra-high temperature applications, above 1300 K, we include data for carbides and borides as these represent some of the most promising materials for such demanding environments. Finally, we include three families of ‘exotic’ materials with relatively modest properties, namely FeGa_3 materials, actinides and lanthanides. For these materials, the structures and chemistry offer alternative atomic interactions and bonding scenarios for the regulation of charge carrier and transport properties. Developing a better understanding of the relationships between crystal chemistry, chemical bonding and electronic structure should allow the tailoring and enhancement of their thermoelectric properties. The approaches may be relevant and transferable to other families of materials. Indeed, we hope this review encourages the scientific community to investigate the full range of available materials using the spectrum of modern tools.

As all the material families have different temperature dependencies, we include data relevant to temperatures for peak performance (on the basis of zT or power factor), and also properties close to room temperature, to enable comparison between the families of materials. Whilst the room temperature properties provide a useful baseline, it is accepted that such thermoelectric parameters will be modest for the high temperature materials, and the documented high temperature performance will be more relevant and representative.

Thermoelectric parameters and relationships

At a particular temperature, T (K), data for up to 12 thermoelectric performance-related parameters are reported, depending on the data available. We first present abbreviations (and units) for these parameters, and then outline important inter-relationships.

Abbreviations and units

- Weighted mobility, μ_w ($\text{cm}^2 \text{V}^{-1} \text{s}^{-1}$)
- Hall mobility, μ_H ($\text{cm}^2 \text{V}^{-1} \text{s}^{-1}$)
- Intrinsic mobility, μ_o ($\text{cm}^2 \text{V}^{-1} \text{s}^{-1}$)
- Lattice thermal conductivity, κ_L ($\text{W m}^{-1} \text{K}^{-1}$)
- Seebeck coefficient, S ($\mu\text{V K}^{-1}$)
- Electrical conductivity, σ ($\Omega^{-1} \text{cm}^{-1}$)
- Thermoelectric quality factor, zT
- Bandgap, E_g (eV)
- Effective mass, m_s^* (m_e)
- Static dielectric constant/relative permittivity, ϵ_r
- Thermal conductivity, κ ($\text{W m}^{-1} \text{K}^{-1}$)
- Carrier concentration, n (cm^{-3})

Inter-relationships

All the parameters contributing to zT (equation (1)), i.e. Seebeck coefficient, electrical resistivity and thermal conductivity vary significantly with charge carrier concentration in contrasting ways. Achieving high zT in a material typically requires optimization of the charge-carrier concentration. As the charge-carrier concentration can be controlled by intrinsic defects (such as vacancies and interstitials) as well as extrinsic dopants (impurities), then the search for (or comparison between) good thermoelectric materials is really a search for a material with the highest potential for high zT assuming it can be optimally doped. This potential high zT is determined by the *thermoelectric quality factor* B [5, 6], defined in equation (3), which at a particular temperature is directly proportional to zT [7]:

$$B = \frac{8\pi k_B (2m_e)^{3/2}}{3eh^3} (k_B T)^{5/2} \frac{\mu_w}{\kappa_L}. \quad (3)$$

Here k_B , m_e , e and h are the Boltzmann constant, electron rest mass, electron charge and Planck’s constant respectively; thus except for temperature, the quality factor is proportional to μ_w/κ_L . This indicates the

quality of a thermoelectric material can be divided into the quality of its electronic properties, given by the weighted mobility μ_w , and the quality of its thermal properties, given by the lattice thermal conductivity κ_L [8]. Hence, improvements in ‘electronic properties’ can be defined as a higher μ_w , while improved ‘thermal properties’ means a lower κ_L for all material changes other than doping.

Several types of mobility are reported in the literature, most commonly the Hall mobility, intrinsic mobility, and weighted mobility. The Hall mobility, μ_H , is directly obtained from measurements of the Hall coefficient and resistivity. The intrinsic mobility, μ_o , is usually calculated using a single parabolic band (SPB) model, and can be viewed as an estimate of μ_H at the limit of very low carrier concentration (i.e. intrinsic behavior). Thus, for a given material and temperature, $\mu_o > \mu_H$. Hall mobility (μ_H) is reported for over half the material families in the compilation and intrinsic mobility (μ_o) for most of the remainder; this reflects the available data in the source publications.

Finally, the weighted mobility, μ_w , is generally described as the drift mobility, μ , weighted by the density-of-states effective mass (m_{DOS}^*). Equation (4) further relates μ_w to the effective valley degeneracy (N_V) and inertial effective mass, m_1^* [9]:

$$\mu_w = \mu \left(\frac{m_{DOS}^*}{m_e} \right)^{3/2} \sim \frac{N_V}{m_1^*}. \quad (4)$$

High weighted mobility is achieved in materials with lighter inertial effective mass m_1 (which is equal to the single band effective mass m_b^* for an isotropic band) and/or higher effective valley degeneracy. The advantage of comparing weighted mobility values among various materials is that it does not require Hall measurements (and is therefore widely accessible) and it combines two different parameters (m_{DOS}^* and μ) that should be maximized to increase thermoelectric performance.

The weighted mobility has been calculated for all material families in this paper using equation (5), where S and ρ are the experimental values of Seebeck coefficient and electrical resistivity, respectively, at temperature T [7]:

$$\mu_w = \frac{331}{\rho} \left(\frac{T}{300} \right)^{-3/2} \left[\frac{\exp \left[\frac{|S|}{k_B/e} - 2 \right]}{1 + \exp \left[-5 \left(\frac{|S|}{k_B/e} - 1 \right) \right]} + \frac{\frac{3}{\pi^2} \frac{|S|}{k_B/e}}{1 + \exp \left[5 + \left(\frac{|S|}{k_B/e} - 1 \right) \right]} \right]. \quad (5)$$

2. New entries

Since this is the first release of the Key Properties of Inorganic Thermoelectric Materials, all the entries in the tables can be treated as ‘new’. Therefore, we present and discuss here the most important materials and the trends observed in the tables. The reader is referred to the original publications for further details.

3. Data tables and commentaries

The data tables are presented in the following sequence as sections 3.1–3.12:

(3.1) Tellurides, (3.2) Skutterudites, (3.3) Half Heuslers, (3.4) Zintl, (3.5) Antimonides (Mg_3Sb_2), (3.6) Clathrates, (3.7) FeGa_3 -type materials, (3.8) Actinides and Lanthanides, (3.9) Oxides, (3.10) Sulfides and Selenides, (3.11) Silicides, (3.12) Borides and Carbides.

To set the scene and highlight the relationships between the different families of materials we show in figure 1, typical zT values as a function of temperature for each of the families. This provides a very limited representation of the available data, but highlights the similarities and differences between current materials. Whilst the highest zT values (above 1.5) are available in the low and medium temperature ranges, there are many high-temperature materials with peak zT values well above 1.0. A clear feature across all the materials is the temperature dependencies; most medium and high temperature materials only really reach peak zT at the highest temperatures, whilst some of the low temperature tellurides (e.g. 1a p -type; 1d n -type) soon reach a very clear peak after which zT decreases rapidly with increasing temperature. Such behavior defines the range of temperatures (or operating window) for which the material will be most suitable as a thermoelectric. In this way the average zT (over a range of temperatures) can be more important, in determining performance, than the peak zT at one temperature.

A common, though not universal, feature across many materials is that the n -type materials exhibit higher zT values than their p -type counterparts. There are clear exceptions to this trend; notably among the sulfides, where a high-performance n -type material continues to be elusive. Consequently, there is considerable effort to develop related p -type and n -type materials of comparable performance to maximize the efficiency of thermoelectric modules. Looking at examples of material families, it is evident that skutterudites have their peak zT values at medium temperatures; the n -type skutterudites exhibit much higher zT values than the p -type skutterudites due to superior electrical transport performance. However, there can also be stark contrasts within individual families; the Sn clathrates display peak zT values at low-to-medium temperatures, whilst the Ge clathrates are best suited for medium-to-high temperature applications. The n -type Mg_3Sb_2 – Mg_3Bi_2 alloys have only a relatively short history as thermoelectrics, but show promising performance from room temperature to around 700 K. The peak zT temperature can be easily adjusted by just changing the Sb:Bi ratio. Finally, carbides, such as SiC, are ideally suited to ‘ultra high temperature’ thermoelectric applications. Whilst their performance is average to good at 1200 K (curve 12a: p -type; curve 12b: n -type data) their zT values are still increasing and will not reach their peak until much higher temperatures, still within their stability range.

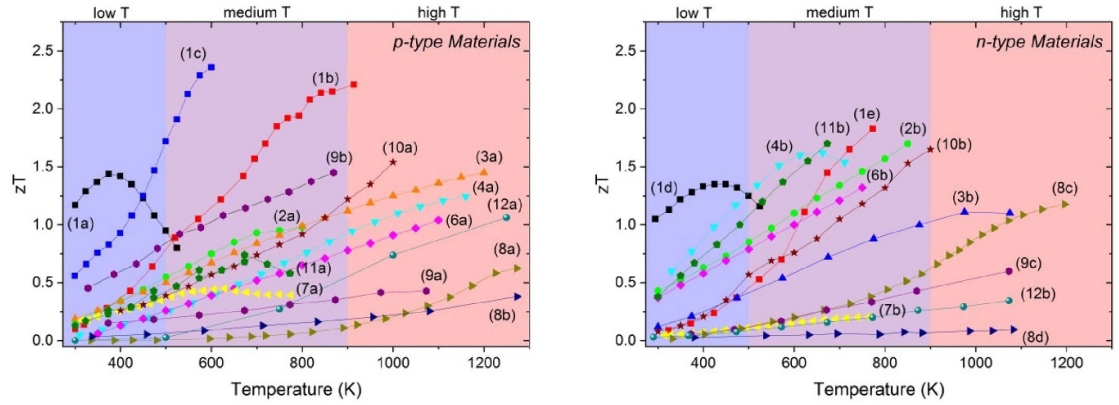


Figure 1. Thermoelectric figure of merit (zT) as a function of temperature for the families of materials. Details: (1) tellurides: *p*-type—(1a) $\text{Bi}_{0.5}\text{Sb}_{1.5}\text{Te}_3$, (1b) $\text{Pb}_{0.98}\text{Na}_{0.02}\text{Te}-4\%\text{SrTe}$, (1c) $\text{Ge}_{0.86}\text{Pb}_{0.1}\text{Bi}_{0.04}\text{Te}$, *n*-type—(1d) $\text{Bi}_{1.8}\text{Sb}_{0.2}\text{Te}_{2.7}\text{Se}_{0.3}$, (1e) $\text{PbTe}-4\%\text{InSb}$; (2) skutterudites: *p*-type—(2a) $\text{CeFe}_{3.85}\text{Mn}_{0.15}\text{Sb}_{12}$, *n*-type—(2b) $\text{Ba}_{0.08}\text{La}_{0.05}\text{Yb}_{0.04}\text{Co}_4\text{Sb}_{12}$; (3) half Heuslers: *p*-type—(3a) $\text{Nb}_{0.88}\text{Hf}_{0.12}\text{FeSb}$, *n*-type—(3b) $\text{Zr}_{0.2}\text{Hf}_{0.8}\text{NiSn}_{0.985}\text{Sb}_{0.015}$; (4) Zintl (including Mg_3Sb_2): *p*-type—(4a) $\text{Yb}_{14}\text{Mn}_{0.2}\text{Al}_{0.8}\text{Sb}_{11}$, *n*-type—(4b) $\text{Mg}_3\text{Sb}_{1.5}\text{Bi}_{0.5}$; (6) clathrates: *p*-type—(6a) $\text{Ba}_8\text{Ga}_{15.8}\text{Cu}_{0.033}\text{Sn}_{30.1}$, *n*-type—(6b) $\text{Ba}_8\text{Ga}_{16.6}\text{Ge}_{28.7}$; (7) FeGa_3 -type materials: *p*-type—(7a) $\text{RuGa}_{2.95}\text{Zn}_{0.05}$, *n*-type—(7b) $\text{FeGa}_{2.80}\text{Ge}_{0.20}$; (8) actinides and lanthanides: *p*-type—(8a) $\text{Yb}_{3.8}\text{Sm}_{0.2}\text{Sb}_3$, (8b) USi_3 , *n*-type—(8c) La_3Te_4 , (8d) URu_2Si_2 ; (9) oxides: *p*-type—(9a) $\text{Ca}_{2.8}\text{Bi}_{0.2}\text{Co}_4\text{O}_9$, (9b) $\text{Bi}_{0.94}\text{Pb}_{0.06}\text{Cu}_{0.99}\text{Fe}_{0.01}\text{SeO}$, *n*-type—(9c) $\text{Sr}_{0.95}(\text{Ti}_{0.8}\text{Nb}_{0.2})_{0.95}\text{Ni}_{0.05}\text{O}_3$; (10) sulfides and selenides: *p*-type—(10a) Cu_2Se , *n*-type—(10b) $\text{Pb}_{0.93}\text{Sb}_{0.05}\text{S}_{0.5}\text{Se}_{0.5}$; (11) silicides: *p*-type—(11a) $\text{Mg}_2\text{Li}_{0.25}\text{Si}_{0.4}\text{Sn}_{0.6}$, *n*-type—(11b) $\text{Mg}_{1.98}\text{Cr}_{0.02}(\text{Si}_{0.3}\text{Sn}_{0.7})_{0.98}\text{Bi}_{0.02}$; (12) Borides and Carbides: *p*-type—(12a) Boron carbide (13.3 at.% C), *n*-type—(12b) $\text{Ca}_{0.5}\text{Sr}_{0.5}\text{B}_6$.

3.1. Tellurides

Thermoelectrics based on metal tellurides

Tanmoy Ghosh¹ and Kanishka Biswas^{1,2,3}

¹ New Chemistry Unit, Jawaharlal Nehru Centre for Advanced Scientific Research (JNCASR), Jakkur PO, Bangalore 560064, India

² School of Advanced Materials, Jawaharlal Nehru Centre for Advanced Scientific Research (JNCASR), Jakkur PO, Bangalore 560064, India

³ International Centre for Materials Science, Jawaharlal Nehru Centre for Advanced Scientific Research (JNCASR), Jakkur PO, Bangalore 560 064, India

E-mail: kanishka@jncasr.ac.in

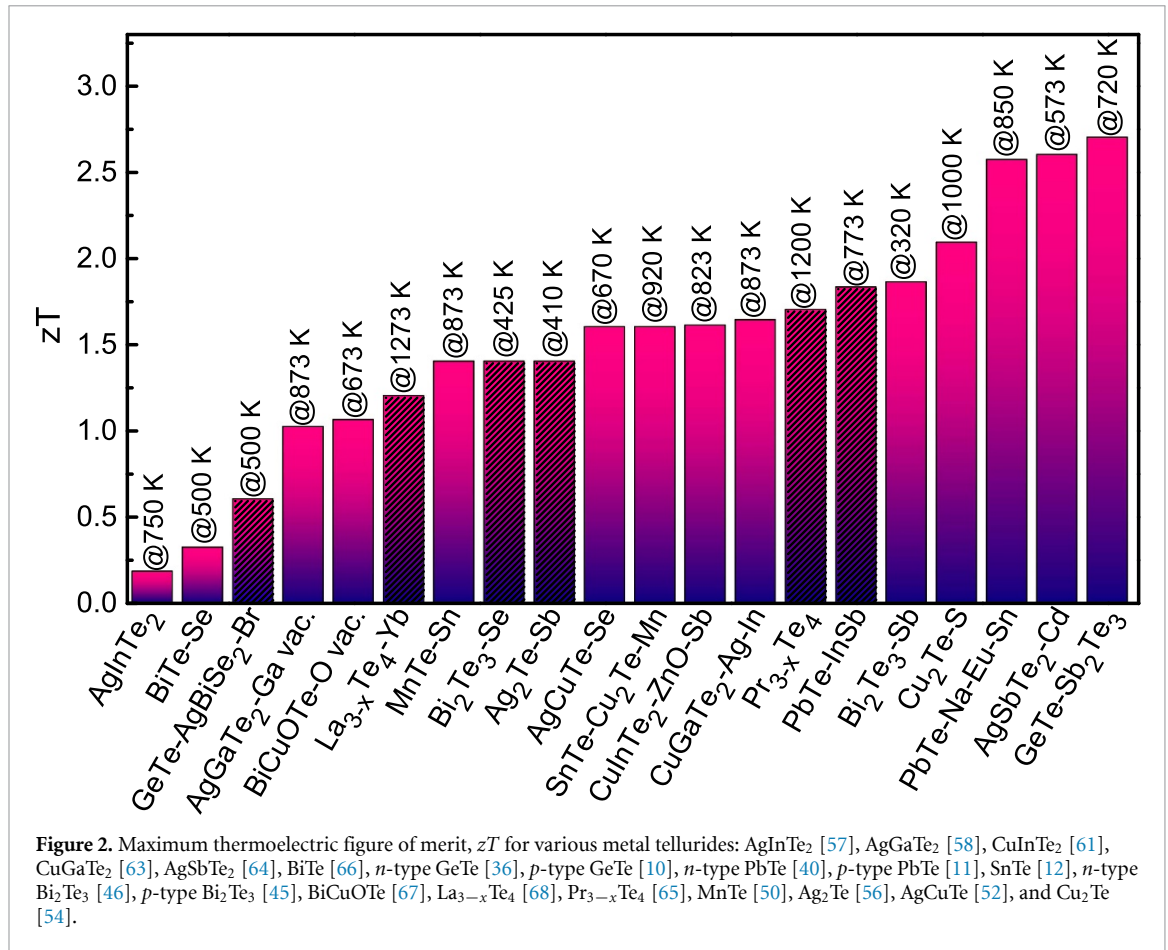
Introduction

Metal tellurides are among the most extensively studied families of thermoelectric materials for near room temperature to mid-temperature thermoelectric power generation. Particularly, the IV–VI semiconductors like GeTe, SnTe, and PbTe and tetradymites Bi₂Te₃-based thermoelectric materials have attracted wide attention in the community. Many of the modern-day approaches of improving thermoelectric performance, based on either electronic structure modulation or phonon scattering manipulation strategies, were first demonstrated on these materials. These families of materials, such as (GeTe)_x(AgSbTe₂)_{100-x}-based TAGS-*x* and Bi₂Te₃-based materials are some of the most widely used thermoelectrics for commercial applications. Figure 2 exhibits the maximum thermoelectric figure of merit, *zT* for a range of current metal telluride thermoelectric materials. Here, we outline the status of these metal telluride-based thermoelectric materials, the challenges, and recent progress. Typical thermoelectric performance-related parameters and *zT* values for various Te-based thermoelectric materials are listed in table 1.

IV–VI tellurides

While both SnTe and PbTe crystallize in the cubic rocksalt structure at ambient conditions, GeTe has a rhombohedral crystal structure at room temperature. However, GeTe undergoes a rhombohedral to cubic phase transition at ~720 K. All three are narrow band gap semiconductors with band gap in the range ~0.18–0.32 eV. As a result of this favorable band gap, highly-symmetric crystal structure leading to degenerate electronic bands, easy tuneability of electronic structure via chemical doping and alloying, and heavy constituent elements, they are ideal for exploring high thermoelectric performance. At present, a thermoelectric figure of merit, *zT* as high as ~2.7 at 720 and ~2.57 at 850 K can be achieved in GeTe [10] and PbTe [11] based *p*-type thermoelectric materials, respectively. While SnTe is much less toxic than PbTe, the maximum *zT* obtained so far is only 1.6 at 720 K [12, 13].

PbTe is a very important thermoelectric material; both band convergence and resonant level formation strategies were first demonstrated in PbTe. Resonant level formation in PbTe upon Tl doping [14] and valence band convergence in PbTe_{1-x}Se_x:Na [15] resulted in maximum *zT* ~ 1.5 and 1.8 in 2008 and 2011, respectively. Since then, these electronic structure modulation strategies have been followed up for numerous materials, and many 2nd ($1 \leq zT \leq 2$) and 3rd ($zT > 2$) generation thermoelectric materials have been achieved, including in GeTe and SnTe. For example, In doping has been very effective in inducing resonant levels in both SnTe [16] and GeTe [17], significantly improving their thermoelectric performance. Similarly, doping or alloying of Sb [18], Mn [19], Zn [20], Cd [21] in GeTe is also highly effective in inducing valence band convergence. While PbTe and SnTe have the same rocksalt crystal structure, the larger energy gap (~0.35 eV) between the primary and secondary valence bands in SnTe results in low Seebeck coefficients and consequently poor thermoelectric performance. Doping and alloying of many elements like Mn [22], Mg [23], Cd [24], Hg [25] etc are highly effective in reducing the gap between the primary and secondary valence bands. It has also been demonstrated that synergistic effects of band convergence and resonant level can further improve the thermoelectric performance. This has been achieved in SnTe via co-doping of In and Cd [26], and In and Ag [27]. Another highly successful strategy, based on phonon scattering manipulation, namely, all-scale hierarchical architecture, was first demonstrated in PbTe, resulting in maximum *zT* ~ 2.2 at 915 K [28]. Recently, lattice strain in Na–Eu–Sn doped PbTe has been shown to be very effective in reducing lattice thermal conductivity without compromising the carrier mobility; it resulted in *zT* ~ 2.57 at 850 K [11]. Many synergistic effects of electronic structure modulation and thermal transport optimization have also been achieved via co-doping in GeTe and SnTe. For example, complementary effects of resonant state formation via In doping, and reduced thermal conductivity due to solid solution point defects with Bi doping, results in high thermoelectric performance with *zT* ~ 2.1 at 723 K in In and Bi co-doped GeTe [29].



Similarly, synergistic effects have also been achieved in GeTe by co-doping Sb and Bi [18], and in SnTe via co-doping of Ag and Mn [30].

One major problem in SnTe and GeTe is their high *p*-type carrier concentration due to cation vacancies. Doping, such as Bi in GeTe [21, 31] and self-compensation in SnTe [30] have been effective in reducing the hole concentration. The rhombohedral to cubic phase transition in GeTe has been used as an added control parameter to achieve high thermoelectric performance. The high temperature cubic phase of GeTe possesses a four-fold degenerate light L band at higher energy and 12-fold degenerate heavy Σ band at lower energy. The polar distortion along the [1 1 1] crystallographic direction in the rhombohedral phase, however, splits the 4 L pockets into 3 L and 1 Z pockets, and the 12 Σ pockets into 6 Σ and 6 η pockets. Moreover, in the rhombohedral phase, the Σ band becomes the principal valance band with higher energy. This reduction of band degeneracy, and practical problems arising from the high-temperature phase transition, led to much effort on reducing the phase transition temperature and achieving higher thermoelectric performance in the cubic phase at lower temperature. For example, In and Sb co-doping [32], Bi and Mn co-doping [33] and MnTe alloying [19] have been successful. In recent years, however, it has been shown that precise control of the rhombohedral distortion can be used to achieve a higher degree of effective band degeneracy due to band orbital overlap and reduced lattice thermal conductivity using Bi doping [34]. This resulted in a maximum $zT \sim 2.4$ at 600 K. Very recently, it was shown that Rashba spin splitting can be used to achieve effective band convergence in Sn doped GeTe [35].

As can be seen from figure 2, high thermoelectric performance has been achieved in these materials with *p*-type thermoelectric transport. In fact, because of intrinsic Sn and Ge vacancies, it is very difficult to achieve *n*-type thermoelectric transport. Only recently *n*-type thermoelectric transport has been reported in GeTe through AgBiSe₂ alloying [36]. However, the $zT \sim 0.6$ at 500 K is much lower than that of the high zT of *p*-type, GeTe-based thermoelectric materials. Indeed, *n*-type thermoelectric transport is far more explored in PbTe. Still, the presence of a single conduction band at the L point, compared to the multivalley degenerate valence band structure at L and Σ points, makes it challenging to achieve high *n*-type thermoelectric transport in PbTe. Introduction of mid-gap states through In [37] and Ga [38] doping in PbTe was highly effective in enhancing the *n*-type thermoelectric performance. The *n*-type thermoelectric performance of PbTe has also benefited from enhanced effective mass by conduction band flattening through MnTe alloying

[39]. In a recent study, introduction of energy filtering through multiphase nano-structuring in a PbTe–InSb composite greatly improved the *n*-type thermoelectric performance of PbTe, with zT of 1.83 at 773 K [40].

Bi₂Te₃

Bi₂Te₃ and its solid solution alloys with Sb₂Te₃ and Bi₂Se₃ have been used in practical applications since the 1950s [41], and today they are still the most widely used thermoelectric materials for near room temperature applications. These are layered materials and have hexagonal close packed arrangement of anions. The structure comprises quintuple atomic layers of Te(1)–Bi–Te(2)–Bi–Te(1) along the crystallographic *c*-direction and two successive quintuple layers are held together by weak van der Waals' (vdW) interactions between two Te(1) layers. Such a layered structure causes anisotropic electrical and thermal transport properties when measured parallel and perpendicular to the layered plane. The highly polarizable Bi–Te bonds, the presence of weak vdW bonds within the layered structure and the constituent heavy elements result in strong lattice anharmonicity and consequently a low lattice thermal conductivity. Bi₂Te₃ is an indirect narrow band gap semiconductor with $E_g \sim 0.15$ eV. A low band effective mass and a highly degenerate electronic band structure also results in high Seebeck coefficient with high charge carrier mobility. Phonon scattering from point defects due to Bi and Sb disorder in Bi_{0.5}Sb_{1.5}Te₃ also markedly reduces lattice thermal conductivity. These combinations of low lattice thermal conductivity, favorable electronic band structure and high charge carrier mobility makes Bi₂Te₃ based materials good candidate thermoelectric materials. The thermoelectric properties of these materials have been greatly improved recently by microstructural engineering and nanostructuring, which result in lower lattice thermal conductivity while retaining relatively high carrier mobility with optimized μ/κ_L ; *p*-type $zT \sim 1.4$ at 373 K was obtained in Bi_{*x*}Sb_{2–*x*}Te₃ alloys by hot pressing ball-milled nanopowders [42]. Recently, nanostructuring with secondary phase nanoprecipitates has also been achieved in BiSbTe–Zn alloys [43]. Melt-centrifugation has been very effective in controlling the microstructure in (Bi,Sb)₂Te₃, with microscale dislocation arrays and a porous network, giving superior thermoelectric performance than zone-melted and hot pressed ingots [44]. While point defects scatter high frequency phonons, boundary scattering targets the low frequency phonons. Recently, liquid phase sintering was adopted to produce low energy grain boundaries with dense dislocation arrays which include scattering of mid-frequency phonons without simultaneously decreasing the charge carrier mobility. This resulted in a record high thermoelectric *p*-type figure of merit $zT \sim 1.86$ at 320 K in (Bi,Sb)₂Te₃ alloy [45]. Such liquid phase sintering has also been applied in Sb doped Bi₂Te_{2.7}Se_{0.3} to obtain a high zT *n*-type material and a large density of dislocation arrays has been observed in the sample. The consequent decrease of lattice thermal conductivity while retaining high charge carrier mobility resulted in *n*-type $zT \sim 1.4$ at 425 K [46]. Bi₂Te_{2.7}Se_{0.3} nanoplates have also been synthesized in a microwave-assisted synthesis route, which have $zT \sim 1.23$ at 480 K [47]. While many studies have focused on microstructure engineering to optimize the thermal transport, recently K doping has been used to modulate the electrical transport in Bi₂Te₃; for *n*-type material, $zT \sim 1.1$ was obtained at 350 K [48].

Transition metal (TM) tellurides

In this section, we discuss the TM based tellurides including MnTe, Ag₂Te, Cu₂Te and AgCuTe. MnTe crystallizes in a hexagonal structure and is an indirect band gap semiconductor with $E_g \sim 0.8$ eV. While MnTe exhibits high Seebeck coefficient, its low carrier concentration (10^{18} cm^{–3}) results in poor thermoelectric performance. Many dopants, such as Cu, Ag, Na have been introduced to improve the carrier concentration, which resulted in a maximum $zT \sim 1.09$ at 873 K [49]. Recently, the incorporation of SnTe nanocrystals was very effective in improving $zT \sim 1.4$ at 873 K [50]. Another novel concept based on paramagnon drag enhancement of the Seebeck coefficient has been used to improve thermoelectric performance [51]. This resulted in maximum $zT \sim 1$ at 923 K in Li doped MnTe. On the other hand, Cu₂Te, Ag₂Te and AgCuTe are superionic conductors. At room temperature, they have a complex crystal structure: for example, the ambient structure of AgCuTe and Ag₂Te are hexagonal and monoclinic, respectively. However, at high temperature, these materials have a cubic structure and exhibit superionic conduction. In the superionic phase, the anions form a rigid framework which supports high electrical conduction while the cations become superionic and impede phonon propagation. Such a resemblance to the phonon-glass electron-crystal (PGEC) scenario drives thermoelectric interest in these materials. However, high hole concentrations due to cation vacancies causes metallic conduction and low Seebeck coefficients. Recently, Se alloying in AgCuTe was very effective in suppressing cation vacancies due to stronger Ag–Se/Cu–Se bonds compared to Ag–Te/CuTe bonds. Additionally, dynamic cation disorder decreases lattice thermal conductivity, and an impressive $zT \sim 1.6$ at 670 K was obtained in Se doped AgCuTe [52]. Similarly, Sn doping has been used to tune the high hole concentration of Cu₂Te and $zT \sim 1.5$ has been achieved at 1000 K [53]. A mosaic crystal of Cu₂(Te,S) has also been reported with $zT \sim 2.09$ at 1000 K [54]. In contrast to *p*-type electronic transport of Cu₂Te and AgCuTe, Ag₂Te exhibits *n*-type conduction. In Ag₂Te, increased band conduction in PbTe alloyed Ag₂Te

resulted in $zT \sim 1$ at 550 K in the high temperature superionic phase [55]. In contrast, Sb doping has been shown to be effective in increasing the carrier concentration and electrical conductivity in the low temperature monoclinic phase of Ag_2Te and $zT \sim 1.4$ has been achieved at 410 K [56].

Chalcopyrites

The I–III–VI₂ (I = Ag, Cu; III = Ga, In; VI = Te) semiconductors, with unique electronic and thermal transport properties, are potential high performance thermoelectric materials. These materials have diamond like structures formed by the interconnected (I–VI)₄ and (III–VI)₄ tetrahedra. Compared to IV–VI semiconductors, these chalcopyrites are wide band gap semiconductors with $E_g \sim 0.8$ – 1.2 eV. Despite having similar crystal structures, all the I–III–VI₂ (I = Ag, Cu; III = Ga, In; VI = Te) semiconductors have distinctly different electrical and thermal transport properties [57]. AgGaTe_2 and AgInTe_2 possess low thermal conductivity; however, their low electrical conductivity renders them unsuitable as high-performance thermoelectric materials. The presence of Ga vacancies in AgGaTe_2 greatly improves thermoelectric performance, with $zT \sim 1.02$ at 873 K [58]. The related tellurides CuGaTe_2 and CuInTe_2 possess both high electrical conductivity and high thermal conductivity. Therefore, much effort has been devoted to lowering the lattice thermal conductivity of CuGaTe_2 and CuInTe_2 via a range of strategies based on inclusions and point defects. For example, the inclusion of nanophase Cu_2Se in CuGaTe_2 significantly reduces lattice thermal conductivity [59]. Similarly, ZnS nanoscale heterostructures [60] and In_2O_3 nano-inclusions [61] have been incorporated in CuInTe_2 to lower its lattice thermal conductivity. Solid solution alloying of Ag into CuInTe_2 lowers lattice thermal conductivity by forming weak Ag–Te bonds, which results in a high $zT \sim 1.6$ at 850 K [62]. Multicomponent alloying of Ag and In in CuGaTe_2 has also been very successful in lowering the lattice thermal conductivity, yielding $zT \sim 1.64$ at 873 K [63].

Concluding remarks

Many metal tellurides materials are used in practical applications because of their high thermoelectric performance. Recent advances in understanding of electronic structure, electrical and thermal transport properties, and sophisticated material processing techniques have led to important improvements in their thermoelectric performance in recent years. Furthermore, a range of novel strategies have been developed, including the precise control of the rhombohedral distortion [34] and Rashba spin splitting in GeTe [35], engineering ferroelectric instability in SnTe [13], and greatly improved material processing techniques for Bi_2Te_3 based materials [45] for microstructure and nanostructure engineering. Recently, a very high $zT \sim 2.6$ at 573 K was achieved in I–IV–VI₂ compound AgSbTe_2 by inducing nanoscale ordering [64]. Similarly, the novel concept of paramagnon drag in MnTe was employed to improve thermoelectric performance [51]. In recent years, rare earth tellurides like $\text{Pr}_{3-x}\text{Te}_4$ have also been introduced with high $zT \sim 1.7$ at 1200 K [65]. In addition to developing new high performance thermoelectric materials, unique strategies of electronic structure and phonon transport manipulation are necessary to achieve higher thermoelectric performance. Currently, the inferior performance of the counterpart *n*-type thermoelectric materials is major drawback, which needs to be addressed. Similarly, Te-based oxide thermoelectric materials, which have great potential in practical applications for high resistance against corrosion and thermal degradation, are worthy of attention.

Table 1. Tellurides thermoelectric properties.

Material	T (K)	μ_w ($\text{cm}^2 \text{V}^{-1} \text{s}^{-1}$)	κ_L ($\text{W m}^{-1} \text{K}^{-1}$) ^a	S ($\mu\text{V K}^{-1}$)	σ ($\Omega^{-1} \text{cm}^{-1}$)	zT	E_g (eV)	μ_0 ($\text{cm}^2 \text{V}^{-1} \text{s}^{-1}$)	m_s^a (m_e)	ϵ_T or ϵ (ϵ_0)	References
$\text{Bi}_x\text{Sb}_{2-x}\text{Te}_3$	300	479.5	0.6	186	1242	1.2	—	—	—	—	[42]
$\text{Bi}_x\text{Sb}_{2-x}\text{Te}_3$	373	318.4	0.44	212	845	1.4	—	—	—	—	[42]
$\text{Bi}_{0.5}\text{Sb}_{1.5}\text{Te}_3$	320	429.4	0.33	241	647	1.86	—	—	—	—	[45]
$\text{Bi}_{0.3}\text{Sb}_{1.625}\text{In}_{0.075}\text{Te}_3$	300	339.6	0.61	185	890	0.75	0.12	—	1.6	—	[69]
$\text{Bi}_{0.3}\text{Sb}_{1.625}\text{In}_{0.075}\text{Te}_3$	500	164.6	1.09 (kT)	220	618	1.4	—	—	—	—	[69]
$\text{Bi}_{0.5}\text{Sb}_{1.495}\text{Cu}_{0.005}\text{Te}_3$	300	363.5	0.34	154	1371	0.97	—	—	—	—	[70]
$\text{Bi}_{0.5}\text{Sb}_{1.495}\text{Cu}_{0.005}\text{Te}_3$	450	152.6	0.31	201	610	1.4	—	—	—	—	[70]
$\text{Bi}_{0.5}\text{Sb}_{1.5}\text{Te}_3$	350	332.4	0.65	237	600	1.24	—	—	—	—	[71]
$\text{Zn}_{0.015}\text{Bi}_{0.46}\text{Sb}_{1.54}\text{Te}_{3.015}$	300	465.6	0.52	185	1220	1.14	—	—	1.03	—	[43]
$\text{Zn}_{0.015}\text{Bi}_{0.46}\text{Sb}_{1.54}\text{Te}_{3.015}$	373	305.7	0.5	208	850	1.4	—	—	—	—	[43]
$\text{Bi}_{0.4}\text{Sb}_{1.6}\text{Te}_3$	323	458.7	1.03 (kT)	232	778	1.38	0.25	320	1.4	—	[72]
$\text{Bi}_2\text{Te}_{2.7}\text{Se}_{0.3}$	300	389.5	0.7	-190	963	0.9	—	—	—	—	[73]
$\text{Bi}_2\text{Te}_{2.7}\text{Se}_{0.3}$	398	221.2	1.14 (kT)	-209	670	1.04	—	—	—	—	[73]
$\text{Bi}_2\text{Te}_2\text{S}$	300	159.9	1.01 (kT)	-148	648	0.4	0.2	—	—	—	[74]
$\text{Bi}_2\text{Te}_2\text{S}$	573	52.8	0.93 (kT)	-171	430	0.8	—	—	—	—	[74]
$\text{K}_{0.06}\text{Bi}_2\text{Te}_{3.18}$	300	455.4	0.66	-180	1265	0.98	—	—	—	—	[48]
$\text{K}_{0.06}\text{Bi}_2\text{Te}_{3.18}$	350	359.4	0.66	-197	1032	1.1	—	—	—	—	[48]
$\text{Bi}_2\text{Te}_{2.7}\text{Se}_{0.3}$	300	182.7	0.44	-167	591	0.68	0.25	—	0.76	—	[47]
$\text{Bi}_2\text{Te}_{2.7}\text{Se}_{0.3}$	480	105.3	0.36	-198	480	1.23	—	—	—	—	[47]
$\text{Bi}_{1.8}\text{Sb}_{0.2}\text{Te}_{2.7}\text{Se}_{0.3} + 15\% \text{Te}$	300	398.8	0.41	-171	1231	1	—	100	1.7	—	[46]
$\text{Bi}_{1.8}\text{Sb}_{0.2}\text{Te}_{2.7}\text{Se}_{0.3} + 15\% \text{Te}$	425	215.6	0.38	-198	819	1.4	—	—	—	—	[46]
GeTe	300	310.2	2.62	32	8069	0.03	0.2	—	1.43	—	[75]
GeTe	673	148.4	0.74	137	2307	0.93	—	—	—	—	[75]
$\text{Ge}_{0.87}\text{Pb}_{0.13}\text{Te}$	723	115.9	1.2 (kT)	196	1000	2.27	—	—	—	—	[76]
$\text{Ge}_{0.87}\text{Pb}_{0.13}\text{Te} - 5\% \text{Bi}_2\text{Te}_3$	373	155.5	1.05 (kT)	130	1087	0.66	—	75	—	—	[77]
$\text{Ge}_{0.87}\text{Pb}_{0.13}\text{Te} - 5\% \text{Bi}_2\text{Te}_3$	690	86.5	0.78 (kT)	243	403	2.1	—	—	—	—	[77]
$(\text{CoGe}_2)_{0.2}(\text{GeTe})_{1.7}\text{Sb}_2\text{Te}_3$	723	135.9	0.64	258	571	1.9	—	—	—	—	[78]
$\text{Ge}_{0.9}\text{Sb}_{0.1}\text{Te}$	300	222.2	1.42	107	1503	0.22	0.08	—	—	—	[75]
$\text{Ge}_{0.9}\text{Sb}_{0.1}\text{Te}$	725	179	1.15	256	773	1.85	—	—	—	—	[75]
$\text{Ge}_{0.94}\text{Bi}_{0.06}\text{Te}$	300	236.9	1.13	71	2680	0.14	0.08	—	—	—	[79]
$\text{Ge}_{0.94}\text{Bi}_{0.06}\text{Te}$	725	130.5	1.2	217	886	1.3	—	—	—	—	[79]
$\text{Ge}_{0.85}\text{Bi}_{0.05}\text{Sb}_{0.1}\text{Te}$	300	159.7	0.48	130	805	0.47	0.08	—	2.44	—	[18]
$\text{Ge}_{0.85}\text{Bi}_{0.05}\text{Sb}_{0.1}\text{Te}$	725	128.3	0.65	232	732	1.8	—	—	—	—	[18]

(Continued.)

Table 1. (Continued.)

Material	T (K)	μ_w (cm ² V ⁻¹ s ⁻¹)	κ_L (W m ⁻¹ K ⁻¹) ^a	S (μ V K ⁻¹)	σ (Ω^{-1} cm ⁻¹)	zT	E_g (eV)	μ_0 (cm ² V ⁻¹ s ⁻¹)	m_s^a (m _e)	ϵ_T or ϵ (ϵ_0)	References
Ge _{0.9} Sb _{0.1} Te _{0.9} Se _{0.05} S _{0.05}	300	172.5	0.96	148	699	0.29	—	—	—	—	[80]
Ge _{0.9} Sb _{0.1} Te _{0.9} Se _{0.05} S _{0.05}	630	191	0.65	260	638	2.1	—	—	—	—	[80]
Ge _{0.9} Cd _{0.05} Bi _{0.05} Te	300	205.6	1.06	105	1428	0.32	—	43	1.7	—	[21]
Ge _{0.9} Cd _{0.05} Bi _{0.05} Te	650	149.7	0.48	232	725	2.23	—	—	—	—	[21]
Ge _{0.89} Sb _{0.1} In _{0.01} Te	300	167.7	0.73	192	405	0.4	—	—	3.8	—	[32]
Ge _{0.89} Sb _{0.1} In _{0.01} Te	780	99.9	0.52	245	547	2.3	—	—	6.2	—	[32]
Ge _{0.86} Pb _{0.1} Bi _{0.04} Te	300	243.1	0.63	138	1111	0.55	—	69	1.94	—	[34]
Ge _{0.86} Pb _{0.1} Bi _{0.04} Te	600	151.7	0.49	282	365	2.4	—	7	5.92	—	[34]
Ge _{0.86} Sb _{0.1} Zn _{0.04} Te	300	183.5	0.74	157	668	0.46	—	24	2.8	—	[20]
Ge _{0.86} Sb _{0.1} Zn _{0.04} Te	780	109.3	0.55	235	672	2.2	—	—	—	—	[20]
Ge _{0.93} In _{0.01} Bi _{0.06} Te	300	233.8	0.46	87	2082	0.33	0.09	—	1.9	—	[29]
Ge _{0.93} In _{0.01} Bi _{0.06} Te	723	212.5	0.72	246	1026	2.1	—	—	—	—	[29]
(GeTe) _{0.8} (AgBiSe ₂) _{0.2}	300	91.7	0.28	242	124	0.63	—	—	—	—	[36]
(GeTe) _{0.8} (AgBiSe ₂) _{0.2}	467	87.7	0.32	279	150	1.3	—	—	—	—	[36]
(Ge _{0.9} Sb _{0.1} Te) _{0.95} (SnSe) _{0.025} (SnS) _{0.025}	300	129.4	0.27	86	1169	0.26	—	—	—	—	[81]
(Ge _{0.9} Sb _{0.1} Te) _{0.95} (SnSe) _{0.025} (SnS) _{0.025}	710	97.1	0.32	206	726	1.9	—	—	—	—	[81]
Ge _{0.87} Sn _{0.05} Sb _{0.08} Te	300	173.4	0.92	89	1501	0.25	—	62	1.57	—	[35]
Ge _{0.87} Sn _{0.05} Sb _{0.08} Te	735	125.3	0.53	205	998	2.2	—	—	3.73	—	[35]
(GeTe) _{0.95} (Sb ₂ Te ₃) _{0.05}	323	204.8	1.44 (kT)	115	1394	0.4	—	—	—	—	[10]
(GeTe) _{0.95} (Sb ₂ Te ₃) _{0.05}	720	136.5	1.19 (kT)	217	917	2.7	—	—	—	—	[10]
(GeTe) _{0.5} (AgBiSe _{1.995} Br _{0.005}) _{0.5}	300	15.7	0.21	-149	63	0.15	0.36	—	—	—	[36]
(GeTe) _{0.5} (AgBiSe _{1.995} Br _{0.005}) _{0.5}	500	16.2	0.19	-167	113	0.6	—	—	—	—	[36]
SnTe	300	188.5	2.88	19	8261	—	—	—	—	—	[82]
SnTe	710	58.1	1.06	91	1779	0.29	—	—	—	—	[82]
Sn _{0.9975} In _{0.0025} Te	300	260.8	1.61	50	4300	0.09	0.18	—	—	—	[16]
Sn _{0.9975} In _{0.0025} Te	873	45	0.88	162	767	1.1	—	—	—	—	[16]
SnCd _{0.03} Te-2%CdS	300	130.8	1.31	47	2300	0.06	—	—	—	—	[24]
SnCd _{0.03} Te-2%CdS	873	40.6	0.63	205	419	1.3	—	—	—	—	[24]
Sn _{0.985} In _{0.015} Te _{0.85} Se _{0.15}	300	136.4	1.28	66	1674	0.09	—	—	—	—	[83]
Sn _{0.985} In _{0.015} Te _{0.85} Se _{0.15}	860	43.2	1.26	172	639	0.8	—	—	—	—	[83]
Sn _{0.94} Mg _{0.09} Te	300	131.6	2.72	35	3126	—	—	—	0.69	—	[23]
Sn _{0.94} Mg _{0.09} Te	860	70.6	0.79	174	1021	1.2	—	—	—	—	[23]
Sn _{0.98} Bi _{0.02} Te-3%HgTe	300	229.8	1.13	67	2774	0.13	—	—	—	—	[25]

(Continued.)

Table 1. (Continued.)

Material	T (K)	μ_w (cm ² V ⁻¹ s ⁻¹)	κ_L (W m ⁻¹ K ⁻¹) ^a	S (μ V K ⁻¹)	σ (Ω^{-1} cm ⁻¹)	zT	E_g (eV)	μ_0 (cm ² V ⁻¹ s ⁻¹)	m_s^a (m _e)	ϵ_T or ϵ (ϵ_0)	References
Sn _{0.98} Bi _{0.02} Te-3%HgTe	910	59.1	0.66	182	847	1.35	—	—	—	—	[25]
Sn _{0.97} In _{0.015} Cd _{0.015} Te-3%CDs	300	132.7	1.64	92	1101	0.13	—	—	—	—	[26]
Sn _{0.97} In _{0.015} Cd _{0.015} Te-3%CDs	923	44	0.59	196	548	1.4	—	—	—	—	[26]
Sn _{0.94} Ca _{0.09} Te	325	257.6	1	44	5466	0.2	—	0.35	—	—	[84]
Sn _{0.94} Ca _{0.09} Te	873	56.9	0.79	185	740	1.35	—	—	—	—	[84]
Sn _{0.97} Bi _{0.03} Te-3%SrTe	300	289.4	1.56	82	2770	0.17	—	—	—	—	[85]
Sn _{0.97} Bi _{0.03} Te-3%SrTe	823	47.4	0.86	173	649	1.2	—	—	—	—	[85]
Sn _{0.85} Sb _{0.15} Te	300	150.9	0.67	33	3806	—	—	—	—	—	[82]
Sn _{0.85} Sb _{0.15} Te	800	56.2	—	151	956	1	—	—	—	—	[82]
SnAg _{0.025} In _{0.025} Te _{1.05}	300	239	2.39	98	1825	0.08	—	—	—	—	[27]
SnAg _{0.025} In _{0.025} Te _{1.05}	856	69.7	1.17	167	1087	1	—	—	—	—	[27]
Sn _{0.97} Bi _{0.03} Te-3%PbTe	300	157.1	1.15	27	4847	—	—	—	—	—	[86]
Sn _{0.97} Bi _{0.03} Te-3%PbTe	900	54.2	1.1	197	642	1.1	—	—	—	—	[86]
(Sn _{0.89} Mn _{0.14} Te)(Cu ₂ Te) _{0.05}	300	102.6	1.72	45	1886	0.06	—	—	—	—	[12]
(Sn _{0.89} Mn _{0.14} Te)(Cu ₂ Te) _{0.05}	920	34.4	0.51	200	407	1.6	—	—	—	—	[12]
Sn _{0.915} Mn _{0.11} In _{0.005} Te	300	106.8	1.64	117	634	0.13	—	—	—	—	[87]
Sn _{0.915} Mn _{0.11} In _{0.005} Te	823	47.6	0.92	237	310	1.15	—	—	—	—	[87]
(Sn _{0.91} Mg _{0.12} Te)(Cu ₂ Te) _{0.05}	300	138.9	1.23	28	4132	—	—	—	—	—	[88]
(Sn _{0.91} Mg _{0.12} Te)(Cu ₂ Te) _{0.05}	900	32.7	0.55	198	383	1.4	—	—	—	—	[88]
Sn _{0.57} Sb _{0.13} Ge _{0.3} Te	300	166	0.48	67	2004	0.16	—	—	—	—	[13]
Sn _{0.57} Sb _{0.13} Ge _{0.3} Te	721	77.8	0.3	174	864	1.6	—	—	—	—	[13]
Sn _{0.83} Ag _{0.03} Mn _{0.17} Te	300	148	1.64	46	2669	0.05	—	—	—	—	[30]
Sn _{0.83} Ag _{0.03} Mn _{0.17} Te	865	55	0.3	164	908	1.45	—	—	—	—	[30]
Sb ₂ Te ₃ (Sn _{0.996} Re _{0.004} Te) ₈	325	190.8	0.72	84	2000	0.2	—	—	—	—	[89]
Sb ₂ Te ₃ (Sn _{0.996} Re _{0.004} Te) ₈	773	77.1	0.48	183	855	1.4	—	—	—	—	[89]
Sn _{1.03} Te _{0.85} Se _{0.075} So _{0.075} -2%Ag-2%In	300	162.6	1.21	90	1387	0.16	—	—	—	—	[90]
Sn _{1.03} Te _{0.85} Se _{0.075} So _{0.075} -2%Ag-2%In	854	62	0.6	182	808	1.3	—	—	—	—	[90]
Na _{0.95} Pb ₂₀ SbTe ₂₂	300	190.6	0.74	94	1538	0.25	—	—	—	—	[91]
Na _{0.95} Pb ₂₀ SbTe ₂₂	650	126	0.55	330	196	1.7	—	—	—	—	[91]
Pb _{0.98} Tl _{0.02} Te	300	93.2	2.17 (kT)	137	431	0.1	—	0.93	—	—	[14]
Pb _{0.98} Tl _{0.02} Te	773	87.3	0.95 (kT)	332	172	1.5	—	—	—	—	[14]
PbTe-12%PbS-2%Na	315	136	1.61	69	1710	0.09	—	—	—	—	[92]
PbTe-12%PbS-2%Na	800	75.6	0.73	263	349	1.8	—	—	—	—	[92]

(Continued.)

Table 1. (Continued.)

Material	T (K)	μ_w ($\text{cm}^2 \text{V}^{-1} \text{s}^{-1}$)	κ_L ($\text{W m}^{-1} \text{K}^{-1}$) ^a	S ($\mu\text{V K}^{-1}$) ^a	σ ($\Omega^{-1} \text{cm}^{-1}$)	zT	E_g (eV)	μ_0 ($\text{cm}^2 \text{V}^{-1} \text{s}^{-1}$)	m_s^a (m_e)	ϵ_r or ϵ (ϵ_0)	References
PbTe-1%Na ₂ Te-6%CaTe	300	179.4	1.32	65	2239	0.09	0.26	—	—	—	[93]
PbTe-1%Na ₂ Te-6%CaTe	765	66.6	0.48	259	301	1.5	—	—	—	—	[93]
PbTe _{0.85} Se _{0.15} -2%Na	300	147.2	1.41	50	2427	0.06	—	—	—	—	[15]
PbTe _{0.85} Se _{0.15} -2%Na	850	59.7	0.52	222	485	1.8	—	—	—	—	[15]
Mg _x Pb _{1-x} Te:Na(9E19) ^b	300	197.1	1.73	105	1369	0.19	—	—	—	—	[94]
Mg _x Pb _{1-x} Te:Na(9E19) ^b	725	92.1	0.64	269	342	1.7	—	—	—	—	[94]
PbTe:Na(9E19) ^b	300	216.2	2.05	62	2840	0.1	—	—	—	—	[95]
PbTe:Na(9E19) ^b	750	87.5	0.8	270	338	1.4	—	—	—	—	[95]
Pb _{0.96} Mn _{0.04} Te:Na	300	190.4	1.33	101	1396	0.2	0.38	—	—	—	[96]
Pb _{0.96} Mn _{0.04} Te:Na	700	86	0.64	263	325	1.6	—	—	—	—	[96]
PbTe-4%SrTe-2%Na	300	145.1	1.96	79	1452	0.09	—	—	—	—	[28]
PbTe-4%SrTe-2%Na	915	64.8	0.52	281	297	2.2	—	—	—	—	[28]
K _{0.02} Pb _{0.98} Te _{0.75} Se _{0.25}	300	98.4	1.49	53	1526	0.06	—	—	—	—	[97]
K _{0.02} Pb _{0.98} Te _{0.75} Se _{0.25}	773	78.5	0.8	312	195	1.6	—	—	—	—	[97]
PbTe-2%MgTe-2%Na ₂ Te	300	197.9	2.05	67	2388	0.1	—	—	—	—	[98]
PbTe-2%MgTe-2%Na ₂ Te	780	76.8	0.74	250	397	1.6	—	—	—	—	[98]
Pb _{0.98} Na _{0.02} Te-6%MgTe	300	175.3	1.73	110	1140	0.16	0.39	1.18	—	—	[99]
Pb _{0.98} Na _{0.02} Te-6%MgTe	823	74.6	0.53	295	248	2	—	—	—	—	[99]
PbTe _{0.7} Se _{0.3} -2.5%K	300	127	0.64	70	1460	0.14	—	—	—	—	[100]
PbTe _{0.7} Se _{0.3} -2.5%K	923	42.7	0.37	299	161	2.2	—	—	—	—	[100]
(PbTe) _{0.86} (PbSe) _{0.07} (PbS) _{0.07} -2%Na	300	163.3	0.61	69	1908	0.1	0.28	—	—	—	[101]
(PbTe) _{0.86} (PbSe) _{0.07} (PbS) _{0.07} -2%Na	823	82.7	0.61	265	389	2	—	—	—	—	[101]
Pb _{0.98} Na _{0.02} Te-8%SrTe	300	242.6	1.7	91	2041	0.18	0.34	1.37	—	—	[102]
Pb _{0.98} Na _{0.02} Te-8%SrTe	923	80.9	0.57	294	323	2.5	—	—	—	—	[102]
Pb _{0.953} Na _{0.04} Ge _{0.007} Te	300	251.7	2.15	69	2941	0.1	0.4	0.8	—	—	[103]
Pb _{0.953} Na _{0.04} Ge _{0.007} Te	805	89.5	0.67	263	417	1.9	—	—	—	—	[103]
Na _{0.03} Eu _{0.03} Sn _{0.02} Pb _{0.92} Te	300	88.2	0.87	104	621	0.14	—	—	—	—	[11]
Na _{0.03} Eu _{0.03} Sn _{0.02} Pb _{0.92} Te	850	62.9	0.42	273	283	2.57	—	—	—	—	[11]
PbTe-1%CdTe-0.055%PbI ₂	300	330.5	0.89	-88	2901	0.21	0.3	—	—	—	[104]
PbTe-1%CdTe-0.055%PbI ₂	720	52.6	0.5	-225	322	1.2	—	—	—	—	[104]
PbTe _{0.9988} I _{0.0012}	300	364.2	1.53	-83	3436	0.27	—	0.25	—	—	[105]
PbTe _{0.9988} I _{0.0012}	723	74.4	0.78	-206	571	1.4	—	—	—	—	[105]

(Continued.)

Table 1. (Continued.)

Material	T (K)	μ_w ($\text{cm}^2 \text{V}^{-1} \text{s}^{-1}$)	κ_L ($\text{W m}^{-1} \text{K}^{-1}$) ^a	S ($\mu\text{V K}^{-1}$)	σ ($\Omega^{-1} \text{cm}^{-1}$)	zT	E_g (eV)	μ_0 ($\text{cm}^2 \text{V}^{-1} \text{s}^{-1}$)	m_s^a (m_e)	ε_r or ε (ε_0)	References
PbTe:1(1.8E19) ^b	300	392.8	3.32 (kT)	-81	3816	0.22	—	1120	0.25	—	[106]
PbTe:1(1.8E19) ^b	725	—	—	-212	—	1.39	—	—	—	—	[106]
PbTe-4%InSb	323	78	2.25	-132	428	0.09	—	—	—	—	[40]
PbTe-4%InSb	773	56	0.25	-205	484	1.83	—	—	—	—	[40]
PbTe-4%MnTe	300	171	1.15	-88	1500	0.15	0.34	—	0.4	—	[39]
PbTe-4%MnTe	773	60	0.53	-238	353	1.6	—	—	—	—	[39]
Pb _{0.9965} In _{0.0035} Te _{0.996} Io _{0.004}	300	301.5	1.33	-140	1345	0.4	—	—	0.4	—	[37]
Pb _{0.9965} In _{0.0035} Te _{0.996} Io _{0.004}	773	56.9	0.7	-224	392	1.4	—	—	—	—	[37]
(Pb _{0.93} Sn _{0.07})(Te _{0.93} Se _{0.07})	300	152.8	1.35	-54	2324	0.08	—	—	0.31	—	[107]
(Pb _{0.93} Sn _{0.07})(Te _{0.93} Se _{0.07})	773	47.5	0.6	-199	437	1.4	—	—	—	—	[107]
Pb _{0.98} Ga _{0.02} Te-5%GeTe	300	330.2	1.13	-222	563	0.59	—	—	0.4	—	[38]
Pb _{0.98} Ga _{0.02} Te-5%GeTe	673	86.4	0.66	-287	233	1.47	—	—	—	—	[38]
AgSbTe ₂	300	137.4	0.5	279	121	0.55	—	—	—	—	[64]
AgSbTe ₂	573	58.5	0.5	328	77	0.89	—	—	—	—	[64]
AgSb _{0.96} Zn _{0.04} Te ₂	300	107.9	0.52	234	160	0.56	—	—	2.65	—	[108]
AgSb _{0.96} Zn _{0.04} Te ₂	585	96.5	0.35	289	206	1.9	—	—	—	—	[108]
AgSbTe _{1.85} Se _{0.15}	300	84.2	0.37	203	179	0.53	—	20	2.32	—	[109]
AgSbTe _{1.85} Se _{0.15}	573	92	0.29	309	151	2.1	—	4	3.38	—	[109]
AgSb _{0.94} Cd _{0.06} Te ₂	300	174.4	0.15	248	220	1.5	—	—	—	—	[64]
AgSb _{0.94} Cd _{0.06} Te ₂	573	92.6	0.17	265	253	2.6	—	—	—	—	[64]
MnTe	300	14.1	1.18	463	1.47	—	0.82	—	7	—	[110]
MnTe	900	17.7	0.67	302	62	0.67	—	—	—	—	[110]
Mn _{0.98} Na _{0.02} Te	300	51.8	0.82	192	125	0.15	—	—	7.7	—	[110]
Mn _{0.98} Na _{0.02} Te	900	19.7	0.58	270	100	0.89	—	—	—	—	[110]
MnTe+0.5%Na ₂ S	300	79.4	1.56	185	208	0.1	—	—	—	—	[49]
MnTe+0.5%Na ₂ S	873	25.9	0.56	267	130	1.09	—	—	—	—	[49]
MnTe+3%Li	923	20.5	0.9 (kT)	208	222	1	—	—	1.05	—	[51]
Mn _{1.06} Te+2%SnTe	323	—	1.48	522	—	—	0.84	—	2.69	—	[50]
Mn _{1.06} Te+2%SnTe	873	64.9	0.66	379	89	1.4	—	—	—	—	[50]
Ag ₂ Te	300	213.1	0.25	-90	1818	0.45	0.04	—	<0.1	—	[55]
Ag ₂ Te	550	32.2	0.23	-119	463	0.62	0.2	—	—	—	[55]
(Ag _{1.9996} Te) _{0.9} (PbTe) _{0.1}	300	177.2	0.38	-101	1299	0.38	—	—	—	—	[55]
(Ag _{1.9996} Te) _{0.9} (PbTe) _{0.1}	550	34.1	0.23	-178	241	1	0.28	—	—	—	[55]

(Continued.)

Table 1. (Continued.)

Material	T (K)	μ_w ($\text{cm}^2 \text{V}^{-1} \text{s}^{-1}$)	κ_L ($\text{W m}^{-1} \text{K}^{-1}$) ^a	S ($\mu\text{V K}^{-1}$)	σ ($\Omega^{-1} \text{cm}^{-1}$)	zT	E_g (eV)	μ_0 ($\text{cm}^2 \text{V}^{-1} \text{s}^{-1}$)	m_s^a (m_e)	ε_r or ε (ε_0)	References
Ag ₂ Sb _{0.02} Te _{0.98}	300	99.2	0.36	-105	689	0.35	0.08	—	—	—	[56]
Ag ₂ Sb _{0.02} Te _{0.98}	410	80.6	—	-106	883	1.4	—	—	—	—	[56]
Cu ₂ Te	320	79.9	6.1 (kT)	15	4878	—	0.26	1.5	—	—	[53]
Cu ₂ Te	1000	20.2	2.36 (kT)	93	1008	0.37	—	—	—	—	[53]
Cu _{1.98} Ag _{0.2} Te	300	128.3	1.98 (kT)	47	2256	0.08	—	—	—	—	[111]
Cu _{1.98} Ag _{0.2} Te	900	30.8	1.3 (kT)	158	575	1	—	—	—	—	[111]
Cu ₂ S _{0.52} Te _{0.48}	300	20.2	0.49 (kT)	62	265	—	—	4.5	—	—	[54]
Cu ₂ S _{0.52} Te _{0.48}	1000	15.5	0.38 (kT)	218	168	2.09	—	—	—	—	[54]
Cu _{1.9} Sn _{0.1} Te	320	109.6	1.22 (kT)	38	2638	0.1	0.25	2.56	—	—	[53]
Cu _{1.9} Sn _{0.1} Te	1000	27.7	0.97 (kT)	133	819	1.5	—	—	—	—	[53]
Cu ₂ Te+50%Ag ₂ Te	300	67.5	1.32 (kT)	54	1027	0.07	—	—	—	—	[112]
Cu ₂ Te+50%Ag ₂ Te	1000	20.1	0.64 (kT)	178	348	1.8	—	—	—	—	[112]
AgCuTe	300	39.3	0.35	31	1055	0.15	—	—	—	—	[52]
AgCuTe	660	29.9	0.23	228	155	1.3	—	—	—	—	[52]
AgCuTe _{0.9} Se _{0.1}	300	31.2	0.15	70	359	0.36	—	—	—	—	[52]
AgCuTe _{0.9} Se _{0.1}	670	38.4	0.25	223	216	1.6	—	—	—	—	[52]
AgCuTe _{0.9} Io _{0.1}	300	39	0.21	143	168	0.35	—	1.21	—	—	[113]
AgCuTe _{0.9} Io _{0.1}	463	33.8	0.17	287	52	0.9	—	—	—	—	[113]
AgGaTe ₂	300	—	1.42	—	—	—	1.06	—	—	—	[57]
AgGaTe ₂	750	16.5	0.33	414	12	0.48	—	—	—	—	[57]
Ag _{0.95} GaTe ₂	300	26.2	1.26 (kT)	673	0.24	—	—	—	—	—	[114]
Ag _{0.95} GaTe ₂	850	14.1	0.2 (kT)	382	18	0.77	—	—	—	—	[114]
AgGa _{0.93} Te ₂	300	—	1.16 (kT)	—	—	—	—	—	—	—	[58]
AgGa _{0.93} Te ₂	873	11.9	0.18 (kT)	396	13.4	1.02	—	—	—	—	[58]
AgInTe ₂	300	—	1.42	—	—	—	0.87	—	—	—	[57]
AgInTe ₂	750	14.2	0.33	570	1.7	0.18	—	—	—	—	[57]
CuGaTe ₂	300	76.9	6.7	380	21	—	1.2	—	—	—	[115]
CuGaTe ₂	950	30.5	0.51	244	227	1.4	—	—	—	—	[115]
CuGaTe ₂	300	117.6	6.7	395	27	—	1.18	—	—	—	[57]
CuGaTe ₂	875	38	0.95	281	163	1	—	—	—	—	[57]
CuGa _{0.36} In _{0.64} Te ₂	320	36.6	1.48	390	9.8	—	0.85	—	—	—	[116]
CuGa _{0.36} In _{0.64} Te ₂	701	39.2	0.56	285	115	0.91	—	—	—	—	[116]

(Continued.)

Table 1. (Continued.)

Material	T (K)	μ_w ($\text{cm}^2 \text{V}^{-1} \text{s}^{-1}$)	κ_L ($\text{W m}^{-1} \text{K}^{-1}$) ^a	S ($\mu\text{V K}^{-1}$)	σ ($\Omega^{-1} \text{cm}^{-1}$)	zT	E_g (eV)	μ_0 ($\text{cm}^2 \text{V}^{-1} \text{s}^{-1}$)	m_s^a (m_e)	ε_r or ε (ε_0)	References
Cu _{0.98} GaSb _{0.02} Te ₂	310	14.4	3.1	176	44	—	0.95	—	—	—	[117]
Cu _{0.98} GaSb _{0.02} Te ₂	721	40.6	0.48	262	162	1.07	—	—	—	—	[117]
Cu _{0.7} Ag _{0.3} Ga _{0.4} In _{0.6} Te ₂	300	252.7	—	588	6.2	—	—	—	—	—	[63]
Cu _{0.7} Ag _{0.3} Ga _{0.4} In _{0.6} Te ₂	873	32.9	0.25	406	33	1.64	—	—	—	—	[63]
CuInTe ₂	300	112.7	6 (kT)	247	144	—	1.02	—	0.52	—	[118]
CuInTe ₂	850	35.8	1.05 (kT)	270	167	1.18	—	—	—	—	[118]
CuInTe ₂	300	155	5.9	464	16	—	0.92	—	—	—	[57]
CuInTe ₂	875	28	0.81	290	108	0.9	—	—	—	—	[57]
Cu _{0.9} InTe ₂	300	78.8	3 (kT)	170	246	0.11	—	—	0.6–0.8	—	[119]
Cu _{0.9} InTe ₂	710	35.5	1.33 (kT)	214	242	0.54	—	—	—	—	[119]
Cu _{0.75} Ag _{0.2} InTe ₂	300	46.5	1.86 (kT)	234	69	0.07	—	—	—	—	[120]
Cu _{0.75} Ag _{0.2} InTe ₂	850	27.6	0.52 (kT)	320	72	1.25	—	—	—	—	[120]
CuInTe _{1.99} Sb _{0.01} +1%ZnO	300	86.6	3.6	104	610	—	—	—	—	—	[61]
CuInTe _{1.99} Sb _{0.01} +1%ZnO	823	47.7	0.45	284	180	1.61	—	—	—	—	[61]
CuInTe ₂ +6%ZnS	300	85.7	3.54	157	312	—	—	—	—	—	[60]
CuInTe ₂ +6%ZnS	823	37.5	0.44	282	145	1.52	—	—	—	—	[60]
Cu _{0.89} Ag _{0.2} In _{0.91} Te ₂	300	149.4	2.68 (kT)	446	19	—	0.9	—	—	—	[62]
Cu _{0.89} Ag _{0.2} In _{0.91} Te ₂	850	31.8	0.47 (kT)	315	88	1.6	—	—	—	—	[62]
BiTe	300	149.3	0.72	−37	3352	0.05	0.1	—	—	—	[66]
BiTe	500	78.8	0.76	−61	2267	0.13	—	—	—	—	[66]
BiTe _{0.5} Se _{0.5}	300	170.6	1.8 (kT)	−49	2873	0.12	—	—	—	—	[66]
BiTe _{0.5} Se _{0.5}	500	93.5	2.1 (kT)	−79	2014	0.32	—	—	—	—	[66]
BiCuOTe	300	62.7	0.68 (kT)	173	189	0.4	0.21	—	—	—	[121]
BiCuOTe	673	24.2	0.73 (kT)	183	218	0.66	—	—	—	—	[121]
BiCuO _{0.88} Te	323	114.8	0.59	185	336	0.48	—	—	—	—	[67]
BiCuO _{0.88} Te	673	29.6	0.33	207	202	1.06	—	—	—	—	[67]
La _{3−x} Te ₄ (1.2E21) ^b	1275	9.3	0.5 (kT)	−300	56	1.13	—	—	—	—	[122]
La _{3−x} Te ₄ (1.2E21) ^b	300	—	—	—	—	—	0.83	—	2.75	—	[122]
La _{2.6} Yb _{0.4} Te ₄ (3E20) ^b	1273	11.1	0.66 (kT)	−289	76	1.2	—	—	—	—	[68]
Pr _{2.74} Te ₄	300	58.1	0.846	−48	1000	0.03	—	—	—	—	[65]
Pr _{2.74} Te ₄	1200	18.1	0.427	−240	200	1.7	—	—	—	—	[65]

^a kT—indicates total thermal conductivity.^b (1.2E21)—numbers of this type after the material name indicates the carrier concentration (cm^{-3}).

3.2. Skutterudites

Skutterudite thermoelectrics

Pengfei Qiu^{1,4}, Shun Wan^{2,4} and Lidong Chen^{1,3}

¹ State Key Laboratory of High Performance Ceramics and Superfine Microstructure, Shanghai Institute of Ceramics, Chinese Academy of Sciences, Shanghai 200050, People's Republic of China

² Center for High Pressure Science and Technology Advanced Research (HPSTAR), Shanghai 201203, People's Republic of China

³ Center of Materials Science and Optoelectronics Engineering, University of Chinese Academy of Sciences, Beijing 100049, People's Republic of China

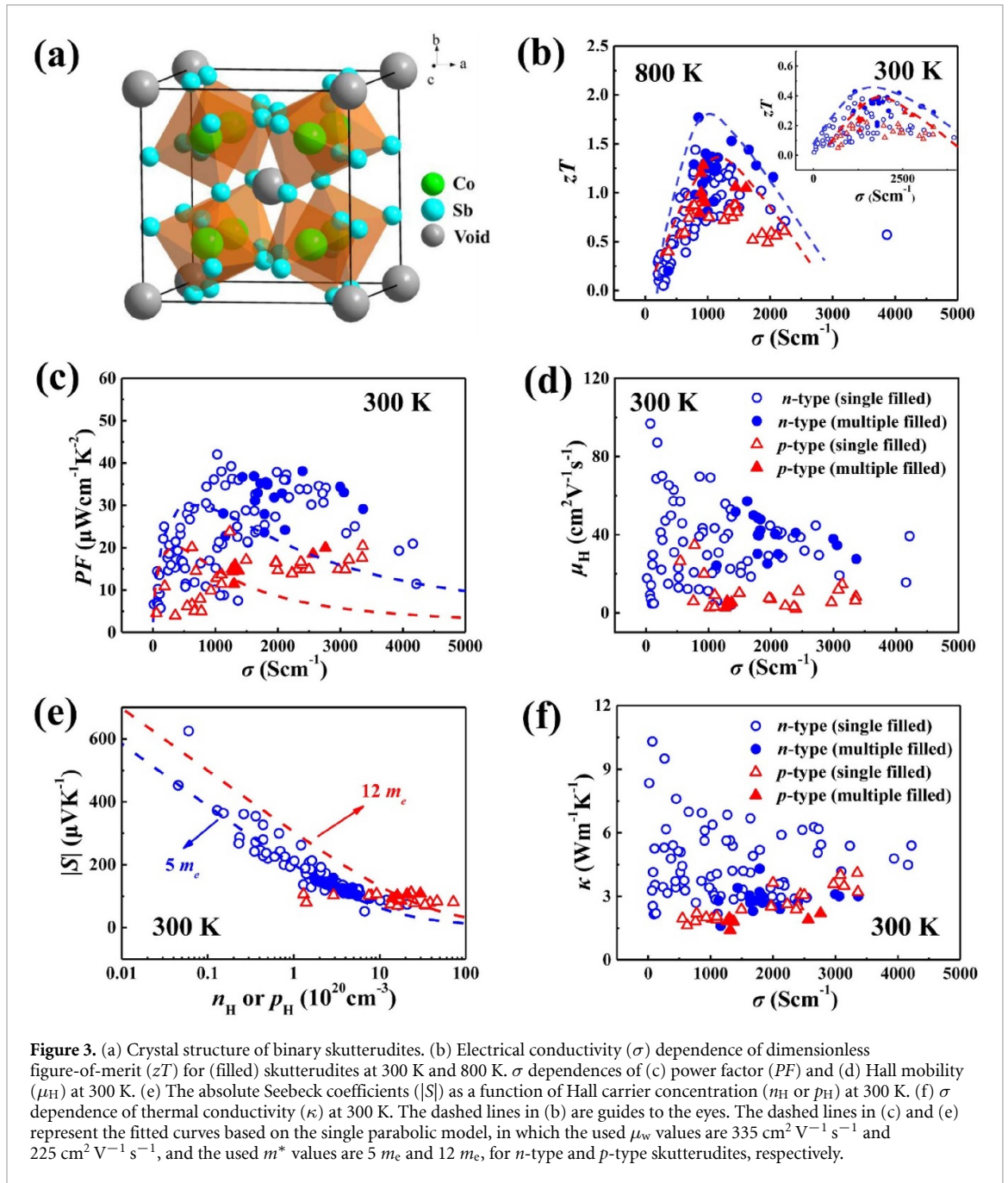
⁴ Equally contributed to this work.

Skutterudites (table 2) are among the best thermoelectric materials for applications in intermediate temperatures [123–125]. Binary skutterudites, with the chemical formula of MX_3 ($M = \text{Co, Rh, or Ir, } X = \text{P, As, or Sb}$), crystallize in a body-centered cubic structure ($Im\bar{3}$), with the structure shown in figure 3(a). There are two large icosahedral voids per unit (M_8X_{24}), which can be filled with guest atoms (e.g. alkalis, alkaline earths, rare earths, and others) forming filled skutterudites. The chemical formula of filled skutterudites can be written as $G_yM_4X_{12}$, where G represents the fillers and y is the filling fraction. The fillers G are weakly bonded with the surrounding atoms with large atomic displacement parameters, which can strongly interrupt the normal transport of phonons by introducing additional localized vibrational modes and therefore significantly lower the lattice thermal conductivity (κ_L). By the combination of significantly reduced thermal conductivity and (maintaining) good electrical transport, the filled skutterudites well satisfy the PGEC concept proposed by Slack [126, 127].

Cobalt antimonide (CoSb_3) based filled skutterudites are reported to show excellent thermoelectric performance among the skutterudite family [128–149]. When rare earth, alkaline earths, or alkali metals are accommodated in the Sb-icosahedral voids without additional charge compensation, the resulting filled skutterudites $G_y\text{Co}_4\text{Sb}_{12}$ usually show n -type conductivity due to the extra electrons introduced into the $[\text{Co}_4\text{Sb}_{12}]$ framework by the filler, while the fillers hardly modify the band structure near the conduction band minimum. The maximum filling fraction increases with the type of filler, roughly following the sequence of rare earths, alkaline earths, and alkali metals, although it is also affected by the electronegativity, radius, and valence of the filler ions. The optimal filling fraction for maximum power factors (PFs) roughly obeys a '0.5 electron per unit cell' rule, in which the carrier concentration reaches $\sim 10^{20} \text{ cm}^{-3}$ [150]. Binary CoSb_3 has an intrinsic high κ_L of about $\sim 10 \text{ W m}^{-1} \text{ K}^{-1}$ at 300 K. Introducing foreign elements into the Sb-icosahedral voids can greatly lower κ_L due to the filler-introduced resonant scattering of phonons. One important realization is that these resonant scattering centers are tuned to a particular spectrum of phonons. By filling the voids with different types of elements possessing different resonant frequencies, it enables phonons with a broad range of frequencies to be scattered, leading to a significant reduction of lattice thermal conductivity in the so-called multiple-filled skutterudites. With comprehensive strategies, combining the optimization of carrier concentration by optimizing the filling fraction, the reduction of κ_L through multiple-filling, as well as the introduction of magnetic nanocomposites, the maximum zT has been enhanced to a very high level, exceeding 1.7 in CoSb_3 -based n -type filled skutterudites [144, 149].

It is easy to obtain p -type filled skutterudites by alloying Fe at the Co-site or Ge/Sn at the Sb-site in $G_y\text{Co}_4\text{Sb}_{12}$. $G_y\text{Co}_{4-x}\text{Fe}_x\text{Sb}_{12}$ (where x is the Fe doping content) represents one of the most promising p -type filled skutterudites [149, 151–157]. The x in $G_y\text{Co}_{4-x}\text{Fe}_x\text{Sb}_{12}$ is usually in the range of 1.5–4. The maximum filling fraction y in $G_y\text{Co}_{4-x}\text{Fe}_x\text{Sb}_{12}$ is usually less than x/n , where n is the valence state of fillers. In $G_y\text{Fe}_4\text{Sb}_{12}$, the electrical transport is sensitively dependent on the valence states of the fillers, while the lattice thermal resistivity $W_L (= 1/\kappa_L)$ obeys the relationship of $W_L \sim (r_{\text{cage}} - r_{\text{ion}})^3$, where r_{cage} and r_{ion} are the radii of Sb-icosahedron void and filler, respectively [151]. It should be noted that the Sb in p -type filled skutterudites is easier to volatilize at elevated temperature than in n -type filled skutterudites, thus the maximum measurement temperature for p -type filled skutterudites is usually around 800 K, about 50–100 K lower than that for n -type filled skutterudites. The maximum zT is around unity for p -type $G_y\text{Co}_{4-x}\text{Fe}_x\text{Sb}_{12}$, which is much lower than for n -type $G_y\text{Co}_4\text{Sb}_{12}$ (figure 3(b)) [151–153].

Figures 3(b)–(f) present the collected physical properties (electrical conductivity, thermal conductivity, Seebeck coefficient, and carrier mobility) and thermoelectric parameters (PF and zT) of p - and n -type skutterudites at 300 K [128–149, 151–157]. These parameters are plotted as the dependencies of electrical conductivity or carrier concentration. All these dependencies show similar trends even at high temperature. As shown in figure 3(b), at 300 K, the zT s of p -type skutterudites are smaller than those for n -type materials across the whole range of electrical conductivity (σ), although the optimal electrical conductivity for peak zT



takes occurs in the same range, around $1500\text{--}2500 \text{ S cm}^{-1}$. The disparity between the optimal zT values of n - and p -type skutterudites is numerically determined by the different levels of PF as shown in figure 3(c). For example, the maximum PF for n -type skutterudites at 300 K is approximately $40 \mu\text{W cm}^{-1} \text{ K}^{-2}$, while that for p -type materials is only around $20 \mu\text{W cm}^{-1} \text{ K}^{-2}$.

Generally, the weighted mobility $\mu_w (= \mu_0(m^*/m_0)^{3/2})$, where μ_0 is the drift mobility and m^* is the density-of-state effective mass) is an important factor to discuss the PF . Since the m^* varies with the variation of carrier concentration in skutterudites, it is difficult to achieve a satisfactory fit to all data by using fixed μ_w , but the general trend should be valuable and meaningful from the estimated μ_w [158]. In figure 3(c), the PF — σ lines for n - and p -type skutterudites are drawn using the estimated μ_w ($335 \text{ cm}^2 \text{ V}^{-1} \text{ s}^{-1}$ and $225 \text{ cm}^2 \text{ V}^{-1} \text{ s}^{-1}$ for n - and p -type skutterudites, respectively, estimated from all collected data) and m^* ($5m_e$ and $12m_e$, for n - and p -type, respectively, estimated from all collected data). As shown in figures 1(d) and (e), the much larger μ_H guarantees the larger PF s for n -type skutterudites although their m^* values are smaller than in p -type ones. This scenario is consistent with analyses based on band structure. For n -type skutterudites, the conduction band edge is dominated by the Sb-dominated threefold degenerated bands. However, for p -type skutterudites, there is one Sb-dominated light band and one Fe-dominated heavy band in the valence band edge. Considering the heavily doped character of $G_y\text{Co}_{4-x}\text{Fe}_x\text{Sb}_{12}$, the Fermi level crosses

the Fe-dominated heavy band. The localized nature of Fe 3d orbitals is responsible for the large m^* but small μ_0 observed in p -type skutterudites. This implies that, efforts to optimize the band structure through exploring new alloy systems (if possible) to enhance the carrier mobility may be worthwhile for the development of p -type filled skutterudites with higher thermoelectric performance.

Figure 3(f) shows that the p -type (filled) skutterudites generally exhibit lower total thermal conductivity (κ) and κ_L than the n -type (filled) skutterudites under the comparable range of σ . This is reasonable since the p -type skutterudites usually possess higher filling fractions, which can lead to stronger scattering of phonons. In addition, the coexistence of Fe and Co at the same atomic site introduces extra point defects to scatter phonons, which are also responsible for the lower κ_L values observed in p -type skutterudites. However, in figure 3(f), it can be seen that many n -type samples exhibit comparable κ to the p -type samples in the optimal σ range. It is noted that these low κ values are obtained in the multiple-filled skutterudites. The combination of the low κ and reduced influence on electrical transport by multiple-filling guarantees the realization of high zT in n -type filled skutterudites.

Although skutterudites have been widely studied in the aspects of both material optimization and device development, there are still great challenges for skutterudite thermoelectrics. Firstly, the current TE performance of p -type skutterudites is behind that of the n -type skutterudites, which limits the development of high efficiency devices. Considering that the localized 3d orbitals of Fe is the main reason for the low carrier mobilities and poor zTs of existing p -type skutterudites, alternative doping elements should be explored to develop new p -type skutterudites. Secondly, the κ_L of n -type skutterudites below 700 K still has much scope for reduction. Novel approaches, such as nanostructure engineering, are to be encouraged to further strengthen phonon scattering, which is beneficial for enhancing the average zT of n -type skutterudites over the entire temperature range and therefore effectively improving the conversion efficiency of the devices. Furthermore, at high temperatures, skutterudites face severe oxidation and Sb volatilization issues, leading to relatively poor reliability during service. Developing effective protective coating or sealing technology against oxidation and volatilization is also important for their practical applications.

Acknowledgments

The work of Lidong Chen and Pengfei Qiu is supported by the National Key Research and Development Program of China (2018YFB0703600) and the National Natural Science Foundation of China (91963208).

Table 2. Skutterudite thermoelectrics properties.

Material/actual composition	μ_{av} ($\text{cm}^2 \text{V}^{-1} \text{s}^{-1}$)	κ ($\text{W m}^{-1} \text{K}^{-1}$)	κ_L ($\text{W m}^{-1} \text{K}^{-1}$)	S ($\mu\text{V K}^{-1}$)	σ ($\Omega^{-1} \text{cm}^{-1}$)	zT	n or p (10^{20}cm^{-3})	E_g (eV)	μ_{HI} ($\text{cm}^2 \text{V}^{-1} \text{s}^{-1}$)	m_s^* (m_e)	ε_r or ε (ε_0)	References
$\text{K}_{0.09}\pm 0.01 \text{Co}_4\text{Sb}_{12}$ (300 K)	339.5	7.0	6.6	-212	650	0.1	—	—	—	—	—	[128]
$\text{K}_{0.09}\pm 0.01 \text{Co}_4\text{Sb}_{12}$ (800 K)	39.4	4.4	3.8	-193	410	0.3	—	—	—	—	—	[128]
$\text{K}_{0.22}\pm 0.01 \text{Co}_4\text{Sb}_{12}$ (300 K)	286.9	6.7	5.7	-120	1640	0.1	—	—	—	—	—	[128]
$\text{K}_{0.22}\pm 0.01 \text{Co}_4\text{Sb}_{12}$ (800 K)	53.7	4.3	3.3	-180	650	0.4	—	—	—	—	—	[128]
$\text{K}_{0.38}\pm 0.02 \text{Co}_4\text{Sb}_{12}$ (300 K)	430.9	6.3	4.7	-114	2660	0.2	—	—	—	—	—	[128]
$\text{K}_{0.38}\pm 0.02 \text{Co}_4\text{Sb}_{12}$ (800 K)	125.8	3.9	2.0	-199	1220	1.0	—	—	—	—	—	[128]
$\text{K}_{0.45}\pm 0.02 \text{Co}_4\text{Sb}_{12}$ (300 K)	398.2	6.2	4.5	-106	2730	0.2	—	—	—	—	—	[128]
$\text{K}_{0.45}\pm 0.02 \text{Co}_4\text{Sb}_{12}$ (800 K)	113.7	4.1	1.9	-181	1360	0.9	—	—	—	—	—	[128]
CoSb_3 (300 K)	164.3	8.5	8.1	145	690	0.1	—	—	—	—	—	[129]
CoSb_3 (600 K, peak)	51.2	3.9	3.5	197	330	0.2	—	—	—	—	—	[129]
CoSb_3 (850 K)	2.2	3.8	3.3	28	310	0.2	—	—	—	—	—	[129]
$\text{Na}_{0.13} \text{Co}_4\text{Sb}_{12}$ (300 K)	390.8	6.9	6.4	-200	860	0.2	0.8	—	69.7	2.4	—	[129]
$\text{Na}_{0.13} \text{Co}_4\text{Sb}_{12}$ (700 K, peak)	103.6	3.8	3.2	-259	410	0.5	0.8	—	33.2	1.7	—	[129]
$\text{Na}_{0.13} \text{Co}_4\text{Sb}_{12}$ (850 K)	37.2	3.3	2.6	-200	390	0.4	0.8	—	31.6	0.9	—	[129]
$\text{Na}_{0.23} \text{Co}_4\text{Sb}_{12}$ (300 K)	401.9	6.8	6.1	-169	1270	0.2	1.4	—	55.8	2.8	—	[129]
$\text{Na}_{0.23} \text{Co}_4\text{Sb}_{12}$ (700 K, peak)	119.5	3.7	2.8	-237	610	0.7	1.4	—	26.8	2.1	—	[129]
$\text{Na}_{0.23} \text{Co}_4\text{Sb}_{12}$ (850 K)	53.4	3.7	2.7	-200	560	0.5	1.4	—	24.6	1.3	—	[129]
$\text{Na}_{0.36} \text{Co}_4\text{Sb}_{12}$ (300 K)	415.9	6.1	4.7	-117	2470	0.2	4.0	—	38.7	3.3	—	[129]
$\text{Na}_{0.36} \text{Co}_4\text{Sb}_{12}$ (850 K)	99.2	3.8	1.8	-190	1170	1.0	4.0	—	18.4	2.4	—	[129]
$\text{Na}_{0.48} \text{Co}_4\text{Sb}_{12}$ (300 K)	431.6	5.4	3.8	-111	2770	0.2	5.9	—	29.5	4.0	—	[129]
$\text{Na}_{0.48} \text{Co}_4\text{Sb}_{12}$ (850 K)	119.4	3.4	1.3	-203	1210	1.3	5.9	—	12.9	1.4	—	[129]
$\text{Ba}_{0.07} \text{Co}_4\text{Sb}_{11.88}$ (300 K)	228.5	6.4	5.8	-139	1032	0.1	—	—	—	—	—	[130]
$\text{Ba}_{0.07} \text{Co}_4\text{Sb}_{11.88}$ (850 K)	49.2	4.4	3.5	-192	567	0.4	—	—	—	—	—	[130]
$\text{Ba}_{0.16} \text{Co}_4\text{Sb}_{11.85}$ (300 K)	434.6	5.9	4.6	-132	2138	0.2	—	—	—	—	—	[130]
$\text{Ba}_{0.16} \text{Co}_4\text{Sb}_{11.85}$ (850 K)	95.8	4.4	2.5	-190	1130	0.8	—	—	—	—	—	[130]
$\text{Ba}_{0.24} \text{Co}_4\text{Sb}_{11.87}$ (300 K)	368.4	5.4	3.4	-88	3234	0.1	—	—	—	—	—	[130]
$\text{Ba}_{0.24} \text{Co}_4\text{Sb}_{11.87}$ (850 K)	126	4.2	1.3	-178	1709	1.1	—	—	—	—	—	[130]
$\text{Ba}_{0.38} \text{Co}_4\text{Sb}_{11.74}$ (300 K)	342.6	4.8	2.4	-70	3939	0.1	—	—	—	—	—	[130]
$\text{Ba}_{0.38} \text{Co}_4\text{Sb}_{11.74}$ (850 K)	92.6	3.9	0.5	-137	2044	0.8	—	—	—	—	—	[130]
$\text{Ba}_{0.44} \text{Co}_4\text{Sb}_{11.90}$ (300 K)	537.2	6.6	2.8	-68	6378	0.1	—	—	—	—	—	[130]
$\text{Ba}_{0.44} \text{Co}_4\text{Sb}_{11.90}$ (850 K)	115.6	5.9	0.1	-114	3404	0.6	—	—	43.4	1.9	—	[131]
$\text{Sr}_{0.12} \text{Co}_4\text{Sb}_{12.46}$ (300 K)	195.3	5.6	5.1	-137	903.6	0.1	1.3	—	30	1.0	—	[131]
$\text{Sr}_{0.12} \text{Co}_4\text{Sb}_{12.46}$ (850 K)	47.2	3.8	2.7	-180	625	0.5	1.3	—	52.9	2.1	—	[131]
$\text{Sr}_{0.17} \text{Co}_4\text{Sb}_{12.88}$ (300 K)	265.4	5.4	4.6	-129	1355	0.7	1.6	—	29.5	1.3	—	[131]
$\text{Sr}_{0.17} \text{Co}_4\text{Sb}_{12.88}$ (850 K)	67.9	3.3	2.0	-195	755	0.1	1.6	—	48.6	2.4	—	[131]
$\text{Sr}_{0.22} \text{Co}_4\text{Sb}_{12.72}$ (300 K)	309.4	5.2	4.1	-119	1791	0.2	2.3	—	26.9	1.5	—	[131]
$\text{Sr}_{0.22} \text{Co}_4\text{Sb}_{12.72}$ (850 K)	73.9	3.3	1.7	-179	990	0.8	2.3	—	44.6	3.0	—	[131]
$\text{Sr}_{0.28} \text{Co}_4\text{Sb}_{12.88}$ (300 K)	417.8	5.1	3.4	-110	2717	0.2	3.8	—	18.2	2.0	—	[131]
$\text{Sr}_{0.28} \text{Co}_4\text{Sb}_{12.88}$ (850 K)	80	3.3	1.4	-176	1110	0.9	3.8	—	39.3	2.0	—	[131]
$\text{Sr}_{0.40} \text{Co}_4\text{Sb}_{12.54}$ (300 K)	266.6	5.4	2.9	-52	4220	0.1	6.7	—	19.2	1.8	—	[131]
$\text{Sr}_{0.40} \text{Co}_4\text{Sb}_{12.54}$ (850 K)	78.5	4.1	0.6	-123	2060	0.7	6.7	—	29.6	2.2	—	[131]
$\text{Ga}_{0.03} \text{Co}_4\text{Sb}_{11.985} \text{Ga}_{0.015}$ (300 K)	137.7	3.5	3.5	-286.6	111	0.1	0.2	—	—	—	—	[132]

(Continued.)

Table 2. (Continued.)

Material/actual composition	μ_{av} ($\text{cm}^2 \text{V}^{-1} \text{s}^{-1}$)	κ ($\text{W m}^{-1} \text{K}^{-1}$)	κ_L ($\text{W m}^{-1} \text{K}^{-1}$)	S ($\mu\text{V K}^{-1}$)	σ ($\Omega^{-1} \text{cm}^{-1}$)	zT	n or p (10^{20}cm^{-3})	E_g (eV)	μ_{H} ($\text{cm}^2 \text{V}^{-1} \text{s}^{-1}$)	m_s^* (m_e)	ε_r or ε (ε_0)	References
Ga _{0.03} Co ₄ Sb _{11.985} Ga _{0.015} (600 K)	78.2	2.4	2.3	-323	117	0.3	0.2	—	31.8	1.5	—	[132]
Ga _{0.03} Co ₄ Sb _{11.985} Ga _{0.015} (650 K)	37	2.6	2.4	-268	118	0.2	0.2	—	32	0.9	—	[132]
Ga _{0.06} Co ₄ Sb _{11.97} Ga _{0.03} (300 K)	249.9	3.4	3.3	-272.6	237	0.2	0.4	—	41.1	2.7	—	[132]
Ga _{0.06} Co ₄ Sb _{11.97} Ga _{0.03} (600 K)	114.6	2.4	2.2	-315	188	0.5	0.4	—	32.6	1.9	—	[132]
Ga _{0.06} Co ₄ Sb _{11.97} Ga _{0.03} (650 K)	77.2	2.6	2.3	-289	193	0.4	0.4	—	33.5	1.4	—	[132]
Ga _{0.10} Co ₄ Sb _{11.95} Ga _{0.05} (300 K)	281.2	3.4	3.2	-228.6	444	0.2	0.4	—	63	2.1	—	[132]
Ga _{0.10} Co ₄ Sb _{11.95} Ga _{0.05} (600 K)	158	2.6	2.1	-285	367	0.7	0.4	—	52.1	1.7	—	[132]
Ga _{0.10} Co ₄ Sb _{11.95} Ga _{0.05} (650 K)	127.2	2.7	2.2	-281	349	0.7	0.4	—	49.5	1.5	—	[132]
Ga _{0.15} Co ₄ Sb _{11.925} Ga _{0.075} (300 K)	241.3	3.2	3.0	-246.4	310	0.2	0.4	—	47.2	2.4	—	[132]
Ga _{0.15} Co ₄ Sb _{11.925} Ga _{0.075} (600 K)	117.7	2.4	2.1	-291	255	0.5	0.4	—	38.8	1.7	—	[132]
Ga _{0.15} Co ₄ Sb _{11.925} Ga _{0.075} (650 K)	94.7	2.5	2.2	-285	248	0.5	0.4	—	37.8	1.5	—	[132]
In _{0.075} Co ₄ Sb _{11.975} (300 K)	307.1	3.7	3.5	-237	440	0.2	0.5	—	57.2	2.4	—	[133]
In _{0.075} Co ₄ Sb _{11.975} (600 K, peak)	157.8	2.5	2.1	-289	350	0.7	0.5	—	45.5	1.9	—	[133]
In _{0.075} Co ₄ Sb _{11.975} (800 K)	45.3	3.4	2.9	-221	340	0.4	0.5	—	44.2	0.8	—	[133]
In _{0.15} Co ₄ Sb _{11.95} (300 K)	479	3.2	2.6	-202	1030	0.4	0.9	—	69.1	2.8	—	[133]
In _{0.15} Co ₄ Sb _{11.95} (700 K, peak)	144.1	2.5	1.7	-259	570	1.1	0.9	—	38.3	1.9	—	[133]
In _{0.15} Co ₄ Sb _{11.95} (800 K)	96.2	2.8	1.9	-243	560	1.0	0.9	—	37.6	1.5	—	[133]
In _{0.225} Co ₄ Sb _{11.925} (300 K)	384.8	3.0	2.3	-173	1160	0.4	2.4	—	30.8	4.0	—	[133]
In _{0.225} Co ₄ Sb _{11.925} (700 K, peak)	139.5	2.5	1.6	-241	680	1.1	2.4	—	18.1	3.1	—	[133]
In _{0.30} Co ₄ Sb _{11.90} (300 K)	399.3	2.9	2.0	-234	640	1.0	2.4	—	17	2.6	—	[133]
In _{0.30} Co ₄ Sb _{11.90} (750 K, peak)	136.2	2.7	1.6	-162	1370	0.4	1.7	—	49.1	3.0	—	[133]
In _{0.30} Co ₄ Sb _{11.90} (800 K)	117.8	2.8	1.6	-236	780	1.2	1.7	—	28	2.3	—	[133]
p-type CoSb ₃ (300 K)-121OB22	66.2	—	—	-233	770	1.2	1.7	—	27.6	2.1	—	[133]
p-type CoSb ₃ -121OB22	0.9	—	—	280	57.6	—	—	From resistivity: 0.75 eV	2996.3	0.1	—	[134]
p-type CoSb ₃ (300 K)-10OB22	136.3	—	—	10 (890 K)	400 (930 K)	—	—	From Hall: 0.63 eV	2675.6	0.1	—	[134]
p-type CoSb ₃ -10OB22	0.9	—	—	240	188.6	—	—	—	—	—	—	[134]
p-type CoSb ₃ (300 K)-23NB12	222.9	—	—	179	626.6	—	—	—	2590.3	0.2	—	[134]
p-type CoSb ₃ (300 K)-23NB12	272.7	—	—	139	400 (930 K)	—	—	—	—	—	—	[134]
p-type CoSb ₃ -2NB13	8.5	—	—	85 (890 K)	1231.5	—	—	—	1976.2	0.2	—	[134]
p-type CoSb ₃ (300 K)-2NB9	234.8	—	—	80	2314.8	—	—	—	1529	0.2	—	[134]
p-type CoSb ₃ -2NB9	1.1	—	—	10 (890 K)	476 (850 K)	—	—	—	—	—	—	[134]
n-type CoSb ₃ (300 K)-1CS10-0.08 at.% Te	593.7	10.3	10.3	-452	70.42	0.04	0.05	0.55 eV	96.8	2.8	—	[134]
n-type CoSb ₃ -1CS10-0.08 at.% Te	4.6	—	—	46 (800 K)	358 (800 K)	—	—	—	—	—	—	[134]
n-type CoSb ₃ (300 K)-1CS11-0.15 at.% Te	606	—	—	-373	179.53	—	—	—	87.1	3.0	—	[134]
n-type CoSb ₃ -1CS11-0.15 at.% Te	4.1	—	—	44 (800 K)	334.45 (800 K)	—	—	—	—	—	—	[134]
n-type CoSb ₃ (300 K)-2CS9-0.12 at.% Te	507.7	—	—	-364	166.94	—	—	—	68.6	3.1	—	[134]
n-type CoSb ₃ -2CS9-0.12 at.% Te	4.1	—	—	38 (800 K)	393.7 (800 K)	—	—	—	—	—	—	[134]
n-type CoSb ₃ (300 K)-4OB25-0.6 at.% Pd	302.4	9.5	9.3	-280	263.16	0.1	0.4	—	37.2	3.3	—	[134]
n-type CoSb ₃ -4OB25-0.6 at.% Pd	11	—	—	-103 (780 K)	330 (800 K)	—	—	—	—	—	—	[134]
n-type CoSb ₃ (300 K)-OB26 ~1 at.% Pd	327.3	6.1	5.6	-180	909.09	0.1	1.4	—	41.1	3.0	—	[134]
n-type CoSb ₃ -OB26 ~1 at.% Pd	69.6	4.1 (770 K)	—	-207 (770 K)	581 (800 K)	—	1.4	—	—	—	—	[134]

(Continued.)

Table 2. (Continued.)

Material/actual composition	μ_{w} ($\text{cm}^2 \text{V}^{-1} \text{s}^{-1}$)	κ ($\text{W m}^{-1} \text{K}^{-1}$)	κ_{L} ($\text{W m}^{-1} \text{K}^{-1}$)	S ($\mu\text{V K}^{-1}$)	σ ($\Omega^{-1} \text{cm}^{-1}$)	zT	n or p (10^{20}cm^{-3})	E_{g} (eV)	μ_{H} ($\text{cm}^2 \text{V}^{-1} \text{s}^{-1}$)	m_s^* (m_e)	ϵ_r or ϵ (ϵ_0)	References
CoSb ₃ (300 K)	1064	8.3	8.3	-625	17	0.02	0.1	—	17.7	12.8	—	[135]
CoSb ₃ (600 K, peak)	31	4.2	4.0	205	182	0.1	0.1	—	189.3	0.2	—	[135]
CoSb ₃ (850 K)	4.1	4.7	4.2	56	284	0.02	0.1	—	295.5	0.0	—	[135]
Co ₄ Sb _{11.95} Te _{0.05} (300 K)	191.1	7.6	7.3	-194	451	0.1	0.9	—	30.9	2.6	—	[135]
Co ₄ Sb _{11.95} Te _{0.05} (600 K, peak)	159.3	4.0	3.7	-310	277	0.4	0.9	—	19	3.4	—	[135]
Co ₄ Sb _{11.95} Te _{0.05} (850 K)	26.1	5.0	4.6	-218	222	0.2	0.9	—	15.2	1.1	—	[135]
Co ₄ Sb _{11.7} Te _{0.3} (300 K)	129.1	5.1	4.8	-148	523	0.1	1.8	—	18	2.7	—	[135]
Co ₄ Sb _{11.7} Te _{0.3} (850 K)	45.1	3.9	3.3	-231	330	0.4	1.8	—	11.4	2.0	—	[135]
Co ₄ Sb _{11.5} Te _{0.5} (300 K)	182.5	3.9	3.3	-123	1004	0.1	5.7	—	11	4.5	—	[135]
Co ₄ Sb _{11.5} Te _{0.5} (850 K)	62.7	3.1	2.0	-200	658	0.7	5.7	—	7.2	3.3	—	[135]
Co _{0.98} Ni _{0.02} Sb ₃ (300 K)	184.8	—	—	-243	247	—	0.7	—	22	3.3	—	[136]
Co _{0.98} Ni _{0.02} Sb ₃ (800 K)	39.2	—	—	-203	363	—	0.7	—	32.4	0.9	—	[136]
Co _{0.97} Ni _{0.03} Sb ₃ (300 K)	176	—	—	-207	357	—	1.5	—	14.9	4.0	—	[136]
Co _{0.97} Ni _{0.03} Sb ₃ (800 K)	58.9	—	—	-217	463	—	1.5	—	19.3	1.6	—	[136]
Co _{0.955} Ni _{0.045} Sb ₃ (300 K)	122.6	—	—	-144	521	—	2.5	—	13	3.2	—	[136]
Co _{0.955} Ni _{0.045} Sb ₃ (800 K)	81.6	—	—	-225	585	—	2.5	—	14.6	2.5	—	[136]
Co _{0.94} Ni _{0.06} Sb ₃ (300 K)	137.5	—	—	-133	668	—	3.4	—	12.3	3.5	—	[136]
Co _{0.94} Ni _{0.06} Sb ₃ (800 K)	85.6	—	—	-210 (700 K)	730	—	3.4	—	13.4	—	—	[136]
Co _{0.925} Ni _{0.075} Sb ₃ (300 K)	135.8	—	—	-113	849	—	4.4	—	12	3.4	—	[136]
Co _{0.925} Ni _{0.075} Sb ₃ (800 K)	64.7	—	—	-180	783	—	4.4	—	11.1	2.4	—	[136]
Co _{0.91} Ni _{0.09} Sb ₃ (300 K)	135.6	—	—	-101	994	—	5.5	—	11.3	3.5	—	[136]
Co _{0.91} Ni _{0.09} Sb ₃ (800 K)	82.7	—	—	-180 (700 K)	1000	—	5.5	—	11.3	—	—	[136]
Co _{0.88} Ni _{0.12} Sb ₃ (300 K)	129.4	—	—	-88	1136	—	12.0	—	5.9	5.0	—	[136]
Co _{0.88} Ni _{0.12} Sb ₃ (800 K)	78.9	—	—	-167	1111	—	12.0	—	5.8	4.2	—	[136]
Co _{0.85} Ni _{0.15} Sb ₃ (300 K)	126.3	—	—	-74	1364	—	20.9	—	4.1	6.0	—	[136]
Co _{0.85} Ni _{0.15} Sb ₃ (800 K)	75.3	—	—	-151	1282	—	20.9	—	3.8	5.3	—	[136]
Yb _{0.066} Co ₄ Sb ₁₂ (300 K)	185.3	5.1	4.8	-186	480	0.1	—	—	—	—	—	[137]
Yb _{0.066} Co ₄ Sb ₁₂	148.1	—	—	-259 (600 K)	465 (700 K)	0.43 (600 K)	—	—	—	—	—	[137]
Yb _{0.19} Co ₄ Sb ₁₂ (300 K)	372.1	4.1	2.9	-141	1640	0.3	—	—	—	—	—	[137]
Yb _{0.19} Co ₄ Sb ₁₂ (640 K)	158	—	—	-216 (640 K)	900 (640 K)	1.2	—	—	—	—	—	[137]
Yb _{0.3} Co ₄ Sb ₁₂ (300 K)	434.5	3.0	1.9	-138	1986	0.4	2.8	—	44.6	3.2	—	[138]
Yb _{0.3} Co ₄ Sb ₁₂ (823 K)	109.7	3.3	1.7	-199	1110	1.1	2.8	—	24.9	2.1	—	[138]
Yb _{0.35} Co ₄ Sb ₁₂ (300 K)	422.6	2.9	1.8	-130	2131	0.4	3.3	—	40.1	3.4	—	[138]
Yb _{0.35} Co ₄ Sb ₁₂ (823 K)	118	3.3	1.4	-193	1280	1.2	3.3	—	24.1	2.2	—	[138]
Yb _{0.40} Co ₄ Sb ₁₂ (300 K)	410.6	2.9	1.6	-120	2347	0.4	3.8	—	38.5	3.3	—	[138]
Yb _{0.40} Co ₄ Sb ₁₂ (823 K)	115.7	3.5	1.4	-183	1410	1.1	3.8	—	23.1	2.2	—	[138]
Yb _{0.5} Co ₄ Sb ₁₂ (300 K)	385.5	2.9	1.6	-109	2540	0.3	5.0	—	31.8	3.5	—	[138]
Yb _{0.5} Co ₄ Sb ₁₂ (823 K)	106.4	3.7	1.4	-170	1510	1.0	5.0	—	18.9	2.4	—	[138]
Eu _{0.03} Co ₄ Sb ₁₂ (300 K)	197.1	6.2	6.0	-235	289	0.1	—	—	—	—	—	[139]
Eu _{0.03} Co ₄ Sb ₁₂ (850 K)	16.3	4.1	3.5	-146	323	0.1	—	—	—	—	—	[139]

(Continued.)

Table 2. (Continued.)

Material/actual composition	μ_w ($\text{cm}^2 \text{V}^{-1} \text{s}^{-1}$)	K ($\text{W m}^{-1} \text{K}^{-1}$)	k_L ($\text{W m}^{-1} \text{K}^{-1}$)	S ($\mu\text{V K}^{-1}$)	σ ($\Omega^{-1} \text{cm}^{-1}$)	zT	n or p (10^{20}cm^{-3})	E_g (eV)	μ_{H} ($\text{cm}^2 \text{V}^{-1} \text{s}^{-1}$)	m_s^* (m_e)	ϵ_r or ϵ (ϵ_0)	References
Eu _{0.10} Co ₄ Sb ₁₂ (300 K)	167.2	4.1	3.8	-171	516	0.1	1.4	—	23	2.8	—	[139]
Eu _{0.10} Co ₄ Sb ₁₂ (850 K)	58	3.0	2.2	-217	500	0.7	1.4	—	22.3	1.5	—	[139]
Eu _{0.19} Co ₄ Sb ₁₂ (300 K)	260.1	4.2	3.3	-118	1525	0.2	4.0	—	23.7	3.4	—	[139]
Eu _{0.19} Co ₄ Sb ₁₂ (850 K)	76.6	3.4	1.9	-191	893	0.8	4.0	—	13.9	2.4	—	[139]
Eu _{0.27} Co ₄ Sb ₁₂ (300 K)	347.7	4.2	2.3	-87	3096	0.2	10.1	—	19.1	4.4	—	[139]
Eu _{0.27} Co ₄ Sb ₁₂ (850 K)	87.4	3.6	1.2	-163	1414	0.9	10.1	—	8.7	3.4	—	[139]
Eu _{0.34} Co ₄ Sb ₁₂ (300 K)	367.8	4.5	2.0	-71	4162	0.1	16.7	—	15.6	4.9	—	[139]
Eu _{0.34} Co ₄ Sb ₁₂ (850 K)	98.8	4.1	0.8	-148	1910	0.9	16.7	—	7.1	4.2	—	[139]
Ce _{0.14} Co ₄ Sb ₁₂ (300 K)	384.5	3.7	2.4	-121	2170	0.3	3.3	—	41	3.1	—	[140]
Ce _{0.14} Co ₄ Sb ₁₂ (850 K)	121.2	3.4	1.1	-196	1333	1.3	3.3	—	25.2	2.2	—	[140]
Ce _{0.14} Co ₄ Sb ₁₂ (300 K)	386.3	3.5	2.2	-121	2180	0.3	4.8	—	28.3	3.9	—	[140]
Ce _{0.14} Co ₄ Sb ₁₂ (850 K)	115.7	3.2	0.9	-192	1333	1.3	4.8	—	17.3	2.7	—	[140]
Ce _{0.16} Co ₄ Sb ₁₂ (300 K)	334.3	3.4	2.2	-118	1960	0.2	4.2	—	29.1	3.5	—	[140]
Ce _{0.16} Co ₄ Sb ₁₂ (850 K)	101.2	3.2	1.0	-184	1280	1.2	4.2	—	19	2.3	—	[140]
Ce _{0.15} Co ₄ Sb ₁₂ (300 K)	261.7	3.3	2.4	-119	1515	0.2	4.6	—	20.5	3.7	—	[140]
Ce _{0.15} Co ₄ Sb ₁₂ (850 K)	102.2	3.0	1.1	-194	1150	1.2	4.6	—	15.6	2.7	—	[140]
Yb _{0.20} Co ₄ Sb ₁₂ (300 K)	330	3.0	2.1	-139	1490	0.3	—	—	—	—	—	[140]
Yb _{0.20} Co ₄ Sb ₁₂ (850 K)	101.4	3.0	1.3	-208	970	1.2	—	—	70	1.9	—	[140]
Dy _{0.02} Co ₄ Sb ₁₂ (300 K)	257.9	5.3	5.2	-268	258	0.1	0.2	—	61.3	1.4	—	[141]
Dy _{0.02} Co ₄ Sb ₁₂ (550 K, peak)	136.6	3.7	3.4	-303	226	0.3	0.2	—	87.7	0.2	—	[141]
Dy _{0.02} Co ₄ Sb ₁₂ (800 K)	14.9	4.4	3.9	-131	323	0.1	0.2	—	65.3	2.1	—	[141]
Tb _{0.03} Co ₄ Sb ₁₂ (300 K)	270.7	4.8	4.6	-242	366	0.1	0.4	—	53.7	1.4	—	[141]
Tb _{0.03} Co ₄ Sb ₁₂ (600 K, peak)	122.3	3.3	2.9	-280	301	0.4	0.4	—	69	0.4	—	[141]
Tb _{0.03} Co ₄ Sb ₁₂ (800 K)	30.5	4.0	3.4	-176	387	0.2	0.4	—	57	2.6	—	[141]
Gd _{0.04} Co ₄ Sb ₁₂ (300 K)	336.7	4.4	4.1	-226	548	0.2	0.6	—	45.9	1.6	—	[141]
Gd _{0.04} Co ₄ Sb ₁₂ (650 K, peak)	133.5	3.3	2.7	-265	441	0.6	0.6	—	48.1	0.9	—	[141]
Gd _{0.04} Co ₄ Sb ₁₂ (800 K)	62.2	3.8	3.1	-222	462	0.5	0.6	—	26.5	3.8	—	[141]
Nd _{0.15} Co ₄ Sb ₁₂ (300 K)	334.2	3.0	2.1	-133	1624	0.3	3.8	—	18.1	2.5	—	[141]
Nd _{0.15} Co ₄ Sb ₁₂ (800 K, peak)	109.3	2.9	1.1	-195	1110	1.2	3.8	—	41.7	3.3	—	[141]
Sm _{0.15} Co ₄ Sb ₁₂ (300 K)	421.7	3.6	2.3	-204	2100	0.3	3.1	—	22.1	2.4	—	[141]
Sm _{0.15} Co ₄ Sb ₁₂ (800 K, peak)	121.3	2.9	1.1	-204	1110	1.3	3.1	—	49.8	2.2	—	[141]
Ba _{0.03} Co ₄ Sb _{12.05} (300 K)	228.7	5.4	5.1	-220	399	0.1	0.5	—	46.2	0.5	—	[142]
Ba _{0.03} Co ₄ Sb _{12.05} (800 K)	24.5	3.8	3.3	-161	370	0.2	0.5	—	39.9	2.9	—	[142]
Ba _{0.15} Yb _{0.01} Co ₄ Sb _{12.08} (300 K)	333.4	4.3	3.0	-125	1789	0.2	2.8	—	—	—	—	[142]

(Continued.)

Table 2. (Continued.)

Material/actual composition	μ_{fw} ($\text{cm}^2 \text{V}^{-1} \text{s}^{-1}$)	κ ($\text{W m}^{-1} \text{K}^{-1}$)	κ_L ($\text{W m}^{-1} \text{K}^{-1}$)	S ($\mu\text{V K}^{-1}$)	σ ($\Omega^{-1} \text{cm}^{-1}$)	zT	n or p (10^{20}cm^{-3})	E_g (eV)	μ_{TH} ($\text{cm}^2 \text{V}^{-1} \text{s}^{-1}$)	m_s^* (m_e)	ϵ_r or ϵ (ϵ_0)	References
Ba _{0.15} Yb _{0.01} Co ₄ Sb _{12.08} (800 K)	92.9	3.6	2.0	-190	1000	0.8	2.8	—	22.3	2.0	—	[142]
Ba _{0.11} Yb _{0.03} Co ₄ Sb _{12.07} (300 K)	293.3	3.2	1.9	-115	1787	0.2	3.7	—	30.1	3.1	—	[142]
Ba _{0.11} Yb _{0.03} Co ₄ Sb _{12.07} (800 K)	89.9	3.1	1.3	-179	1100	0.9	3.7	—	18.6	2.2	—	[142]
Yb _{0.12} Co ₄ Sb _{12.11} (800 K)	184.3	2.7	2.2	-146	765	0.2	2.3	—	20.8	3.1	—	[142]
Yb _{0.12} Co ₄ Sb _{12.11} (300 K)	89.5	2.7	1.6	-220	680	1.0	2.3	—	18.5	2.2	—	[142]
Ba _{0.05} Yb _{0.09} Co ₄ Sb _{12.13} (300 K)	313	2.8	2.0	-158	1126	0.3	2.9	—	24.2	4.0	—	[142]
Ba _{0.05} Yb _{0.09} Co ₄ Sb _{12.13} (800 K)	119.4	2.6	1.4	-233	780	1.3	2.9	—	16.8	2.9	—	[142]
Ba _{0.08} Yb _{0.09} Co ₄ Sb _{12.12} (300 K)	390.2	2.5	1.0	-126	2068	0.4	3.2	—	40.3	3.2	—	[142]
Ba _{0.08} Yb _{0.09} Co ₄ Sb _{12.12} (800 K)	107.7	2.5	0.6	-190	1160	1.4	3.2	—	22.6	2.2	—	[142]
Ba _{0.11} Yb _{0.08} Co ₄ Sb _{12.08} (300 K)	312.5	2.4	0.9	-107	2114	0.3	4.4	—	30	3.2	—	[142]
Ba _{0.11} Yb _{0.08} Co ₄ Sb _{12.08} (800 K)	89.4	2.3	0.5	-177	1120	1.2	4.4	—	15.9	2.4	—	[142]
Ba _{0.25} Co ₄ Sb _{11.91} (300 K)	312.4	5.6	4.9	-145	1312	0.2	2.0	—	40.3	2.8	—	[143]
Ba _{0.25} Co ₄ Sb _{11.91} (850 K)	67.3	4.5	3.2	-192	775	0.5	2.0	—	23.8	1.5	—	[143]
Ba _{0.21} In _{0.04} Co ₄ Sb _{11.93} (300 K)	408.2	3.4	2.5	-160	1434	0.3	1.7	—	51.7	2.9	—	[143]
Ba _{0.21} In _{0.04} Co ₄ Sb _{11.93} (850 K)	83.8	2.9	1.6	-209	792	1.0	1.7	—	28.6	1.6	—	[143]
Ba _{0.19} In _{0.07} Co ₄ Sb _{11.85} (300 K)	414.2	3.0	2.0	-151	1619	0.4	1.8	—	57.1	2.7	—	[143]
Ba _{0.19} In _{0.07} Co ₄ Sb _{11.85} (850 K)	88.1	2.8	1.2	-199	935	1.1	1.8	—	33	1.5	—	[143]
Ba _{0.16} In _{0.12} Co ₄ Sb _{11.85} (300 K)	400	2.8	1.8	-143	1721	0.4	2.2	—	50	2.9	—	[143]
Ba _{0.16} In _{0.12} Co ₄ Sb _{11.85} (850 K)	86.5	2.6	1.0	-194	973	1.2	2.2	—	28.2	1.6	—	[143]
Ba _{0.15} In _{0.16} Co ₄ Sb _{11.83} (300 K)	405	2.7	1.6	-139	1829	0.4	2.7	—	42.3	3.2	—	[143]
Ba _{0.15} In _{0.16} Co ₄ Sb _{11.83} (850 K)	94.2	2.5	0.9	-200	989	1.3	2.7	—	22.9	2.0	—	[143]
Ba _{0.15} In _{0.20} Co ₄ Sb _{11.84} (300 K)	405.7	2.8	1.8	-140	1810	0.4	2.9	—	39.6	3.4	—	[143]
Ba _{0.15} In _{0.20} Co ₄ Sb _{11.84} (850 K)	90.9	2.8	1.1	-198	977	1.2	2.9	—	21.4	2.0	—	[143]
Ba _{0.14} In _{0.23} Co ₄ Sb _{11.84} (300 K)	376.1	2.6	1.5	-128	1944	0.4	4.8	—	25.2	4.2	—	[143]
Ba _{0.14} In _{0.23} Co ₄ Sb _{11.84} (850 K)	95	2.6	0.7	-190	1120	1.3	4.8	—	14.5	2.7	—	[143]
Ba _{0.06} La _{0.05} Yb _{0.06} Co ₄ Sb ₁₂ (300 K)	400.8	3.0	1.9	-138	1832	0.4	2.4	—	47.8	2.9	—	[144]
Ba _{0.06} La _{0.05} Yb _{0.06} Co ₄ Sb ₁₂ (850 K)	113.2	2.9	1.1	-211	1046	1.4	2.4	—	27.3	2.0	—	[144]
Ba _{0.08} La _{0.05} Yb _{0.08} Co ₄ Sb ₁₂ (300 K)	452.5	2.7	1.3	-126	2398	0.4	3.7	—	40.9	3.5	—	[144]
Ba _{0.08} La _{0.05} Yb _{0.08} Co ₄ Sb ₁₂ (850 K)	125.1	2.6	0.4	-198	1344	1.7	3.7	—	22.9	2.4	—	[144]
Ba _{0.10} La _{0.05} Yb _{0.10} Co ₄ Sb ₁₂ (300 K)	443.5	3.1	1.3	-107	3000	0.3	5.0	—	37.8	3.4	—	[144]
Ba _{0.10} La _{0.05} Yb _{0.10} Co ₄ Sb ₁₂ (850 K)	130.5	3.0	0.3	-185	1631	1.6	5.0	—	20.6	2.6	—	[144]
Ba _{0.10} La _{0.05} Yb _{0.15} Co ₄ Sb ₁₂ (300 K)	434.3	3.0	1.2	-104	3058	0.3	5.5	—	34.6	3.6	—	[144]
Ba _{0.10} La _{0.05} Yb _{0.15} Co ₄ Sb ₁₂ (850 K)	120.7	3.2	0.3	-174	1715	1.4	5.5	—	19.4	2.5	—	[144]
Ba _{0.10} La _{0.05} Yb _{0.20} Co ₄ Sb ₁₂ (300 K)	411.6	3.0	1.0	-93	3367	0.3	7.6	—	27.5	3.9	—	[144]
Ba _{0.10} La _{0.05} Yb _{0.20} Co ₄ Sb ₁₂ (850 K)	121.3	3.4	0.1	-164	1938	1.3	7.6	—	15.8	2.9	—	[144]
Co ₄ Sb _{11.46} Te _{0.43} (300 K)	293.9	4.9	3.9	-120	1680	0.2	5.6	—	18.5	4.3	—	[145]
Co ₄ Sb _{11.46} Te _{0.43} (850 K)	102.6	3.7	2.0	-203	1040	1.0	5.6	—	11.5	3.3	—	[145]

(Continued.)

Table 2. (Continued.)

Material/actual composition	μ_{av} ($\text{cm}^2 \text{V}^{-1} \text{s}^{-1}$)	κ ($\text{W m}^{-1} \text{K}^{-1}$)	κ_L ($\text{W m}^{-1} \text{K}^{-1}$)	S ($\mu\text{V K}^{-1}$)	σ ($\Omega^{-1} \text{cm}^{-1}$)	zT	n or p (10^{20}cm^{-3})	E_g (eV)	μ_{H} ($\text{cm}^2 \text{V}^{-1} \text{s}^{-1}$)	m_n^* (m_e)	ϵ_r or ϵ (ϵ_0)	References
$\text{S}_{0.26} \text{Co}_4 \text{Sb}_{11.11} \text{Te}_{0.73}$ (300 K)	239.9	2.2	1.5	-137	1110	0.3	3.1	—	22.1	3.5	—	[145]
$\text{S}_{0.26} \text{Co}_4 \text{Sb}_{11.11} \text{Te}_{0.73}$ (850 K)	98.5	2.2	0.9	-221	810	1.5	3.1	—	16.3	2.6	—	[145]
$\text{S}_{0.17} \text{Co}_4 \text{Sb}_{11.31} \text{Te}_{0.53}$ (300 K)	243.4	3.0	2.4	-142	1060	0.2	3.2	—	20.4	3.7	—	[145]
$\text{S}_{0.17} \text{Co}_4 \text{Sb}_{11.31} \text{Te}_{0.53}$ (850 K)	91.3	2.5	1.3	-220	760	1.2	3.2	—	14.7	2.6	—	[145]
$\text{Br}_{0.16} \text{Co}_4 \text{Sb}_{11.34} \text{Te}_{0.52}$ (300 K)	288.2	4.2	3.4	-136	1350	0.2	3.7	—	22.5	3.8	—	[145]
$\text{Br}_{0.16} \text{Co}_4 \text{Sb}_{11.34} \text{Te}_{0.52}$ (850 K)	94	3.2	1.6	-207	910	1.1	3.7	—	15.2	2.6	—	[145]
$\text{S}_{0.18} \text{Co}_3.4 \text{Ni}_{0.58} \text{Sb}_{11.94}$ (300 K)	126.6	2.9	2.2	-90	1080	0.1	16.0	—	4.2	6.2	—	[145]
$\text{S}_{0.18} \text{Co}_3.4 \text{Ni}_{0.58} \text{Sb}_{11.94}$ (850 K)	67.3	3.4	1.7	-171	990	0.7	16.0	—	3.8	5.0	—	[145]
$\text{Se}_{0.03} \text{Co}_4 \text{Sb}_{11.94} \text{Se}_{0.06}$ (300 K)	305.5	5.3	5.2	-361	104	0.1	0.3	0.3	24.7	4.4	—	[146]
$\text{Se}_{0.03} \text{Co}_4 \text{Sb}_{11.94} \text{Se}_{0.06}$ (600 K, peak)	100.2	3.4	3.2	-334	132	0.3	0.3	—	31.3	1.8	—	[146]
$\text{Se}_{0.03} \text{Co}_4 \text{Sb}_{11.94} \text{Se}_{0.06}$ (800 K)	12.8	4.1	3.7	-152	215	0.1	0.3	—	51	0.3	—	[146]
$\text{Se}_{0.05} \text{Co}_4 \text{Sb}_{11.9} \text{Se}_{0.1}$ (300 K)	222.1	4.1	4.1	-354	82	0.1	0.4	0.4	14.1	5.1	—	[146]
$\text{Se}_{0.05} \text{Co}_4 \text{Sb}_{11.9} \text{Se}_{0.1}$ (600 K, peak)	115.9	2.9	2.8	-354	121	0.3	0.4	—	20.9	2.6	—	[146]
$\text{Se}_{0.05} \text{Co}_4 \text{Sb}_{11.9} \text{Se}_{0.1}$ (800 K)	16.5	3.5	3.1	-172	219	0.2	0.4	—	37.8	4.7	—	[146]
$\text{Se}_{0.1} \text{Co}_4 \text{Sb}_{11.8} \text{Se}_{0.2}$ (300 K)	128.7	3.3	3.2	-327	65	0.1	0.4	0.4	9.2	4.7	—	[146]
$\text{Se}_{0.1} \text{Co}_4 \text{Sb}_{11.8} \text{Se}_{0.2}$ (600 K, peak)	68	2.4	2.3	-328	96	0.3	0.4	—	13.6	2.4	—	[146]
$\text{Se}_{0.1} \text{Co}_4 \text{Sb}_{11.8} \text{Se}_{0.2}$ (800 K)	15.8	3.0	2.7	-175	202	0.2	0.4	—	28.7	0.5	—	[146]
$\text{Se}_{0.15} \text{Co}_4 \text{Sb}_{11.7} \text{Se}_{0.3}$ (300 K)	111.5	2.5	2.5	-300	77	0.1	0.7	0.7	7.1	5.1	—	[146]
$\text{Se}_{0.15} \text{Co}_4 \text{Sb}_{11.7} \text{Se}_{0.3}$ (600 K, peak)	82.1	2.0	1.9	-339	102	0.4	0.7	—	9.4	3.5	—	[146]
$\text{Se}_{0.15} \text{Co}_4 \text{Sb}_{11.7} \text{Se}_{0.3}$ (800 K)	24.9	2.6	2.2	-214	203	0.3	0.7	—	18.8	0.9	—	[146]
$\text{Se}_{0.2} \text{Co}_4 \text{Sb}_{11.6} \text{Se}_{0.4}$ (300 K)	87.7	2.2	2.1	-262	94	0.1	1.2	0.4	4.8	5.5	—	[146]
$\text{Se}_{0.2} \text{Co}_4 \text{Sb}_{11.6} \text{Se}_{0.4}$ (600 K, peak)	77.1	1.9	1.8	-324	114	0.4	1.2	—	5.8	4.6	—	[146]
$\text{Se}_{0.2} \text{Co}_4 \text{Sb}_{11.6} \text{Se}_{0.4}$ (800 K)	27.6	2.6	2.2	-218	215	0.3	1.2	—	11	1.4	—	[146]
$\text{Se}_{0.3} \text{Co}_4 \text{Sb}_{11.4} \text{Se}_{0.6}$ (300 K)	66.6	2.2	2.1	-213	126	0.1	1.6	0.3	4.8	4.5	—	[146]
$\text{Se}_{0.3} \text{Co}_4 \text{Sb}_{11.4} \text{Se}_{0.6}$ (750 K, peak)	36.1	2.3	1.9	-233	214	0.4	1.6	—	8.2	2.1	—	[146]
$\text{Se}_{0.3} \text{Co}_4 \text{Sb}_{11.4} \text{Se}_{0.6}$ (800 K)	30.7	2.5	2.1	-212	256	0.4	1.6	—	9.8	1.7	—	[146]
$\text{Pd}_{0.20(\pm 0.03)} \text{Co}_3.80 \text{Sb}_{12.01(\pm 0.07)}$ (300 K)	435.2	5.6	4.9	-177	1252	0.2	2.1	0.3	38.1	3.8	—	[147]
$\text{Pd}_{0.20(\pm 0.03)} \text{Co}_3.80 \text{Sb}_{12.01(\pm 0.07)}$ (700 K)	126.1	4.2	3.0	-217	812	0.6	2.1	—	24.7	2.3	—	[147]
$\text{Pd}_{0.20(\pm 0.03)} \text{Co}_3.80 \text{Sb}_{12.01(\pm 0.07)}$ (850 K)	77	4.6	3.3	-203	781	0.6	2.1	—	23.8	1.7	—	[147]
$\text{S}_{0.02(\pm 0.01)} \text{Pd}_{0.20(\pm 0.02)} \text{Co}_3.80 \text{Sb}_{12.06(\pm 0.07)}$ (300 K)	423.9	4.1	3.4	-186	1098	0.3	1.6	0.3	43.4	3.5	—	[147]
$\text{S}_{0.02(\pm 0.01)} \text{Pd}_{0.20(\pm 0.02)} \text{Co}_3.80 \text{Sb}_{12.06(\pm 0.07)}$ (700 K)	133.9	3.5	2.5	-233	716	0.8	1.6	—	28.3	2.2	—	[147]
$\text{S}_{0.02(\pm 0.01)} \text{Pd}_{0.20(\pm 0.02)} \text{Co}_3.80 \text{Sb}_{12.06(\pm 0.07)}$ (850 K)	78.9	4.0	2.8	-189	704	0.7	1.6	—	27.8	1.6	—	[147]
$\text{S}_{0.04(\pm 0.01)} \text{Pd}_{0.20(\pm 0.01)} \text{Co}_3.80 \text{Sb}_{11.99(\pm 0.08)}$ (300 K)	341	3.7	3.2	-189	853	0.3	1.4	0.3	39.2	3.2	—	[147]
$\text{S}_{0.04(\pm 0.01)} \text{Pd}_{0.20(\pm 0.01)} \text{Co}_3.80 \text{Sb}_{11.99(\pm 0.08)}$ (700 K)	123.2	3.3	2.4	-244	580	0.7	1.4	—	26.6	2.2	—	[147]
$\text{S}_{0.04(\pm 0.01)} \text{Pd}_{0.20(\pm 0.01)} \text{Co}_3.80 \text{Sb}_{11.99(\pm 0.08)}$ (850 K)	67.6	3.8	2.8	-216	589	0.6	1.4	—	27	1.4	—	[147]
$\text{S}_{0.08(\pm 0.01)} \text{Pd}_{0.20(\pm 0.02)} \text{Co}_3.80 \text{Sb}_{12.04(\pm 0.11)}$ (300 K)	310.3	3.3	2.9	-212	594	0.2	1.0	0.3	36.4	3.3	—	[147]

(Continued.)

Table 2. (Continued.)

Material/actual composition	μ_w ($\text{cm}^2 \text{V}^{-1} \text{s}^{-1}$)	κ ($\text{W m}^{-1} \text{K}^{-1}$)	κ_L ($\text{W m}^{-1} \text{K}^{-1}$)	S ($\mu\text{V K}^{-1}$)	σ ($\Omega^{-1} \text{cm}^{-1}$)	zT	n or p (10^{20}cm^{-3})	E_g (eV)	μ_H ($\text{cm}^2 \text{V}^{-1} \text{s}^{-1}$)	m_s^* (m_e)	ϵ_r or ϵ (ϵ_0)	References
$\text{S}_{0.08}(\pm 0.01)\text{Pd}_{0.20}(\pm 0.02)\text{Co}_{3.80}\text{Sb}_{12.04}(\pm 0.11)$ (600 K)	144.8	2.9	2.4	-262	439	0.6	1.0	—	26.9	2.5	—	[147]
$\text{S}_{0.08}(\pm 0.01)\text{Pd}_{0.20}(\pm 0.02)\text{Co}_{3.80}\text{Sb}_{12.04}(\pm 0.11)$ (850 K)	52.7	3.6	2.8	-213	476	0.5	1.0	—	29.1	1.2	—	[147]
$\text{S}_{0.05}(\pm 0.01)\text{Pd}_{0.15}(\pm 0.01)\text{Co}_{3.85}\text{Sb}_{12.03}(\pm 0.14)$ (300 K)	356.4	3.7	3.4	-226	580	0.2	0.8	0.3	45.8	3.1	—	[147]
$\text{S}_{0.05}(\pm 0.01)\text{Pd}_{0.15}(\pm 0.01)\text{Co}_{3.85}\text{Sb}_{12.03}(\pm 0.14)$ (600 K)	162.5	3.1	2.6	-276	419	0.6	0.8	—	33.1	2.3	—	[147]
$\text{S}_{0.05}(\pm 0.01)\text{Pd}_{0.15}(\pm 0.01)\text{Co}_{3.85}\text{Sb}_{12.03}(\pm 0.14)$ (850 K)	44.5	3.9	3.1	-202	456	0.4	0.8	—	36	0.9	—	[147]
$\text{S}_{0.04}(\pm 0.01)\text{Pd}_{0.21}(\pm 0.02)\text{Co}_{3.75}\text{Sb}_{11.92}(\pm 0.09)$ (300 K)	405.3	3.4	2.8	-192	979	0.3	2.1	0.3	29.5	4.4	—	[147]
$\text{S}_{0.04}(\pm 0.01)\text{Pd}_{0.21}(\pm 0.02)\text{Co}_{3.75}\text{Sb}_{11.92}(\pm 0.09)$ (700 K)	139.5	3.1	2.3	-244	657	0.9	2.1	—	19.8	3.4	—	[147]
$\text{S}_{0.04}(\pm 0.01)\text{Pd}_{0.21}(\pm 0.02)\text{Co}_{3.75}\text{Sb}_{11.92}(\pm 0.09)$ (850 K)	76.1	3.7	2.6	-216	663	0.7	2.1	—	20	1.9	—	[147]
$\text{CeFe}_4\text{As}_{12}$	—	—	—	—	—	—	—	0.2	—	—	34.4 (static)	[159]
$\text{CeFe}_4\text{Sb}_{12}$	—	—	—	—	—	—	—	0.1	—	—	39.8 (static)	[159]
CoSb_3	—	—	—	—	—	—	—	—	—	—	$\epsilon_\infty = 31.67$	[160]
$\text{TiFeCo}_3\text{Sb}_{12}$	—	—	—	—	—	—	—	—	—	—	$\epsilon_\infty = 38.57$	[160]
CoSb_3	—	—	—	—	—	—	—	—	—	—	$\epsilon_\infty = 25.6$ (130 K), $\epsilon_\infty = 24.3$ (623 K)	[161]
$\text{UFe}_4\text{P}_{12}$	—	—	—	—	—	—	—	—	—	—	$\epsilon_\infty = 17$	[162]
$\text{CeFe}_4\text{P}_{12}$	—	—	—	—	—	—	—	—	—	—	$\epsilon_\infty = 31$	[162]
$\text{LaFe}_3\text{CoSb}_{12}$ (300 K)	87.6	1.6	1.3	103	625	0.1	—	—	—	—	—	[148]
$\text{LaFe}_3\text{CoSb}_{12}$	55.3	1.6 (740 K)	1.0 (740 K)	203 (700 K)	455 (700 K)	0.9 (740 K)	—	—	—	—	—	[148]
$\text{CeFe}_3\text{CoSb}_{12}$ (300 K)	74.9	—	—	87	667	—	—	—	—	—	—	[148]
$\text{CeFe}_3\text{CoSb}_{12}$	37.6	—	—	150 (680 K)	508 (680 K)	0.7 (800 K)	—	—	—	—	—	[148]
$\text{CeFe}_{2.5}\text{Co}_{1.5}\text{Sb}_{12}$ (300 K)	51.8	—	—	105	360	—	—	0.43	—	—	—	[148]
$\text{CeFe}_{2.5}\text{Co}_{1.5}\text{Sb}_{12}$ (680 K)	25.7	—	—	161	304	—	—	—	—	—	—	[148]
$\text{La}_{0.89}\text{Fe}_4\text{Sb}_{12.02}$ (300 K)	241.3	3.1	1.6	78.3	2440	0.2	13.8	—	11	4.8	—	[151]
$\text{La}_{0.89}\text{Fe}_4\text{Sb}_{12.02}$ (800 K)	81.3	3.4	1.1	150	1400	0.8	13.8	—	6.3	4.0	—	[151]
$\text{Ce}_{0.91}\text{Fe}_4\text{Sb}_{11.97}$ (300 K)	224.2	2.6	1.3	79.4	2230	0.2	38.6	—	3.6	9.7	—	[151]
$\text{Ce}_{0.91}\text{Fe}_4\text{Sb}_{11.97}$ (800 K)	86.8	3.1	0.8	152	1460	0.9	38.6	—	2.4	8.0	—	[151]
$\text{Pt}_{0.90}\text{Fe}_4\text{Sb}_{12.00}$ (300 K)	248.9	2.5	1.1	81.5	2400	0.2	71.9	—	2.1	15.1	—	[151]
$\text{Pt}_{0.90}\text{Fe}_4\text{Sb}_{12.00}$ (800 K)	84.4	3.0	0.8	152	1420	0.9	71.9	—	1.2	12.2	—	[151]
$\text{Nd}_{0.85}\text{Fe}_4\text{Sb}_{12.00}$ (300 K)	253.8	2.4	1.0	83.7	2370	0.2	46.6	—	3.2	11.6	—	[151]

(Continued.)

Table 2. (Continued.)

Material/actual composition	μ_{av} ($\text{cm}^2 \text{V}^{-1} \text{s}^{-1}$)	κ ($\text{W m}^{-1} \text{K}^{-1}$)	κ_L ($\text{W m}^{-1} \text{K}^{-1}$)	S ($\mu\text{V K}^{-1}$)	σ ($\Omega^{-1} \text{cm}^{-1}$)	zT	n or p (10^{20}cm^{-3})	E_g (eV)	μ_{H1} ($\text{cm}^2 \text{V}^{-1} \text{s}^{-1}$)	m_s^* (m_e)	ε_r or ε (ε_0)	References
Nd _{0.85} Fe ₄ Sb _{12.00} (800 K)	84.6	3.0	0.7	151	1440	0.9	46.6	—	1.9	9.0	—	[151]
Eu _{0.96} Fe ₄ Sb _{11.94} (300 K)	261.7	3.6	1.8	70.8	2970	0.1	34.3	—	5.4	7.9	—	[151]
Eu _{0.96} Fe ₄ Sb _{11.94} (800 K)	79	4.0	1.0	124	1870	0.6	34.3	—	3.4	5.6	—	[151]
Yb _{0.99} Fe ₄ Sb _{12.07} (300 K)	330.3	3.2	1.2	77.9	3360	0.2	25.4	—	8.3	7.2	—	[151]
Yb _{0.94} Fe ₄ Sb _{12.07} (800 K)	93.1	4.4	0.9	123	2230	0.6	25.4	—	5.5	4.6	—	[151]
Ca _{0.98} Fe ₄ Sb _{12.08} (300 K)	290.4	3.5	1.6	73.9	3140	0.2	13.4	—	14.6	4.4	—	[151]
Ca _{0.98} Fe ₄ Sb _{12.08} (800 K)	84.3	4.2	0.9	123	2020	0.6	13.4	—	9.4	3.0	—	[151]
St _{0.94} Fe ₄ Sb _{12.08} (300 K)	303.2	4.1	2.1	72.5	3350	0.1	33.6	—	6.2	8.0	—	[151]
St _{0.94} Fe ₄ Sb _{12.08} (800 K)	86.5	4.5	1.1	122	2100	0.6	33.6	—	3.9	5.4	—	[151]
Ba _{0.92} Fe ₄ Sb _{12.04} (300 K)	265.4	4.0	2.2	69.4	3080	0.1	16.1	—	11.9	4.7	—	[151]
Ba _{0.92} Fe ₄ Sb _{12.04} (800 K)	74.8	4.4	1.2	116	1960	0.5	16.1	—	7.6	3.1	—	[151]
Ce _{0.2} FeCo ₃ Sb ₁₂ (300 K)	80.2	2.0	1.7	106	550	0.1	1.3	—	26.4	1.4	—	[152]
Ce _{0.2} FeCo ₃ Sb ₁₂ (700 K, peak)	42	2.2	1.7	193	357	0.4	1.3	—	17.1	1.4	—	[152]
Ce _{0.2} FeCo ₃ Sb ₁₂ (800 K)	31.6	2.5	1.9	182	373	0.4	1.3	—	17.9	1.1	—	[152]
Ce _{0.5} Fe ₂ Co ₂ Sb ₁₂ (300 K)	105.1	1.8	1.4	102	760	0.1	8.0	—	5.9	4.5	—	[152]
Ce _{0.5} Fe ₂ Co ₂ Sb ₁₂ (700 K, peak)	64.8	2.0	1.3	190	571	0.7	8.0	—	4.5	4.5	—	[152]
Ce _{0.5} Fe ₂ Co ₂ Sb ₁₂ (800 K)	41.9	2.3	1.4	171	563	0.6	8.0	—	4.4	3.4	—	[152]
Ce _{0.9} Fe ₃ CoSb ₁₂ (300 K)	161	1.9	1.3	112	1020	0.2	23.3	—	2.7	10.2	—	[152]
Ce _{0.9} Fe ₃ CoSb ₁₂ (700 K, peak)	81.5	2.0	0.9	184	770	0.9	23.3	—	2.1	8.8	—	[152]
Ce _{0.9} Fe ₃ CoSb ₁₂ (800 K)	64.7	2.4	1.2	185	738	0.9	23.3	—	2	7.8	—	[152]
CeFe ₄ Sb ₁₂ (300 K)	222.9	2.6	1.3	79	2230	0.2	0.2	—	—	—	—	[152]
CeFe ₄ Sb ₁₂ (775 K, peak)	86.9	3.1	0.8	147	1480	0.8	0.8	—	—	—	—	[152]
CeFe ₄ Sb ₁₂ (800 K)	81.3	3.1	0.8	146	1470	0.8	0.8	—	—	—	—	[152]
Yb _{0.3} FeCo ₃ Sb ₁₂ (300 K)	78.9	2.2	1.7	80	778	0.1	1.4	—	34.7	1.1	—	[152]
Yb _{0.3} FeCo ₃ Sb ₁₂ (700 K, peak)	52.7	2.0	1.1	164	630	0.6	1.4	—	28.1	1.1	—	[152]
Yb _{0.3} FeCo ₃ Sb ₁₂ (800 K)	44	2.4	1.3	165	634	0.6	1.4	—	28.3	1.0	—	[152]
Yb _{0.5} Fe _{1.5} Co _{2.5} Sb ₁₂ (300 K)	130.3	2.0	1.4	103	930	0.2	2.9	—	20	2.3	—	[152]
Yb _{0.5} Fe _{1.5} Co _{2.5} Sb ₁₂ (700 K, peak)	67.3	1.9	0.9	171	740	0.8	2.9	—	15.9	2.0	—	[152]
Yb _{0.5} Fe _{1.5} Co _{2.5} Sb ₁₂ (800 K)	53.3	2.3	1.1	173	700	0.7	2.9	—	15.1	1.7	—	[152]
Yb _{0.7} Fe ₂ Co ₂ Sb ₁₂ (300 K)	152.1	1.9	1.2	102	1100	0.2	7.5	—	9.2	4.3	—	[152]
Yb _{0.7} Fe ₂ Co ₂ Sb ₁₂ (700 K, peak)	73.7	2.0	0.8	166	860	0.8	7.5	—	7.2	3.5	—	[152]

(Continued.)

Table 2. (Continued.)

Material/actual composition	μ_w ($\text{cm}^2 \text{V}^{-1} \text{s}^{-1}$)	κ ($\text{W m}^{-1} \text{K}^{-1}$)	κ_L ($\text{W m}^{-1} \text{K}^{-1}$)	S ($\mu\text{V K}^{-1}$)	σ ($\Omega^{-1} \text{cm}^{-1}$)	zT	n or p (10^{20}cm^{-3})	E_g (eV)	μ_{H} ($\text{cm}^2 \text{V}^{-1} \text{s}^{-1}$)	m_s^* (m_e)	ϵ_r or ϵ (ϵ_0)	References
$\text{Yb}_{0.7}\text{Fe}_2 \text{Co}_2\text{Sb}_{12}$ (800 K)	60	2.3	1.0	168	835	0.8	7.5	—	6.9	3.1	—	[152]
$\text{Yb}_{0.9}\text{Fe}_{2.5} \text{Co}_{1.5}\text{Sb}_{12}$ (300 K)	221	2.4	1.5	107	1495	0.2	9.2	—	10.1	5.2	—	[152]
$\text{Yb}_{0.9}\text{Fe}_{2.5} \text{Co}_{1.5}\text{Sb}_{12}$ (700 K, peak)	88.3	2.5	1.0	162	1080	0.8	9.2	—	7.3	3.9	—	[152]
$\text{Yb}_{0.9}\text{Fe}_{2.5} \text{Co}_{1.5}\text{Sb}_{12}$ (800 K)	71.6	3.0	1.4	166	1020	0.8	9.2	—	6.9	3.5	—	[152]
$\text{YbFe}_3 \text{CoSb}_{12}$ (300 K)	237.5	2.5	1.4	92	1970	0.2	16.4	—	7.5	6.4	—	[152]
$\text{YbFe}_3 \text{CoSb}_{12}$ (700 K, peak)	101.2	2.7	0.8	151	1410	0.8	16.4	—	5.4	5.1	—	[152]
$\text{YbFe}_3 \text{CoSb}_{12}$ (800 K)	80.6	3.1	0.9	153	1340	0.8	16.4	—	5.1	4.6	—	[152]
$\text{YbFe}_{3.5} \text{Co}_{0.5}\text{Sb}_{12}$ (300 K)	242.4	3.1	1.6	77	2500	0.2	—	—	—	—	—	[152]
$\text{YbFe}_{3.5} \text{Co}_{0.5}\text{Sb}_{12}$ (700 K, peak)	92	3.6	1.0	121	1850	0.5	—	—	—	—	—	[152]
$\text{YbFe}_{3.5} \text{Co}_{0.5}\text{Sb}_{12}$ (800 K)	71.8	4.0	1.3	123	1720	0.5	—	—	—	—	—	[152]
$\text{BaFe}_3 \text{CoSb}_{12}$ (300 K)	220.2	3.6	2.4	85.6	2000	0.1	17.8	—	7	6.3	—	[153]
$\text{BaFe}_3 \text{CoSb}_{12}$ (800 K)	76.7	3.3	1.3	154	1260	0.7	17.8	—	4.4	4.9	—	[153]
$\text{Ce}_{0.9}\text{Fe}_3 \text{CoSb}_{12}$ (300 K)	172.5	2.0	1.4	111.5	1100	0.2	23.1	—	3	10.1	—	[153]
$\text{Ce}_{0.9}\text{Fe}_3 \text{CoSb}_{12}$ (750 K, peak)	76.4	2.2	1.0	183	810	0.9	23.1	—	2.2	8.1	—	[153]
$\text{Ce}_{0.9}\text{Fe}_3 \text{CoSb}_{12}$ (800 K)	68.3	2.4	1.2	184	788	0.9	23.1	—	2.1	7.6	—	[153]
$\text{YbFe}_3 \text{CoSb}_{12}$ (300 K)	235.5	2.5	1.3	91.4	1970	0.2	16.4	—	7.5	6.4	—	[153]
$\text{YbFe}_3 \text{CoSb}_{12}$ (700 K, peak)	99.5	2.7	0.7	149	1420	0.8	16.4	—	5.4	5.0	—	[153]
$\text{YbFe}_3 \text{CoSb}_{12}$ (800 K)	79.7	3.1	0.9	152	1340	0.8	16.4	—	5.1	4.5	—	[153]
$\text{Ba}_{0.4}\text{Ce}_{0.6}\text{Fe}_3 \text{CoSb}_{12}$ (300 K)	160.5	2.0	1.2	93.7	1300	0.2	13.9	—	5.8	5.9	—	[153]
$\text{Ba}_{0.4}\text{Ce}_{0.6}\text{Fe}_3 \text{CoSb}_{12}$ (750 K, peak)	63.9	2.2	0.8	160	888	0.8	13.9	—	4	4.7	—	[153]
$\text{Ba}_{0.4}\text{Ce}_{0.6}\text{Fe}_3 \text{CoSb}_{12}$ (800 K)	58.9	2.3	1.0	163	869	0.8	13.9	—	3.9	4.5	—	[153]
$\text{Ce}_{0.45}\text{Nd}_{0.45}\text{Fe}_3 \text{CoSb}_{12}$ (300 K)	191.7	1.8	1.1	108.6	1270	0.3	29.7	—	2.7	11.6	—	[153]
$\text{Ce}_{0.45}\text{Nd}_{0.45}\text{Fe}_3 \text{CoSb}_{12}$ (750 K, peak)	83.7	2.1	0.8	182	898	1.1	29.7	—	1.9	9.5	—	[153]
$\text{Ce}_{0.45}\text{Nd}_{0.45}\text{Fe}_3 \text{CoSb}_{12}$ (800 K)	72.2	2.3	0.8	178	894	1.0	29.7	—	1.9	8.6	—	[153]
$\text{Ce}_{0.6}\text{Yb}_{0.4}\text{Fe}_3 \text{CoSb}_{12}$ (300 K)	193.5	1.9	1.1	105.8	1330	0.2	20.8	—	4	8.9	—	[153]
$\text{Ce}_{0.6}\text{Yb}_{0.4}\text{Fe}_3 \text{CoSb}_{12}$ (750 K, peak)	79.7	2.1	0.7	173	950	1.0	20.8	—	2.9	6.9	—	[153]
$\text{Ce}_{0.6}\text{Yb}_{0.4}\text{Fe}_3 \text{CoSb}_{12}$ (800 K)	69.6	2.3	0.8	172	925	0.9	20.8	—	2.8	6.4	—	[153]
$\text{Ce}_{0.4}\text{Yb}_{0.6}\text{Fe}_3 \text{CoSb}_{12}$ (300 K)	192.3	1.8	1.0	103.1	1370	0.2	16.0	—	5.3	7.2	—	[153]
$\text{Ce}_{0.4}\text{Yb}_{0.6}\text{Fe}_3 \text{CoSb}_{12}$ (750 K, peak)	76.3	2.1	0.6	167	975	1.0	16.0	—	3.8	5.5	—	[153]
$\text{Ce}_{0.4}\text{Yb}_{0.6}\text{Fe}_3 \text{CoSb}_{12}$ (800 K)	66.3	2.3	0.8	165	956	0.9	16.0	—	3.7	5.0	—	[153]

(Continued.)

Table 2. (Continued.)

Material/actual composition	μ_{av} ($\text{cm}^2 \text{V}^{-1} \text{s}^{-1}$)	κ ($\text{W m}^{-1} \text{K}^{-1}$)	κ_L ($\text{W m}^{-1} \text{K}^{-1}$)	S ($\mu\text{V K}^{-1}$)	σ ($\Omega^{-1} \text{cm}^{-1}$)	zT	n or p (10^{20}cm^{-3})	m_s^* (m_e)	ϵ_r or ϵ (ϵ_0)	References
DD _{0.86} Fe ₄ Sb ₁₂ (300 K)	301.4	2.2	0.5	85	2762	0.3	—	—	—	[154]
DD _{0.86} Fe ₄ Sb ₁₂ (800 K)	91.3	2.9	0.6	157	1447	1.1	—	—	—	[154]
DD _{0.78} Fe _{3.2} Co _{0.8} Sb ₁₂ (300 K)	300	2.0	0.3	83	2830	0.3	2.8	1.8	—	[154]
DD _{0.78} Fe _{3.2} Co _{0.8} Sb ₁₂	97.7	3.1 (675 K)	—	152 (800 K)	1643 (800 K)	—	—	—	—	[154]
DD _{0.44} Fe _{2.1} Co _{1.9} Sb ₁₂ (300 K)	185.1	1.9	1.2	103	1321	0.2	3.4	2.6	—	[154]
DD _{0.44} Fe _{2.1} Co _{1.9} Sb ₁₂	53.6	2.8 (725 K)	—	159 (800 K)	830 (800 K)	0.4 (800 K)	—	—	—	[154]
DD _{0.25} Fe _{1.2} Co _{2.8} Sb ₁₂ (300 K)	153.2	2.7	2.0	98	1170	0.1	1.7	1.5	—	[154]
DD _{0.25} Fe _{1.2} Co _{2.8} Sb ₁₂	65.2	3.4 (775 K)	—	198 (800 K)	640 (800 K)	0.4 (800 K)	—	—	—	[154]
DD _{0.12} FeCo ₃ Sb ₁₂ (300 K)	111.7	3.5	2.7	69	1305	0.1	1.5	1.0	—	[154]
DD _{0.12} FeCo ₃ Sb ₁₂	85.1	4.4 (675 K)	—	168 (800 K)	1076 (750 K)	0.5 (800 K)	—	—	—	[154]
DD _{0.08} FeCo ₃ Sb ₁₂ (300 K)	166.6	3.4	3.3	-228	265	0.1	1.0	3.7	—	[154]
DD _{0.08} FeCo ₃ Sb ₁₂	49.3	4.88 (775 K)	—	-230 (750 K)	303 (800 K)	0.3 (800 K)	—	—	—	[154]
DD _{0.68} Fe _{3.2} Ni _{0.8} Sb ₁₂ (300 K)	304.9	2.3	1.4	132	1500	0.3	0.8	1.3	—	[154]
DD _{0.68} Fe _{3.2} Ni _{0.8} Sb ₁₂ (800 K)	104.7	2.9	2.4	211	883	1.1	0.8	2.7	—	[154]
DD _{0.76} Fe _{3.4} Ni _{0.6} Sb ₁₂ (300 K)	251.1	2.0	0.8	94	2026	0.3	1.4	1.3	—	[154]
DD _{0.76} Fe _{3.4} Ni _{0.6} Sb ₁₂ (800 K)	81.6	2.8	2.0	155	1325	0.9	1.4	2.4	—	[154]
DD _{0.40} Fe _{2.8} Ni _{1.2} Sb ₁₂ (300 K)	54.4	2.1	2.0	135	258	0.1	0.5	1.0	—	[154]
DD _{0.40} Fe _{2.8} Ni _{1.2} Sb ₁₂ (800 K)	5.3	3.4	2.8	20	957	0.01	0.5	0.1	—	[154]
DD _{0.08} Fe ₂ Ni ₂ Sb ₁₂ (300 K)	23.2	2.2	2.0	-70	267	0.02	0.7	0.6	—	[154]
DD _{0.08} Fe ₂ Ni ₂ Sb ₁₂ (800 K)	108.4	4.3	0.6	-62	6200	0.4	0.7	0.5	—	[154]
ST _{0.03} Ba _{0.03} Yb _{0.1} Co ₄ Sb ₁₂ (300 K)	357.5	2.7	1.7	-138	1634	0.4	—	—	—	[149]
ST _{0.03} Ba _{0.03} Yb _{0.1} Co ₄ Sb ₁₂ (800 K)	121	2.8	1.3	-217	952	1.3	—	—	—	[149]
ST _{0.07} Ba _{0.07} Yb _{0.07} Co ₄ Sb ₁₂ (300 K)	376.8	2.3	1.3	-140	1681	0.4	—	—	—	[149]
ST _{0.07} Ba _{0.07} Yb _{0.07} Co ₄ Sb ₁₂ (800 K)	111.1	2.4	0.9	-208	970	1.4	—	—	—	[149]
ST _{0.07} Ba _{0.07} Yb _{0.07} Co ₄ Sb ₁₂ (300 K), HPT	260.7	1.6	0.9	-140	1163	0.4	—	—	—	[149]
ST _{0.07} Ba _{0.07} Yb _{0.07} Co ₄ Sb ₁₂ (800 K), HPT	103.8	1.8	0.4	-213	855	1.8	—	—	—	[149]
DD _{0.88} Fe ₄ Sb ₁₂ (300 K)	279.8	1.9	0.4	85	2564	0.3	—	—	—	[155]
DD _{0.88} Fe ₄ Sb ₁₂ (800 K)	105.4	3.2	0.6	160	1613	1.1	—	—	—	[155]
Mm _{0.68} Fe ₄ Sb ₁₂ (300 K)	202.4	1.4	0.6	110	1316	0.3	—	—	—	[155]
Mm _{0.68} Fe ₄ Sb ₁₂ (800 K)	81	2.1	0.7	188	893	1.2	—	—	—	[155]
DD _{0.60} Fe ₃ CoSb ₁₂ (300 K)	187	1.8	1.1	106	1282	0.2	—	—	—	[155]
DD _{0.60} Fe ₃ CoSb ₁₂ (800 K)	79.4	1.9	0.5	183	927	1.3	—	—	—	[155]
DD _{0.88} Fe ₄ Sb ₁₂ (300 K)	279.8	1.9	0.4	85	2564	0.3	—	—	—	[155]

For simplicity, the carrier concentration values at high temperature are taken as the same values at room temperature to calculate the m^* in this table.

3.3. Half Heuslers

Half-Heusler thermoelectric materials

Shen Han, Chenguang Fu and Tiejun Zhu

State Key Laboratory of Silicon Materials, and School of Materials Science and Engineering, Zhejiang University, Hangzhou 310027, People's Republic of China

E-mail: zhutj@zju.edu.cn

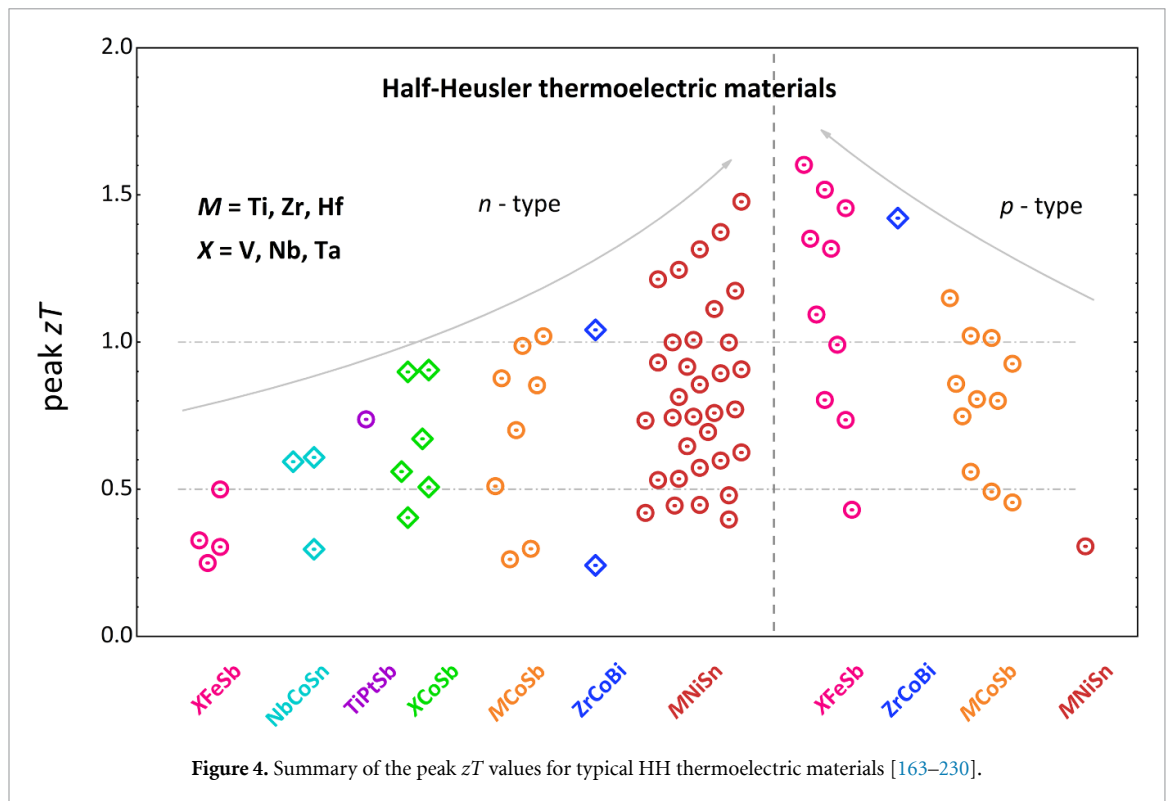
Studies of thermoelectric properties of half-Heusler (HH) compounds have been carried out since the end of the 20th century, focusing on compositions with 18 valence electrons represented by three typical systems, i.e. $MNiSn$ ($M = Ti, Zr, Hf$), $MCoSb$ and $XFeSb$ ($X = V, Nb, Ta$). In recent years, the 18-electron $NbCoSn$, $ReNiSb$ (Re is a rare earth element), and nominal 19-electron $XCoSb$ compounds have also attracted increasing attention. A summary of the peak zT values obtained for different HH compounds is shown in figure 4, and a detailed compilation of representative data are given in table 3. These advances make HH compounds promising thermoelectric candidates for power generation applications with advantages of mechanical robustness, thermal stability, and relatively low-cost constituents.

The intermetallic $MNiSn$, found to exhibit semiconducting behavior around 1988 [231], was the first HH system to seriously arouse the interest of the thermoelectric community before the end of the 20th century [232]. With the efforts in the past two decades, $MNiSn$ -based HH compounds have now been developed into the best n -type HH thermoelectric materials with peak zT above unity [164, 188, 192, 193, 233]. $MCoSb$ has attracted research attention since 2000 and rapidly developed as a representative p -type thermoelectric system with a zT of about unity [168, 214]. It is worth noting that n -type $MCoSb$ has recently been found to show a similar high zT value as its p -type counterpart [169–171], making it the first HH system with both good n -type and p -type thermoelectric performance. The studies on the thermoelectric properties of $XFeSb$ started as early as those on $MNiSn$ and $MCoSb$ [172], but it did not attract much attention at that time, owing to the poor thermoelectric properties. Since 2014, with guidance of the band engineering concept and the selection of rational dopants, the heavy-band $XFeSb$ -based HH system has been developed as high-performance p -type thermoelectric materials with a peak zT value of about 1.5 through rational compositional design and optimal doping [173–177, 179]. Very recently, prototype eight-pair HH thermoelectric modules using n -type $MNiSn$ and p -type $XFeSb$ were assembled [234, 235]; they show a maximum conversion efficiency of 10.5% and power density of 3.1 W cm^{-2} for a temperature difference of 680 K, demonstrating the encouraging prospect of HH compounds for power generation.

The nominal 19-electron HH system was usually thought to show metallic behavior and thus, it was unexpected that $NbCoSb$ exhibited a respectable zT value of 0.4 in 2015 [180]. Subsequently, with the knowledge of defect chemistry [236], $XCoSb$ was identified to be a defective HH compound with a considerable fraction of cation vacancies (up to $\sim 20\%$). Through tuning the content of cation vacancies that lead to suppressed lattice thermal conductivity and optimized electrical properties, a peak $zT \sim 0.9$ was achieved in $Nb_{1-x}CoSb$ [181], demonstrating that the nominal 19-electron HH system provides a new class of material for the exploration of high-performance thermoelectrics and the understanding of the relationship between vacancies and transport properties.

In addition, some other HH compounds have also attracted some attention, including $ZrCoBi$, which was reported to show a peak zT of ~ 1.4 for p -type and ~ 1.0 for n -type [185, 186]. The thermoelectric properties of $ReNiSb$, a family of HH compounds with rare-earth elements, were also studied [191]. Further performance improvement is expected if the optimization strategies, generally used for $MNiSn$, $MCoSb$, and $XFeSb$, are successfully applied to $ReNiSb$. Similarly, $NbCoSn$, another 18-electron system with the predicted high PF for both p -type and n -type [237], has also been investigated. A peak zT of ~ 0.6 was reported when it was doped as n -type [187, 189], whereas optimal p -type doping for $NbCoSn$ is still not successful.

Different from many other good thermoelectric materials, HH compounds are characterized by their high PF ($S^2\sigma$), which directly contributes to their high zT value. The high crystal symmetry, from their cubic structure, leads to multiple carrier pockets and high band degeneracy N_V near the band edge, such as the N_V of 8 for p -type $NbFeSb$ and $ZrCoSb$ [238, 173]. Thus, a large density of states (DOS) effective mass is obtained, resulting in a large Seebeck coefficient even at a high carrier concentration. In addition, the low deformation potential guarantees weak carrier scattering by phonons and thus the relatively high carrier mobility in the heavy-band HH system [175, 188]. Another distinct feature of the heavy-band HH system is the high optimal carrier concentration n_{opt} , defined as the carrier concentration where the peak zT occurs. In a single-band system, the n_{opt} is approximately proportional to $(m_d^*T)^{3/2}$ under the classical statistics approximation [239], where m_d^* is the DOS effective mass. For the HH system, n_{opt} increases from



$\sim 4 \times 10^{20} \text{ cm}^{-3}$ for n -type ZrNiSn, $\sim 2.6 \times 10^{21} \text{ cm}^{-3}$ for p -type NbFeSb, to $\sim 4 \times 10^{21} \text{ cm}^{-3}$ for n -type TiPtSb, whilst the m_d^* increases from $2.8 m_e$, $6.4 m_e$, to $14.5 m_e$, respectively [174, 184, 188]. In comparison, the n_{opt} of PbTe is about $3 \times 10^{19} \text{ cm}^{-3}$ [240], one or two orders of magnitude lower than that of the HH system. High n_{opt} indicates that a high level of chemical doping is required for optimizing the electrical performance, which could also bring additional point-defect scattering of phonons. Thus, the selection of a rational doping element is important for the simultaneous optimization of PF and strong suppression of lattice thermal conductivity in the heavy-band HH system [175, 179].

Knowledge of the intrinsic electronic structure of thermoelectric materials is of vital importance for the selection of optimization strategies. The bandgap E_g is considered to be the foremost parameter for a semiconductor. The calculated E_g for MNiSn, MCoSb, and XFeSb by density functional theory (DFT) is 0.4–0.5 eV, 0.95–1.13 eV, and 0.34–0.86 eV, respectively [163, 172, 173, 237, 238, 241–243]. Experimentally, polycrystalline MNiSn samples, synthesized using high-temperature techniques and probably having excess Ni-induced in-gap states, show E_g values of 0.1–0.36 eV by different experimental methods. Recently, using high-quality ZrNiSn single crystals, a combined study involving resistivity and optical measurements together with angle-resolved photoemission spectroscopy (ARPES) gave experimental E_g values of 0.5–0.66 eV [244]. These results demonstrate the effect of defects on the electronic structure and thermoelectric properties of HH compounds. Experimental studies on the interplay between defects and electronic structure for the other HH compounds are required.

Most HH compounds with high thermoelectric performance are generally heavily doped narrow-bandgap semiconductors. The dominant scattering mechanism is acoustic phonon scattering (APS) and the electrical transport properties can be explained using the SPB model. Under the assumption of SPB and APS, the weighted mobility μ_w performs as a good descriptor characterizing the electrical performance for thermoelectric materials [245]. The μ_w values of MNiSn and XFeSb are above $300 \text{ cm}^2 \text{ V}^{-1} \text{ s}^{-1}$ at room temperature and above $60 \text{ cm}^2 \text{ V}^{-1} \text{ s}^{-1}$ at temperatures higher than 900 K. In contrast, the MCoSb system shows values of $100\text{--}250 \text{ cm}^2 \text{ V}^{-1} \text{ s}^{-1}$ at room temperature and less than $60 \text{ cm}^2 \text{ V}^{-1} \text{ s}^{-1}$ at high-temperature, corresponding to the lower zT compared with that of MNiSn and XFeSb. It is worth noting that ZrCoBi and NbCoSn also have a μ_w above $300 \text{ cm}^2 \text{ V}^{-1} \text{ s}^{-1}$ at room temperature, implying their potential as good TEs.

High lattice thermal conductivity, κ_L , is the main disadvantage of HH compounds that prevents high thermoelectric figures of merit. By introducing multiple phonon scattering mechanisms through alloying, nanostructuring, the formation of nanocomposites, and phase separation, the κ_L , at the temperature where the peak zT occurs, can be largely suppressed to values of $2\text{--}3 \text{ W m}^{-1} \text{ K}^{-1}$, which, however, is still higher than its minimum value ($\sim 1 \text{ W m}^{-1} \text{ K}^{-1}$ above 300 K) estimated using the Cahill model [246]. In comparison,

the nominal 19-electron HH compounds, such as unalloyed XCoSb and TiPtSb, show significantly lower κ_L below $2 \text{ W m}^{-1} \text{ K}^{-1}$ in the high-temperature region [182–184], which can be ascribed to strong point defect scattering resulting from the existence of substantial intrinsic cation vacancies. However, the net lower carrier mobility, compared to the routine 18-electron HH systems, limits their thermoelectric performance. This highlights the dilemma in developing high-performance HH thermoelectric materials, specifically, how to maximally suppress lattice thermal conductivity while maintaining high carrier mobility [124].

In summary, the past two decades have witnessed significant development of HH thermoelectric materials with the establishment of several low-cost, high-performance material systems. Targeting the future optimization of thermoelectric performance and practical application of HH compounds, several future directions are suggested:

- (a) The interplay of point defects, electronic structures and transport properties is an appealing theme, including intrinsic defects in the 18-electron HH system and short-range order in the defective 19-electron HH system.
- (b) Further reduction in thermal conductivity, especially near room-temperature, is highly desirable, with the aim of improving the average zT .
- (c) The development of devices using the current best HH thermoelectric compounds is progressing but the related interfacial issues need to be solved. In addition, active Peltier coolers, which requires materials with high PF and high κ also brings new potential applications for HH compounds [247].
- (d) HH is a large compound family with many members; the exploration of new thermoelectric candidates in the HH system is always attractive. To aid exploration and development, guidance from accurate, rapid electronic and phonon calculations is important.

Acknowledgments

Tiejun Zhu and Chenguang Fu acknowledge the support from the National Key Research and Development Program of China (2019YFA0704902) and the National Science Fund for Distinguished Young Scholars (No. 51725102).

Table 3. Half Heusler thermoelectric properties.

Material	T (K)	μ_w ($\text{cm}^2 \text{V}^{-1} \text{s}^{-1}$)	κ_L ($\text{W m}^{-1} \text{K}^{-1}$)	S ($\mu\text{V K}^{-1}$)	σ ($\Omega^{-1} \text{cm}^{-1}$)	zT	E_g (eV) (Exp.) 0.5 (DFT) 0.66 (ARPES)	μ_0 ($\text{cm}^2 \text{V}^{-1} \text{s}^{-1}$)	m_s^* (m_e)	ϵ_r or ϵ (ϵ_0)	κ ($\text{W m}^{-1} \text{K}^{-1}$)	References
MNiSn (M = Ti, Zr, Hf) system												
ZrNiSn	309	172.7	—	−224.7	298.1	0.07	0.1–0.36 (Exp.) 0.5 (DFT) 0.66 (ARPES)	37.1	2.8	20.6–26(Cal.)	6.06	[163, 188, 237, 241, 244, 248–250]
ZrNiSn _{0.99} Sb _{0.01}	874	89.6	—	−222.6	754.4	0.60	—	—	—	—	5.22	
	309	301.4	7.35	−129.2	1604.6	0.10	—	48.1	2.8	—	7.44	
	874	122.9	4.48	−205.7	1259.1	0.77	—	—	—	—	5.45	
Hf _{0.5} Zr _{0.5} Ni _{0.88} Pd _{0.2} Sn _{0.99} Sb _{0.01}	300	300.5	—	−104.0	2115.5	0.15	—	—	—	—	4.52	[192]
	800	71.3	—	−153.2	1182.7	0.69	—	—	—	—	3.07	
Hf _{0.75} Zr _{0.25} NiSn _{0.975} Sb _{0.025}	312	316.5	—	−73.1	3663.5	0.09	—	—	—	—	7.04	[193]
	977	92.6	—	−158.3	1950.2	0.81	—	—	—	—	5.83	
Hf _{0.6} Zr _{0.4} NiSn _{0.98} Sb _{0.02}	291	301.1	—	−92.1	2377.3	0.12	—	45.0	2.8	—	5.00	[233]
	1030	75.4	—	−170.6	1485.4	1.01	—	—	—	—	4.28	
Ti _{0.5} Zr _{0.25} Hf _{0.25} NiSn _{0.998} Sb _{0.002}	373	202.6	2.88	−215.8	515.2	0.26	—	—	—	—	3.34	[164]
	824	92.1	0.76	−206.5	854.6	1.21	—	—	—	—	2.47	
MCoSb (M = Ti, Zr, Hf) system												
ZrCoSb	334	0.8	—	−121.4	5.4	—	1.06 (DFT)	—	—	17.9–19(Cal.)	16.36	[165, 238, 249–251]
	991	2.4	—	−149.1	56.7	0.02	—	—	—	—	6.56	
ZrCoSn _{0.1} Sb _{0.9}	328	241.4	—	161.2	956.0	0.08	—	10.5	9.2	—	9.87	
	956	59.2	—	257.1	382.3	0.45	—	—	—	—	5.40	
Zr _{0.5} Hf _{0.5} CoSb _{0.8} Sn _{0.2}	322	151.3	—	109.7	1100.0	0.11	—	10.9	5–9	—	4.04	[166]
	965	35.6	—	173.8	613.1	0.49	—	—	—	—	3.61	
Zr _{0.5} Hf _{0.5} CoSb _{0.8} Sn _{0.2}	301	214.1	2.85	146.3	887.6	0.17	—	—	—	—	3.40	[167]
	974	53.4	2.19	216.7	565.8	0.80	—	—	—	—	3.24	
Ti _{0.25} Hf _{0.75} CoSb _{0.85} Sn _{0.15}	391	192.4	2.98	196.1	659.2	0.29	—	4.9	—	—	3.43	[168]
	981	71.2	1.99	266.3	429.5	1.15	—	—	—	—	2.68	
Zr _{0.5} Hf _{0.5} Co _{0.9} Ni _{0.1} Sb	300	107.7	5.07	−112.7	677.6	0.05	—	6.3	6	—	5.44	[169]
	1074	58.8	2.37	−226.9	641.2	1.02	—	—	—	—	3.44	
(Zr _{0.4} Hf _{0.6}) _{0.88} Nb _{0.12} CoSb	300	184.4	3.86	−98.9	1391.4	0.08	—	9.2	6.5	—	4.68	[170]

(Continued.)

Table 3. (Continued.)

Material	T (K)	μ_{av} ($\text{cm}^2 \text{V}^{-1} \text{s}^{-1}$)	κ_L ($\text{W m}^{-1} \text{K}^{-1}$)	S ($\mu\text{V K}^{-1}$)	σ ($\Omega^{-1} \text{cm}^{-1}$)	zT	E_g (eV)	μ_0 ($\text{cm}^2 \text{V}^{-1} \text{s}^{-1}$)	m_s^* (m_e)	ϵ_r or ϵ (ϵ_0)	κ ($\text{W m}^{-1} \text{K}^{-1}$)	References
(Hf _{0.3} Zr _{0.7}) _{0.88} Nb _{0.12} CoSb	1174 301 1123	40.1 129.2 39.3	2.04 4.15 2.22	-212.7 -114.8 -228.2	588.9 794.5 451.0	0.99 0.07 0.85	—	— 6.9 —	— 6.5 —	—	3.15 4.60 3.04	[171]
XFeSb (X = V, Nb, Ta) system	300	—	—	-2.7	7.2	—	0.54 (DFT)	—	—	23(Cal.)	—	[172, 173, 242, 249, 250]
NbFeSb	300	—	—	—	—	—	—	—	—	—	—	—
V _{0.95} Ti _{0.05} FeSb	300	—	—	57.6	2125.6	—	—	—	—	—	—	—
(V _{0.6} Nb _{0.4}) _{0.8} Ti _{0.2} FeSb	300 900	267.2 64.6	3.09 2.37	143.5 214.1	1142.7 626.7	0.19 0.80	—	7.6	10	—	3.70 3.24	[173]
Nb _{0.8} Ti _{0.2} FeSb	300	431.6	4.54	71.6	4833.5	0.09	—	24.9	—	80(Exp.)	7.47	[174, 252]
Nb _{0.88} Hf _{0.12} FeSb	1100 301	71.1 723.5	2.68 4.82	204.0 93.7	1048.4 5893.6	1.09 0.19	—	32.5	6.9	—	4.55 8.31	[175]
Nb _{0.95} Ti _{0.05} FeSb	1200 304 975	79.9 1150.4 144.4	2.62 —	246.1 175.6 306.3	823.5 3427.8 542.6	1.45 0.25 0.74	—	35.8	7.5	—	4.21 13.09 6.57	[176]
(Nb _{0.6} Ta _{0.4}) _{0.8} Ti _{0.2} FeSb	300	508.3	1.76	74.7	5416.4	0.18	—	25.0	6.9	—	5.07	[177]
NbFe _{0.94} Ir _{0.06} Sb	1200 300	63.9 164.4	1.43 6.21	218.2 -76.8	910.1 1700.2	1.60 0.04	—	81.0	1.6	—	3.19 6.89	[178]
Ta _{0.74} V _{0.1} Ti _{0.16} FeSb	1101 304 969	24.0 460.8 93.8	3.46 2.33 1.56	-205.9 116.0 227.7	346.3 2832.2 868.8	0.50 0.29 1.52	—	—	—	20(Exp.)	4.11 3.93 2.91	[179]
19-electron HH materials												
NbCoSb	303 974	170.7 38.8	3.98 3.04	-59.2 -139.8	2393.7 1013.8	0.04 0.40	—	3.7	—	—	5.56 4.80	[180]
Nb _{0.8} CoSb	299	68.7	4.17	-174.2	203.3	0.04	1.0 (DFT) 0.5 (GSF)	2.9	—	—	4.26	[181, 236]
Nb _{0.83} CoSb	1123 299	21.1 155.6	1.92 4.83	-225.7 -87.4	249.4 1372.9	0.62 0.06	—	7.0	7.7	—	2.36 5.64	—
Nb _{0.8} Co _{0.92} Ni _{0.08} Sb	1123 299	36.8 118.0	1.93 3.85	-204.0 -106.3	558.8 801.0	0.90 0.07	—	—	—	—	2.93 4.31	[182]
V _{0.855} Ti _{0.1} CoSb	1123 300 972	32.5 148.2 50.0	1.69 2.20 1.73	-213.0 -57.9 -147.5	445.1 2093.7 1188.4	0.90 0.06 0.67	—	—	—	—	2.49 3.56 3.74	[183]

(Continued.)

Table 3. (Continued.)

Material	T (K)	μ_w ($\text{cm}^2 \text{V}^{-1} \text{s}^{-1}$)	κ_L ($\text{W m}^{-1} \text{K}^{-1}$)	S ($\mu\text{V K}^{-1}$)	σ ($\Omega^{-1} \text{cm}^{-1}$)	zT	E_g (eV)	μ_0 ($\text{cm}^2 \text{V}^{-1} \text{s}^{-1}$)	m_s^* (m_e)	ϵ_r or ϵ (ϵ_0)	κ ($\text{W m}^{-1} \text{K}^{-1}$)	References
Ti _{0.82} PtSb	301	131.8	2.53	-78.1	1339.0	0.08	0.33 (GSF)	2.0	14.5	—	3.34	[184]
	1072	32.2	1.55	-164.0	728.5	0.74	—	—	—	—	2.86	
Other HH materials												
ZrCoBi _{0.65} Sb _{0.15} Sn _{0.20}	303	293.1	2.18	129.9	1501.0	0.26	—	—	12	—	2.98	[185]
	973	83.2	1.59	232.2	735.8	1.42	—	—	—	—	2.73	
ZrCo _{0.9} Ni _{0.1} Bi _{0.85} Sb _{0.15}	302	147.4	3.25	-111.4	951.0	0.09	—	—	6.8	—	3.78	[186]
	972	61.7	1.86	-212.0	687.9	1.04	—	—	—	—	2.92	
NbCoSn	301	—	7.94	-65.4	—	—	1 (DFT)	—	—	22.6(Cal.)	7.95	[187, 249, 250]
	972	33.4	4.36	-284.9	160.2	0.26	—	—	—	—	4.63	
NbCoSn _{0.9} Sb _{0.1}	302	301.1	7.64	-85.6	2758.3	0.07	—	18.9	6	—	9.31	
	973	60.9	3.53	-179.8	989.8	0.61	—	—	—	—	5.15	
NbCo _{0.95} Pt _{0.05} Sn	319	226.4	4.65	-123.2	1358.7	0.13	—	14.3	6.5	—	5.45	[189]
	770	92.1	3.26	-198.7	845.6	0.59	—	—	—	—	4.34	
ErPdSb	333	119.1	—	241.2	189.7	0.07	0.28 (AF)	—	—	—	5.55	[190]
	698	45.8	—	141.6	710.8	0.16	—	—	—	—	6.37	
ErPdBi	332	126.9	—	82.8	1398.9	0.06	0.05 (AF)	—	—	—	5.30	
	495	75.3	—	71.0	1806.9	0.08	—	—	—	—	6.50	
ScNiSb	341	54.3	—	221.4	113.0	0.02	0.38 (AF) 0.21 (GSF)	30.6	1.52	—	9.74	[191]
	807	26.0	—	122.5	634.1	0.10	—	—	—	—	7.55	
DyNiSb	329	30.2	—	46.9	612.1	0.01	0.13 (AF) 0.09 (GSF)	53.5	0.56	—	3.67	
	717	35.6	—	72.5	1452.6	0.11	—	—	—	—	4.90	
ErNiSb	343	28.7	—	80.6	342.5	0.01	0.17 (AF) 0.13 (GSF)	10.9	10.9	—	4.13	
	688	47.3	—	106.7	1115.6	0.17	—	—	—	—	5.31	
TmNiSb	318	96.7	—	205.1	218.7	0.07	0.21 (AF) 0.15 (GSF)	17.1	17.1	—	3.82	
	698	55.3	—	130.0	989.0	0.26	—	—	—	—	4.53	
LuNiSb	323	59.9	—	113.3	416.2	0.03	0.19 (AF) 0.12 (GSF)	29.1	29.1	—	5.06	
	699	56.6	—	113.6	1247.8	0.18	—	—	—	—	5.88	

Notes:

AF—Arrhenius formula.

APERS—angle-resolved photoemission spectroscopy.

Cal.—calculation.

DFT—density functional theory.

Exp.—experiment.

GSF—Goldsmid-Sharp formula.

3.4. Zintl

Thermoelectric performance in Zintl phases: a bird's-eye view

A K M Ashiquzzaman Shawon and Alexandra Zevalkink

Chemical Engineering and Materials Science Department, Michigan State University, East Lansing, MI 48824, United States of America

E-mail: alexzev@msu.edu

One of the most recent additions to the thermoelectric material realm, Zintl phases are a class of intermetallic compounds following the Zintl-Klemm concept, with structures consisting of both covalent and ionic bonding. The cations (typically alkali, alkaline-earth or rare-earth metals) are treated as fully ionized, providing valence electrons to main group metalloids, which in turn form covalent bonds to achieve a closed-shell configuration. Although united by a common bonding scheme, the crystal structures of Zintl phases vary widely. Enthusiasm for Zintl thermoelectrics stems primarily from their structural complexity and diversity, with novel structures and compounds being reported regularly [253]. Further, many Zintls exhibit salt-like behavior with high melting points and brittle mechanical properties.

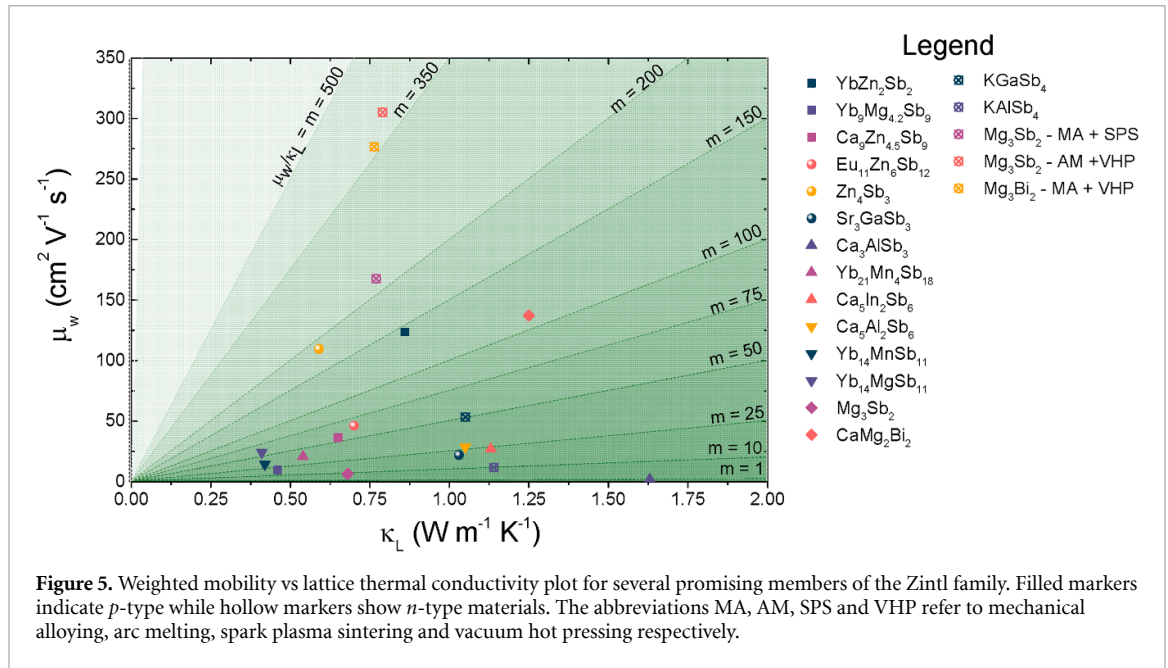
Zintl compounds are often structurally complex, which leads to very low thermal conductivities, comparable in most cases with the amorphous limit. This, along with the prospect of tuning carrier transport properties through doping, makes Zintl phases ideal thermoelectric materials. Of the Zintl phases studied in the last two decades, the $A_{14}MX_{11}$ ($A = \text{Ca, Sr, Ba, Yb, Eu}$; $M = \text{Zn, Cd, Mn, Mg}$; $X = \text{As, Sb, Bi}$) and AM_2X_2 ($A = \text{Ca, Sr, Ba, Yb, Eu, Mg}$; $M = \text{Zn, Cd, Mn, Mg, Ga}$; $X = \text{As, Sb, Bi}$) compounds have been most widely investigated. Other important classes of Zintl phases include those with compositions $A_5M_2X_6$, $A_{11}M_6X_{12}$, A_3MX_3 and $A_9M_{4.5}X_9$. These materials have significant promise, as depicted by both theoretical modeling and experimental results. With the exception of the AM_2X_2 family, the compounds above exhibit extremely low inherent lattice thermal conductivities. Their optimized thermoelectric properties are found at various temperatures depending on the compositions. This opens up the possibility of applications at low, mid and high temperatures. $\text{Yb}_{14}\text{MnSb}_{11}$ and $\text{Yb}_{14}\text{MgSb}_{11}$ are two of the most promising *p*-type thermoelectric materials available for high-temperature applications. At intermediate temperatures, *p*-type AM_2X_2 compounds have zT values as high as 1.3, and compounds like $\text{Ca}_9\text{Zn}_{4.5+x}\text{Sb}_9$ have already reached a zT value of 1.1.

Most Zintl thermoelectrics are *p*-type, as they have a tendency to form intrinsic acceptor type defects (e.g. cation vacancies). However, recent progress has uncovered strategies to achieve *n*-type behavior. The most prominent and successful examples are Mg_3Sb_2 -based compounds, which are now important enough to deserve their own section 3.5. The only other *n*-type Zintl phases with promising performance, to date, are the AMX_4 ($A = \text{Na, K, Rb, Cs}$; $M = \text{Al, Ga, In}$; $X = \text{As, Sb, Bi}$) compounds. While their properties are impressive, reaching zT values >1 , there is still much need for newer *n*-type compound discovery.

Two sets of data are presented in table 4 for each composition, for room temperature and for the temperature with the maximum thermoelectric figure of merit. To ensure a consistent approach to calculating κ_L , we used the reported total thermal conductivity, and estimated the electronic contribution (κ_E) using the Wiedemann–Franz law [3]. The Lorenz number was calculated using the equation of Kim *et al* [254]. The values of κ_L reported in the table are then given by $\kappa - \kappa_E$.

Figure 5 shows the weighted mobility vs lattice thermal conductivity for selected Zintl compounds at 300 K, including both *n*-type (open symbols) and *p*-type (filled symbols). The contour lines represent slopes, denoted by m . The ratio of weighted mobility to lattice thermal conductivity is directly proportional to the thermoelectric quality factor, B , which indicates the potential zT that *could* be achieved under optimal doping concentrations [245]. The relationship is given in equation (3). Therefore, as a general rule, compounds closer to the top left corner of the plot are expected to have better thermoelectric performance when optimally doped. Indeed, the *n*-type $\text{Mg}_3\text{Sb}_{2-x}\text{Bi}_x$ compounds show the most promising ratio of μ_w/κ_L at room temperature.

The introduction of Zintl phases for thermoelectric applications has provided the option to find inherently low lattice thermal conductivity materials made of earth-abundant, non-toxic elements. While many *p*-type Zintl compounds have been discovered with respectable zT values, tuning Zintl compounds *n*-type is particularly challenging. This is primarily the case due to the low band degeneracy in conduction bands, which are largely dominated by the *s*-orbitals of the cation [255]. The discovery of *n*-type Mg_3Sb_2 phases are attributed largely to the low formation energy of Mg vacancies, but this is not a common phenomenon. Therefore, new Zintl phases new phases are being actively pursued computationally and experimentally. Furthermore, the elements generally used to make Zintl compounds are highly reactive.



Though most Zintls studied for thermoelectrics are stable in air, such is not the case for the entire family. This is a hindrance when it comes to the pursuit of new *n*-type Zintl compounds.

Acknowledgment

A K M Ashiquzzaman Shawon has received funding from the National Science Foundation (Award No. 2045122).

Table 4. Zintl thermoelectric properties.

Material	T (K)	μ_{sc} ($\text{cm}^2 \text{V}^{-1} \text{s}^{-1}$)	κ ($\text{W m}^{-1} \text{K}^{-1}$)	κ_L ($\text{W m}^{-1} \text{K}^{-1}$)	S ($\mu\text{V K}^{-1}$)	σ ($\Omega^{-1} \text{cm}^{-1}$)	zT	E_g (eV)	n (10^{20}cm^{-3})	μ_0 ($\text{cm}^2 \text{V}^{-1} \text{s}^{-1}$)	μ_{HI} ($\text{cm}^2 \text{V}^{-1} \text{s}^{-1}$)	m_k^* (m_e)	ϵ_r, OT ϵ (ϵ_0)	L ($10^{-8} \text{W } \Omega \text{K}^{-2}$)	κ_E ($\text{W m}^{-1} \text{K}^{-1}$)	References
Ca ₁₄ MgSb _{10.80} Sb _{0.20}	300	5.1	0.52	0.50	115.3	31.25	0.02	0.6	—	—	—	—	—	1.87	0.02	[256]
Ca ₁₄ MgSb _{10.80} Sb _{0.20}	1075	4.9	0.76	0.61	193	80	0.49	—	—	—	—	—	—	1.69	0.15	[256]
Sr ₁₄ MgSb ₁₁	300	1.6	0.55	0.55	230	2.45	0.007	1.18	—	—	—	—	—	—	—	[257]
Sr ₁₄ MgSb ₁₁	773	1.9	0.8	0.69	110	50	0.067	—	—	—	—	—	—	—	—	[257]
Eu ₁₄ MgSb ₁₁	300	3.6	0.775	0.58	12.5	241.4	0.002	—	—	—	—	—	—	—	—	[257]
Eu ₁₄ MgSb ₁₁	823	3.1	0.82	0.45	55	210.5	0.08	—	—	—	—	—	—	—	—	[257]
Yb ₁₄ Mn _{0.2}	300	14.4	0.75 (500 K)	0.42 (500 K)	50	238.1	0.08	0.55	4.35	—	5.5	2.75	—	—	—	[253]
Al _{0.8} Sb ₁₁	—	—	—	—	—	—	—	—	—	—	—	—	—	—	—	—
Yb ₁₄ Mn _{0.2}	1223	9.7	0.5	0.25	240	109.9	1.3	—	—	—	—	—	—	—	—	[253]
Al _{0.8} Sb ₁₁	—	—	—	—	—	—	—	—	—	—	—	—	—	—	—	—
Yb ₁₄ MgSb ₁₁	300	24.3	0.67	0.41	50	400	0.005	0.56	5.3	—	4.66	—	—	2.15	0.26	[258, 259]
Yb ₁₄ MgSb ₁₁	1200	10.7	0.73	0.46	228	136.4	1.26	—	11.2	—	0.7	—	—	1.64	0.27	[258]
Yb ₁₄ MgBi ₁₁	300	22.2	1.56	0.97	25	740.7	0.015	—	6.9	—	8	—	—	—	—	[260]
Yb ₁₄ MgBi ₁₁	1073	12.3	1.6	0.56	110	540.5	0.42	—	7.25	—	6.1 (573 K)	—	—	—	—	[260]
Eu ₁₄ MgBi ₁₁	300	18.5	1.55	1.07	27	571.4	0.015	—	7.25	—	5.2	—	—	—	—	[260]
Eu ₁₄ MgBi ₁₁	1073	12.2	1.6	0.70	121	465.1	0.46	—	7.8	—	4.15 (573 K)	—	—	—	—	[260]
Ca ₁₄ MgBi ₁₁	300	13.7	0.75	0.61	56	200	0.046	1.06	5.9	—	2.2	—	—	—	—	[260]
Ca ₁₄ MgBi ₁₁	1073	6.4	1.6	0.92	97.5	333.33	0.21	—	6.75	—	2.3 (573 K)	—	—	—	—	[260]
Sr ₁₄ MgBi ₁₁	300	24.0	1.26	0.78	32	625	0.03	—	4.75	—	9.8	—	—	—	—	[260]
Sr ₁₄ MgBi ₁₁	1073	16.6	1.48	0.54	140	500	0.72	—	5.3	—	7.05 (573 K)	—	—	—	—	[260]
CaZn ₃ Sb ₂	300	73.8	2.6	2.37	120	421.9	0.075	0.33	1.9	—	45	0.6	—	1.86	0.23	[255, 261, 262]
CaZn ₃ Sb ₂	773	30.8	1.42	0.95	178.9	358.42	0.56	—	—	—	—	—	—	1.71	0.47	[255, 261, 262]
Yb _{0.3} Mg _{0.1}	300	123.6	1.225	0.95	157	450	0.3	0.44	0.26	—	106.67	0.82	—	—	—	[255, 263]
Mg _{0.8} Zn _{1.1} Sb _{0.8}	773	46.3	0.76	0.47	256	220	1.5	—	—	—	35	—	—	—	—	[255, 263]
Ag _{0.002} Sb ₂	—	—	—	—	—	—	—	—	—	—	—	—	—	—	—	—
Mg ₈ Sb _{1.8} Pb _{0.2}	300	6.3	0.69	0.68	183	17	0.025	0.8	5.8	—	12.1	1.21	32.04	—	—	[255, 264, 265]
Mg ₈ Sb _{1.8} Pb _{0.2}	773	10.1	0.30	0.25	280	36.25	0.84	—	—	—	—	1.21	—	—	—	[255, 264, 265]
Ca _{0.99} Na _{0.01} MgZnSb ₂	300	70.5	1.39	1.27	167.5	226.67	0.16	1.12	0.32	60	—	1.1	—	—	—	[262, 266]
Ca _{0.99} Na _{0.01} MgZnSb ₂	850	54.6	0.82	0.35	245	340	0.87	—	0.5	22	—	—	—	—	—	[262, 266]

(Continued.)

Table 4. (Continued.)

Material	T (K)	μ_w (cm ² V ⁻¹ s ⁻¹)	κ (W m ⁻¹ K ⁻¹)	κ_L (W m ⁻¹ K ⁻¹)	S (μ V K ⁻¹)	σ (Ω^{-1} cm ⁻¹)	zT	E_g (eV)	n (10 ²⁰ cm ⁻³)	μ_0 (cm ² V ⁻¹ s ⁻¹)	μ_H (cm ² V ⁻¹ s ⁻¹)	m_e^* (m _e)	ϵ_f or $\epsilon(\epsilon_0)$	L (10 ⁻⁸ W Ω K ⁻²)	κ_E (W m ⁻¹ K ⁻¹)	References
EuCd _{1.4} Zn _{0.6} Sb ₂	300	128.0	1.76	1.43	130	645.16	0.18	0.5	0.21	—	182.4	0.56	—	—	—	[255, 267]
EuCd _{1.4} Zn _{0.6} Sb ₂	700	45.4	1	0.72	219	285.71	0.96	0.5	0.23	—	80	0.62	—	—	—	[255, 267]
Ba _{0.975} Yb _{0.2} Na _{0.025}	300	81.6	1.65	1.30	100	606	0.1	0.7	0.4	—	12	0.315	0.29	—	—	[268]
Cd ₂ Sb ₂	—	—	—	—	—	—	—	—	—	—	—	—	—	—	—	—
Ba _{0.975} Yb _{0.2} Na _{0.025}	700	34.1	0.83	0.55	208	244	0.92	—	0.42	—	13	0.37	—	—	—	[268]
Cd ₂ Sb ₂	—	—	—	—	—	—	—	—	—	—	—	—	—	—	—	—
YbCd _{1.6} Zn _{0.4} Sb ₂	300	159.0	1.85	1.19	102	1150	0.2	0.63	0.6	—	118	0.74	—	—	—	[255, 269]
YbCd _{1.6} Zn _{0.4} Sb ₂	700	58.2	1.1	0.44	184	550	1.2	—	—	—	—	—	—	1.70	—	[255, 269]
Eu _{0.2} Yb _{0.2} Ca _{0.6} Mg ₂ Bi ₂	300	137.2	1.5	1.25	165	454.5	0.25	0.46	0.177	—	171	0.77	—	—	—	[255, 270]
Eu _{0.2} Yb _{0.2} Ca _{0.6} Mg ₂ Bi ₂	873	33.0	0.925	0.52	217.5	294.1	1.3	—	—	—	—	—	—	—	—	[255, 270]
Ca _{0.5} Yb _{0.5} Mg ₂ Bi ₂	300	68.3	1.25	1.20	260	75	0.12	0.5	0.033	—	138	0.61	—	—	—	[255, 271]
Ca _{0.5} Yb _{0.5} Mg ₂ Bi ₂	873	28.7	1.115	0.55	188	360	0.98	—	—	—	—	—	—	—	—	[255, 271]
Ba _{1.975} Na _{0.025} Ga ₂ Sb ₂	300	53.4	1.46	1.27	140	238.1	0.1	0.4	1.02	—	15.2	—	—	—	—	[272]
Ba _{1.975} Na _{0.025} Ga ₂ Sb ₂	750	22.5	0.98	0.72	200	196.1	0.65	—	1.6	—	7.1	1.7	—	—	—	[272]

(Continued.)

Table 4. (Continued.)

Material	T (K)	μ_w ($\text{cm}^2 \text{V}^{-1} \text{s}^{-1}$)	κ ($\text{W m}^{-1} \text{K}^{-1}$)	κ_L ($\text{W m}^{-1} \text{K}^{-1}$)	S ($\mu\text{V K}^{-1}$)	σ ($\Omega^{-1} \text{cm}^{-1}$)	zT	E_g (eV)	n (10^{20}cm^{-3})	μ_0 ($\text{cm}^2 \text{V}^{-1} \text{s}^{-1}$)	μ_{H} ($\text{cm}^2 \text{V}^{-1} \text{s}^{-1}$)	m_s^* (m_e)	ϵ_r or $\epsilon(\epsilon_0)$	L ($10^{-8} \text{W} \Omega \text{K}^{-2}$)	κ_E ($\text{W m}^{-1} \text{K}^{-1}$)	References
$\text{Yb}_9 \text{Mn}_{4.2} \text{Sb}_9$	300	9.5	0.675	0.46	60	307.7	0.033	0.4	2.1	—	10	1.2	—	—	—	[273]
$\text{Yb}_9 \text{Mn}_{4.2} \text{Sb}_9$	973	20.7	0.59	0.39	186	129	0.75	—	2	5	4	—	—	—	—	[273]
$\text{Eu}_9 \text{Cd}_{3.76} \text{Ag}_{0.43} \text{Sb}_9$	300	56.6	1.44	0.84	39	1204.8	0.03	—	1.6	—	36	0.44	—	—	—	[274]
$\text{Eu}_9 \text{Cd}_{3.76} \text{Ag}_{0.43} \text{Sb}_9$	773	13.6	0.92	0.40	85	515.5	0.29	—	2	—	15	—	—	—	—	[274]
$\text{Ca}_9 \text{Zn}_{4.6} \text{Sb}_9$	300	36.4	0.67	0.65	170	113.6	0.1	0.35	0.22	—	30.5	0.56	—	—	—	[275]
$\text{Ca}_9 \text{Zn}_{4.6} \text{Sb}_9$	875	18.2	0.47	0.36	268	90.9	1.1	—	0.46	—	11	—	—	—	—	[275]
$\text{Eu}_{11} \text{Cd}_6 \text{Sb}_{12}$	300	24.4	0.82	0.71	118	142.9	0.06	—	0.35	—	33.5	—	—	—	—	[276]
$\text{Eu}_{11} \text{Cd}_6 \text{Sb}_{12}$	773	5.2	0.68	0.54	132	105.3	0.23	—	1.2	—	7	—	—	—	—	[276]
$\text{Eu}_{11} \text{Cd}_{4.5} \text{Zn}_{1.5} \text{Sb}_{12}$	300	46.2	0.88	0.70	132	227.2	0.11	0.1	0.25	—	53	0.6	—	—	—	[277]
$\text{Eu}_{11} \text{Cd}_{4.5} \text{Zn}_{1.5} \text{Sb}_{12}$	800	12.6	0.65	0.42	188	138.9	0.51	—	0.75	—	10	—	—	—	—	[277]
$\text{Ca}_5 \text{Al}_{0.95} \text{In}_{0.95} \text{Zn}_{0.1} \text{Sb}_6$	300	28.7	1.12	1.05	140	128.2	0.02	0.65	2	—	4.9	1.92	—	1.80	0.07	[278, 279]
$\text{Ca}_5 \text{Al}_{0.95} \text{In}_{0.95} \text{Zn}_{0.1} \text{Sb}_6$	900	16.4	0.81	0.56	210	166.67	0.7	—	4	—	2	—	—	1.66	0.25	[278, 279]
$\text{Ca}_5 \text{Ga}_{1.9} \text{Zn}_{0.1} \text{Sb}_6$	300	24.5	1.65	1.50	60	333.33	0.04	0.43	5	—	8	1.46	—	—	—	[279, 280]
$\text{Ca}_5 \text{Ga}_{1.9} \text{Zn}_{0.1} \text{Sb}_6$	773	15.1	1.1	0.70	150	246.9	0.37	—	6.5	—	3.5	—	—	—	—	[279, 280]
$\text{Ca}_5 \text{In}_{1.9} \text{Zn}_{0.1} \text{Sb}_6$	300	26.9	1.25	1.13	100	323 K	0.025	0.64	2	—	5.5	1.8	—	—	—	[279, 281]
$\text{Ca}_5 \text{In}_{1.9} \text{Zn}_{0.1} \text{Sb}_6$	973	11.5	0.75	0.53	190	166.67	0.72	0.44	3.8	—	2.2	—	—	—	—	[279, 281]
$\text{Sr}_5 \text{In}_{1.9} \text{Zn}_{0.1} \text{Sb}_6$	300	3.8	1.14	1.10	155	325 K	0.01	—	0.7	—	2.1	—	—	—	—	[282]
$\text{Sr}_5 \text{In}_{1.9} \text{Zn}_{0.1} \text{Sb}_6$	750	15.3	0.78	0.70	275	55.6	0.4	—	1.6	—	2.5	—	—	—	—	[282]
$\text{Eu}_5 \text{In}_{1.9} \text{Zn}_{0.1} \text{Sb}_6$	300	9.3	1.16	1.12	92	76.9	0.018	0.29	—	—	5	1.5	—	—	—	[283]
$\text{Eu}_5 \text{In}_{1.9} \text{Zn}_{0.1} \text{Sb}_6$	673	18.0	0.84	0.80	200	133.33	0.39	—	—	—	8.5	0.8	—	—	—	[283]
$\text{Ca}_{2.97} \text{N}_{0.03} \text{AlSb}_3$	1050	12.4	0.67	0.58	285	66.67	0.8	—	0.65	—	5.74	—	—	—	—	[284]
$\text{Sr}_3 \text{AlSb}_3$	300	1.8	1.1	1.10	325	0.95	~	0.6	0.8	—	1.25	—	—	1.56	0.00	[285]
$\text{Sr}_3 \text{AlSb}_3$	800	14.6	0.575	0.57	450	7.69	0.15	—	4	—	1.5	—	—	1.52	0.01	[285]
$\text{Sr}_3 \text{Ga}_{0.93} \text{Zn}_{0.07} \text{Sb}_3$	300	22.0	1.1	1.03	110	142.9	0.015	0.75	1.01	—	13	0.9	—	—	—	[286]
$\text{Sr}_3 \text{Ga}_{0.93} \text{Zn}_{0.07} \text{Sb}_3$	1000	11.1	0.65	0.43	215	125	0.9	—	0.7	—	7	—	—	—	—	[286]
$\text{K}_{0.99} \text{Ba}_{0.01} \text{AlSb}_4$	298	11.6	1.16	1.05	—150	45.5	0.025	0.5	0.1	—	18	0.5	—	—	—	[287]
$\text{K}_{0.99} \text{Ba}_{0.01} \text{AlSb}_4$	643	29.0	0.645	0.52	—260	100	0.72	—	0.1	—	52	—	—	—	—	[287]
$\text{K}_{0.985} \text{Ba}_{0.015} \text{GaSb}_4$	323	53.3	1.25	1.14	—145	250	0.143	0.39	0.021	—	70	0.6	—	—	—	[288]
$\text{K}_{0.985} \text{Ba}_{0.015} \text{GaSb}_4$	673	30.0	0.6	0.45	—238	142.9	0.94	—	0.019	—	50	—	—	—	—	[288]
$\text{Yb}_{20.6} \text{Na}_{0.4} \text{Mn}_4 \text{Sb}_{18}$	300	20.7	0.6	0.54	125	111.11	0.07	0.4	2.2	—	2.75	5.7	—	—	—	[289]
$\text{Yb}_{20.6} \text{Na}_{0.4} \text{Mn}_4 \text{Sb}_{18}$	800	16.5	0.45	0.38	290	55.56	0.78	—	3.2	—	0.75	—	—	—	—	[289]
LiZnSb	300	160.0	5.5	3.50	45	2941	0.034	—	3.5	—	52	0.7	—	—	—	[290]
LiZnSb	525	58.9	4.5	2.20	58	1923	0.075	—	5	—	24	—	—	—	—	[290]
$\text{Ca}_{0.84} \text{Ce}_{0.16} \text{Ag}_{0.07} \text{Sb}$	300	79.3	1.75	—	33	2000	0.05	0.18	—	—	—	0.82	—	—	—	[291, 292]
$\text{Ca}_{0.84} \text{Ce}_{0.16} \text{Ag}_{0.07} \text{Sb}$	1073	20.9	1.55	—	100	1052.6	0.66	—	—	—	—	—	—	—	—	[291, 292]
$\text{Mg}_{0.97} \text{Zn}_{0.03} \text{Ag}_{0.9} \text{Sb}_{0.95}$	323	177.9	0.62	0.54	284	165.5	1.11	—	0.25	—	49.1	—	1.54	0.08	—	[293]
$\text{Mg}_{0.97} \text{Zn}_{0.03} \text{Ag}_{0.9} \text{Sb}_{0.95}$	423	142.8	0.70	0.52	246	307.21	1.4	—	0.54	—	33.9	—	1.55	0.18	—	[293]
$(\text{Zn}_{1.98} \text{Pb}_{0.02} \text{Sb}_3)_{0.97} (\text{Cu}_3 \text{SbSe}_4)_{0.03}$	300	109.6	0.95	0.59	125	588.2	0.28	0.26	2.24	—	16.8	2.14	—	—	—	[294]
$(\text{Zn}_{1.98} \text{Pb}_{0.02} \text{Sb}_3)_{0.97} (\text{Cu}_3 \text{SbSe}_4)_{0.03}$	650	61.1	0.7	0.20	195	454.5	1.25	—	—	—	—	—	—	—	—	[294]

L = Lorenz number.

3.5. Mg₃Sb₂

High thermoelectric performance of *n*-type Mg₃Sb₂-Mg₃Bi₂ alloys

Kazuki Imasato^{1,2} and G Jeffrey Snyder¹

¹ Department of Materials Science and Engineering, Northwestern University, Evanston, IL, United States of America

² Global Zero Emission Research Center, National Institute of Advanced Industrial Science and Technology, Tsukuba (AIST), Japan

The *n*-type Mg₃Sb₂-Mg₃Bi₂ alloys (Mg₃X₂ where X is a group 15 element, often a mixture of Sb and Bi) are receiving heightened attention as one of the most prominent thermoelectric materials with high performance in the range of room temperature (~300 K) to mid-temperature (~700 K) [295–298]. Owing to their highly degenerate conduction band structure (Valley degeneracy $N_v = 6$) [295, 296, 299] and extremely low phonon thermal conductivity ($\kappa_L \sim 0.5 \text{ W m}^{-1} \text{ K}^{-1}$), Peng *et al* [300] reported zT values are higher than 1.5 at 700 K and reaching 1.0 around room temperature. Since the discovery of *n*-type Mg₃Sb_{1.5}Bi_{0.5} [295], extensive research has been conducted to optimize their thermoelectric performance by engineering the electronic band structure [301–303], chemical doping [304–310], and the optimization of microstructure [311–314]. The crystal structure of Mg₃Sb₂ and Mg₃Bi₂ is identical to that of a relatively large class of AM_2X_2 Zintl phases. The space group is $P-3m1$ (No. 164). Mg₃Sb₂ and Mg₃Bi₂ can be treated as the special cases of AM_2X_2 in which Mg atoms occupy both the A and M sites. Twelve different reports for the most studied composition Mg₃Sb_{1.5}Bi_{0.5} and some other compositions with different Sb:Bi ratios are summarized in table 5.

To synthesize *n*-type Mg₃X₂ an excess of Mg ($x > 0$) is required, such that the typical *nominal* stoichiometry is Mg_{3+x}X₂, to suppress the formation of Mg vacancies which are an electron killer defect [297]. Note that the actual composition of the Mg₃X₂ phase, written with nonstoichiometry as Mg_{3+ δ} X₂ will have δ much smaller (possibly even $\delta < 0$) than the nominal x needed for processing. The amount of excess Mg required varies, depending on the synthesis route and starting materials (powder, turnings, shot, granules etc). *n*-type conduction can be achieved as long as the sample is in the Mg-excess thermodynamic condition. This sensitivity of the thermodynamic chemical potential of Mg implies the *n*-type conduction can be lost during high temperature ($T > 700 \text{ K}$) processing as the high vapor pressure and reactivity of Mg leads to a net loss of Mg at elevated temperature [306, 308, 315, 316]. The charge carrier concentration is controlled by using aliovalent substitution, i.e. group 3 elements (e.g. Sc, Y, La) substituting for Mg or group 16 elements (e.g. S, Se or Te) on anion sites, as extrinsic dopants. All good thermoelectric Mg₃X₂ materials contain such an extrinsic dopant (e.g. nominal composition Mg_{3+x}Sb_{1.5}Bi_{0.49}Te_{0.01} [295]) but for convenience they may be formulated simply as Mg₃Sb_{1.5}Bi_{0.5}. Te substitution on the anion site has been known as an effective dopant [295–298, 317, 318], while Se and S do not have enough dopability to achieve optimum carrier concentration [319, 320]. Recently, cation site substitutions are reported with higher doping efficiency and thermal stability compared to the anion alternatives [304–310, 321–324].

As Mg₃Sb₂ and Mg₃Bi₂ make a solid solution for the entire composition range, the effect of the Sb:Bi ratio has been studied to optimize the thermoelectric performance. In addition to a more than 50% reduction in the lattice thermal conductivity because of alloy scattering [325], Mg₃Bi₂ alloying with Mg₃Sb₂ was proven to be an effective way to engineer the electronic band structure [301, 303, 326]. As the Bi content increases, the weighted mobility [245] increases with the reduced effective mass and smaller band gap. The band gap of pure Mg₃Sb₂ is around 0.5–0.6 eV [296, 306] and decreases with Bi content x in Mg₃(Sb_{1-x}Bi_x)₂ [296, 302, 303]. Considering the operating temperature of thermoelectric materials, the Bi 25% composition (Mg₃Sb_{1.5}Bi_{0.5}) is the most commonly studied and recognized as the highest zT composition for mid temperature (~700 K) [301]. The higher Bi compositions (Bi content greater than 50%) were suggested as the optimized composition for lower temperatures including room temperature with reduced band gap [303, 326–330]. On the other hand, alloying on the cation (Mg) site causes a significant reduction in the performance due to the decreased carrier mobility [315]. The reason for this degraded performance is mainly due to disruption in the conduction band because the six degenerate U^* (CB1) pockets originate from Mg orbital interaction [306, 315, 331, 332].

Grain boundaries play a significant role in the thermoelectric performance of Mg₃X₂. They have been important since the initial studies where undesirable low electronic conductivity led to low performance ($zT \sim 0.1$ is reported below ~500 K [295, 317, 333]). Although often not identified as due to grain boundaries, and sometimes suggested as due to ionized impurity scattering, [298, 317, 334], the effect is significant in most polycrystalline samples. This thermally activated resistivity is particularly strong in Mg₃X₂ but can be found in other high-efficiency thermoelectric materials as well [335]. The grain boundary effect can be described by a series circuit model including a bulk phase and a grain boundary

phase [311, 333, 336, 337]. Highly resistive grain boundaries can be attributed to charged defects that collect at the grain boundaries that trap and scatter the mobile charge carriers. The grain boundary charge is screened by the dielectric response of the material making grain boundary resistance more observable in low dielectric constant materials such as Mg_3Sb_2 (DFT calculated relative isotropic dielectric constant of Mg_3Sb_2 $\epsilon_r = 32$ [338]). This grain boundary effect can be mitigated by increasing the grain size through various methods. Some samples optimized for lower temperature ranges possess a performance comparable to the commercialized Bi_2Te_3 around room temperature [302, 303, 308, 309, 327–329]. While the thermal resistance of the grain boundaries is not very noticeable the dramatically reduced electrical conductivity of the overall sample leads one to expect the electronic contribution to the thermal conductivity within the grains to be much less than it actually is. This leads to a significant overestimation of the lattice thermal conductivity that is commonly reported in systems with grain boundary effects which includes not only Mg_3X_2 but many other good thermoelectric materials as well [335].

Some of the recent studies coupled with *p*-type Bi_2Te_3 [339] and *p*-type MgAgSb [340] showed a high conversion efficiency of more than 7% under a temperature difference of ~ 300 K at the hot-side temperature around 573 K. Further improvement in the performance could lead to energy harvesting and Internet of things (IoT) thermoelectric devices. Mg_3X_2 may have better mechanical properties [341, 342] as well as containing more abundant elements than commercially used Bi_2Te_3 – Sb_2Te_3 alloys [330]. However, as with any new material, there will be some new challenges to overcome for making devices with *n*-type Mg_3Sb_2 – Mg_3Bi_2 alloys. For example, thermal stability will be one of the most important issues in this material. With the reactive nature of Mg and its importance to the *n*-type behavior, the degradation of performance has been observed. Improved stability has been reported with a chemical substitution/ addition [306, 308, 315, 343] and use of coatings [316]; however, the fundamental mechanism of this degradation needs to be further studied. Beyond high zT and degradation, an assessment of mechanical robustness [302, 343] and processing cost are required to make commercial thermoelectric devices with Mg_3Sb_2 – Mg_3Bi_2 alloys.

Table 5. Mg₃Sb₂ thermoelectric properties.

Composition (dopant/additive)	Bi content	Dopant/additive	T (K)	μ_{av} (cm ² V ⁻¹ s ⁻¹)	κ_L (W m ⁻¹ K ⁻¹)	S (μ V K ⁻¹)	σ (Ω^{-1} cm ⁻¹)	zT	E _g (eV)	μ_0 (cm ² V ⁻¹ s ⁻¹)	m [*] (m _e)	ϵ_r or ϵ (ϵ_0)	References
Mg _{3.2} Sb _{1.5} Bi _{0.49} Te _{0.01}	25%	Te	350	47.1	0.85	-214.8	110.1	0.19	—	41.7	1.08	—	[295]
—	—	—	550	81.0	0.64	-254.4	235.4	0.98	—	76.1	1.04	—	—
—	—	—	700	67.6	0.56	-281.6	206.0	1.44	—	53.9	1.16	—	—
Mg _{3.2} Sb _{1.5} Bi _{0.49} Te _{0.01}	25%	Te	350	192.0	0.74	-203.0	514.6	0.71	—	148.6	1.19	—	[298]
—	—	—	550	99.7	0.64	-247.7	313.2	1.15	—	79.3	1.17	—	—
—	—	—	700	66.3	0.59	-275.4	216.9	1.38	—	48.3	1.23	—	—
Mg _{3.2} Sb _{1.5} Bi _{0.49} Te _{0.01}	25%	Te	350	162.9	0.68	-210.4	400.4	0.68	—	129.8	1.16	—	[333]
—	—	—	550	107.2	0.47	-255.0	309.7	1.48	—	82.0	1.20	—	—
—	—	—	700	69.7	0.49	-280.7	214.6	1.63	—	49.4	1.26	—	—
Mg ₃ Sb _{1.48} Bi _{0.48} Te _{0.04}	25%	Te	350	129.3	0.53	-213.9	305.0	0.69	0.6 eV (DFT)	106.7	1.14	—	[318]
—	—	—	550	77.7	0.41	-252.1	232.1	1.32	—	55.4	1.25	—	—
—	—	—	700	50.0	0.35	-264.3	185.9	1.63	—	30.6	1.39	—	—
Mg _{3.2} Sb _{1.5} Bi _{0.49} Te _{0.01}	25%	Te	350	51.7	0.95	-209.1	129.0	0.19	0.433 eV	29.5	1.45	—	[297]
—	—	—	550	88.0	0.67	-251.9	263.2	1.02	—	55.7	1.36	—	—
—	—	—	700	63.5	0.60	-274.5	209.9	1.33	—	42.3	1.31	—	—
Mg _{3+δ} Sb _{1.5} Bi _{0.49} Te _{0.01}	25%	Te	350	219.6	0.67	-200.0	609.3	0.83	—	—	—	—	[313]
—	—	—	550	91.2	0.59	-240.2	312.3	1.15	—	—	—	—	—
Mg _{3.15} Nb _{0.05} Sb _{1.5} Bi _{0.49} Te _{0.01}	25%	Te, Nb	350	153.1	0.76	-204.3	404.1	0.59	—	105.4	1.28	—	[317]
—	—	—	550	112.2	0.71	-249.2	346.2	1.32	—	85.9	1.20	—	—
—	—	—	700	65.9	0.46	-274.5	217.7	1.36	—	53.0	1.16	—	—
Mg _{3.175} Mn _{0.025} Sb _{1.5} Bi _{0.49} Te _{0.01}	25%	Te, Mn	350	165.7	0.77	-232.0	316.9	0.63	—	98.4	1.42	—	[334]
—	—	—	550	132.7	0.60	-271.9	314.9	1.46	—	95.9	1.24	—	—
—	—	—	700	90.7	0.55	-297.5	229.7	1.78	—	65.0	1.25	—	—
Mg _{3.17} B _{0.03} Sb _{1.5} Bi _{0.49} Te _{0.01}	25%	Te, B	350	212.0	0.62	-205.7	550.2	0.87	—	196.0	1.05	—	[343]
—	—	—	550	117.3	0.51	-260.7	317.1	1.50	—	80.1	1.29	—	—
—	—	—	700	75.3	0.49	-287.7	213.7	1.71	—	45.6	1.40	—	—
Mg _{3.2} Nd _{0.03} Sb _{1.5} Bi _{0.5}	25%	Nd	350	78.6	0.82	-152.8	384.6	0.30	—	48.5	1.38	—	[341]

(Continued.)

Table 5. (Continued.)

Composition (dopant/additive)	Bi content	Dopant/additive	T (K)	μ_w ($\text{cm}^2 \text{V}^{-1} \text{s}^{-1}$)	κ_L ($\text{W m}^{-1} \text{K}^{-1}$)	S ($\mu\text{V K}^{-1}$)	σ ($\Omega^{-1} \text{cm}^{-1}$)	zT	E_g (eV)	μ_0 ($\text{cm}^2 \text{V}^{-1} \text{s}^{-1}$)	m_s^* (m_e)	ϵ_r or ϵ (ϵ_0)	References
$\text{Mg}_{3.05}\text{La}_{0.005}\text{Sb}_{1.5}\text{Bi}_{0.5}$	25%	La	350	95.9	0.86	-200.9	263.3	0.37	—	79.2	1.14	—	[306]
$\text{Mg}_{3+\delta}\text{Sb}_{1.5}\text{Bi}_{0.49}\text{Te}_{0.01}\text{Mn}_{0.01}$	25%	Te, Mn	350	225.1	0.80	-213.3	535.3	0.77	0.279 (FTIR)	—	1.12	—	[302]
$\text{Mg}_{3.2}\text{Sb}_{1.99}\text{Te}_{0.01}$	0%	Te	350	51.7	0.93	-209.1	129.0	0.20	0.54	29.5	1.45	—	[301]
$\text{Mg}_3\text{Sb}_{1.25}\text{Bi}_{0.75}\text{Y}_{0.01}$	37.50%	Y	350	128.3	1.41	-215.5	297.3	0.31	—	47.8	1.93	—	[337]
$\text{Mg}_{3+\delta}\text{Sb}_{1.1}\text{Bi}_{0.89}\text{Te}_{0.01}\text{Mn}_{0.01}$	45%	Te, Mn	350	217.7	0.79	-182.7	740.1	0.70	0.242 (FTIR)	—	—	—	[302]
$\text{Mg}_{3.05}\text{Sb}_{1.0}\text{Bi}_{0.97}\text{Te}_{0.03}$	50%	Te	350	230.9	0.69	-180.9	801.6	0.79	0.364 (DFT)	135.7	1.43	—	[329]
$\text{Mg}_{3.05}(\text{Sb}_{0.3}\text{Bi}_{0.7})_{1.996}\text{Te}_{0.004}$	70%	Te	350	258.4	0.61	-204.7	679.0	0.99	0.208 (G-S gap)	159.3	1.38	—	[303]
$\text{Mg}_{3.2}\text{Sb}_{0.5}\text{Bi}_{1.498}\text{Te}_{0.02}$	75%	Te	350	226.2	0.70	-234.8	419.1	0.86	—	218.4	1.02	—	[327]

3.6. Clathrates

Clathrate thermoelectrics

Melis Ozen^{1,2}, Kivanc Saglik^{1,2} and Umut Aydemir^{1,3}

¹ Koç University Boron and Advanced Materials Application and Research Center (KUBAM), Istanbul 34450, Turkey

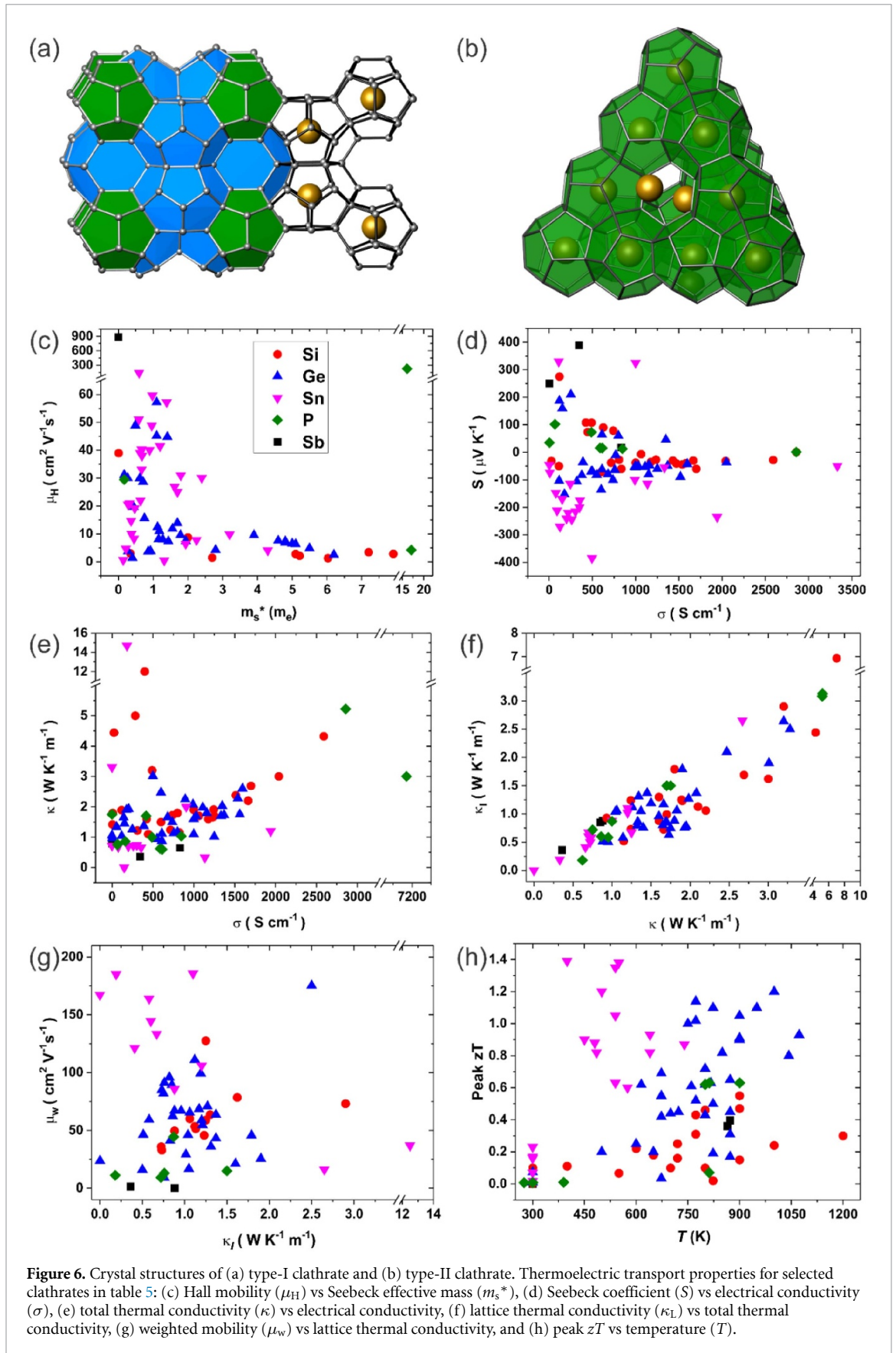
² Graduate School of Sciences and Engineering, Koç University, Istanbul 34450, Turkey

³ Department of Chemistry, Koç University, Istanbul 34450, Turkey

Clathrates are inclusion compounds with a three-dimensional (3D) framework of tetrahedrally-coordinated host structure, encapsulating in large polyhedral cavities guest molecules, atoms, or ions [344]. The classification of clathrate structures is based on packing of different building polyhedra of various sizes, e.g. pentagonal dodecahedron (formed by 12 pentagons: [5¹²]), tetrakaidekahedron (formed by 12 pentagons and 2 hexagons: [5¹²6²]), pentakaidekahedron ([5¹²6²]), or hexakaidekahedron ([5¹²6⁴]). In polyanionic clathrates, the framework structure may bear a negative charge with cations (e.g. Na, K, Rb, Sr, Ba) residing as the guest atoms, whereas, in polycationic clathrates, the framework has a positive charge and the anions (e.g. Te, Cl, Br, I) are the guest atoms [345]. Inorganic clathrates crystallize mostly in two common structure types termed as type-I and type-II clathrates (figures 6(a) and (b)). Type-I clathrates are composed of two pentagonal dodecahedra and eight tetrakaidekahedra per unit cell leading to a general chemical formula of $G'_2G''_8E_{46}$ (G' and G'' indicate guest species in pentagonal dodecahedra and tetrakaidekahedra, respectively) crystallizing in the primitive cubic space group $Pm\bar{3}n$ (no. 223). Type-II clathrates with composition $G'_{16}G''_8E_{136}$ crystallize in the space group $Fd\bar{3}m$ with a framework comprising 16 pentagonal dodecahedra and 8 hexakaidekahedra per unit cell.

The formal electronic structure of intermetallic clathrates can be in most cases adequately described by the Zintl-Klemm concept [346, 347], in which each constituent atom achieves a closed valence shell via a formal charge transfer from the more electropositive atoms to the more electronegative ones. Zintl-Klemm formalism provides a guiding relationship between stoichiometry, structure, and electronic properties. Clathrates with large and weakly bounded ions that can ‘rattle’ inside oversized cages of the rigid host framework have been discussed in the context of the PGEC concept [348]. These compounds display low lattice thermal conductivity as an inherent property of their complex crystal structure, which is ascribed to the interaction of the heat-carrying phonons with the local vibration modes of guest atoms in the polyhedral cages [349, 350]. The guest-host interactions do not substantially degrade the electronic properties. It is possible to finely adjust the electronic properties of clathrates from metallic to semiconducting behavior by tuning the chemical composition and forming vacancies in their crystal structures. By controlling the concentration of guest atoms in the cages and substituting the framework atoms, the charge carrier concentrations of clathrates can be adjusted effectively. Besides, vacancies in these materials’ crystal structures can turn the electrical conduction from n -type to p -type even in the same material system and thus change their thermoelectric properties [351, 352].

Transport properties of different clathrate families (arranged for the majority atoms forming the framework structure) are presented in figures 6(c)–(h). Figure 6(c) shows the trend for Hall mobility (μ_H) vs Seebeck effective mass (m_s^*) at 300 K for the clathrates tabulated in table 6. Except for three clathrate compounds, $K_{7.1}Ba_{16.9}Ga_{41.3}Sn_{94.7}$, $Cs_8In_{27}Sb_{19}$, and $Ba_{6.4}La_{1.6}Cu_{16}P_{30}$, μ_H values are almost exclusively well below $60 \text{ cm}^2 \text{ V}^{-1} \text{ s}^{-1}$, which are relatively low compared to other families of thermoelectrics. Low effective masses provide much higher Hall mobility values, mainly observed for the Sn and Ge clathrates. Clathrates can be obtained both n - and p -type as illustrated in figure 6(d) even for the same family of compounds. Clathrates with the homoatomic framework of four-bonded E_{14} elements do not require additional electrons based on the $8-N$ rule. Such compounds containing excess electrons are generally observed for silicon clathrates in which the electrons transferred from the guest atoms fill up antibonding conduction bands of the corresponding empty Si_{46} framework. Clathrates of the heavier homologous (Ge and Sn) may accommodate excess electrons by forming vacancies. Therefore, Si clathrates show relatively low Seebeck coefficient values due to their metallic nature. As the framework is built up of heavier (same group) elements of Ge and Sn, the variation and the absolute values of S increase. This trend can be correlated with doping behavior along with respective changes in the Fermi level of these clathrate families. Higher Seebeck values



can be obtained with charge-balanced compositions, which in turn can be achieved more easily for the Ge and especially Sn clathrates thanks to easier substitution with other elements and higher possibility of vacancy formation (note that the bond strengths between the framework atoms decrease down the group for Group 14 elements).

All known P clathrates show *p*-type conduction. Sn clathrates generally show much lower σ values in comparison to those of Si and Ge clathrates due to their tendency to have charge-balanced compositions. Figure 5(e) reveals the phonon-glass nature of the clathrates' thermal conductivity with a majority of phases possessing κ below $3 \text{ W K}^{-1} \text{ m}^{-1}$ irrespective of the framework atoms. Heavier Sn clathrates with large cage volumes display the lowest κ values compared to Si and Ge homologous. Based on a linear fit analysis, κ_L contributes on average $\sim 70\%$ to κ (figure 6(f)). High μ_w (calculated by equation (5)) and low κ_L are desirable to achieve better thermoelectrics efficiencies. Sn clathrates satisfy this condition best among all families of clathrates (figure 6(g)), which manifest themselves with the highest peak zT values attained at low-to-mid temperatures (figure 6(h)). Ge clathrates show moderate μ_w and little higher κ_L values compared to the Sn counterparts and display high peak zT values at mid-to-high temperatures. Si clathrates have relatively low μ_w and peak zT values but are the most stable phases ($T_{mSi} > T_{mGe} > T_{mSn}$; Tm: melting T) make them attractive for high-temperature thermoelectrics applications. P and Sb cationic clathrates possess the lowest μ_w values and generally show low thermoelectric efficiencies.

Widespread use of thermoelectric generators necessitates stable *n*- and *p*-type materials of almost equal thermoelectric potential and compatibility in thermal expansion to minimize stress effects. For such module applications, inorganic clathrates displaying both *n*- and *p*-type conduction in the same material systems with high thermoelectric efficiencies are very suitable materials. However, in targeting large-scale industrial applications, cheap, earth-abundant, and non-toxic raw materials should be preferred during their synthesis. As mentioned above, Sn, Ge, and Si clathrates show the best thermoelectric performances at low, mid, and high temperatures, respectively. Combinatorial use of these framework elements in the same clathrate framework could lead to superior thermoelectric properties along with better thermal management. Besides, band structure engineering through proper substitution of the framework atoms or tuning the vacancy concentration on the framework sites and the guest atom concentrations inside the polyhedral cages with novel synthetic techniques, e.g. low-temperature redox reactions [353, 354] melt-centrifugation [44, 314] or liquid phase sintering [355, 356] may potentially lead to enhanced thermoelectric properties. Leveraging high-throughput calculations and data mining [357–360], the selection process of inorganic clathrates can be accelerated, and unexplored clathrate phases may be uncovered with high thermoelectric performance. Exploring novel clathrate types with unique cage structures should be another motivation for discovering high-efficiency materials for this family of compounds.

Acknowledgment

This work is supported by the Scientific and Technological Research Council of Turkey (TÜBİTAK) with Grant Number 118M371.

Table 6. Clathrate thermoelectric properties.

Material	T (K)	μ_{av} (cm ² V ⁻¹ s ⁻¹)	κ (W m ⁻¹ K ⁻¹)	ϵ_{Lz} (W m ⁻¹ K ⁻¹)	ϵ_{Lz} (W m ⁻¹ K ⁻¹)	S (μ V K ⁻¹)	σ (Ω^{-1} cm ⁻¹)	zT	E_g (eV)	μ_{Hl} (cm ² V ⁻¹ s ⁻¹)	m_{Hl}^* (m _e)	ϵ_r or $\epsilon(\epsilon_0)$	η (10 ¹⁹ cm ⁻³)	References
Silicides														
Ba ₈ Cu ₆ Si ₄₀	323	34.9	1.7	0.6	0.6	-26	1250	—	—	—	—	—	—	[361]
	723	15.3	1.3	0.1	0.1	-65	714.3	—	—	—	—	—	—	
Ba ₈ Cu ₆ Si ₄₀ (4 GPa)	300	49.5	1.6	0.9	0.9	-35	1176	0.01	—	5.2	2.18	—	140	[362]
	773	18.7	1.3	0.1	0.1	-84.3	717.4	0.31	—	—	—	—	—	[362]
Ba ₈ Cu ₆ Si ₄₀ (3 GPa)	300	40	1.8	1	1	-27	1234	0.01	—	4.9	1.84	—	160	[362]
	773	17.8	1.4	0.3	0.3	-78.3	744	0.27	—	4.6	1.73	—	175	[362]
Ba ₈ Cu ₆ Si ₄₀ (2 GPa)	300	37.4	2.1	1.3	1.3	-24	1299	0.002	—	4.6	1.73	—	175	[362]
	773	18	1.6	0.4	0.4	-74.2	799	0.16	—	—	—	—	—	[362]
Ba ₈ Cu ₆ Si ₄₀ (1 GPa)	300	35	2.3	1.5	1.5	-21	1389	0.002	—	4.2	1.69	—	205	[362]
	773	18.2	1.8	0.4	0.4	-69.3	874.9	0.14	—	—	—	—	—	[361]
Ba ₈ Cu _{3.89} Si _{40.16}	320	35.9	1.7	0.7	0.7	-26.7	1234	0.02	—	—	—	—	—	[361]
	720	14.5	1.26	0	0	-62	709.7	0.16	—	—	—	—	—	[361]
Ba _{7.78} Eu _{0.22}	320	29	1.9	1	1	-21.4	1244	0.01	—	—	—	—	—	[361]
Cu _{3.83} Si _{36.47}	720	15.1	1.7	0	0	-51.5	898.5	0.1	—	—	—	—	—	[361]
Ba _{7.23} Eu _{0.73}	320	27.9	3.1	2.3	2.3	-25	1026	0.002	—	—	—	—	—	[361]
Cu _{3.81} Si _{39.23}	720	6.4	2.2	1.3	1.3	-40	492.4	0.03	—	—	—	—	—	[361]
Ba ₈ Cu ₆ Si ₄₀	300	49.1	2.4	—	—	27	1515	0.01	—	—	—	—	—	[363]
	673	27	2	—	—	74	980.4	0.18	—	—	—	—	—	[363]
Ba ₈ Cu ₆ Ce ₈ Si ₃₂	300	43.5	1.9	—	—	45	800	0.03	—	—	—	—	—	[363]
	673	22.6	1.5	—	—	109	500	0.28	—	—	—	—	—	[363]
Ba ₈ Cu ₆ Ce ₁₆ Si ₂₄	300	46.9	1.5	—	—	63	606	0.05	—	—	—	—	—	[363]
	673	22.7	1.3	—	—	125	409.8	0.37	—	—	—	—	—	[363]
Ba ₈ Cu ₆ Ce ₂₄ Si ₁₆	300	41.2	1.1	—	—	74	444.4	0.07	—	—	—	—	—	[363]
	673	20.9	1.2	—	—	141.2	308.6	0.42	—	—	—	—	—	[364]
Ba ₈ Cu ₆ Ce ₁₅ Si ₂₅	323	66.3	1.7	—	—	79	740.7	0.07	—	—	—	—	—	[364]
	773	20	1.2	—	—	121.3	465.1	0.43	—	—	—	—	—	[365]
Ba ₈ Al ₆ Si ₄₀	298	—	—	—	—	—	—	—	0.5	—	—	—	—	[366]
Ba ₈ Al ₆ Si ₃₆	320	11	—	—	—	-9	1104	—	—	—	—	—	—	[366]
	670	10.5	—	—	—	-27	1079	—	—	—	—	—	—	[366]
Ba ₈ Al ₆ Si ₃₀	320	11.7	—	—	—	-11.5	925	—	—	—	—	—	—	[366]
	670	9.1	—	—	—	-32.8	769.2	—	—	—	—	—	—	[366]

(Continued.)

Table 6. (Continued.)

Material	T (K)	μ_{hw} ($\text{cm}^2 \text{V}^{-1} \text{s}^{-1}$)	κ ($\text{W m}^{-1} \text{K}^{-1}$)	κ_L ($\text{W m}^{-1} \text{K}^{-1}$)	S ($\mu\text{V K}^{-1}$)	σ ($\Omega^{-1} \text{cm}^{-1}$)	zT	E_g (eV)	μ_{H0} ($\text{cm}^2 \text{V}^{-1} \text{s}^{-1}$)	μ_{H1} ($\text{cm}^2 \text{V}^{-1} \text{s}^{-1}$)	m_e^* (m_e)	ϵ_r or ϵ (ϵ_0)	n (10^{19}cm^{-3})	References
Ba ₈ Al ₁₄ Si ₃₁	300	15.7	1.9	1.2	-13	1000	0.01	—	6.8	1.5	—	—	—	[367]
	1100	7.7	1.9	0.9	-80	534.7	0.18	—	—	—	6.94	—	400	[367]
Ba ₈ Al ₁₅ Si ₃₀	300	45.7	1.9	1.2	-38	1000	0.02	0.2	4.1	1.5	2.7	—	—	[367]
	1000	9.7	1.7	0.7	-90	505	0.24	—	—	—	6.62	—	300	[368]
Ba ₈ Al _{13,6} Si _{32,4}	317	53	3.5	—	-24	2000	0.01	—	—	—	—	—	—	[368]
	865	24.4	3.7	—	-78.5	1205	0.17	—	—	—	—	—	—	[368]
Ba ₇ Dy _{0.3}	317	4.3	3.5	—	-3.5	1053	—	—	—	—	—	—	—	[368]
Al _{1,2,8} Si _{33,2}	865	9.6	3.6	—	-53.8	719.4	0.05	—	—	—	—	—	—	[368]
Ba _{7,5} Dy _{0.5}	317	76	2.3	—	-44.4	1539	0.04	—	—	—	—	—	—	[368]
Al _{1,4,7} Si _{31,3}	865	25.4	2.3	—	-105	865	0.36	—	—	—	—	—	—	[368]
Ba _{7,3} Dy _{0.7}	317	65.7	3.1	—	-35.6	1667	0.02	—	—	—	—	—	—	[368]
Al _{1,4,4} Si _{31,6}	863	24.3	3	—	-93	970.8	0.24	—	—	—	—	—	—	[368]
Ba ₇ Dy ₁	317	85	3.3	—	-21.3	3610	0.02	—	—	—	—	—	—	[368]
Al _{1,3,8} Si _{32,2}	863	38.9	3.3	—	-65	2370	0.27	—	—	—	—	—	—	[369]
Ba ₇ Si ₁	300	60	2.2	1.1	-30	1667	0.03	—	—	—	—	—	—	[370]
Al _{1,6} Si ₃₀	1200	12	2.6	0.3	-92	793.6	0.3	—	18.6	—	—	—	—	[370]
Ba ₇ Eu ₁	300	—	1.7	1	-7	1064	0.01	—	—	3	0.35	—	100	[370]
Al _{1,3} Si ₃₁	1200	6.8	2.6	0.8	-71.1	614.6	0.14	—	—	—	—	—	—	[370]
Ba ₈ Bi _{0.32}	300	51.5	2.1	1.1	-30	1429	0.03	—	—	—	—	—	—	[370]
Al _{1,4,2} Si _{30,5}	900	14.5	2.5	1.9	-67	909	0.15	—	—	—	—	—	—	[352]
Ba ₈ Au _{4,75}	300	12.7	2.7	2.5	-36	293.2	4×10^{-3}	—	—	—	—	—	—	[352]
Si _{4,1,2,5}	680	6.1	2.8	2.5	-71	234.7	0.03	—	—	—	—	—	—	[352]
Ba ₈ Au _{5,15} Si _{40,85}	300	42.8	1.7	1.55	-104	301.2	0.07	0.1	—	—	3.7	—	650	[352]
	480	26.5	1.7	1.4	-123.7	292.4	0.12	—	—	—	—	—	—	[352]
Ba ₈ Au _{5,30} Si _{40,70}	300	39.8	1.5	1.4	143.2	170.6	0.06	0.1	—	—	6.8	—	80	[352]
	530	19.4	1.8	1.5	129.4	232	0.13	—	—	—	—	—	—	[352]
Ba ₈ Au _{5,45} Si _{40,55}	300	63.6	1.6	1.3	108.2	423.7	0.1	0.2	—	—	5.28	—	150	[352]
	600	27.5	1.9	1.7	135.8	364.9	0.22	—	—	—	—	—	—	[352]
Ba ₈ Au ₆ Si ₄₀	300	86.2	2.2	1.1	47	1515	0.05	—	—	—	8.72	—	720	[352]
	650	80.3	2.9	1.2	127.4	1333	0.18	—	—	—	—	—	—	[352]

(Continued.)

Table 6. (Continued.)

Material	T (K)	μ_w (cm ² V ⁻¹ s ⁻¹)	κ (W m ⁻¹ K ⁻¹)	κ_L (W m ⁻¹ K ⁻¹)	S (μ V K ⁻¹)	σ (Ω^{-1} cm ⁻¹)	zT	E_g (eV)	μ_0 (cm ² V ⁻¹ s ⁻¹)	μ_H (cm ² V ⁻¹ s ⁻¹)	m_s^* (m _e)	ϵ_r or $\epsilon(\epsilon_0)$	n (10 ¹⁹ cm ⁻³)	References
Ba _{7,0} Eu _{1,07} Al _{5,16} Si _{41,84}	300	73.3	—	—	90	625	—	—	—	—	—	—	—	[371]
Ba _{6,19} Eu _{1,68} Al _{5,89} Si _{40,11}	300	61.3	—	—	-60	833.3	—	—	—	—	—	—	—	[371]
Ba _{8,0} Al _{5,59} Si _{39,01}	300	73.1	3.2	2.9	107.6	490.2	0.1	—	5.7	3.4	7.2	—	150	[372]
Ba ₇ Ce ₁ Al _{5,5} Si _{40,5}	300	36.1	1.8	1.6	-150	142.8	0.05	—	1.9	1.3	6.03	—	92.9	[373]
Ba ₇ La ₁ Al ₆ Si ₄₀	500	29.4	1.8	1.5	-175	186.2	0.1	—	—	—	—	—	—	[373]
Ba ₇ La ₁ Al ₆ Si ₄₀	300	127.5	1.9	1.8	275	117.6	0.1	—	3.3	2.8	7.91	—	26.9	[373]
Ba ₇ La ₁ Al ₆ Si ₄₀	400	104.5	1.9	1.8	300	111.1	0.11	—	—	—	—	—	—	[373]
Ba ₈ Ni _{3,8} Si _{42,2}	300	12.6	—	—	-13	806.5	—	—	—	—	—	—	—	[374]
Ba ₈ Ni _{3,8} Si _{42,2}	823	3.8	2	1	-27	534.7	0.02	—	—	—	—	—	—	[374]
Ba ₈ Ni _{3,6} Si _{42,4}	300	78.5	3	1.6	-32	2041	0.02	—	—	—	—	—	—	[375]
Ba ₈ Ni _{3,8} Si _{42,4}	800	25.2	4	1	-58.6	1531	0.1	—	—	—	—	—	—	[375]
Ba ₈ Ni _{3,8} Si _{42,4}	300	82.7	—	—	-40.4	1698	—	0.1	7.4	2.8	5.1	—	400	[375]
Ba ₈ Ni _{3,8} □ ₁ Si _{42,2-y}	790	26.8	—	—	-70	1314	—	—	—	—	—	—	—	[375]
Ba ₈ Ni _{3,8} □ ₁ Si _{42,2-y}	300	85.8	4.3	2.4	-27.6	2591	—	—	—	—	—	—	—	[376]
Ba ₈ Pt _{1,5} Ni _{3,5} Si ₄₁	700	34.5	3.9	0.7	-54.5	1852	0.1	—	—	—	—	—	—	[376]
Ba ₈ Pt _{1,5} Ni _{3,5} Si ₄₁	300	76.2	—	—	-40	1580	—	—	—	—	—	—	—	[377]
Ba ₈ Pt _{1,5} Ni _{3,5} Si ₄₁	1040	11.8	—	—	-44	1429	—	—	—	—	—	—	—	[377]
Ba ₈ Pt _{1,5} Ni _{3,5} Si ₄₁	300	30.7	—	—	35	728.8	—	—	—	—	—	—	—	[378]
Ba ₈ Pt _{1,5} Ni _{3,5} Si ₄₁	1040	4.8	—	—	20	1287	—	—	—	—	—	—	—	[378]
K ₇ BaAl ₉ Si ₃₇	300	4.8	1.2	1	—	309.6	—	—	—	—	—	—	29.1	[378]
K _{6,3} Ba _{1,5} Al _{9,5} Si _{36,5}	873	6.7	—	—	-166	108.7	0.23	—	—	—	—	—	—	[378]
K _{6,3} Ba _{1,5} Al _{9,5} Si _{36,5}	300	—	1.1	0.5	—	826.4	0.35	—	—	1.2	—	—	449	[378]
K ₆ Ba ₂ Al ₁₀ Si ₃₆	873	8.8	—	—	-133	212.7	0.4	—	—	—	—	—	—	[378]
K ₆ Ba ₂ Al ₁₀ Si ₃₆	300	—	0.8	0.7	—	259.7	—	—	—	13.2	—	—	12.5	[378]
K _{7,6} Ga _{3,1} Al _{4,6} Si _{38,7}	873	55	—	—	-184	724.6	0.28	—	—	—	—	—	—	[379]
K _{7,6} Ga _{3,1} Al _{4,6} Si _{38,7}	300	7.2	—	—	-300	5	0.02	—	—	—	—	—	—	[379]
Ba ₈ Ga ₁₇ Si ₂₉	550	—	—	—	—	5	0.07	—	—	—	—	—	—	[380]
Ba ₈ Ga ₁₇ Si ₂₉	300	53.4	1.5	1.1	-71.5	600	0.06	—	17.5	8.8	2	—	44	[380]
Ba ₈ Ga ₁₇ Si ₂₉	900	17	—	—	-165.8	290	0.55	—	—	—	—	—	—	[380]

(Continued.)

Table 6. (Continued.)

Material	T (K)	μ_{av} ($\text{cm}^2 \text{V}^{-1} \text{s}^{-1}$)	κ ($\text{W m}^{-1} \text{K}^{-1}$)	κ_L ($\text{W m}^{-1} \text{K}^{-1}$)	S ($\mu\text{V K}^{-1}$)	σ ($\Omega^{-1} \text{cm}^{-1}$)	zT	F_g (eV)	μ_0 ($\text{cm}^2 \text{V}^{-1} \text{s}^{-1}$)	μ_H ($\text{cm}^2 \text{V}^{-1} \text{s}^{-1}$)	m_t^* (m_e)	ϵ_r or ϵ (ϵ_0)	n (10^{19}cm^{-3})	References
Ba ₈ Cu _{0.2} Si ₃₂ Ga _{13.8}	300	72.7	—	—	-41	1471	—	—	—	—	0.6	—	16	[381]
Si ₄₆	835	23.9	—	—	-101	813	—	—	—	—	—	—	—	[382]
Si ₁₃₆	400	—	59.9	—	—	9×10^{-7}	—	—	—	—	—	—	—	[383]
Si ₂₃₀	300	—	—	—	—	—	—	1.7-1.9	—	—	—	—	—	[382]
Si ₄₄₄	400	—	21.9	—	—	—	—	—	—	—	—	—	—	[382]
Si ₆₄₄	400	—	13.4	—	—	—	—	—	—	—	—	—	—	[382]
Ba ₈ Si ₄₆	400	—	12.6	7.6	—	6×10^{-7}	—	—	—	—	—	—	—	[382]
BaSi ₄₆	300	125	2.7	1.7	-60	1700	0.05	—	—	—	2.99	—	100	[384]
BaSi ₄₆	800	75.7	—	—	-141.2	1450	0.46	—	—	—	—	—	—	[384]
Ba ₈ Si ₃₀	400	—	8.7	—	—	—	—	—	—	—	—	—	—	[382]
Ba ₈ Si ₆₄	400	—	8.7	—	—	—	—	—	—	—	—	—	—	[382]
Nd _{5.1} Si ₁₃₆	300	6.7	7	6.9	-50	111.1	1.2×10^{-3}	—	—	—	—	—	—	[385]
Nd _{8.2} Si ₁₃₆	300	16.8	12	11.7	-35	400	1.2×10^{-3}	—	—	—	—	—	—	[385]
K ₉ Al ₈ Si ₃₈	300	1.1	1.8	1.8	-90	9.1	1.2×10^{-3}	69.8	—	39	0.01	—	0.031	[386]
C ₅₈ Ga ₈ Si ₃₈	300	0	1.7	1.7	24	0.1	1×10^{-6}	1.1	—	—	—	—	—	[386]
K ₉ Ga ₈ Si ₃₈	300	0.2	0.5	0.5	-33	4.5	3×10^{-4}	1.2	239.6	82	—	—	—	[386]
C ₆ Al ₈ Si ₃₈	400	—	—	—	—	—	1×10^{-4}	—	—	—	—	—	—	[387]
Rb ₉ Al ₈ Si ₃₈	300	0	0.93	0.9	-300	1.8×10^{-3}	2×10^{-5}	0.8	—	—	—	—	—	[387]
K ₉ Al ₈ Si ₃₈	300	0.3	1.24	1.2	-252	0.3	5×10^{-4}	0.7	—	—	—	—	—	[388]
Ca ₈ Na ₁₆ Al ₂₄ Si ₁₁₂	300	—	1.65	—	—	—	—	0.3	—	—	—	—	—	[389]
Si _{30.3} P _{15.7} Se _{7.93}	300	1	4.5	—	-32	24.8	—	—	—	—	—	—	—	[390]
Ba ₈ Al ₁₆ Ga ₂ Si ₂₆ P ₂	300	58.8	1.8	1.3	-60	800	0.06	0.7	—	—	—	—	30	[389]
	900	19.5	—	—	-150	400	0.47	—	—	—	—	—	—	[390]
Germanides														
Ge ₁₃₆	300	—	—	—	—	—	—	0.6-0.8	—	—	—	—	—	[383]
Ba ₈ Ge ₁₃ □ ₃	300	—	3.2	2.6	-10	769.2	0	—	—	—	—	—	—	[391]
	673	65.8	3.8	2	-39.4	4660	0.04	—	—	—	—	—	—	[392]
Ba ₈ Zr _{7.66} Ge _{3.65} Sb _{1.79}	300	70.6	1	—	-74	762.8	0.13	27.5	—	14	1.7	—	30	[392]
	850	22.3	0.9	0.4	-187	272.8	0.82	—	—	—	—	—	—	[392]

(Continued.)

Table 6. (Continued.)

Material	T (K)	μ_{sc} ($\text{cm}^2 \text{V}^{-1} \text{s}^{-1}$)	κ ($\text{W m}^{-1} \text{K}^{-1}$)	κ_L ($\text{W m}^{-1} \text{K}^{-1}$)	S ($\mu\text{V K}^{-1}$)	σ ($\Omega^{-1} \text{cm}^{-1}$)	zT	E_g (eV)	μ_0 ($\text{cm}^2 \text{V}^{-1} \text{s}^{-1}$)	μ_{HI} ($\text{cm}^2 \text{V}^{-1} \text{s}^{-1}$)	m_s^* (m_e)	ϵ_r or ϵ (ϵ_0)	n (10^{19}cm^{-3})	References
$\text{Ba}_8\text{Au}_{5.3}\text{Ge}_{10.7}$	300	95.9	1.3	0.8	112.2	606	0.2	0.3	—	—	0.49	—	4	[393]
	683	44	0.9	0.5	173.5	452.5	0.9	—	—	—	—	—	—	—
$\text{Ba}_{24}\text{Ge}_{100}$	300	54.4	2.6	1.3	-21.6	2100	0.01	—	8.6	2.4	3.35	—	550	[394]
	873	22	3.8	0.6	-50	1800	0.11	—	—	—	—	—	—	—
$\text{Ba}_{24}\text{Ag}_8\text{Ge}_{94}$	300	82	1.8	0.8	-42.5	1597	0.04	—	20.2	7.8	2.25	—	110	[394]
	873	24.2	2.3	0.5	-85	1100	0.31	—	—	—	—	—	—	—
$\text{Ba}_{24}\text{Cu}_8\text{Ge}_{94}$	300	21.3	2.3	1.6	-19.7	898	0.01	—	19.1	5.1	—	—	111	[394]
	873	12.3	2.2	1.3	-80	600	0.17	—	—	—	—	—	—	—
$\text{Ba}_8\text{Cu}_{5.1}\text{Ce}_{10.2}\text{Sh}_{0.7}$	300	89.4	1.7	0.9	-55	1333	0.07	0.2	27.1	11.9	1.56	—	43	[395]
	800	24.3	1.2	0.6	-153	403.2	0.62	—	—	—	—	—	—	—
$\text{Ba}_8\text{Cu}_{5.7}\text{Ce}_{10.3}$	329	111.1	1.3	1.1	210	250	0.26	0.3	12	9.6	3.9	—	—	[396]
	615	43.2	1.1	0.9	229	199.2	0.62	—	—	—	—	—	—	—
$\text{Ba}_8\text{Cu}_{5.13}\text{Ge}_{10.87}$	329	51.4	1.9	1.1	-44	1111	0.04	—	—	—	—	—	—	[396]
	773	25	1.6	0.9	-137	478.4	0.42	—	—	—	—	—	—	—
$\text{Ba}_8\text{Cu}_{5.93}\text{Ge}_{10.07}$	329	83	1.2	1.1	300	65.8	0.17	—	12.7	11	1.18	—	—	[396]
	573	35.7	1.1	1.1	299	65.8	0.3	—	—	—	—	—	—	—
$\text{Ba}_8\text{Cu}_6\text{Si}_{16}\text{Ge}_{24}$	300	41.2	1.1	0.9	-74	444.4	0.07	—	28.3	14.4	1.26	—	20	[397]
	673	20.8	1	0.6	-141	307.7	0.43	—	—	—	—	—	—	—
$\text{Eu}_{10.5}\text{Ba}_{7.5}\text{Cu}_6\text{Si}_{16}\text{Ge}_{24}$	300	42.4	1	0.7	-70	487.8	0.07	—	19.9	9.8	1.56	—	30	[397]
	673	22.4	0.85	0.4	-137	348.7	0.53	—	—	—	—	—	—	—
$\text{Eu}_1\text{Ba}_7\text{Cu}_6\text{Si}_{16}\text{Ge}_{24}$	300	44.5	1	0.65	-67	537.6	0.07	—	17.3	8.4	1.81	—	40	[397]
	673	24.3	0.7	0.2	-133.6	393.7	0.66	—	—	—	—	—	—	—
$\text{Eu}_{1.5}\text{Ba}_{6.5}\text{Cu}_6\text{Si}_{16}\text{Ge}_{24}$	300	46.4	0.9	0.5	-62	609.7	0.08	—	16.1	7.5	1.94	—	50	[397]
	673	24.1	0.7	0.1	-125	434.8	0.69	—	—	—	—	—	—	—
$\text{Ba}_8\text{Cu}_{15}\text{Si}_3\text{Ge}_{38}$	300	67	1.6	1	-55	1000	—	—	—	—	—	—	—	[398]
	823	22.5	1.5	0.6	-141	450.5	0.5	—	—	—	—	—	—	—
$\text{Ba}_8\text{Cu}_{15}\text{Ge}_{41}$	300	55.4	1.3	0.8	-80	546.5	0.08	—	23.7	12.5	1.13	—	—	[399]
	673	28.4	1.3	0.8	-170	298.5	0.44	—	—	—	—	—	—	—
$\text{Ba}_8\text{Cu}_{15}\text{Si}_6\text{Ge}_{45}$	300	60.6	1.4	0.5	-50	1000	0.05	—	17.6	7.4	1.44	—	—	[399]
	823	20.2	1.4	0.5	-139.7	411.5	0.45	—	—	—	—	—	—	—
$\text{Ba}_8\text{Cu}_{15}\text{Si}_{10}\text{Ge}_{31}$	300	61.2	1.7	0.9	-60	833.3	0.05	—	—	—	—	—	—	[399]
	773	23.3	1.7	0.9	-139.7	431	0.4	—	—	—	—	—	—	—

(Continued.)

Table 6. (Continued.)

Material	T (K)	μ_w ($\text{cm}^2 \text{V}^{-1} \text{s}^{-1}$)	κ ($\text{W m}^{-1} \text{K}^{-1}$)	κ_L ($\text{W m}^{-1} \text{K}^{-1}$)	S ($\mu\text{V K}^{-1}$)	σ ($\Omega^{-1} \text{cm}^{-1}$)	zT	E_g (eV)	μ_0 ($\text{cm}^2 \text{V}^{-1} \text{s}^{-1}$)	μ_{H} ($\text{cm}^2 \text{V}^{-1} \text{s}^{-1}$)	m_s^* (m_e)	ϵ_r or ϵ (ϵ_0)	n (10^{19}cm^{-3})	References
$\text{Ba}_8\text{Cu}_{15}\text{Si}_{18}\text{Ge}_{23}$	300	54.7	1.4	1.1	-115	333.3	0.09	—	13.0	8.2	1.16	—	18	[399]
	573	27.3	1.4	1.1	-160	253.1	0.3	—	—	—	—	—	—	[400]
$\text{Ba}_8\text{Cu}_6\text{Ge}_{20}\text{Si}_{20}$	300	32.9	1.3	0.7	-38.2	715.3	0.03	—	—	—	—	—	—	[400]
	720	13.2	1.15	0.6	-112.7	307.7	0.25	—	—	—	—	—	—	[377]
$\text{Ba}_8\text{Cu}_6\text{Si}_{16}\text{Ge}_{24}$ (4 GPa)	300	48.3	1.1	—	64.3	609.7	0.07	—	—	—	—	—	—	[377]
	673	23.8	0.8	—	129	408.1	0.55	—	—	—	—	—	—	[377]
$\text{Ba}_8\text{Cu}_6\text{Si}_{16}\text{Ge}_{24}$ (5 GPa)	300	41.8	1.05	—	50	689.6	0.05	—	—	—	—	—	—	[401]
	673	22.4	0.8	—	116	452.5	0.52	—	—	—	—	—	—	[401]
$\text{Ba}_8\text{Cu}_{4.5}\text{Si}_6\text{Ge}_{35.5}$	300	30	1.1	—	-25	1000	0.06	—	—	—	—	—	—	[401]
	873	22	2	0.8	-115	666.7	0.45	—	—	—	—	—	—	[401]
$\text{Ba}_8\text{Cu}_{4.8}\text{Ga}_{1.0}\text{Ge}_{40.2}$	300	—	2	0.7	—	—	0.05	—	—	—	—	—	—	[401]
	900	—	1.4	0.7	—	—	0.9	—	—	—	—	—	—	[401]
$\text{Ba}_8\text{Cu}_{4.65}\text{Ga}_{1.01}\text{Ge}_{40.35}$	300	91.2	—	—	-37	2049	—	58.5	—	21.2	1.29	—	56	[401]
$\text{Ba}_8\text{Cu}_{4.63}\text{Ga}_{1.02}\text{Ge}_{40.35}$	300	91.3	1.9	0.8	-37	2049	0.04	—	58.5	—	1.29	—	—	[401]
	900	29.8	1.4	0.7	-157	564.8	0.9	—	—	—	—	—	—	[401]
$\text{Ba}_8\text{Cu}_{4.78}\text{Ga}_{0.89}\text{Ge}_{40.33}$	300	86.5	—	—	-40.4	1776	—	51	—	19.3	1.35	—	—	[401]
	900	27.9	—	—	-159	515.5	—	38.8	—	15.1	1.36	—	—	[401]
$\text{Ba}_8\text{Cu}_{4.92}\text{Ga}_{0.75}\text{Ge}_{40.33}$	300	66.3	—	—	-42.9	1280	—	—	—	—	—	—	—	[401]
	900	24.4	—	—	-162	434.8	—	—	—	—	—	—	—	[402]
$\text{Ba}_8\text{Cu}_{4.6}\text{In}_{1.4}\text{Ge}_{40.0}$	300	92.5	1	—	-60.4	1250	0.1	—	97.4	44.8	1.41	—	40	[402]
$\text{Ba}_8\text{Ni}_{3.8}\text{Ge}_{42.2}$	300	1.8	0.9	0.9	125	10.1	—	—	—	—	—	—	—	[374]
	823	0.9	0.9	0.8	-83	40	0.02	—	—	—	—	—	—	[374]
$\text{Ba}_8\text{Ni}_{3.8}\text{Si}_{10}\text{Ge}_{32.2}$	300	26.2	1.3	0.8	-40.9	531.9	—	—	—	—	—	—	—	[374]
	823	10.2	1.4	0.8	-106	319.5	0.19	—	—	—	—	—	—	[351]
$\text{Ba}_8\text{Ni}_2\text{Ge}_{43-yy}$	300	27.6	2.2	—	-25.5	900.9	0.01	—	—	—	4.24	—	610	[351]
	650	42.6	2.9	2.2	-83.6	1269	0.2	—	—	—	4.5	—	360	[351]
$\text{Ba}_8\text{Ni}_3\text{Ge}_{42-yy}$	300	23.9	1.9	1.5	-38.5	515.5	0.01	—	—	—	—	—	—	[351]
	650	15.4	2.5	2	-104.8	341.3	0.1	—	—	—	—	—	—	[351]
$\text{Ba}_8\text{Ni}_{3.5}\text{Ge}_{42.5-yy}$	300	108	2.3	1.4	-67.2	1299	0.08	0.2	—	—	4.57	—	160	[351]
	600	13	2.4	—	-100	273.9	0.15	—	—	—	—	—	—	[351]
$\text{Ba}_8\text{Ni}_{3.8}\text{Ge}_{42.2-yy}$	300	45.8	1.9	1.8	-152	176.7	0.06	0.2	—	—	3.6	—	26	[351]
	500	34	2.6	1.9	-159.4	259	0.2	—	—	—	—	—	—	[351]
$\text{Ba}_8\text{Ni}_4\text{Ge}_{42-yy}$	300	51.1	1.9	1.8	-172	156	0.07	0.1	—	—	—	—	19	[351]
	450	25	1.6	1.6	-172	140.2	0.13	—	—	—	—	—	—	[351]
$\text{Ba}_8\text{Ni}_{4.2}\text{Ge}_{41.8-yy}$	300	52.7	1.5	1.4	215	97.4	0.07	0.1	—	—	9	—	75	[351]
$\text{Ba}_8\text{Ni}_{3.5}\text{Ge}_{42.1}\square_{0.4}$	300	63.7	2.1	1.4	-52.9	990	0.05	—	—	—	—	—	—	[403]
	680	34.5	3.1	—	-119.6	675.6	0.21	—	—	—	—	—	—	[403]

(Continued.)

Table 6. (Continued.)

Material	T (K)	μ_{av} ($\text{cm}^2 \text{V}^{-1} \text{s}^{-1}$)	κ ($\text{W m}^{-1} \text{K}^{-1}$)	κ_L ($\text{W m}^{-1} \text{K}^{-1}$)	S ($\mu\text{V K}^{-1}$)	σ ($\Omega^{-1} \text{cm}^{-1}$)	zT	E_g (eV)	μ_0 ($\text{cm}^2 \text{V}^{-1} \text{s}^{-1}$)	μ_{HI} ($\text{cm}^2 \text{V}^{-1} \text{s}^{-1}$)	m_s^* (m_e)	ϵ_r or ϵ (ϵ_0)	n (10^{19}cm^{-3})	References
$\text{Ba}_8\text{Ga}_{16.61}\text{Ge}_{29.30}$	300	65.7	1.8	—	38	1435	0.03	—	—	—	0.53	—	15	[404]
	773	56.3	1.7	—	177	670	0.93	—	—	—	—	—	—	
$\text{Ba}_8\text{Ga}_{16}\text{Ga}_{16.68}\text{Ge}_{29.16}$	300	75	1.7	—	46	1349	0.04	—	—	—	0.62	—	14.2	[404]
	773	56.5	1.6	—	192	564	1.02	—	—	—	—	—	—	
$\text{Ba}_8\text{Ga}_{16.81}\text{Ge}_{29.14}$	300	70.4	1.5	—	52	1115	0.05	—	—	—	0.56	—	10	[404]
	823	35.1	1.3	—	200	351	0.88	—	—	—	—	—	—	
$\text{Ba}_{7.9}\text{Ga}_{16.90}\text{Ge}_{29.20}$	300	60.9	1.3	—	62	800	0.06	—	—	—	0.47	—	6	[404]
	823	34.7	1.2	—	206	324	0.94	—	—	—	—	—	—	
$\text{Ba}_8\text{Ga}_{16.98}\text{Ge}_{28.97}$	300	58.2	1.2	—	77	600	0.07	—	—	—	0.11	—	0.8	[404]
	823	13.3	1	—	165	200	0.42	—	—	—	—	—	—	
$\text{Ba}_8\text{Ga}_{15.83}\text{In}_{0.09}\text{Ge}_{29.03}$	321	25.8	1	0.9	-126	151.5	0.08	—	—	—	—	—	—	[405]
	876	8.9	1.1	0.9	-212	84.7	0.31	—	—	—	—	—	—	
$\text{Ba}_8\text{Ga}_{15.59}\text{In}_{0.15}\text{Ge}_{27.27}$	321	29.2	1.2	1	-111	207.5	0.07	—	—	—	—	—	—	[405]
	876	9.4	1.2	0.9	-199	104.7	0.31	—	—	—	—	—	—	
$\text{Ba}_8\text{Ga}_{15.83}\text{In}_{0.31}\text{Ge}_{25.94}$	325	50.9	1	0.5	-82	549.5	0.13	—	—	—	—	—	—	[405]
	773	15.7	0.8	0.6	-203	137.7	0.52	—	—	—	—	—	—	
$\text{Ba}_8\text{Ga}_{16}\text{Ge}_{30}$ (3 GPa)	300	53.3	1.3	0.8	-66.8	645.1	0.07	—	—	—	—	—	—	[406]
	773	27.9	0.9	0.2	-173.1	347.2	0.97	—	—	—	—	—	—	
$\text{Ba}_8\text{Ga}_{16}\text{Ge}_{30}$ (4 GPa)	300	59.3	1.1	0.6	-63.6	757.6	0.08	—	—	—	—	—	—	[406]
	773	28.2	0.7	0	-170.2	363.6	1.14	—	—	—	—	—	—	
$\text{Ba}_8\text{Ga}_{16}\text{Ge}_{30}$ (5 GPa)	300	65.1	1.5	0.8	-61	869.5	0.07	—	—	—	—	—	—	[406]
	773	31.1	1	0.2	-167.6	413.2	0.92	—	—	—	—	—	—	
$\text{Ba}_8\text{Ga}_{16}\text{Ge}_{30}$	300	25.5	3	1.9	-70	500	0.04	0.5	—	—	2.48	—	60	[407]
	600	52.8	2.5	1.1	-140	400	0.25	—	—	—	3.61	—	50	
$\text{Ba}_8(\text{Ga}_{16})_{16}\text{Ge}_{30}$	373	56.2	1.4	1.2	-230	200	0.12	—	—	—	—	—	—	[408]
	823	27.2	1.1	—	-225	166.6	0.69	—	—	—	—	—	—	
$\text{Ba}_8(\text{Al}_{0.2}\text{Ga}_{0.8})_{16}\text{Ge}_{30}$	373	42.7	1.6	0.9	-58	833.3	0.07	—	—	—	—	—	—	[408]
	923	21	1.4	0.7	-156	400	0.67	—	—	—	—	—	—	
$\text{Ba}_8(\text{Al}_{0.23}\text{Ga}_{0.77})_{16}\text{Ge}_{30}$	373	51	—	—	-53	1053	0.1	—	—	—	—	—	—	[408]
	1073	—	—	—	-178	518	—	—	—	—	—	—	—	
$\text{Ba}_8(\text{Al}_{0.25}\text{Ga}_{0.75})_{16}\text{Ge}_{30}$	373	56.2	1.7	0.6	-49	1370	0.07	—	—	—	—	—	—	[408]
	1073	—	2.1	1	-163	515.5	0.93	—	—	—	—	—	—	
$\text{Ba}_8(\text{Al}_{0.33}\text{Ga}_{0.67})_{16}\text{Ge}_{30}$	373	30	1.9	1	-32.5	1053	0.02	—	—	—	—	—	—	[408]
	973	—	2.6	1.4	-113	724.6	0.33	—	—	—	—	—	—	

(Continued.)

Table 6. (Continued.)

Material	T (K)	μ_{Hv} ($\text{cm}^2 \text{V}^{-1} \text{s}^{-1}$)	κ ($\text{W m}^{-1} \text{K}^{-1}$)	κ_L ($\text{W m}^{-1} \text{K}^{-1}$)	S ($\mu\text{V K}^{-1}$)	σ ($\Omega^{-1} \text{cm}^{-1}$)	zT	E_g (eV)	μ_0 ($\text{cm}^2 \text{V}^{-1} \text{s}^{-1}$)	μ_{HI} ($\text{cm}^2 \text{V}^{-1} \text{s}^{-1}$)	m_s^* (m_e)	ϵ_r or ϵ (ϵ_0)	n (10^{19}cm^{-3})	References
$\text{Ba}_8(\text{Al}_{0.5}\text{Ga}_{0.5})_{16}\text{Ge}_{30}$	373	26.7	—	—	-26	1163	—	—	—	—	—	—	—	[408]
$\text{Ba}_8(\text{Al})_{16}\text{Ge}_{30}$	373	20	—	—	-12.5	1755	—	—	—	—	—	—	—	[408]
$\text{Ba}_8\text{Ga}_{16.1}\text{Zn}_{3.3}\text{Ge}_{26.9}$	300	35.8	1.4	1.4	162	123	0.07	—	41.4	30.1	0.27	—	0.7	[409]
	690	27.3	1.3	—	230	148	0.42	—	—	—	—	—	—	[409]
$\text{Ba}_8\text{Ga}_{16.2}\text{Zn}_{3.3}\text{Ge}_{26.8}$	300	43.3	1.4	1.4	160	152	0.08	—	39.6	28.7	0.71	—	3.3	[409]
	700	23.8	1.3	—	208	170	0.44	—	—	—	—	—	—	[409]
$\text{Ba}_8\text{Ga}_{16.3}\text{Zn}_{3.3}\text{Ge}_{26.7}$	300	39	1.5	1.5	140	174	0.06	—	36.4	24.9	0.7	—	4.3	[409]
	650	23.9	1.3	—	188	193	0.34	—	—	—	—	—	—	[410]
$\text{Ba}_8\text{Ga}_{16}\text{Zn}_{3.0}\text{Ge}_{27.0}$	300	36.1	1.3	1.3	230	56	0.07	—	59.7	48.9	0.49	—	0.7	[410]
	790	24.6	1.3	—	294	77.9	0.38	—	—	—	—	—	—	[410]
$\text{Ba}_8\text{Ga}_{16}\text{Zn}_{3.2}\text{Ge}_{26.8}$	300	27.6	1.4	1.3	250	34	0.06	—	35	29.3	0.58	—	0.7	[410]
	700	18.3	1.2	—	270	63.7	0.32	—	—	—	—	—	—	[411]
$\text{Ba}_8\text{Ga}_{16}\text{Ge}_{28}\text{Zn}_2$	300	50.1	1.3	0.2	-125	268.8	0.1	—	—	—	—	—	—	[411]
	773	24.5	1.2	1.1	-250	125	0.51	—	—	—	—	—	—	[411]
$\text{Ba}_8\text{Ga}_{16}\text{Ge}_{30}$	300	68.5	0.9	0.5	-79.5	680.2	0.09	—	—	—	—	—	—	[411]
	873	22.7	1.4	0.9	-205.7	232.5	0.65	—	—	—	—	—	—	[412]
$\text{Ba}_{8.01}\text{Ga}_{15.79}\text{Al}_{2.95}\text{Ge}_{26.91}$	300	46.2	1.1	1	187	118.2	0.12	—	5.6	4.3	2.8	—	17.4	[412]
	760	23.4	1	1	255	109.7	0.61	—	—	—	—	—	—	[412]
$\text{Ba}_{7.92}\text{Ga}_{15.84}\text{Al}_{3.38}\text{Ge}_{26.50}$	300	38.8	1.2	1.2	168	123.9	0.09	—	5.9	4.3	2.43	—	18.3	[412]
	780	26	1.1	1.1	247	138.8	0.55	—	—	—	—	—	—	[412]
$\text{Ba}_{7.89}\text{Ga}_{15.92}\text{Al}_{1.89}\text{Ge}_{27.12}$	300	34.2	1.1	1.1	200	75.3	0.09	—	4.9	3.8	2.51	—	12.4	[412]
	850	18.9	1	1	264	94.4	0.53	—	—	—	—	—	—	[413]
$\text{Ba}_8\text{Ga}_{15}\text{Ge}_{31}$	300	65.4	1.8	1.1	-47	1150	0.45	—	19.6	8	2.1	—	5.6	[413]
	723	30	1.4	—	-121	632.9	0.05	—	—	—	—	—	—	[414]
$\text{Ba}_8\text{Ga}_{16}\text{Ge}_{30}$	300	85	1.8	0.7	-45	1562	0.05	0.3	—	—	2.6	—	27.8	[414]
	1043	22.3	1.7	0.2	-150	571.4	0.8	—	—	—	—	—	—	[415]
$\text{Ba}_8\text{Ga}_{16.6}\text{Ge}_{28.7}$	300	58.8	—	1.2	60	800	0.06	—	—	—	0.29	—	3	[415]
	823	44.2	1.2	0.7	234	298	1.1	—	—	—	—	—	—	[416]
$\text{Yb}_{0.3}\text{Ba}_{7.7}\text{Ga}_{16}\text{Ge}_{30}$	300	31.8	1.6	1.2	-56.9	457.1	0.03	—	23.7	10.6	1.25	—	29.3	[416]
	950	24.1	1.3	0.8	-206	278.2	0.83	—	—	—	—	—	—	[416]
$\text{Yb}_{0.5}\text{Ba}_{7.5}\text{Ga}_{16}\text{Ge}_{30}$	300	34.5	1.5	1.1	-60	469.6	0.03	—	17.4	8	1.78	—	46.2	[416]
	950	26.6	1.2	0.6	-198.3	336.8	1.02	—	—	—	—	—	—	[416]
$\text{Yb}_{0.7}\text{Ba}_{7.3}\text{Ga}_{16}\text{Ge}_{30}$	300	62.5	1.7	0.9	-50	1030	0.04	—	22.9	9.6	1.79	—	61.2	[416]
	950	32.3	1.5	0.6	-176	530	1.1	—	—	—	—	—	—	[416]

(Continued.)

Table 6. (Continued.)

Material	T (K)	μ_{av} (cm ² V ⁻¹ s ⁻¹)	κ (W m ⁻¹ K ⁻¹)	κ_L (W m ⁻¹ K ⁻¹)	S (μ V K ⁻¹)	σ (Ω^{-1} cm ⁻¹)	zT	E_g (eV)	μ_0 (cm ² V ⁻¹ s ⁻¹)	μ_H (cm ² V ⁻¹ s ⁻¹)	m_s^* (m _e)	ϵ_r or ϵ (ϵ_0)	n (10 ¹⁹ cm ⁻³)	References
Ba ₈ Ni _{0.31} Zn _{0.32} Ga _{13.06} Ge _{32.2}	300	67.2	1.8	0.9	-47.8	1160	0.06	—	41.8	17.2	—	—	—	[417]
	1000	28	1.3	—	-193	406.9	1.2	—	—	—	—	—	—	[418]
Ba _{7.7} Yb _{0.3} Ni _{0.1} Zn _{0.54} Ga _{13.8} Ge _{31.56}	300	6.9	1.7	0.8	-40	142.8	0.05	—	—	—	—	—	—	[419]
	900	2.7	1.3	0.3	-150	55.6	0.91	—	—	—	—	—	—	[420]
Ba ₈ Sb ₂ Ga ₁₄ Ge ₃₀	300	70.8	2	1.3	-52.5	1110	0.05	—	—	—	—	—	—	[420]
	900	39	1.7	0.4	-154.4	760	1.05	—	—	—	—	—	—	[420]
Ba ₈ Ga ₁₆ Si ₁₁ Ge ₁₉	300	16.1	—	0.5	-103	114.9	0.07	—	6.6	3.9	0.92	—	18.4	[420]
Ba ₈ Ga ₁₆ Si ₁₃ Ge ₁₇	300	14.4	—	0.4	-88	126.5	0.06	—	6.7	3.7	0.86	—	21.6	[420]
Ba ₈ Ga ₁₆ Si ₁ Ge ₂₆	300	2	—	0.5	-67	24.2	0.01	—	2.9	1.4	0.41	—	11.2	[420]
Ba ₈ Ga ₁₆ Sb ₉ Ge ₂₁	300	15.5	—	0.6	-112	98	0.06	—	6.1	3.8	0.93	—	16.1	[420]
Si ₈ Ga ₁₆ Ge ₃₀	300	99.3	1.5	1.2	-100	738	0.11	—	13.6	8	1.28	—	41.4	[420]
	800	—	1.5	0.9	-160	—	0.72	—	—	—	—	—	—	[420]
Si ₈ Ga _{15.5} In _{0.5} Ge ₃₀	300	104.5	1.3	0.7	-80	1030	0.16	—	29.6	15.6	0.75	—	43	[420]
	800	28.7	1.2	0.5	-152	483	0.65	—	—	—	—	—	—	[420]
Si ₈ Ga ₁₅ In ₁ Ge ₃₀	300	125.3	1.5	0.7	-70	1440	0.13	—	37.5	19.8	0.44	—	40.1	[420]
	800	32.6	1.5	0.4	-132	698	0.51	—	—	—	—	—	—	[421]
Na ₈ Ga _{8.4} Ge _{16-8.4}	300	81.9	2.1	2	-270	80	0.07	—	5.8	4.9	5.5	—	10.3	[421]
Na ₈ Ga _{8.1} Ge _{16-8.1}	300	85.4	2.3	2.1	-160	300	0.1	0.5	10.2	7.4	4.8	—	26	[421]
	817	30.3	1.7	1.5	-242.5	183	0.48	—	—	—	—	—	—	[421]
Na ₈ Ga _{8.1} Ge _{16-8.1}	300	128.1	2.5	2.1	-136	600	0.13	—	11.2	7.6	4.6	—	26	[421]
	817	38.2	1.9	1.5	-212.5	327	0.63	—	—	—	—	—	—	[421]
Na ₈ Ge _{7.8} Ge _{16-7.8}	300	126.3	2.7	2.3	-112	800	0.1	—	11.1	6.9	4.8	—	72	[421]
	817	36.6	2.1	1.5	-184	436	0.56	—	—	—	—	—	—	[421]
Na ₈ Ge _{7.5} Ge _{16-7.5}	300	129.6	3	2.5	-105	900	0.11	—	10.6	6.4	5.1	—	90	[421]
	817	36.4	2.3	1.6	-174	487	0.53	—	—	—	—	—	—	[421]
Na ₈ Ge _{7.4} Ge _{16-7.4}	300	175.3	3.3	2.5	-89	1517	0.87	—	11.9	6.6	5	—	120	[421]
	817	39.8	2.5	1.7	-160	628	0.47	—	—	—	—	—	—	[421]
K ₈ Al ₈ Ge ₃₈	300	16.8	1.3	0.9	-35.8	390	0.01	—	10.5	3.7	0.28	—	6.3	[422]
K ₈ Ga ₈ Ge ₃₈	300	—	1.1	—	4.2	0.9	2 × 10 ⁻⁶	—	—	—	—	—	—	[422]
Rb _{7.88} Au _{0.47} Ge _{13.53}	300	—	2	2	-13	5	1.3 × 10 ⁻⁵	—	—	—	—	—	—	[423]
K ₇ Sr ₁₇ Ga ₁₀ Ge ₉₆	300	23.7	2.3	2.2	-80	280	0.02	—	56.9	30	0.62	—	5.7	[424]
	800	39.1	1.9	1.4	-170	330	0.43	—	—	—	—	—	—	[425]
Si _{7.92} Ga _{15.04} Sn _{0.35} Ge _{30.69}	298	117.8	1.7	—	-80	1150	0.15	—	59.1	31.2	0.17	—	2.3	—
	750	61.4	1.6	—	-190	600	1	—	—	—	—	—	—	(Continued.)

Table 6. (Continued.)

Material	T (K)	μ_{Hv} ($\text{cm}^2 \text{V}^{-1} \text{s}^{-1}$)	κ ($\text{W m}^{-1} \text{K}^{-1}$)	κ_L ($\text{W m}^{-1} \text{K}^{-1}$)	S ($\mu \text{V K}^{-1}$)	σ ($\Omega^{-1} \text{cm}^{-1}$)	zT	E_g (eV)	μ_0 ($\text{cm}^2 \text{V}^{-1} \text{s}^{-1}$)	μ_{Hl} ($\text{cm}^2 \text{V}^{-1} \text{s}^{-1}$)	m_{H^*} (m_e)	ϵ_r or ϵ (ϵ_0)	n (10^{19}cm^{-3})	References
Stannides														
$\text{Ba}_8\text{Ga}_{16}\text{Sn}_{30}$ (SC)	300	17.3	0.7	—	-138.8	78.5	0.11	—	30.6	20.9	0.33	—	3.8	[426]
$\text{Ba}_8\text{Ga}_{16}\text{Zn}_{0.5}\text{Sn}_{30}$ (SC)	510	24.8	0.8	—	-221.3	94.5	0.31	—	—	—	—	—	—	[426]
$\text{Ba}_8\text{Ga}_{16}\text{Zn}_{0.5}\text{Sn}_{30}$ (SC)	300	13.7	0.7	—	-115.7	82.8	0.08	—	32.8	20.6	0.28	—	3.7	[426]
$\text{Ba}_8\text{Ga}_{16}\text{Zn}_1\text{Sn}_{30}$ (SC)	510	16.9	0.8	—	-196	86.3	0.22	—	—	—	—	—	—	[426]
$\text{Ba}_8\text{Ga}_{16}\text{Zn}_1\text{Sn}_{30}$ (SC)	300	18.9	0.7	—	-147.8	76.6	0.13	—	21	14.7	0.37	—	5.5	[426]
$\text{Ba}_8\text{Ga}_{16}\text{Zn}_{1.5}\text{Sn}_{30}$ (SC)	300	43.6	0.8	—	-270	94.5	0.45	—	—	—	—	—	—	[426]
$\text{Ba}_8\text{Ga}_{16}\text{Zn}_{1.5}\text{Sn}_{30}$ (SC)	300	47.9	0.7	—	-212	91.7	0.22	—	24	19.2	0.47	—	3.6	[426]
$\text{Ba}_8\text{Ga}_{16}\text{Zn}_{1.5}\text{Sn}_{30}$ (SC)	540	84.8	0.8	—	-346	83	0.63	—	—	—	—	—	—	[427]
$\text{Ba}_8\text{Ga}_{15.82}\text{Sn}_{30.18}$ (SC)	300	—	—	—	-200	333.3	—	—	—	—	1.46	—	5.5	[427]
$\text{Ba}_8\text{Ga}_{15.88}\text{Sn}_{30.11}$ (SC)	300	144.6	0.7	0.6	-240	200	0.45	0.4	—	—	1.5	—	4.3	[427]
$\text{Ba}_8\text{Ga}_{15.92}\text{Sn}_{30.08}$ (SC)	490	100.5	0.8	0.5	-303	139.8	0.85	—	—	—	—	—	—	[427]
$\text{Ba}_8\text{Ga}_{15.93}\text{Sn}_{30.07}$ (SC)	300	148.3	—	—	370	45.5	—	—	—	—	—	—	11	[427]
$\text{Ba}_8\text{Ga}_{15.94}\text{Sn}_{30.06}$ (SC)	300	191.4	—	—	280	166.6	—	—	—	—	—	—	17	[427]
$\text{Ba}_8\text{Ga}_{15.95}\text{Sn}_{30.03}$ (SC)	300	184.2	—	—	-290	142.8	—	—	—	—	—	—	3.3	[427]
$\text{Ba}_8\text{Ga}_{15.97}\text{Sn}_{30.02}$ (SC)	300	182.6	—	—	320	100	—	0.4	—	—	4.3	—	14	[427]
$\text{Ba}_8\text{Ga}_{15.82}\text{Sn}_{30.22}$ (SC)	300	31.8	0.7	0.7	220	55.5	0.04	—	—	—	—	—	—	[398]
$\text{Ba}_8\text{Ga}_{15.92}\text{Sn}_{30.12}$ (SC)	300	48.1	1.2	1	-110	312.5	0.06	—	—	—	0.43	—	3.4	[398]
$\text{Ba}_8\text{Ga}_{15.92}\text{Sn}_{30.12}$ (SC)	300	36.2	0.8	0.8	-300	25	0.03	—	—	—	2.34	—	3.2	[398]
$\text{Ba}_8\text{Ga}_{16.02}\text{Sn}_{30.02}$ (SC)	300	85.7	1	0.9	-180	238.1	0.23	—	—	—	0.95	—	3.8	[398]
$\text{Ba}_8\text{Ga}_{16.12}\text{Sn}_{29.92}$ (SC)	300	42.1	1	0.9	150	166.6	0.06	—	—	—	2.71	—	28	[398]
$\text{Ba}_8\text{Ga}_{15.8}\text{Cu}_{0.033}\text{Sn}_{30.17}$ (SC)	300	163.9	0.7	0.6	-215	303	0.55	—	71.2	57.2	1.1	—	35	[428]
$\text{Ba}_8\text{Ga}_{15.8}\text{Cu}_{0.018}\text{Sn}_{30.19}$ (SC)	550	118.5	0.7	—	-307	187.2	1.38	—	—	—	—	—	—	[428]
$\text{Ba}_{7.99}\text{Ga}_{15.84}\text{Cu}_{0.004}\text{Sn}_{30.16}$ (SC)	300	158.6	0.7	0.6	-235	232.5	0.51	—	54.9	45.2	1.1	—	31	[428]
$\text{Ba}_8\text{Ga}_{15.8}\text{In}_{0.1}\text{Sn}_{30.1}$ (SC)	550	102.3	0.8	—	-311	154.3	1.1	—	—	—	—	—	—	[428]
$\text{Ba}_8\text{Ga}_{15.8}\text{In}_{0.1}\text{Sn}_{30.1}$ (SC)	300	315.7	0.8	—	395.7	71.9	0.39	—	2.8	2.5	6.2	—	18	[429]
$\text{Ba}_8\text{Ga}_{15.8}\text{In}_{0.1}\text{Sn}_{30.1}$ (SC)	460	321.7	0.8	—	470	58.8	0.71	—	—	—	—	—	—	[429]
$\text{Ba}_8\text{Ga}_{15.66}\text{In}_{0.2}\text{Sn}_{30.14}$ (SC)	300	107.2	0.7	0.5	-195	250	0.42	—	62.6	48.8	0.96	—	3.1	[429]
$\text{Ba}_8\text{Ga}_{15.66}\text{In}_{0.2}\text{Sn}_{30.14}$ (SC)	525	71	—	0.4	-272	157	0.95	—	—	—	—	—	—	[429]
$\text{Ba}_8\text{Ga}_{15.66}\text{In}_{0.2}\text{Sn}_{30.14}$ (SC)	300	121.3	0.7	0.4	-175	357.1	0.5	—	79.5	59.6	0.98	—	3.8	[430]
$\text{Ba}_8\text{Ga}_{15.7}\text{Cu}_{0.3}\text{Sn}_{30}$ (SC)	540	79.2	0.8	0.4	-250	235.8	1.05	—	—	—	—	—	—	[430]
$\text{Ba}_8\text{Ga}_{15.7}\text{Cu}_{0.3}\text{Sn}_{30}$ (SC)	300	0	0.7	0.5	-210	0	0.53	—	71.7	57.2	1.39	—	4.5	[430]
$\text{Ba}_8\text{Ga}_{15.7}\text{Cu}_{0.3}\text{Sn}_{30}$ (SC)	540	0	0.7	0.4	-303	0	1.35	—	—	—	—	—	—	[430]

(Continued.)

Table 6. (Continued.)

Material	T (K)	μ_w ($\text{cm}^2 \text{V}^{-1} \text{s}^{-1}$)	κ ($\text{W m}^{-1} \text{K}^{-1}$)	κ_L ($\text{W m}^{-1} \text{K}^{-1}$)	S ($\mu\text{V K}^{-1}$)	σ ($\Omega^{-1} \text{cm}^{-1}$)	zT	E_g (eV)	μ_0 ($\text{cm}^2 \text{V}^{-1} \text{s}^{-1}$)	μ_{H} ($\text{cm}^2 \text{V}^{-1} \text{s}^{-1}$)	m_s^* (m_e)	ϵ_r or ϵ (ϵ_0)	n (10^{19}cm^{-3})	References
Ba ₈ Ga ₁₄ Sn ₃₀	300	191.6	—	—	−385	49.4	0.36	—	33.7	30.1	2.40	—	1.2	[431]
485	397.8	—	—	—	−523	42.6	0.82	—	—	—	—	—	—	—
Ba ₈ Ga ₁₂ Sn ₃₀	300	46.3	—	—	−225	76.3	0.28	—	41.4	33.7	—	—	1.0	[431]
485	47.9	—	—	—	−305	64.2	0.5	—	—	—	—	—	—	—
Ba ₈ Ga ₁₈ Sn ₃₀	300	75.9	—	—	275	70	0.2	—	31.5	26.9	1.62	—	2.5	[431]
485	57.7	—	—	—	326	60.6	0.45	—	—	—	—	—	—	—
Ba ₈ Ga ₁₆ Sn ₃₀	300	—	—	—	0	—	0.15	—	—	—	—	—	—	[345]
Ba _{6,03} Ga _{15,7} Zn _{0,07} Sn _{30,3}	300	181.9	—	—	−220	219.3	0.4	—	51.2	41.4	1.2	—	3.3	[432]
550	—	—	—	—	−325	—	0.85	—	—	—	—	—	—	—
Ba _{7,95} Ga _{15,97} Sn _{30,03}	300	231.4	—	—	325	100	0.5	—	—	—	7.65	—	14	[427]
450	135.8	—	—	—	350	83.3	0.9	—	—	—	—	—	—	—
Ba _{7,77} Eu _{0,12} Ga _{15,83} Sn _{30,28}	300	225.6	—	—	330	110	—	—	7.3	6.4	1.94	—	10	[433]
480	244.2	—	—	—	415	90	0.88	—	—	—	—	—	—	—
Ba ₈ Ga ₁₀ Al ₆ Sn ₃₀	300	196.8	0.7	—	−244	260	0.63	—	48.4	40.3	0.67	—	4.6	[434]
500	142.7	—	—	—	−300.8	210	1.2	—	—	—	—	—	—	—
Ba ₈ Ga ₈ Al ₈ Sn ₃₀	300	188.1	0.8	—	−247	240	0.48	—	39.7	33.1	0.67	—	4.5	[434]
500	123.4	—	—	—	−298.7	186	1.03	—	—	—	—	—	—	—
Ba ₂₂ Ga ₁₆ Sn ₉₀	200	0	—	—	95	0.1	—	—	—	—	—	—	—	[435]
300	0	0	3.4	—	−46	0.5	1×10^{-5}	—	11.7	4.7	0.2–0.25	—	0.03	—
400	0.6	—	—	—	−225	1.4	0.02	—	—	—	—	—	—	—
Ba ₂₁ Ga ₁₉ Sn ₈₇	170	0	—	—	45	0	—	—	—	—	—	—	—	[435]
300	0.1	—	3.3	—	−200	0.3	—	—	7.5	5.9	0.03	—	0.01	—
400	1.3	—	—	—	−305	1.3	—	—	—	—	—	—	—	—
Cs ₈ Ba ₁₆ Ga ₄₁ Sn ₉₅	300	28.9	13.7	12.1	−124	157	0.04	—	60.1	39	0.63	—	24	[436]
687	30.9	—	10.9	9.3	−185	281	0.6	—	—	—	—	—	—	—
Cs ₈ Ba ₁₆ Ga ₄₁ Sn ₉₅	300	40	15	13	−115	244	0.06	—	81.3	51	0.59	—	3	[436]
687	40.5	—	11	8.8	−188	355	0.75	—	—	—	—	—	—	—
Cs ₈ Ba ₁₆ Ga ₄₁ Sn ₉₅	300	17.7	13.7	12.5	−117	105	0.03	—	34.8	22	0.64	—	3.1	[436]
687	32.4	—	11.9	10.9	−204	236	0.56	—	—	—	—	—	—	—
Cs ₈ Ba ₁₆ Ga ₄₀ Sn ₉₆	300	37	14.7	12.5	−131	184	0.05	—	57.1	38	0.68	—	3.1	[436]
740	41.1	—	11.3	7.4	−200	350	0.87	—	—	—	—	—	—	—
K ₇ Ba ₉ Ga ₂₆ Sn ₁₁₀	300	8.2	0.4	0.4	−147.7	33.3	0.06	—	—	—	0.45	—	3.1	[437]
575	117.3	—	0.4	0.2	−162.3	1064	0.58	—	—	—	—	—	—	—
K ₅ Ba ₁₃ Ga ₂₃ Sn ₁₁₃	300	185.1	0.3	0.2	−114.4	1136	0.24	—	—	—	0.51	—	6.2	[437]
575	88.5	—	0.4	0.1	−133.3	1136	0.6	—	—	—	—	—	—	—
K _{7,1} Ba _{16,9} Ga _{41,3} Sn _{94,7}	300	133.4	1.3	0.7	−100	991	0.23	—	240.1	141	0.6	—	—	[438]
640	56.3	—	1.2	0.5	−167	567	0.93	—	—	—	—	—	—	—
K ₉ Ba ₁₅ Al ₁₁ Ga ₈ Sn ₉₇	300	77.3	0.5	0.45	−170	150	0.25	—	54	40	0.9	—	2.3	[439]
640	35.4	—	0.6	0.45	−250	100	0.82	—	—	—	—	—	—	—

(Continued.)

Table 6. (Continued.)

Material	T (K)	μ_w ($\text{cm}^2 \text{V}^{-1} \text{s}^{-1}$)	κ ($\text{W m}^{-1} \text{K}^{-1}$)	κ_L ($\text{W m}^{-1} \text{K}^{-1}$)	S ($\mu\text{V K}^{-1}$)	σ ($\Omega^{-1} \text{cm}^{-1}$)	zT	E_g (eV)	μ_0 ($\text{cm}^2 \text{V}^{-1} \text{s}^{-1}$)	μ_{H} ($\text{cm}^2 \text{V}^{-1} \text{s}^{-1}$)	m_e^* (m_e)	ϵ_r or ϵ (ϵ_0)	n (10^{19}cm^{-3})	References
Ba _{13.2} K _{10.8} Ga _{36.7} Sn _{89.4}	300	202.2	—	—	-50	3333	—	—	—	—	—	—	—	[440]
Rb ₈ Sn ₄₄	300	3.7	2	1	-7.3	6291	—	—	3	0.5	1.32	—	—	[441]
C ₈ Sn ₄₄	300	5.8	1.8	1.8	-160	12.5	4.7×10^{-3}	—	13.8	10	0.38	—	—	[442]
C ₈ Zn ₄ Sn ₄₂	300	16.1	2.7	2.7	-212.5	20.8	0.02	—	—	8.3	0.45	—	—	[442]
Rb ₈ Ga ₈ Sn ₃₈	300	5.6	—	—	-143.8	14.3	—	—	—	0.6	0.14	—	—	[442]
Rb ₈ Ga ₈ Sn ₃₈	300	—	1.2	1.2	-145	—	8×10^{-4}	—	—	—	—	—	—	[345]
K ₉ Ga ₇ Sn ₃₉	300	105.9	1.3	1.2	-175	195.7	0.12	—	—	—	—	—	—	[443]
K ₅ Ga ₈ Sn ₃₈	300	185.6	1.2	1.1	-235	194.2	0.17	—	—	—	—	—	—	[443]
K ₉ Ga ₈ Sn ₃₈	300	—	1.2	1.1	-230	—	0.17	—	30.5	25	1.7	—	—	[443]
K ₉ Ga _{7.9} Sn _{37.9}	300	754	2	2	-220	909.1	0.07	—	—	—	—	—	—	[444]
K ₉ Ga ₈ Sn ₃₈	300	167.3	—	0.12	-270	125	0.16	—	36.4	31	1.8	—	3.2	[445]
K ₉ Al ₈ Sn ₃₈	300	70.1	—	0.14	-265	55	0.09	—	4.8	4.1	4.3	—	—	[445]
K ₉ In ₈ Sn ₃₈	300	110.3	—	0.13	-250	100	0.13	—	11.7	9.8	3.2	—	—	[445]
K ₈ Zn ₄ Sn ₄₂	300	45.8	1.6	1.6	-200	66.7	0.08	—	—	—	—	—	—	[446]
Nb ₂ ZnSn ₅	295	258.2	1.9	1.1	-111	1070	0.21	—	—	—	—	—	—	[447]
	400	212.8	2.2	1.3	-130	1000	0.3	—	—	—	—	—	—	[447]
Phosphides														
Ba ₈ Cu ₁₆ P ₃₀	300	13	1.3	0.8	12.7	847.5	0.02	0.5	19.6	4.3	17.1	—	33	[448]
	900	6	1.4	0.4	50.7	510.2	0.09	—	—	—	—	—	—	[448]
Bar _{7.3} La _{0.7} Cu ₁₆ P ₃₀	300	22.4	1	0.7	30	621	0.03	—	90.3	29.5	0.17	—	3.8	[448]
Bar _{7.1} La _{0.9} Cu ₁₆ P ₃₀	900	10.5	1.2	0.6	111	348.4	0.32	—	—	—	—	—	—	[448]
	300	25.8	1.1	0.8	39	549.5	0.03	—	83.4	31	0.09	—	1	[448]
	900	12	1.1	0.5	128	321.5	0.43	—	—	—	—	—	—	[448]
Ba _{6.4} La _{1.6} Cu ₁₆ P ₃₀	300	44.5	1	0.9	73	487.8	0.08	0.4	449.8	227	16.1	—	0.5	[448]
	900	13.9	0.9	0.6	170	225.2	0.63	—	—	—	—	—	—	[448]
Ba ₈ Cu ₁₆ P ₃₀	300	0	1.2	—	12.8	0	4×10^{-3}	—	—	—	—	—	—	[449]
	812	1.3	1.4	—	46	102	0.07	—	—	—	—	—	—	[449]
Ba ₈ Cu ₁₄ Ge ₆ P ₂₆	300	9.2	0.8	—	101.5	66.7	0.03	—	—	—	—	—	—	[449]
	812	0	0.7	—	234	0	0.63	—	—	—	—	—	—	[449]
Ba ₈ Cu ₁₄ Zn ₂ P ₃₀	298	—	—	—	80	—	—	—	—	—	—	—	—	[450]
Ba ₈ Cu ₁₄ Zn ₂ P ₃₀	800	17.4	0.9	0.6	202	162.6	0.62	—	—	—	—	—	—	[450]
Ba ₈ Cu ₁₄ Zn ₂ P ₃₀	300	9.2	0.8	0.7	102	66.6	0.02	—	—	—	—	—	—	[451]
Ba ₈ Cu ₁₄ Ge ₆ P ₂₆ (SC)	812	15.4	0.7	0.6	234	102	0.63	—	—	—	—	—	—	[449]
Ba ₈ Cu ₁₆ P ₃₀	275	15.1	1.1	—	12.5	877.1	3.5×10^{-3}	—	—	—	—	—	—	[452]
	300	—	—	—	12.8	—	—	—	—	—	—	—	—	[452]
Ba ₈ Cu ₄ Au ₁₂ P ₃₀	275	9	0.7	0.4	14.3	458.7	—	—	—	—	—	—	—	[452]
	300	—	—	—	15.3	—	3.8×10^{-3}	—	—	—	—	—	—	[452]
Ba ₈ Cu ₈ Au ₈ P ₃₀	275	9.8	1	0.6	14.8	483	—	—	—	—	—	—	—	[452]
	300	—	—	—	16.1	—	3.1×10^{-3}	—	—	—	—	—	—	[452]

(Continued.)

Table 6. (Continued.)

Material	T (K)	μ_w ($\text{cm}^2 \text{V}^{-1} \text{s}^{-1}$)	κ ($\text{W m}^{-1} \text{K}^{-1}$)	κ_L ($\text{W m}^{-1} \text{K}^{-1}$)	S ($\mu\text{V K}^{-1}$)	σ ($\Omega^{-1} \text{cm}^{-1}$)	zT	F_g (eV)	μ_0 ($\text{cm}^2 \text{V}^{-1} \text{s}^{-1}$)	μ_{H} ($\text{cm}^2 \text{V}^{-1} \text{s}^{-1}$)	m_s^* (m_e)	ϵ_r or ϵ (ϵ_0)	η (10^{19}cm^{-3})	References
Ba ₈ Cu ₁₂ Au ₄ P ₃₀	275	8.3	1	0.6	11	543.5	1.9×10^{-3}	—	—	—	—	—	—	[452]
Ba ₈ Au ₁₀ P ₃₀	275	12.9	0.6	—	15.3	613.5	0.01	—	—	—	—	—	—	[452]
Ba ₈ Au ₁₀ P ₃₀	300	—	—	—	15.3	—	—	—	—	—	—	—	—	[453]
Ba ₈ Au ₁₀ P ₃₀	300	11.1	0.6	0.2	15.8	588.2	—	—	—	—	—	—	—	[454]
Ba ₈ Au ₁₀ P ₃₀	390	7.5	0.7	0.2	16.2	571.4	0.01	—	—	—	—	—	—	[455]
Ba ₈ Au ₁₀ P ₃₀	300	3.9	5.2	3.1	0.9	2857	—	—	—	—	—	—	—	[456]
Ba ₈ Au ₁₀ P ₃₀	300	—	4.5	0.3	—	11933	—	—	—	—	0.37	—	—	[457]
Ba ₈ Au ₁₀ P ₃₀	300	27.3	4.2	—	1.6	12500	2.3×10^{-3}	—	—	—	—	—	—	[458]
Ba ₈ Au ₁₀ P ₃₀	300	15	1.7	1.5	30	416.6	6.6×10^{-3}	—	—	—	—	—	—	[459]
Ba ₈ Au ₁₀ P ₃₀	300	7.2	3	—	0.6	7143	3×10^{-5}	—	—	—	—	—	—	[460]
Ba ₈ Au ₁₀ P ₃₀	300	0	1	—	15	1000	0.05	—	—	—	—	—	—	[461]
Ba ₈ Au ₁₀ P ₃₀	300	1.4	0.4	0.4	389	0.3	4×10^{-4}	0.2	—	—	—	—	—	[462]
Ba ₈ Au ₁₀ P ₃₀	300	0.2	0.9	0.9	250	0.2	4×10^{-4}	0.3	1051.5	880	0.002	—	0.0001	[463]
Ba ₈ Au ₁₀ P ₃₀	300	—	0.8	0.8	150	—	—	0.7	—	—	—	—	—	[464]
Ba ₈ Au ₁₀ P ₃₀	300	—	0.9	0.9	150	—	—	0.6	—	—	—	—	—	[465]
Ba ₈ Au ₁₀ P ₃₀	300	0.4	0.8	—	80	4	1×10^{-3}	0.9	—	—	—	—	—	[466]
Ba ₈ Au ₁₀ P ₃₀	300	0.3	0.6	—	76	3.2	1×10^{-3}	0.1	—	—	—	—	—	[467]
Ba ₈ Au ₁₀ P ₃₀	300	0.2	0.5	—	63	2.6	6×10^{-4}	0.1	—	—	—	—	—	[468]
Ba ₈ Au ₁₀ P ₃₀	300	0.2	0.5	—	26	5.3	2×10^{-4}	0.1	—	—	—	—	—	[469]
Ba ₈ Au ₁₀ P ₃₀	300	17	0.7	—	17	833.3	0.01	2.5×10^{-2}	—	—	—	—	—	[470]
Ba ₈ Au ₁₀ P ₃₀	300	382.3	5	—	270	285.7	0.03	—	—	—	—	—	—	[471]
Ba ₈ Au ₁₀ P ₃₀	750	205.4	3.5	—	330	333.3	0.1	—	—	—	—	—	—	[472]
Ba ₈ Au ₁₀ P ₃₀	300	52.3	4.2	—	310	26.3	0	—	—	—	—	—	—	[473]
Ba ₈ Au ₁₀ P ₃₀	750	19.9	3	—	350	26.3	0.01	—	—	—	—	—	—	[474]
Ba ₈ Au ₁₀ P ₃₀	300	—	—	—	800	0.1	—	0.3	—	—	—	—	—	[475]
Ba ₈ Au ₁₀ P ₃₀	300	—	—	—	—	0	—	0.2	—	—	—	—	—	[476]
Ba ₈ Au ₁₀ P ₃₀	300	19.1	1.5	—	170	37	0.02	—	—	—	—	—	—	[477]
Ba ₈ Au ₁₀ P ₃₀	1100	3.3	1.4	—	210	30.3	0.36	—	—	—	—	—	—	[478]
Ba ₈ Au ₁₀ P ₃₀	300	85.9	3.2	3.1	170	166.7	0.05	—	—	—	—	—	—	[479]
Ba ₈ Au ₁₀ P ₃₀	870	38.7	2.9	2.6	270	142.8	0.3	—	—	—	—	—	—	[480]
Ba ₈ Au ₁₀ P ₃₀	300	—	0.7	—	—600	—	—	0.8	—	—	—	—	—	[481]
Ba ₈ Au ₁₀ P ₃₀	300	—	1.2	—	—800	—	—	1.2	—	—	—	—	—	[482]

GPa: applied pressure for the high pressure synthesis.

□: vacancy.

SC: single crystal.

3.7. FeGa₃-type

Intermetallic compounds with crystal structure of the FeGa₃ type

Raúl Cardoso-Gil

Max-Planck-Institut für Chemische Physik fester Stoffe, Nöthnitzer Straße 40, 01187 Dresden, Germany

Intermetallic compounds with composition $T^{(8)}Tr_3$, where $T^{(8)}$ is a TM of the group 8 and Tr being gallium or indium, are rather unexpectedly semiconductors with narrow band gap, originated by the hybridization of d and p orbitals of the participant atoms [465]. They crystallize in the tetragonal FeGa₃ structure type (space group $P4_2/mnm$, nr.139). In the crystal structure, the Ga2 (8j) atoms form double trigonal prisms capped by four Ga1 (4c) atoms and filled by two TM atoms (4f). The FeGa₃ type considered as a simple crystal structure, shows its complexity in its electronic structure. In FeGa₃ itself, the valence electron count of 17 ve/fu can be rationalized with atomic interactions isolobal to one Fe–Fe and eight Fe–Ga two-center-two electron bonds. The detailed bonding analysis shows the presence of three-center Fe–Ga–Ga' bonding having simultaneously a direct influence on the Fe–Fe bonding in the dumbbell [466]. The knowledge on the atomic interactions and bonding scenario is the key for the regulation of charge carrier and transport properties considering chemical insights. Additionally, the presence of different bonding types (bonding inhomogeneity) allows a reduction of the lattice thermal conductivity [467]. Thus, this particular electronic condition offers a suitable setup to tune the thermoelectric properties via chemical substitution. The consequent improvement of the thermoelectric properties has been accomplished tailoring the band gap with the synthesis of partially substituted derivatives. This concerning, the data compilation (table 7) shows a direct comparative view on the resulting thermoelectric properties of intermetallic compounds of the FeGa₃-type.

The narrow band gap of the binary semiconductors ranges between 0.2 and 0.5 eV. Their electrical conductivity increases significantly by substitution, e.g. from $\sigma(300K) = 3.2 \Omega^{-1} \text{ cm}^{-1}$ in RuIn₃ [468, 469] to $\sigma(300K) = 2128 \Omega^{-1} \text{ cm}^{-1}$ in RuIn_{2.90}Zn_{0.10} [470].

RuIn₃ and RuGa₃ are n -type semiconductors at $T < 360$ K and $T < 468$ K and p -type above these temperatures, respectively. The n - to p -type transition is selectively suppressed in RuIn₃ upon electron or hole doping, reaching $|S|$ values around $200 \mu\text{V K}^{-1}$ [468, 470]. FeGa₃ and OsGa₃ do not present this behavior. Noteworthy, the original binary compounds show high values of Seebeck coefficients at room temperature, e.g. $S = -563 \mu\text{V K}^{-1}$ and $S = -477 \mu\text{V K}^{-1}$ in FeGa₃ and OsGa₃, respectively [471].

The thermal conductivity of binary FeGa₃-type compounds is reduced to $\sim 30\%$ by substitutions, where Ru_{0.99}Ir_{0.01}In₃ with $\kappa = 1.55 \text{ W m}^{-1} \text{ K}^{-1}$ [472], Fe_{0.99}Co_{0.01}Ga_{2.99}Ge_{0.09} with $\kappa = 1.37 \text{ W m}^{-1} \text{ K}^{-1}$ [473] and ReGa₂Ge with $\kappa = 1.1 \text{ W m}^{-1} \text{ K}^{-1}$ [474] are those representatives with the lowest thermal conductivity at room temperature, attributed to the singular chemical substitutions. The ternary derivative ReGa₂Ge is a rather unusual chemical variant of the FeGa₃-type with a TM atom from the group 7 (Re) and Ge substituting gallium. Its stoichiometric composition, yields likewise a defined valence electron count of 17 ve/fu. The presence of Re–Ga and Re–Re interactions is also consistent with the reported band gap (0.23–0.4 eV) and the semiconductor behavior [474].

An essential condition for good thermoelectric materials is a reasonable electrical conductivity associated to a low electronic contribution to the thermal conductivity, this is fulfilled by certain intermetallic compounds with small band gap [475]. For further isostructural TTr_3 intermetallic compounds a theoretical study on their thermoelectric properties has been performed [476], based on these results, the corresponding experimental study is main part of an ongoing project. The acquired knowledge should strengthen the search and the development of further intermetallic compounds with high potential as thermoelectric materials, as well as the better understanding and control of their physical properties.

Table 7. FeGa₃-type thermoelectric properties.

Material	T (K)	μ_{w} (cm ² V ⁻¹ s ⁻¹)	κ_L (W m ⁻¹ K ⁻¹)	S (μ V K ⁻¹)	σ (Ω^{-1} cm ⁻¹)	zT {T}	E _g (eV)	μ_{H} (cm ² V ⁻¹ s ⁻¹)	m_s^* (m _e)	References
FeGa ₃	—	—	—	—	—	—	0.31 ^t	—	—	[465]
FeGa ₃	—	—	—	—	—	—	0.50 ^t	—	—	[477]
FeGa ₃	—	—	—	—	—	—	0.45–0.29 ^e	—	—	[478]
FeGa ₃	—	—	—	—	—	—	0.8 ^c	—	—	[478]
FeGa ₃	—	—	—	—	—	—	0.4 ^e	—	—	[479]
FeGa ₃	—	—	—	—	—	—	0.5 ^t	—	—	[476]
FeGa ₃	313	123.1	3.7	-563	4.3	—	0.3 ^t 0.26 ^c	12 (295)	5	[471]
FeGa ₃	298	0.4	5.3	1.47	183	—	—	—	—	[480]
FeGa ₃	300	1.3	~6.4	-350	0.5	0.000 14	0.47 ^c	—	0.2	[481]
FeGa ₃	290	10.8	2.14	-455	1.18	0.0023 {390 K}	—	—	—	[473]
FeGa _{2.95}	290	9.5	—	-518	0.5	—	—	—	—	[473]
FeGa _{3.05}	290	4.0	—	-400	0.83	—	—	—	—	[473]
FeGa _{2.991} Ge _{0.009}	290	2.8	—	-153	10	—	—	—	—	[473]
FeGa _{2.952} Ge _{0.048}	290	5.9	—	-98	43	—	—	—	—	[473]
FeGa _{2.901} Ge _{0.099}	290	3.4	—	-73	35	—	—	—	—	[473]
Fe _{0.99} Co _{0.01} Ga ₃	290	8.0	—	-196	17.5	—	—	—	—	[473]
Fe _{0.95} Co _{0.05} Ga ₃	290	4.2	—	-93	33	—	—	—	—	[473]
Fe _{0.90} Co _{0.10} Ga ₃	290	5.6	—	-95	42	—	—	—	—	[473]
Fe _{0.99} Co _{0.01} Ga _{2.991} Ge _{0.009}	290	6.8	1.37	-130	32.6	0.013 {390 K}	—	—	—	[473]
FeGa ₃	300	11.6	—	-5	1876	—	—	—	—	[482]
CoGa ₃	300	42.0	—	-6.3	5434	—	—	—	—	[482]
Fe _{0.75} Co _{0.25} Ga ₃	300	22.1	—	-8.1	2242	—	—	—	—	[482]
FeGa ₃	290	11.8	4.4	-360	3.85	—	—	—	—	[483]
FeGa ₃ [001]	290	201.1	4.4	-605	3.85	—	—	—	—	[483]
FeGa ₃ [100]	290	162.4	5.7	-590	3.7	—	—	—	—	[483]
FeGa _{2.95} Al _{0.05}	315	19.5	4.0	-550	0.8	0.020 {750 K}	—	—	—	[484]
FeGa _{2.90} Al _{0.10}	315	0.8	4.3	-140	4	0.015 {750 K}	—	—	—	[484]
FeGa _{2.97} In _{0.03}	315	0.4	4.6	-118	2.6	0.010 {750 K}	—	—	—	[484]
FeGa _{2.94} In _{0.06}	315	0.2	4.4	-48	2.9	0.006 {750 K}	—	—	—	[484]
FeGa _{2.97} Zn _{0.03}	315	2.6	3.6	310	1.7	0.016 {750 K}	—	—	—	[484]
FeGa _{2.94} Zn _{0.06}	315	31.9	3.2	420	5.9	0.016 {750 K}	—	—	—	[484]

(Continued.)

Table 7. (Continued.)

Material	T (K)	μ_{av} ($\text{cm}^2 \text{V}^{-1} \text{s}^{-1}$)	κ_{L} ($\text{W m}^{-1} \text{K}^{-1}$)	S ($\mu\text{V K}^{-1}$)	σ ($\Omega^{-1} \text{cm}^{-1}$)	zT { $\}$	E_{g} (eV)	μ_{H} ($\text{cm}^2 \text{V}^{-1} \text{s}^{-1}$)	m_{s}^* (m_{e})	References
FeGa _{2.95} Ge _{0.05}	315	53.7	3.1	-120	330	0.13 {667 K}	—	—	—	[484]
FeGa _{2.90} Ge _{0.10}	315	31.1	2.3	-70	385	0.10 {716 K}	—	—	—	[484]
FeGa _{2.80} Ge _{0.20}	315	51.1	1.9	-82	526	0.21 {765 K}	—	—	—	[484]
Fe _{0.995} Co _{0.005} Ga ₃	300	21.1	4.0	-213	40	0.014 {400 K}	—	—	—	[485]
Fe _{0.985} Co _{0.015} Ga ₃	300	18.2	3.6	-109	120	0.012 {400 K}	—	—	—	[485]
Fe _{0.975} Co _{0.025} Ga ₃	300	25.3	2.8	-109	167	0.029 {400 K}	—	—	—	[485]
Fe _{0.950} Co _{0.050} Ga ₃	300	28.9	3.4	-94	233	0.052 {400 K}	—	—	—	[485]
Fe _{0.875} Co _{0.125} Ga ₃	300	30.3	2.9	-79	303	0.037 {400 K}	—	—	—	[485]
Fe _{0.500} Co _{0.500} Ga ₃	300	34.9	2.6	-49	588	0.027 {400 K}	—	—	—	[485]
Fe ₂₅ Ga ₇₅	373	11.6	4.0	-334	7.5	~0.002 {773 K}	0.25 ^e	9 (300)	—	[486]
Fe ₂₅ Ga ₇₄ Sn ₁	373	50.8	3.1	-256	81	0.09 {473 K}	—	—	—	[486]
Fe ₂₅ Ga ₇₃ Sn ₂	373	49.3	2.8	-202	147	0.11 {573 K}	—	—	—	[486]
Fe ₂₅ Ga ₇₂ Sn ₃	373	40.1	2.3	-178	158	0.14 {524 K}	—	—	—	[486]
Ru ₂₅ Ga ₇₅	373	19.2	4.7	-522	1.4	0.09 {773 K}	0.33 ^c	10 (300)	—	[486]
Fe ₂₅ Ga ₇₄ Zn ₁	373	117.3	4.5	322	87	0.14 {737 K}	—	—	—	[486]
Fe ₂₅ Ga ₇₃ Zn ₂	373	100.9	5.0	307	89	0.21 {737 K}	—	—	—	[486]
Fe ₂₅ Ga ₇₂ Zn ₃	373	81.9	5.1	294	84	0.14 {737 K}	—	—	—	[486]
FeGa ₃	300	—	—	—	2.5	—	0.35 ^f 4.0 ^e	—	—	[487]
FeGa _{2.98} Zn _{0.02}	300	—	—	—	5.9	—	0.2 ^e	—	—	[487]
FeGa _{2.96} Zn _{0.04}	300	—	—	—	22	—	0.2 ^e	—	—	[487]
FeGa _{2.94} Zn _{0.06}	300	—	—	—	43	—	0.18 ^c	—	—	[487]
Fe _{0.986} Mn _{0.014} Ga ₃	300	—	—	—	0.14	—	0.33 ^c	—	—	[487]
Fe _{0.966} Mn _{0.034} Ga ₃	300	—	—	—	0.37	—	0.23 ^e	—	—	[487]
Fe _{0.916} Mn _{0.084} Ga ₃	300	—	—	—	20	—	0.14 ^f	—	—	[487]
Fe _{0.913} Mn _{0.087} Ga ₃	300	—	—	—	2.5	—	0.13 ^e	—	—	[487]
FeGa _{2.99} Ge _{0.01}	293	—	—	—	—	—	—	24 (300)	—	[488]
FeGa _{2.95} Ge _{0.07}	293	—	—	—	—	—	—	11.5 (300)	—	[488]
FeGa _{2.85} Ge _{0.15}	293	58.8	4.9	-118	333	0.14 {623 K}	—	—	—	[488]
FeGa _{2.75} Ge _{0.25}	293	66.5	4.5	-85	588	0.17 {673 K}	—	—	—	[488]
FeGa _{2.65} Ge _{0.35}	293	59.1	4.1	-77	588	0.20 {673 K}	—	—	—	[488]

(Continued.)

Table 7. (Continued.)

Material	T (K)	μ_{fw} ($\text{cm}^2 \text{V}^{-1} \text{s}^{-1}$)	κ_L ($\text{W m}^{-1} \text{K}^{-1}$)	S ($\mu\text{V K}^{-1}$)	σ ($\Omega^{-1} \text{cm}^{-1}$)	zT {T}	E_g (eV)	μ_H ($\text{cm}^2 \text{V}^{-1} \text{s}^{-1}$)	m_s^* (m_e)	References
Fe _{0.90} Co _{0.10} Ga _{2.65} Ge _{0.35}	293	54.3	2.7	-67	633	—	—	—	—	[488]
Fe _{0.85} Co _{0.15} Ga _{2.65} Ge _{0.35}	325	53.2	2.7	-73	658	0.25 {823 K}	—	—	—	[488]
Fe _{0.75} Co _{0.25} Ga _{2.65} Ge _{0.35}	293	65.5	2.5	-47	1111	0.24 {873 K}	—	—	—	[488]
Fe _{0.50} Co _{0.50} Ga _{2.65} Ge _{0.35}	293	68.7	2.0	-45	1219	0.23 {873 K}	—	—	—	[488]
Fe _{0.95} Co _{0.05} Ga ₃	322	48.9	3.75	-143	234	0.14 {620 K}	—	—	—	[489]
Fe _{0.975} Ni _{0.025} Ga ₃	322	37.7	4.1	-222	71.4	0.09 {620 K}	—	—	—	[489]
FeGa ₃	373	—	—	—	0.36	—	0.46 ^e	—	—	[490]
FeAl _{0.276} Ga _{2.724}	373	—	—	—	0.71	—	0.42 ^e	—	—	[490]
FeAl _{0.366} Ga _{2.634}	373	—	—	—	1.25	—	0.4 ^e	—	—	[490]
FeAl _{0.534} Ga _{2.466}	373	—	—	—	4.35	—	0.35 ^e	—	—	[490]
Fe _{0.96} Re _{0.04} Ga ₃	327	9.0	3.7	217	18.5	0.06 {975 K}	0.46	—	—	[491]
Fe _{0.92} Re _{0.08} Ga ₃	327	0.3	3.6	38.4	8.3	0.05 {825 K}	0.4	—	—	[491]
RuGa ₃	—	—	—	—	—	—	0.3 ^t	—	—	[465]
RuGa ₃	—	—	—	—	—	—	0.26 ^t	—	—	[477]
RuGa ₃	300	—	—	—	3.3	—	~0.5 ^t	—	—	[487]
RuGa ₃	313	1.6	3.3	-274	1.6	0.18 {940 K}	0.3 ^t 0.32 ^e	7.8 (295)	0.5	[471]
RuGa ₃	373	66.9	4.3	-546	3.7	0.13 {973 K}	0.4 ^t 0.33 ^e	10 (300)	—	[469]
RuGa ₃	300	20.3	~7	-477	1.8	—	0.33 ^t	—	—	[492]
RuGa ₃	300	31.6	~7	-463	3.3	0.08 {845 K}	0.33 ^t	—	—	[492]
OsGa ₃	—	—	—	—	—	—	0.68 ^t	—	—	[477]
OsGa ₃	313	84.2	3.5	-577	2.5	—	0.42 ^e	—	—	[471]
ReGa ₂ Ge ⁱ	300	2.1	1.11	-43.5	40	—	0.23-0.4 ^t	12 (300)	1.8	[474]
RuIn ₃	—	—	—	—	—	—	0.31 ^t	—	—	[465]
RuIn ₃	—	—	—	—	—	—	0.3 ^t	—	—	[477]
RuIn ₃	—	—	—	—	—	—	0.41 ^t 0.46-0.51 ^e	—	—	[493]
RuIn ₃	—	—	—	—	—	—	0.3 ^t	—	—	[470]
RuIn ₃	300	14.8	5.7	-400	3.2	0.073 {753 K}	0.45 ^e	—	—	[468]

(Continued.)

Table 7. (Continued.)

Material	T (K)	μ_{sw} ($\text{cm}^2 \text{V}^{-1} \text{s}^{-1}$)	κ_L ($\text{W m}^{-1} \text{K}^{-1}$)	S ($\mu\text{V K}^{-1}$)	σ ($\Omega^{-1} \text{cm}^{-1}$)	zT {T}	E_g (eV)	μ_H ($\text{cm}^2 \text{V}^{-1} \text{s}^{-1}$)	m_s^* (m_e)	References
RuIn _{2.99} Sn _{0.01}	300	66.0	3.2	-170	206	0.10 {464 K}	—	—	—	[468]
RuIn _{2.975} Sn _{0.025}	300	41.0	2.1	-115	250	0.14 {565 K}	—	—	—	[468]
RuIn _{2.950} Sn _{0.050}	300	26.9	2.3	-100	200	0.084 {628 K}	—	—	—	[468]
RuIn _{2.90} Sn _{0.10}	300	47.0	2.3	-82	450	0.17 {676 K}	—	—	—	[468]
RuIn _{2.99} Zn _{0.01}	300	0.1	3.1	54	2	0.13 {789 K}	—	—	—	[468]
RuIn _{2.975} Zn _{0.025}	300	84.0	3.6	253	100	0.24 {235 K}	—	—	—	[468]
RuIn _{2.950} Zn _{0.050}	300	212.9	2.6	140	950	0.45 {629 K}	—	—	—	[468]
RuIn _{2.90} Zn _{0.10}	300	44.1	2.6	175	130	0.18 {637 K}	—	—	—	[468]
RuIn _{2.99} Sn _{0.01}	300	—	—	-99 ^t	—	—	—	—	—	[470]
RuIn _{2.975} Sn _{0.025}	300	—	—	-133 ^t	—	—	—	—	—	[470]
RuIn _{2.950} Sn _{0.050}	300	—	—	-174 ^t	—	—	—	—	—	[470]
RuIn _{2.90} Sn _{0.10}	300	—	—	-218 ^t	—	—	—	—	—	[470]
RuIn _{2.875} Sn _{0.125}	300	—	—	-274 ^t	—	—	—	—	—	[470]
RuIn _{2.99} Zn _{0.01}	300	—	—	222 ^t	—	—	—	—	—	[470]
RuIn _{2.975} Zn _{0.025}	300	316.0	4.0	164 ^t 150 ^e	1250	0.76 {620 K}	—	—	—	[470]
RuIn _{2.950} Zn _{0.050}	300	219.0	3.9	124 ^t 146 ^e	909	0.41 {620 K}	—	—	—	[470]
RuIn _{2.90} Zn _{0.10}	300	477.0	4.4	98 ^t 140 ^e	2128	0.60 {620 K}	—	—	—	[470]
RuIn _{2.875} Zn _{0.125}	300	—	—	85 ^t	—	—	—	—	—	[470]
Ru _{0.95} Rh _{0.05} In ₃	300	36.1	3.3	-150	143	0.05 {472 K}	—	—	—	[494]
Ru _{0.95} Ir _{0.05} In ₃	300	29.2	2.8	-120	167	0.04 {444 K}	—	—	—	[494]
Ru _{0.95} Re _{0.05} In ₃	300	1.5	3.7	-120	8.3	0.15 {786 K}	—	—	—	[494]
Ru _{0.95} Ir _{0.05} In _{2.95} Zn _{0.05}	300	32.8	2.9	-115	200	0.04 {428 K}	—	—	—	[494]
RuIn ₃	300	1.6	3.0	207	3.2	0.17 {773 K}	0.2 ^t 0.19 ^e	11 (300)	—	[469]
Ru ₂₄ In ₇₆	373	1.4	3.5	138	9.1	0.07 {773 K}	—	—	—	[469]
Ru ₂₅ In ₇₅	373	15.2	3.5	324	11	0.11 {873 K}	—	—	—	[469]

(Continued.)

Table 7. (Continued.)

Material	T (K)	μ_{av} ($\text{cm}^2 \text{V}^{-1} \text{s}^{-1}$)	κ_L ($\text{W m}^{-1} \text{K}^{-1}$)	S ($\mu\text{V K}^{-1}$)	σ ($\Omega^{-1} \text{cm}^{-1}$)	zT {T}	E_g (eV)	μ_H ($\text{cm}^2 \text{V}^{-1} \text{s}^{-1}$)	m_s^* (m_e)	References
Ru _{25.4} In _{74.6}	373	7.5	4.2	278	9.3	0.096 {773 K}	—	—	—	[469]
Ru ₂₆ In ₇₄	373	7.7	3.6	295	7.8	0.10 {673 K}	—	—	—	[469]
Co ₁ Ru _{2.5} In ₇₄	373	44.4	2.9	−193	1.47	0.077 {473 K}	—	—	—	[469]
Co ₂ Ru _{2.4} In ₇₄	373	27.2	2.5	−175	1.11	0.10 {473 K}	—	—	—	[469]
RuIn ₃	290	16.5	2	−420	2.7	0.0077 {347 K}	—	—	—	[472]
Ru _{0.995} Ir _{0.005} In ₃	290	10.7	—	−172	31	—	—	—	—	[472]
Ru _{0.99} Ir _{0.01} In ₃	290	21.0	1.6	−172	61	0.053 {380 K}	—	—	—	[472]
Ru _{0.95} Ir _{0.05} In ₃	290	11.2	—	−83	100	—	—	—	—	[472]
Ru _{0.80} Ir _{0.20} In ₃	290	13.4	—	−37	286	—	—	—	—	[472]
Ru _{0.60} Ir _{0.40} In ₃	290	21.6	—	−40.5	420	—	—	—	—	[472]
Ru _{0.20} Ir _{0.80} In ₃	290	12.1	—	−24	400	—	—	—	—	[472]
IrIn ₃ ⁱ	290	31.2	—	−17	1449	—	—	—	—	[472]

Temperature for highest zT in bracket (e.g. 0.14 {524 K}).

t: theoretical.

e: experimental.

i: isostructural compound with 17 ve and transition metal $\neq T^{(8)}$.

3.8. Actinides and lanthanides

Actinide- and lanthanide-based thermoelectrics

E Svanidze

Max-Planck-Institut für Chemische Physik fester Stoffe, Nöthnitzer Straße 40, 01187 Dresden, Germany

The idea of using lanthanide- or actinide-based materials for thermoelectric applications is rather unconventional and, perhaps, even far-fetched. On the one hand, the chemical and radiological attributes of these materials require non-trivial experimental conditions which render scaling-up efforts questionable, while, on the other hand, the complexity of $4f$ - and $5f$ -orbitals often makes their theoretical assessment quantitatively challenging. However, much like other branches of fundamental research on f -electron-based alloys and compounds, understanding their complex properties can provide a convenient avenue towards a targeted discovery of 'simpler' materials containing only s -, p -, and d -electrons.

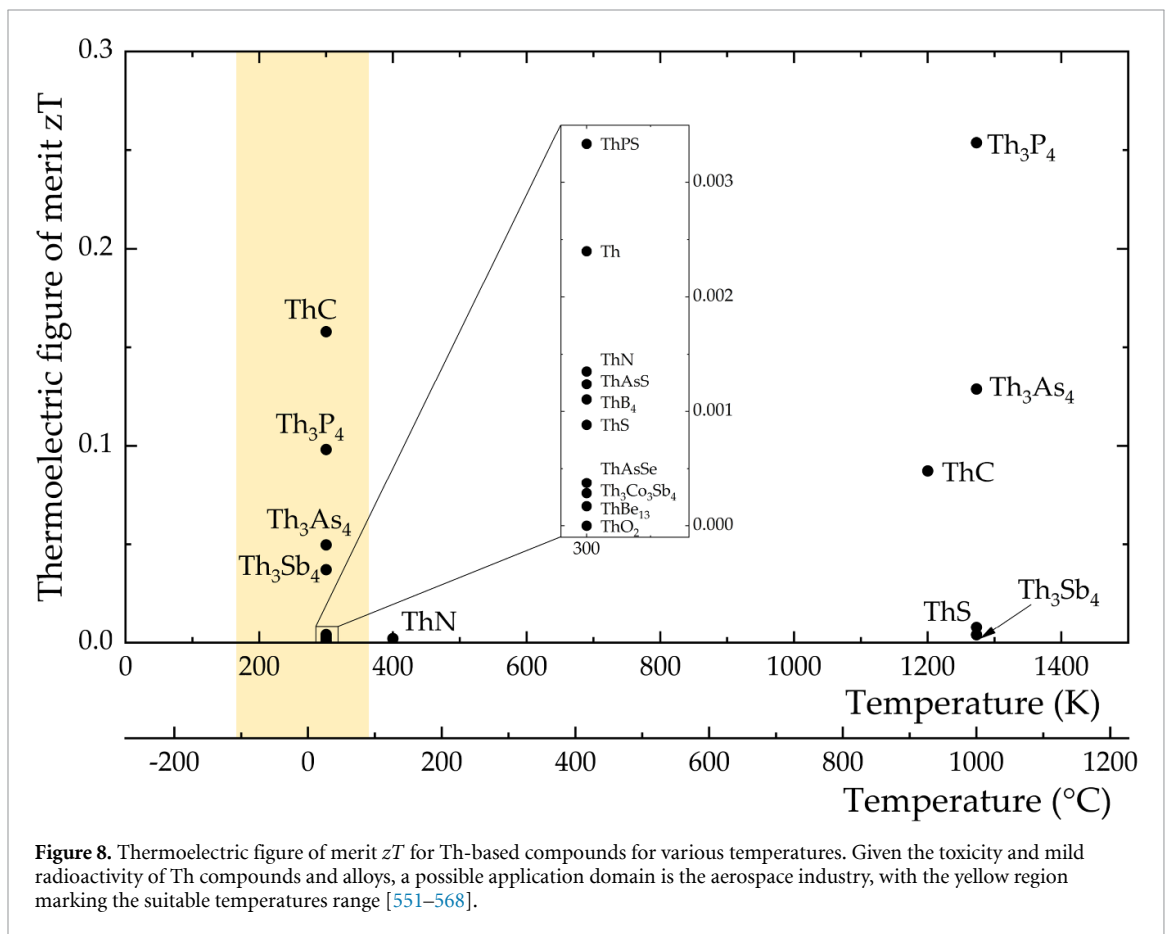
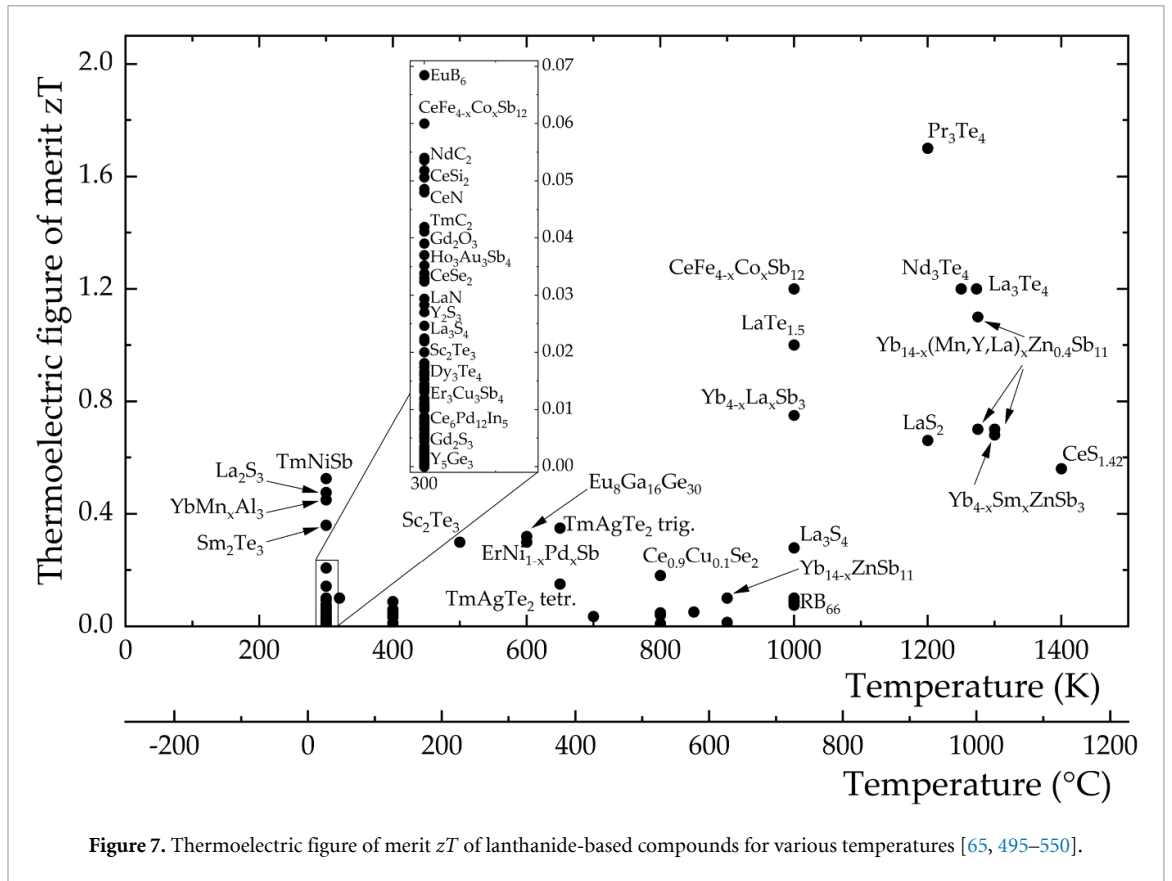
Previous work on lanthanide- [65, 495–550], thorium- [551–568], and uranium-based [521, 551, 557, 560, 564, 569–594] systems is summarized in table 8 and figures 7–9. Some variations in the reported data can probably be attributed to the fragile ground states of f -electron materials and, consequently, sample quality issues [467]. Moreover, for the majority of these systems, values of the thermal conductivity κ , are missing. In order to estimate the value of zT for those compounds, a value of $\kappa = 10 \text{ W m}^{-1} \text{ K}^{-1}$ was used. Based on the existing data, this estimate of κ is comparable to what has been observed in these materials, with average values $\kappa_{\text{ave}}(\text{R}) = \kappa_{\text{ave}}(\text{Th}) = 6.7 \text{ W m}^{-1} \text{ K}^{-1}$, $\kappa_{\text{ave}}(\text{U}) = 10.6 \text{ W m}^{-1} \text{ K}^{-1}$, but, of course, experimentally determined values of κ are highly desired in order to properly assess the thermoelectric potential of these systems. As for the values of the effective mass, a distinction must be made between those obtained from the low-temperature specific heat, ARPES, or de Haas-van Alphen measurements and those extracted from room-temperature Hall or specific heat data. In the case of heavy-fermion lanthanide- and uranium-based systems, it was previously noted [595] that the assumption of a spherical Fermi surface, that is needed for this analysis, is quantitatively not accurate. Moreover, experimentally obtained values of the lattice thermal conductivity, weighed mobility, bandgap, mobility parameter, as well as static dielectric constant are currently lacking. Filling such gaps will enable deeper insight into thermoelectric properties of lanthanide- and actinide-based compounds.

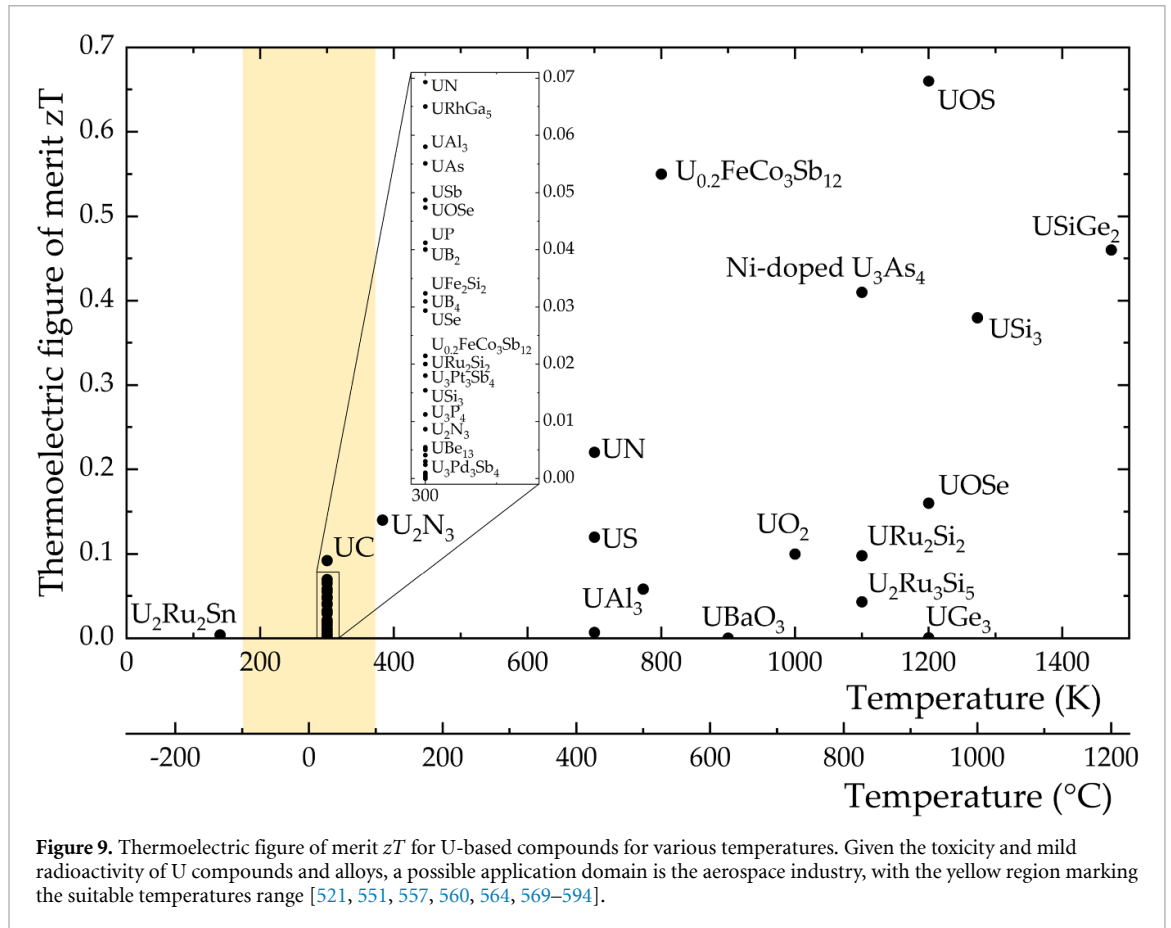
Among lanthanide-containing compounds and alloys, the majority of previous reports have focused on the introduction of large lanthanide atoms into existing materials which show good thermoelectric properties; see, for example, section 3.2 covering skutterudite materials and section 3.9 covering oxide systems. In the current section, we focus on materials for which the starting compound is based on a lanthanide element. As evident from figure 7, room-temperature values of the thermoelectric figure of merit are rather modest, with $zT_{\text{max}} \sim 0.5$ for the HH compound TmNiSb. Interestingly, the high-temperature region shows that more promising materials are likely to be compounds with the Th_3P_4 structure type [65, 506, 511, 525], Zintl phase $\text{Yb}_{14}(\text{Mn}, \text{Y}, \text{La})_x\text{Zn}_y\text{Sb}_{11}$ [541, 542], skutterudite compound $\text{CeFe}_{4-x}\text{Co}_x\text{Sb}_{12}$ [522], as well as lanthanide-based dichalcogenides [504, 519].

When it comes to actinide-based materials, some work has been done for compounds and alloys containing uranium and thorium. Among Th-based materials, very little has been published regarding investigations of their thermoelectric properties. In particular, for the majority of materials provided in table 8, even their thermal conductivity values are missing. Overall, the values of thermoelectric figure of merit, summarized in figure 8, appear to be rather modest (notice a three-fold vertical axis decrease in figure 8 compared to figure 7). For both room temperature and high-temperature regions, two groups of Th-based materials appear to be promising—ThC [562, 563] and compounds with the Th_3P_4 structure type [553–555, 568]. However, more Th-based materials need to be examined in order to evaluate the viability of using these materials for thermoelectric applications.

While the possibility of using uranium-based materials for thermoelectric applications has been proposed over half a century ago [569], very little work has been done in this field in the meantime [582, 593]. The stagnation of this topic is probably due to several factors: the limited number of facilities that carry out uranium work, possible health concerns, as well as the inability to predict new thermoelectric materials using computational means. Nonetheless, given the low cost and abundance of depleted uranium, development of functional uranium-based materials can perhaps contribute to the solution of the nuclear waste problem. Moreover, toxicity and radiological danger of these materials can be avoided if they are used, for example, for aerospace applications [582].

As evident from figure 9, more experimental studies are needed in order to adequately enhance the current maximum value of the thermoelectric figure of merit in uranium-based materials. Given the





currently available data, the most promising systems appear to be compounds with the Th_3P_4 structure type [560, 593], AuCu_3 structure type [578, 584, 593] as well as the skutterudite compound $\text{U}_{0.2}\text{FeCo}_3\text{Sb}_{12}$ [586].

Acknowledgment

Eteri Svanidze would like to acknowledge the support of the Christiane Nüsslein-Volhard-Stiftung.

Table 8. Actinide and lanthanide thermoelectric properties.

Material	T (K)	μ_{av} ($\text{cm}^2 \text{V}^{-1} \text{s}^{-1}$)	κ ($\text{W m}^{-1} \text{K}^{-1}$)	S ($\mu\text{V K}^{-1}$)	σ ($\Omega^{-1} \text{cm}^{-1}$)	zT	E_g (eV)	μ_0 ($\text{cm}^2 \text{V}^{-1} \text{s}^{-1}$)	m_s^* (m_e)	ϵ_r or ϵ (ϵ_0)	zT max	T (K)	References
Sc ₂ Te ₃	300	46.9	—	90	400	0.02	—	—	—	—	0.3	500	[495]
YB ₆	300	22.2	—	-0.5	25000	0.00002	—	—	—	—	—	—	[496, 507, 517]
YB ₆₆	300	0.3	2	450	0.03	0.0001	—	—	—	—	0.1	1000	[528]
YC ₂	300	482.5	—	12	33300	0.01	—	—	—	—	—	—	[539, 547]
Y ₂ O ₃	300	1.8	—	30	50	0.0001	—	—	—	—	—	—	[548]
Y ₂ S ₃	300	360.2	—	30	10000	0.03	—	—	—	—	—	—	[548]
Y ₅ Ge ₃	300	75.9	—	-8.1	7690	0.002	—	—	—	—	—	—	[549]
YGe	300	14.3	—	0.7	12700	0.00002	—	—	—	—	—	—	[549]
YGe ₂	300	12.7	—	0.8	10200	0.00002	—	—	—	—	—	—	[549]
YNiSb	300	86.8	6	40	1800	0.01	—	—	—	—	—	—	[550]
Y ₃ Ru ₄ Ge ₁₃	300	49.4	3.8	37	1110	0.01	—	—	—	—	—	—	[497]
i-Zn-Mg-Y QC	300	55.6	6-7	8	5700	2.5×10^{-7}	—	—	—	—	—	—	[498, 499]
i-Zn-Mg-Y QC	300	35.1	2.6	8	3600	0.003	—	—	—	—	—	—	[500]
LaB ₆	300	27.9	—	0.1	66700	2.0×10^{-6}	—	—	—	—	—	—	[496, 507, 517]
LaC ₂	300	242.7	—	9	22200	0.005	—	—	—	—	—	—	[539, 547]
LaN	300	323.7	—	35	7690	0.03	—	—	—	—	—	—	[501]
La ₂ O ₃	300	2.0	—	33	50	0.0002	—	—	—	—	—	—	[548]
LaSi ₂	300	2228.4	—	-4.2	424000	0.02	—	—	—	—	—	—	[502]
LaS	300	63.2	22.6	4	12600	0.0003	—	—	—	—	—	—	[503]
LaS ₂	300	—	—	—	—	—	—	—	—	—	0.7	1200	[504]
La ₂ S ₃	300	1924.5	9	100	14300	0.5	—	—	—	—	—	—	[548, 505]
La ₃ S ₄	300	32.2	1.3	-40	667	0.03	—	—	—	—	0.3	1000	[506]
La ₅ Ge ₃	300	13.6	—	-1.7	5920	0.00005	—	—	—	—	—	—	[549]
LaGe	300	73.0	—	-3.9	14900	0.0007	—	—	—	—	—	—	[549]
LaGe ₂	300	139.4	—	-10	11500	0.004	—	—	—	—	—	—	[549]
LaSe	300	202.3	24.3	9	18500	0.002	—	—	—	—	—	—	[503]
La ₂ Se ₃	300	1.6	—	340	0.7	0.0002	—	—	—	—	—	—	[548, 508]
La ₂ Te ₃	300	8.1	1.1	40	169	0.007	—	—	—	—	—	—	[548, 509, 510]
La ₃ Te ₄	300	30.0	17	-25	1000	0.001	—	—	—	—	1.2	1250	[65, 511]
LaTe _{1.5}	300	—	—	—	—	—	—	—	—	—	1	1000	[504]

(Continued.)

Table 8. (Continued.)

Material	T (K)	μ_w ($\text{cm}^2 \text{V}^{-1} \text{s}^{-1}$)	κ ($\text{W m}^{-1} \text{K}^{-1}$)	S ($\mu\text{V K}^{-1}$)	σ ($\Omega^{-1} \text{cm}^{-1}$)	zT	E_g (eV)	μ_0 ($\text{cm}^2 \text{V}^{-1} \text{s}^{-1}$)	m_s^* (m_e)	ϵ_r or ϵ (ϵ_0)	zT max	T (K)	References
LaCoO ₃	300	0.0	—	300	0.001	2.7×10^{-7}	—	—	—	—	—	—	[512]
La ₆ Pd ₁₂ In ₅	300	16.1	7.2	-1	10 900	0.00005	—	—	—	—	—	—	[513]
La ₃ Cu ₃ Sb ₄	300	—	2.8	60	—	0.02	—	—	—	—	0.05	400	[514]
LaCrSe ₃	300	40.6	12.5	250	50	0.008	—	—	—	—	—	—	[515]
CeC ₂	300	52.3	—	-2.4	16 700	0.0003	—	—	—	—	—	—	[539, 547]
CeB ₆	300	122.5	—	2.8	34 000	0.0008	—	—	—	—	—	—	[496, 507, 517]
CeN	300	960.5	—	20	40 000	0.05	—	—	—	—	—	—	[501]
CeSi ₂	300	56.8	—	19.3	2450	0.003	—	—	—	—	—	—	[502]
CeS	300	169.5	16.3	12	11 700	0.003	—	—	—	—	—	—	[503]
CeTe	300	50.8	11.3	5	8200	0.0006	—	—	—	—	—	—	[503]
Ce ₅ Ge ₃	300	9.8	—	1.7	4270	0.00004	—	—	—	—	—	—	[549]
CeGe	300	60.5	—	-6.1	8060	0.0009	—	—	—	—	—	—	[549]
CeGe ₂	300	6.8	—	0.7	6060	9.0×10^{-6}	—	—	—	—	—	—	[548]
CeO ₂	300	0.6	—	47	11.1	0.00007	—	—	—	—	—	—	[548]
CeSe ₂	300	1.2	1	480	0.10	0.0007	—	—	—	—	—	—	[516, 518]
Ce _{0.9} Cu _{0.1} Se ₂	300	26.1	1.3	320	14.3	0.03	—	—	—	—	0.2	800	[516]
CeS _{1.42}	300	1.7	0.01	-34	40.8	0.1	—	—	—	—	0.6	1400	[519]
Ce ₃ Se ₄	300	31.6	2.4	-150	125	0.04	—	—	—	—	—	—	[518]
Ce ₂ Se ₃	300	21.1	—	-57	303	0.003	—	—	—	—	—	—	[510, 518]
Ce ₂ Te ₃	300	31.2	1.1	-176	90.9	0.08	—	—	—	—	—	—	[509]
Ce ₃ Te ₄	300	26.8	1.9	-40	556	0.01	—	—	—	—	—	—	[509]
CeRhSn	300	453.1	—	45	8330	0.05	—	—	—	—	—	—	[520]
CeIrSn	300	87.7	—	40	1820	0.009	—	—	—	—	—	—	[520]
Ce ₆ Pd ₁₂ In ₅	300	0	4.2	2	8330	2.4×10^{-10}	—	—	—	—	—	—	[513]
CeCu ₄ Al ₈	300	278.2	—	12	19 200	0.008	—	—	—	—	—	—	[521]
Ce ₃ Cu ₃ Sb ₄	300	—	2	55	—	0.03	—	—	—	—	0.06	400	[514]
CeFe _{4-x} Co _x Sb ₁₂	300	—	—	—	—	—	—	—	—	—	1.2	1000	[522]
Ce _{0.65} Fe ₂ Co ₂ Sb ₁₁ Sn	300	63.4	2	80	625	0.06	—	—	—	—	—	—	[550]
Ce _{0.65} Fe ₂ Co ₂ Sb ₁₀ Ge ₂	300	31.9	3.2	20	1330	0.005	—	—	—	—	—	—	[550]
Ce _{0.65} Fe ₂ Co ₂ Sb ₁₂	300	84.1	3.5	100	625	0.05	—	—	—	—	—	—	[550]
PrB ₆	300	51.7	—	-0.6	51 300	0.00006	—	—	—	—	—	—	[496, 507, 517]
PrSe	300	10.6	0.9	1	7200	0.0002	—	—	—	—	—	—	[503]

(Continued.)

Table 8. (Continued.)

Material	T (K)	μ_{sw} ($\text{cm}^2 \text{V}^{-1} \text{s}^{-1}$)	κ ($\text{W m}^{-1} \text{K}^{-1}$)	S ($\mu\text{V K}^{-1}$)	σ ($\Omega^{-1} \text{cm}^{-1}$)	zT	E_g (eV)	μ_0 ($\text{cm}^2 \text{V}^{-1} \text{s}^{-1}$)	m_s^* (m_e)	ϵ_r or ϵ (ϵ_0)	zT max	T (K)	References
PrS	300	1923.8	—	−19.3	83000	0.09	—	—	—	—	—	—	[503, 523]
PrTe	300	19.7	8.0	2	7400	0.0001	—	—	—	—	—	—	[503]
PrC ₂	300	282.9	—	−9.1	25600	0.006	—	—	—	—	—	—	[539, 547]
PrN	300	389.1	—	−34	9520	0.03	—	—	—	—	—	—	[501]
Pr ₃ Te ₄	300	30.0	31	−25	1000	0.0006	—	—	—	—	1.7	1200	[65]
Pr ₂ Te ₃	300	28.1	1.8	−35	667	0.01	—	—	—	—	—	—	[509, 510]
PrSi ₂	300	20.2	—	−3.2	4950	0.0002	—	—	—	—	—	—	[502]
PrCoO ₃	300	0	1	210	0.05	0.00007	—	—	—	—	0.04	700	[524]
NdBi ₆	300	38.6	—	0.4	50000	0.00002	—	—	—	—	—	—	[496, 507, 517]
NdS	300	34.6	19.3	2	13000	0.00008	—	—	—	—	—	—	[503]
NdC ₂	300	275.1	—	−10	22700	0.007	—	—	—	—	—	—	[539, 547]
NdN	300	576.0	—	−36	13300	0.05	—	—	—	—	—	—	[501]
Nd ₅ Ge ₃	300	47.3	—	−7	5520	0.0008	—	—	—	—	—	—	[549]
NdGe ₂	300	40.8	—	−3.9	8330	0.0004	—	—	—	—	—	—	[549]
Nd ₃ Te ₄	300	60.6	14	−50	1000	0.005	—	—	—	—	1.2	1273	[525]
Nd ₂ Te ₃	300	10.6	1.3	−15	588	0.003	—	—	—	—	—	—	[509, 510]
NdCoO ₃	300	0.0	1.3	300	0.01	0.00002	—	—	—	—	0.04	800	[524]
Nd ₂ CuO ₄	300	62.7	24	−720	0.3	0.0002	—	—	—	—	—	—	[526]
Nd _{1.85} Th _{0.15} CuO ₄	300	1.6	—	−10	133	0.00004	—	—	—	—	—	—	[527]
SmB ₆	300	44.8	—	7.6	4830	0.0008	—	—	—	—	—	—	[496, 507, 517]
SmB ₆₆	300	0.6	2.1	590	0.01	0.00007	—	—	—	—	0.1	1000	[528]
Sm ₂ Te ₃	300	0	—	130	0.004	2.0×10^{-7}	—	—	—	—	—	—	[510]
Sm ₂ O ₃	300	4791.3	—	30	133000	0.4	—	—	—	—	—	—	[548]
Sm ₃ Au ₃ Sb ₄	300	31.1	—	125	167	0.008	—	—	—	—	—	—	[550]
Sm ₂ CuO ₄	300	75.6	20	−840	0.1	0.0001	—	—	—	—	—	—	[526]
EuB ₆	300	251.0	—	−17.7	11800	0.01	—	—	—	—	—	—	[496, 507, 517]
Eu ₈ Ga ₁₆ Ge ₃₀	300	101.2	—	−152	391	0.1	—	—	—	—	0.3	600	[529]
Eu _{1-x} Yb _x Cd ₆ Sb ₁₂	300	21.3	0.8	120	122	0.07	—	—	—	—	0.1	320	[530]
Eu ₂ Pb ₂ Bi ₆ Se ₁₃	300	12.6	—	−35	300	0.001	—	—	—	—	—	—	[550]
Eu ₂ Pb ₂ Bi ₄ Se ₁₀	300	112.1	—	−140	500	0.03	—	—	—	—	—	—	[550]

(Continued.)

Table 8. (Continued.)

Material	T (K)	μ_{sw} ($\text{cm}^2 \text{V}^{-1} \text{s}^{-1}$)	κ ($\text{W m}^{-1} \text{K}^{-1}$)	S ($\mu\text{V K}^{-1}$)	σ ($\Omega^{-1} \text{cm}^{-1}$)	zT	E_g (eV)	μ_0 ($\text{cm}^2 \text{V}^{-1} \text{s}^{-1}$)	m_s^* (m_e)	ϵ_r or ϵ (ϵ_0)	zT max	T (K)	References
GdC ₂	300	299.0	3	-7.4	33 300	0.02	—	—	—	—	—	—	[531]
GdB ₆	300	9.4	—	0.1	22 400	7.0×10^{-7}	—	—	—	—	—	—	[496, 507, 517]
Gd ₃ Se ₄	300	15.3	—	-14	909	0.0005	—	—	—	—	—	—	[518]
Gd ₂ Te ₃	300	19.0	—	160	66.7	0.005	—	—	—	—	—	—	[518]
Gd ₂ O ₃	300	7.2	—	42	143	0.0008	—	—	—	—	—	—	[548]
Gd _{1-x} Sr _x CoO ₃	300	6.7	0.3	100	50.0	0.06	—	—	—	—	—	—	[532]
Gd ₃ Cu ₃ Sb ₄	300	—	3.7	89	—	0.04	—	—	—	—	0.09	400	[514]
Gd ₃ Au ₃ Sb ₄	300	35.7	—	50	588	0.004	—	—	—	—	—	—	[550]
Gd _{1.34} Au _{6.716} Ge _{18.5}	300	18.7	5.2	4.5	3330	0.0004	—	—	—	—	0.03	400	[533]
Gd _{1.19} Au _{6.887} Si _{15.94}	300	5.2	3.1	1.5	2500	0.0005	—	—	—	—	0.01	400	[533]
Gd ₂ CuO ₄	300	7.5	30	-700	0.05	0.0003	—	—	—	—	—	—	[526]
1/1-Au-Ge-Gd AC	300	14.6	5.5	3.5	3300	0.0002	—	—	—	—	—	—	[533]
1/1-Au-Si-Gd AC	300	5.2	3	1.5	2500	0.0006	—	—	—	—	—	—	[533]
1/1-Au-Al-Gd AC	300	37.1	3.7	11	2790	0.003	—	—	—	—	0.006	800	[499]
TbC ₂	300	270.4	3.0	-7.8	28 600	0.02	—	—	—	—	—	—	[531]
TbB ₆	300	42.6	—	-1.1	26 700	0.0001	—	—	—	—	—	—	[496, 507, 517]
TbCoO ₃	300	0	1.8	600	50 000	3.0×10^{-6}	—	—	—	—	0.05	800	[524]
i-Zn-Mg-Tb QC	300	36.2	5-6	6	4900	1.2×10^{-7}	—	—	—	—	—	—	[498]
DyC ₂	300	266.3	3.1	-6.8	32 200	0.01	—	—	—	—	—	—	[531]
DyN	300	360.8	—	-36	8330	0.03	—	—	—	—	—	—	[501]
Dy ₃ Te ₄	300	19.2	2.2	-49	323	0.01	—	—	—	—	—	—	[509]
Dy ₃ Ru ₄ Ge ₁₃	300	52.6	3	35	1250	0.02	—	—	—	—	—	—	[497]
DyCoO ₃	300	0.2	2	800	0.0005	4.8×10^{-6}	—	—	—	—	0.05	850	[524]
HoN	300	445.3	—	-37	10 000	0.04	—	—	—	—	—	—	[501]
HoB ₆	300	0.3	1.9	460	0.03	0.0001	—	—	—	—	—	—	[528]
HoPdSb	300	35.9	6	170	112	0.02	—	—	—	—	0.09	1000	[550, 534]
HoNiSb	300	72.3	5.5	40	1500	0.01	—	—	—	—	—	—	[550]
Ho ₃ Au ₃ Sb ₄	300	40.8	—	140	182	0.01	—	—	—	—	—	—	[550]
Ho ₃ Ru ₄ Ge ₁₃	300	55.7	3.2	37	1250	0.02	—	—	—	—	—	—	[497]
i-Zn-Mg-Ho QC	300	52.6	7-8	8	5400	2.3×10^{-7}	—	—	—	—	—	—	[498]
EuB ₆	300	251.0	—	-17.7	11 800	0.01	—	—	—	—	—	—	[496, 507, 517]

(Continued.)

Table 8. (Continued.)

Material	T (K)	μ_w ($\text{cm}^2 \text{V}^{-1} \text{s}^{-1}$)	κ ($\text{W m}^{-1} \text{K}^{-1}$)	S ($\mu\text{V K}^{-1}$)	σ ($\Omega^{-1} \text{cm}^{-1}$)	zT	E_g (eV)	μ_0 ($\text{cm}^2 \text{V}^{-1} \text{s}^{-1}$)	m_s^* (m_e)	ϵ_r or ϵ (ϵ_0)	zT max	T (K)	References
ErC ₂	300	156.7	2.1	-6.0	21 400	0.01	—	—	—	—	—	—	[531]
ErN	300	412.3	—	-36	9520	0.04	—	—	—	—	—	—	[501]
Er ₂ O ₃	300	2.0	—	33	50.0	0.0002	—	—	—	—	—	—	[548]
Er ₃ Cu ₃ Sb ₄	300	—	3.5	38	—	0.02	—	—	—	—	0.04	400	[514]
ErNiSb	300	113.9	4	160	400	0.07	—	—	—	—	—	—	[550]
ErNi _{1-x} Pd _x Sb	300	—	—	—	—	—	—	—	—	—	0.3	600	[535]
ErNiSb	300	101.1	5	150	400	0.05	—	—	—	—	—	—	[550]
i-Zn-Mg-Er QC	300	53.1	5-6	7	6200	0.002	—	—	—	—	—	—	[498]
TimC ₂	300	17.1	0.3	-7.2	1940	0.01	—	—	—	—	—	—	[531]
TimB ₆₆	300	0.3	2.1	460	0.03	0.0001	—	—	—	—	0.09	1000	[528]
TimNiSb	300	28.4	3	58	400	0.01	—	—	—	—	—	—	[550]
i-Au-Al-Tm QC	300	33.4	4.7	8.7	3160	0.002	—	—	—	—	—	—	[499]
1/1-Au-Al-Tm AC	300	49.5	4.7	13.6	3020	0.004	—	—	—	—	0.01	800	[499]
TimAgTe ₂ trigonal	300	11.5	0.5	500	0.8	0.01	—	—	—	—	0.4	650	[536]
TimAgTe ₂ tetragonal	300	29.4	0.8	570	0.9	0.01	—	—	—	—	0.2	650	[536]
YbB ₆	300	658.0	—	-25.5	21 500	0.04	—	—	—	—	—	—	[496, 507, 517]
YbB ₆₆	300	0.5	2.3	570	0.01	0.00006	—	—	—	—	0.08	1000	[528]
Yb ₂ Te ₃	300	6018.8	—	35	143 000	0.5	—	—	—	—	—	—	[548]
Yb ₂ O ₃	300	1081.3	—	18	50 000	0.05	—	—	—	—	—	—	[548]
YbAl ₃	300	1424.0	14	-88	12 500	0.2	—	—	—	—	—	—	[537]
YbMn _x Al ₃	300	—	—	—	—	—	—	—	—	—	0.5	300	[537]
i-Cd-Yb QC	300	134.7	5.1	16	7000	0.01	—	—	—	—	—	—	[500]
i-Cd-Yb QC	300	87.8	9	13	5600	0.003	—	—	—	—	—	—	[538]
1/1Cd-Yb AC	300	102.9	9	12	7100	0.003	—	—	—	—	—	—	[538]
i-Cd-Yb QC	300	107.8	5-7.5	6-16	2900-5600	0.007	—	—	—	—	—	—	[540]
1/1Cd-Yb AC	300	48.9	7.5	14	2900	0.002	—	—	—	—	—	—	[540]
YbNiSb	300	60.0	4.5	20	2500	0.007	—	—	—	—	—	—	[550]
Yb _{15.78} Au _{65.22} Ge _{19.00}	300	0.6	2.5	-1.2	370	6.0×10^{-6}	—	—	—	—	6.0×10^{-6}	400	[533]
Yb ₁₄ ZnSb ₁₁	300	6.2	12	5	1000	0.00006	—	—	—	—	0.1	900	[541, 542]
Yb ₁₄ MnSb ₁₁	300	30.3	1.4	50	500	0.01	—	—	—	—	—	—	[542]
Yb _{13.5} La _{0.5} ZnSb ₁₁	300	24.0	10.5	20	1000	0.001	—	—	—	—	0.7	1275	[541]

(Continued.)

Table 8. (Continued.)

Material	T (K)	μ_{sw} ($\text{cm}^2 \text{V}^{-1} \text{s}^{-1}$)	κ ($\text{W m}^{-1} \text{K}^{-1}$)	S ($\mu\text{V K}^{-1}$)	σ ($\Omega^{-1} \text{cm}^{-1}$)	zT	E_g (eV)	μ_0 ($\text{cm}^2 \text{V}^{-1} \text{s}^{-1}$)	m_s^* (m_e)	ϵ_r or $\epsilon(\epsilon_0)$	zT max	T (K)	References
Yb _{13.5} Y _{0.5} ZnSb ₁₁	300	36.0	10.5	30	1000	0.003	—	—	—	—	0.7	1300	[541]
Yb _{4-x} Sm _x Sb ₃	300	48.5	35	-10	4000	0.0003	—	—	—	—	0.7	1300	[543]
Yb _{4-x} La _x Sb ₃	300	60.0	25	20	2500	0.001	—	—	—	—	0.8	1000	[543, 544]
i-Au-Al-Yb QC	300	45.9	—	9	4200	0.001	—	—	—	—	—	—	[545]
1/1-Au-Ge-Yb AC	300	0.5	3	-1	370	4.0×10^{-6}	—	—	—	—	—	—	[533]
i-Au-Al-Yb QC	300	72.7	—	11.4	5280	0.002	—	—	—	—	—	—	[499]
1/1-Au-Al-Yb AC	300	80.9	3.7-3.9	9.7-12.9	3010-5200	0.006	—	—	—	—	0.01	900	[499]
Yb ₁₄ Mn _{0.6} Zn _{0.4} Sb ₁₁	300	—	—	—	—	—	—	—	—	—	1.1	1275	[542]
Lu ₃ Ru ₄ Ge ₁₃	300	70.3	3.7	35	1670	0.02	—	—	—	—	—	—	[497]
Th	300	251.0	—	-4	50000	0.002	—	—	—	—	—	—	[551, 552]
ThO ₂	300	—	11	—	—	0	—	—	—	—	—	—	[561]
ThC	300	1279.7	—	50	21100	0.2	—	—	—	—	0.09	1200	[562, 563]
ThN	300	191.9	—	-3	50000	0.001	—	—	—	—	0	400	[564]
ThS	300	73.2	—	-5	11800	0.0009	—	—	—	—	0.01	1273	[565]
ThBe ₁₃	300	29.5	—	-2.5	9090	0.0002	—	—	—	—	—	—	[566]
ThB ₄	300	91.2	—	-5	14700	0.001	—	—	—	—	—	—	[567]
ThB ₆	300	344.8	—	-5	55600	0.004	—	—	—	—	—	—	[567]
Th ₃ P ₄	300	108.0	2.8	-223	182	0.1	—	—	—	—	0.3	1273	[568, 553]
Th ₃ As ₄	300	228.8	5.4	-380	62.5	0.05	—	—	—	—	0.1	1273	[554, 555]
Th ₃ Sb ₄	300	215.1	7.5	-52.5	3370	0.04	—	—	—	—	0	1273	[554]
ThAsSe	300	31.0	—	-5	5000	0.0004	—	—	—	—	—	—	[556, 557]
ThAsS	300	136.8	—	-3.8	28600	0.001	—	—	—	—	—	—	[558]
ThPS	300	159.2	—	-8.5	15400	0.003	—	—	—	—	—	—	[559]
Th ₃ Co ₃ Sb ₄	300	23.6	—	5	3800	0.0003	—	—	—	—	—	—	[560]

(Continued.)

Table 8. (Continued.)

Material	T (K)	μ_{sw} ($\text{cm}^2 \text{V}^{-1} \text{s}^{-1}$)	κ ($\text{W m}^{-1} \text{K}^{-1}$)	S ($\mu\text{V K}^{-1}$)	σ ($\Omega^{-1} \text{cm}^{-1}$)	zT	E_g (eV)	μ_0 ($\text{cm}^2 \text{V}^{-1} \text{s}^{-1}$)	m_s^* (m_e)	ϵ_r or ϵ (ϵ_0)	zT max	T (K)	References
U metal	300	316.9	—	7	37000	0.005	—	—	—	—	—	—	[551, 590, 591]
U ₂ N ₃	300	37.0	—	-107	250	0.009	—	—	—	—	0.1	383	[592, 593]
U ₂ S ₃	300	—	—	—	—	0.005	—	—	—	—	—	—	[593]
U ₂ Se ₃	300	1.2	—	-2	435	0.02	—	—	—	—	—	—	[594]
USb ₂	300	31.2	3.1	20	1300	0.005	—	—	—	—	0.007	700	[569, 593]
USE ₂	300	1.0	—	21	40.0	0.02	—	—	—	—	—	—	[570, 594]
US ₂	300	—	—	—	7.5	0.005	—	—	—	—	—	—	[569, 570]
UO ₂	300	4.0	6.5	500	0.3	0.0003	—	—	—	—	0.1	1000	[569, 571, 593]
UB ₂	300	—	—	—	—	0.04	—	—	—	—	—	—	[572]
US	300	284.8	9.6	55	4250	0.04	—	—	—	—	0.1	700	[573]
UP	300	297.0	10.5	59.2	4100	0.04	—	—	—	—	—	—	[557, 573]
UC	300	1903.6	23.0	45	35000	0.09	—	—	—	—	—	—	[573]
UN	300	517.4	13.4	75	5500	0.07	—	—	—	—	0.2	700	[573, 574]
UAs	300	304.5	8.4	62	4000	0.06	—	—	—	—	—	—	[564, 573]
USb	300	204.9	4.2	40	4250	0.05	—	—	—	—	—	—	[573, 575]
USE	300	197.6	6.7	40	4100	0.03	—	—	—	—	—	—	[573]
UB ₄	300	620.1	—	5	100000	0.03	—	—	—	—	—	—	[576, 577]
UAL ₃	300	—	—	—	—	0.06	—	—	—	—	0.06	773	[593]
USi ₃	300	648.4	21	20	27000	0.02	—	—	—	—	0.4	1273	[578]
UGe ₃	300	244.9	18	12	16900	0.004	—	—	—	—	0.0005	1200	[578]
U ₃ P ₄	300	28.3	1.9	30	785	0.01	—	—	—	—	—	—	[560]
Ni-doped U ₃ As ₄	300	3.3	2.5	-0.6	3300	0.00001	—	—	—	—	0.4	1100	[560, 593]
U ₃ Sb ₄	300	11.1	3.4	-3.5	2500	0.0003	—	—	—	—	—	—	[560]
U ₃ Se ₄	300	15.6	25.5	-8.4	1530	0.0001	—	—	—	—	—	—	[560]
U ₃ Te ₄	300	21.4	30.6	-7.4	2370	0.0001	—	—	—	—	—	—	[560]
UBe ₁₃	300	153.3	—	14	9090	0.005	—	—	—	—	—	—	[521]
URu ₂ Si ₂	300	48.0	—	-20	2000	0.02	—	—	—	—	0.1	1100	[578, 579]
UFe ₂ Si ₂	300	21.6	0.5	-30	600	0.03	—	—	—	—	—	—	[578]
UNi ₂ Si ₂	300	0.2	—	-4	37.0	1.8×10^{-6}	—	—	—	—	—	—	[580]
URhGa ₅	300	612.2	0.3	60	8330	0.07	—	—	—	—	—	—	[581]

(Continued.)

Table 8. (Continued.)

Material	T (K)	μ_w ($\text{cm}^2 \text{V}^{-1} \text{s}^{-1}$)	κ ($\text{W m}^{-1} \text{K}^{-1}$)	S ($\mu\text{V K}^{-1}$)	σ ($\Omega^{-1} \text{cm}^{-1}$)	zT	E_g (eV)	μ_0 ($\text{cm}^2 \text{V}^{-1} \text{s}^{-1}$)	m_s^* (m_e)	ϵ_r or ϵ (ϵ_0)	zT max	T (K)	References
$\text{U}_3\text{Pt}_3\text{Sb}_4$	300	9.8	2.0	193.7	23.3	0.02	—	—	—	—	—	—	[582]
$\text{U}_3\text{Ni}_3\text{Sb}_4$	300	8.2	2.5	10.2	667	0.0006	—	—	—	—	—	—	[582]
$\text{U}_3\text{Pd}_3\text{Sb}_4$	300	4.1	2.9	80.8	40	0.003	—	—	—	—	—	—	[582]
$\text{U}_3\text{Pt}_3\text{Sn}_4$	300	8.4	69	-6.9	1000	0.00001	—	—	—	—	—	—	[582]
$\text{U}_2\text{Ru}_3\text{Si}_5$	300	12.4	—	-5	2000	0.001	—	—	—	—	0.04	1100	[579]
$\text{U}_2\text{Fe}_3\text{Si}_5$	300	34.7	—	-10	2860	0.0009	—	—	—	—	—	—	[583]
U_2FeSi_3	300	20.7	—	12	1430	0.0006	—	—	—	—	—	—	[583]
$\text{U}_3\text{Fe}_2\text{Si}_7$	300	88.7	—	11	6670	0.002	—	—	—	—	—	—	[583]
$\text{U}_{1.2}\text{Fe}_4\text{Si}_{9.7}$	300	5.3	—	4	1050	0.00005	—	—	—	—	—	—	[583]
UOS	300	0.3	3.8	150	1.3	0.0002	—	—	—	—	0.7	1200	[569, 593]
UOSe	300	14.7	0.8	166	48.0	0.05	—	—	—	—	0.2	1200	[569, 593]
USiGe ₂	300	—	—	—	—	—	—	—	—	—	0.5	1473	[584, 593]
UBaO ₃	300	—	0.8	170	—	—	—	—	—	—	0.0002	900	[585]
Fe-doped $\text{UCo}_3\text{Sb}_{12}$	300	60.6	3.5	50	1000.0	0.02	—	—	—	—	0.6	800	[586]
$\text{U}_2\text{Ru}_2\text{Sn}$	300	—	—	—	37.0	—	—	—	—	—	0.004	140	[587, 588]
$\text{U}_2\text{Rh}_2\text{In}$	300	0.6	—	12.5	37.0	0.00002	—	—	—	—	—	—	[589]

3.9. Oxides

Oxide thermoelectrics

Dursun Ekren¹, Robert Freer² and Ryoji Funahashi³

¹ Department of Metallurgy and Materials Engineering, Iskenderun Technical University, Iskenderun 31200, Hatay, Turkey

² Department of Materials, University of Manchester, Oxford Road, M13 9PL, United Kingdom

³ National Institute of Advanced Industrial Science and Technology, 1-8-31 Midorigaoka, Ikeda, Osaka 563-8577, Japan

Oxides, developed from earth abundant materials, having structural/chemical flexibility and high temperature stability, are well suited to medium and high temperature thermoelectric applications. Today there is a wide variety of oxide thermoelectrics (table 9) [596–668], but work on oxide thermoelectrics only began in the 1990s after the discovery of a high PF ($5000 \mu\text{W m}^{-1} \text{K}^{-2}$) in single crystal Na_xCoO_2 (NCO) combined with both high μ ($\sim 13 \text{ cm}^2 \text{V}^{-1} \text{s}^{-1}$ at 300 K) and a large S ($\sim 100 \mu\text{V K}^{-1}$ at 300 K). Whilst polycrystalline NCO presents additional processing challenges and the presence of microstructural features can seriously degrade the transport properties, resulting in very modest zT in the pure material [653], the performance of these p -type materials can, under ideal conditions, reach zT_{max} of 0.92 at 960 K, particularly when prepared as a composite containing 10%Ag [655]. NCO tends to physically degrade at elevated temperatures, but the related p -type, layered compounds $\text{Ca}_3\text{Co}_4\text{O}_9$ (CCO) and $\text{Bi}_2\text{Sr}_2\text{Co}_2\text{O}_y$ do not suffer in the same way and have been exploited in prototype modules [669]. Once again the highest thermoelectric performance has been reported for single crystals, but polycrystalline CCO has achieved zT_{max} of ~ 0.43 at 1073 K for Bi or Ba doped ceramics [640, 641]. For the closely related misfit layered cobaltite $\text{Bi}_2\text{Sr}_2\text{Co}_2\text{O}_y$, the orientation-dependent properties mean that texturing of ceramics is essential to maximize performance. By use of partial melting and/or doping of $\text{Bi}_2\text{Sr}_2\text{Co}_2\text{O}_y$, zT_{max} of 0.27 has been achieved at 973 K [649, 650].

Whilst p -type oxides have been predominantly limited to cobalt-based, layered structured compounds, the n -type materials include a number of different structural families, amongst which, the perovskites have attracted considerable attention. CaMnO_3 (CMO) was one of the first n -type perovskites explored and like many oxides, the undoped material suffers from inherently high thermal conductivity. There is also a metal-insulator transition at high temperature due to a change in the spin state of Mn ions. Substituting Ca with heavy rare earths has been particularly successful in reducing thermal transport [613]; dual doping on both Ca and Mn sites can also enhance charge transport [614, 616]. Theoretical work suggests that zT_{max} of greater than 1.0 can be achieved in CMO [670], but to date the use of soft chemistry processing to develop sub-micron grains with nanosized twinned domains, has produced the best performing CMO with a zT_{max} of 0.32 at 1060 K [613].

The transport properties of perovskite SrTiO_3 (STO) depend critically on processing conditions and composition. Undoped STO processed in air is an insulator, exhibiting a high Seebeck coefficient (S $-380 \mu\text{V K}^{-1}$ at 300 K), but also exceptionally high thermal conductivity ($9\text{--}12 \text{ W m}^{-1} \text{K}^{-1}$) at room temperature [596]. By processing under reducing conditions a high PF, comparable with that of Bi_2Te_3 can be achieved, but reducing thermal conductivity is much more of a challenge as nanostructuring is less effective than in many other materials. Doping on the cation A site, with La in place of $\sim 10\%$ of the Sr has been popular and effective, which under reducing conditions leads to the formation of oxygen vacancies, which enhance electrical conductivity and reduce thermal conductivity [596–612]. On the cation B site, doping with higher valent Nb leads to metallic conduction and simultaneously increases S because the effective mass m^* is increased; consequently, the PF σS^2 is enhanced, with values of $\sim 1500 \mu\text{W m}^{-1} \text{K}^{-2}$ at 1000 K recorded for $\text{SrTi}_{0.8}\text{Nb}_{0.2}\text{O}_3$ epitaxial films and a zT_{max} of 0.37 [596].

By optimized doping of A and or B sites of STO, zT_{max} values at high temperatures have remained stubbornly around 0.38 [597–599, 603, 604, 610]. There have been isolated reports of zT_{max} values above 0.5 for STO-based materials [602, 608, 611], but an interesting development in recent years has been the enhancement of transport properties at lower temperatures through additions of carbon-based species. Lin *et al* [600] showed that incorporation of small amounts of graphene ($<1 \text{ wt}\%$) into STO enabled single crystal-like electronic transport behavior, with high electrical conductivity at temperatures of 373 K or less. The presence of the graphene at the grain boundaries promoted oxygen deficiency, increasing charge transport through an increase in the weighted mobility; at the same time the graphene helped reduce thermal transport. Increased zT values, around 0.4 were achieved over a wide temperature range up to 873 K, thereby greatly enhancing the operational thermal window. Other studies with graphene/graphene oxide

support the enhancement behavior [605–607, 609]. It is predicted that zT values above 0.5 could be achieved for STO-graphene composites by optimizing the grain boundary structure [671].

Semiconducting zinc oxide, ZnO (ZO) is a further oxide having considerable potential because of its high mobility and high PF, but again there is the disadvantage of high thermal conductivity ($\sim 5 \text{ W m}^{-1} \text{ K}^{-1}$). Doping with trivalent elements is usually employed to increase thermoelectric performance; a zT_{max} of 0.30 at 1273 K was achieved with 2% Al doping [618], whilst dual doping with Al and Ga (the latter preventing second phase formation, which limits electrical conductivity) enabled one of the highest zT values to be achieved for an oxide— zT_{max} 0.65 for $\text{Zn}_{0.96}\text{Al}_{0.02}\text{Ga}_{0.02}\text{O}$ at 1273 K [620].

The success with improving the properties of ZnO led to work on the related homologous compounds $\text{In}_2\text{O}_3(\text{ZnO})_m$ (IZO) and $\text{Ga}_2\text{O}_3(\text{ZnO})_m$ (GZO), having structures comprising layers of ZnO separated by integer numbers of layers of gallium or indium oxide. The attraction of these materials is that by changing the number of layers the PF can be adjusted whilst maintaining low thermal conductivity. For many of the simple binary compounds, the zT_{max} is still quite modest, but for $\text{In}_2\text{O}_3(\text{ZnO})_3$ and Ni coated $\text{In}_2\text{O}_3(\text{ZnO})_5$ very useful zT_{max} values of 0.24 and 0.39 at 973 K respectively have been reported [623, 622]. Increasing the value of m can be beneficial for developing superlattice and twin structures for reducing thermal conductivity, but unfortunately there is often a concomitant reduction in electrical conductivity as well.

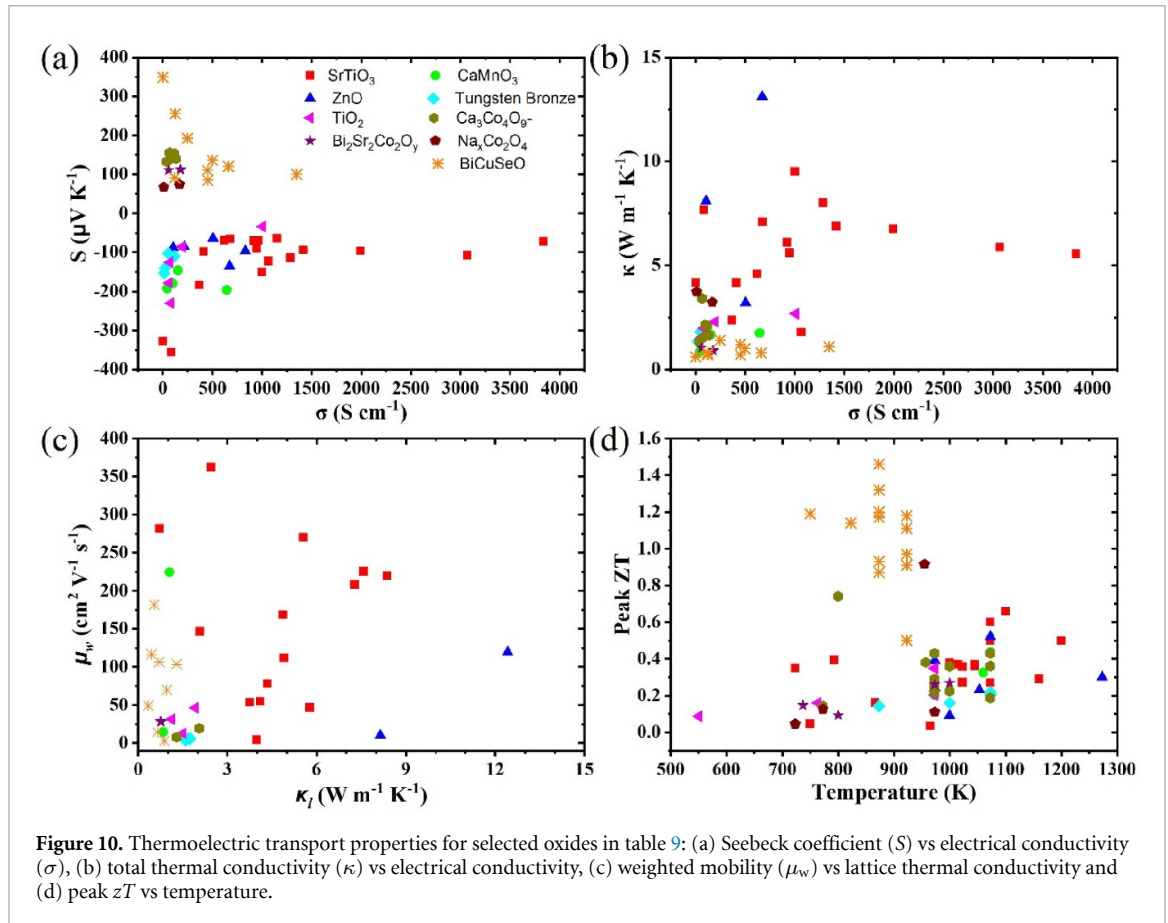
Non-stoichiometric titania, specifically the Magnéli phases $\text{Ti}_n\text{O}_{2n-1}$ ($n = 2, 3, \dots$) have significantly better thermoelectric properties than TiO_2 , as a result of the presence of planar shear defects and oxygen vacancies acting as effective phonon scatterers. With increasing non-stoichiometry electrical conductivity increases and S reduces, but there is often a beneficial reduction in thermal conductivity as well; in $\text{TiO}_{1.76}$ the highest zT_{max} of 0.35 was achieved at 973 K [630]. Simultaneous co-doping by Nb and N has the double benefit of increasing the PF and reducing κ for Magnéli phases, leading to zT_{max} of 0.35 at 973 K for $\text{Ti}_{0.83}\text{Nb}_{0.17}(\text{O,N})_{2\pm\delta}$ [629].

There have also been investigations of materials with the complex tungsten bronze structure based on $(\text{Sr,Ba})\text{Nb}_2\text{O}_6$. With the more complex crystal structure they are expected to have inherently low thermal conductivity; structural anisotropy means that they need to be textured to optimize performance. Both cation and anion doping has been explored; replacing oxygen by fluorine increases the PF through increases in carrier concentration, and helps to reduce κ , leading to a zT_{max} of 0.21 at 1073 K for $\text{Sr}_{0.61}\text{Ba}_{0.39}\text{Nb}_2\text{O}_{5.95}\text{F}_{0.05}$ [624]. Somewhat surprisingly, ferroelectric $\text{Ba}_{6-x}\text{Nd}_{8+2x}\text{Ti}_{18}\text{O}_{54}$ has both a high Seebeck coefficient ($-210 \mu\text{V K}^{-1}$) and an exceptionally low thermal conductivity ($\sim 1.45 \text{ W m}^{-1} \text{ K}^{-1}$); indeed this κ value is one of the lowest for an oxide. With modest electrical conductivity the zT_{max} was limited to 0.16 at 1000 K for $\text{Ba}_{5.19}\text{Nd}_{8.54}\text{Ti}_{18}\text{O}_{54}$ [626]. Nevertheless, it is clear that oxides offer considerable opportunities for medium and high temperature thermoelectrics if the natural advantages of oxides can be exploited to the full. Indeed, the recent work on composites including carbon species [600] suggests that oxides could potentially be used over very much wider temperature ranges, in principle from room temperature.

Finally, new materials from the oxyselenide family, mainly BiCuSeO , have attracted a lot of attention as p -type material candidates due to their intrinsically low thermal conductivity and moderate PF values [657]. These materials have a complex crystal structure consisting of alternating insulating $(\text{Bi}_2\text{O}_2)^{2+}$ layers and conductive $(\text{Cu}_2\text{Se}_2)^{2-}$ layers along the c -axis [672]. The occurrence of low thermal conductivity is linked to the layered crystal structure with low Young's modulus and speed of sound [673]. BiCuSeO exhibits a large Seebeck coefficient varying from $353 \mu\text{V K}^{-1}$ at 300 K to $420 \mu\text{V K}^{-1}$ at 923 K [657]. The high S values is linked to the two dimensional confinement of charge carriers due to the layered crystal structure and alternated stacking of insulating and conductive layers [658]. BiCuSeO has typically low electrical conductivity and exhibits semiconductor-like conduction behavior with temperature [657–659]. PF values generally improved with doping at the Bi site as a result of the significant increase in electrical conductivity; reasonable values were obtained for compositions containing Bi and/or O vacancies. Moreover, co-doping strategies generally resulted in further improvement in PF values due to the increased contribution of charge carriers; thermal conductivity generally increased with doping. However, the increase in the PF with doping compensates for relatively small increase in thermal conductivity, which leads to higher zT values. For example, a zT_{max} value of 1.46 at 873 K is reported for $\text{Bi}_{0.94}\text{Pb}_{0.06}\text{Cu}_{0.99}\text{Fe}_{0.01}\text{SeO}$ [664].

Transport properties for the various oxides (based on data collected for 300 K) are summarized in figure 10. Currently, there are considerably more n -type oxides than p -type materials available and this is reflected in figure 10(a), showing the relationship between Seebeck coefficient and electrical conductivity. Materials such as STO and BiCuSeO which inherently have exceptionally low electrical conductivities exhibit the highest Seebeck coefficients (above $300 \mu\text{V K}^{-1}$). However, by doping, electrical conductivity can be increased for all oxides, and indeed by careful processing, very high σ values (towards 4000 S cm^{-1}) and single-crystal like electrical conductivity have been achieved in STO.

Whilst there is a desire for phonon-glass behavior, and high thermoelectric performance in oxides, it is clear from figure 10(b) that whilst high electrical conductivity can be achieved (e.g. for STO), the problem



continues to be high thermal conductivity, exceptionally high in some cases with the exception of BiCuSeO. However, by selective doping and nanostructuring there has been progress in recent years, and many of the layered structured compounds and the complex tungsten bronze structured materials do exhibit low thermal conductivities (down to $1.45 \text{ W m}^{-1} \text{ K}^{-1}$). Alternatively, intrinsically low thermal conductivity (as low as $0.6 \text{ W m}^{-1} \text{ K}^{-1}$) and moderate electrical conductivity of oxyselenides leads to relatively high zT values. Figure 10(c) shows the weighted mobility (which was calculated via experimental S and σ values using equation (4)) as a function of lattice thermal conductivity for eight oxide families. As noted earlier (in sections 1.4, 3.4 and 3.6) the ratio of weighted mobility to lattice thermal conductivity (denoted by m) is directly proportional to the thermoelectric quality factor, B (equation (3)), which in turn is proportional to the thermoelectric figure of merit, zT . The highest value of m (i.e. high μ_w and low κ_L) is observed for BiCuSeO materials (the highest $m \approx 330$) whilst it is approximately 160–180 for STO and CMO materials. These values are broadly comparable with many of the metallic counterparts, although the best Zintlts reach m values in excess of 350 (figure 5) similar to that for BiCuSeO. Finally figure 10(d) summarizes peak zT values as a function of temperature. Several oxide materials have peak zT values above 0.6 at temperatures above 800 K whereas zT_{max} values are typically >0.8 and even reaching to ~ 1.5 for oxyselenides around 900 K.

With the advances in computational material science [674, 675], many materials can first be theoretically screened and then the promising compositions can be evaluated experimentally. Such studies suggest that oxides with zT values above 1 are possible and the utilization of new material design concepts, such as introducing/controlling interfaces at both atomic [676] and micro [677] scales, will allow control of both phonon and charge carrier transport in oxides. This will enable oxides to be competitive with more established materials, since they can offer much more once they can be utilized to full capacity, including their stability over a wide temperature range, lower density, lower toxicity, and cheaper material production.

The mobility data in table 9 are predominantly obtained from Hall measurements; only one entry has been obtained by SPB method; both types of entry are clearly identified.

Table 9. Oxides—thermoelectric properties.

Material	T (K)	μ_w ($\text{cm}^2 \text{V}^{-1} \text{s}^{-1}$)	κ ($\text{W m}^{-1} \text{K}^{-1}$)	S ($\mu\text{V K}^{-1}$)	σ ($\Omega^{-1} \text{cm}^{-1}$)	zT	μ_{H} ($\text{cm}^2 \text{V}^{-1} \text{s}^{-1}$) ^a	m_s^* (me)	n (10^{20}cm^{-3})	References
<i>n-Type oxides</i>										
La-SrTiO ₃	300	219.7	9.5	-150.0	1000.0	0.08	9.2	—	6.8	[596]
	1073	15.6	3.0	-291.7	80.0	0.27	—	—	—	
Sr _{0.92} La _{0.08} TiO ₃	300	456.8	5.9	-107.3	3070.6	0.19	—	—	—	[597]
	1045	20.6	3.0	-233.1	200.0	0.37	—	—	—	
La _{0.1} Sr _{0.83} Dy _{0.07} TiO ₃	300	107.9	6.1	-70.7	921.1	0.04	—	—	—	[598]
	1045	16.5	2.6	-200.9	234.9	0.36	—	—	—	
Sr _{0.85} Pr _{0.15} TiO ₃	323	309.9	5.5	-72.2	3838.2	0.12	11.8	—	23.0	[599]
	723	45.4	3.8	-161.4	647.4	0.35	—	—	—	
La _{0.067} Sr _{0.9} TiO _{3-δ} + 0.6G	323	173.0	1.8	-122.6	1066.7	0.42	—	—	—	[600]
	1023	9.7	2.1	-221.2	105.0	0.36	—	—	—	
Sr _{0.8} La _{0.067} Ti _{0.8} Nb _{0.2} O ₃	310	50.6	4.6	-69.2	622.8	0.02	1.6	—	28.3	[601]
	1023	15.1	3.1	-167.8	303.4	0.27	—	—	—	
Sr _{0.9} La _{0.1} Ti _{0.9} Nb _{0.1} O ₃	323	48.1	4.2	-98.5	411.8	0.01	0.9	—	15.0	[602]
	1100	31.9	2.8	-287.8	201.8	0.66	—	—	—	
Sr _{0.8} La _{0.06} Ti _{0.8} Nb _{0.2} O ₃ + 2.5 wt%Fe	315	71.0	—	-69.6	966.2	0.02	0.9	—	56.0	[603]
	1000	50.8	2.9	-169.6	882.4	0.38	—	—	—	
Sr _{0.9} Nd _{0.1} TiO ₃ + 0.5%wt B ₂ O ₃ + 0.3 wt% ZrO ₂	310	168.9	6.9	-94.3	1418.9	0.06	2.1	—	42.0	[604]
	1015	18.9	2.9	-215.1	217.6	0.37	—	—	—	
Sr _{0.8} La _{0.067} Ti _{0.8} Nb _{0.2} O _{3-d} + 1 wt% G	310	2.3	4.2	-327.2	1.2	0.002	—	—	—	[605]
	965	0.9	2.8	-360.3	1.8	0.03	—	—	—	
SrTiO ₃ + 0.7 wt% RGO	300	231.7	7.7	-356.1	85.3	0.04	25.4	—	0.9	[606]
	750	11.1	3.6	-343.6	18.2	0.05	—	—	—	
Sr _{0.98} Ti _{0.90} Nb _{0.10} O _{3$\pm\delta$} + 0.6 wt% rGO	315	240.2	6.7	-97.1	1993.6	0.09	23.7	—	5.2	[607]
	1160	11.9	2.9	-221.1	155.6	0.29	—	—	—	
Sr _{0.9} La _{0.1} TiO ₃ + 20 wt% Ti	330	119.3	2.4	-183.3	370.4	0.08	161.4	—	0.1	[608]
	1073	16.2	1.3	-321.4	59.0	0.50	—	—	—	
SrTi _{0.85} Nb _{0.15} O ₃ + 1.5 wt% GO	323	49.6	7.1	-66.2	676.9	0.007	9.0	—	4.7	[609]
	1200	6.3	3.4	-187.7	126.9	0.50	—	—	—	
Sr _{0.9} La _{0.1} Ti _{0.9} Nb _{0.1} O ₃	315	102.2	5.6	-89.2	947.5	0.15	7.2	—	7.0	[610]
	793	38.0	3.9	-162.7	554.1	0.39	—	—	—	
Sr _{0.95} (Ti _{0.8} Nb _{0.2}) _{0.95} Ni _{0.05} O ₃	305	88.4	—	-63.9	1150.0	—	—	—	—	[611]
	1073	13.0	1.4	-206.9	177.3	0.60	—	—	—	

(Continued.)

Table 9. (Continued.)

Material	T (K)	μ_w ($\text{cm}^2 \text{V}^{-1} \text{s}^{-1}$)	κ ($\text{W m}^{-1} \text{K}^{-1}$)	S ($\mu\text{V K}^{-1}$)	σ ($\Omega^{-1} \text{cm}^{-1}$)	zT	μ_{H} ($\text{cm}^2 \text{V}^{-1} \text{s}^{-1}$) ^a	m_s^* (m _e)	n (10^{20}cm^{-3})	References
La _{0.08} Sr _{0.9} TiO _{3-δ}	330	182.9	8.0	-114.7	1287.7	0.07	10.9	4.2	7.4	[612]
CaMn _{0.98} Nb _{0.02} O ₃	867	18.8	4.3	-209.2	182.0	0.16	—	—	—	[613]
	340	15.4	0.9	-192.6	44.4	0.09	—	—	—	
Ca _{0.92} Pr _{0.04} Yb _{0.04} MnO ₃	1060	3.7	0.8	-247.0	31.4	0.32	—	—	—	[614]
	330	32.0	1.7	-145.7	153.3	0.07	—	—	—	
Ca _{0.97} Bi _{0.03} MnCu _{0.04} O _{3-δ}	973	6.3	1.3	-196.3	84.4	0.24	—	—	—	[615]
	377	200.3	1.8	-196.4	645.2	0.51	—	—	—	
Ca _{0.89} Pr _{0.08} St _{0.03} MnO ₃	1073	9.5	1.5	-213.9	120.7	0.44	—	—	—	[616]
	373	25.4	1.8	-179.5	98.2	0.07	24.4	—	1.3	
Ba _{0.1} Eu _{0.9} TiO _{3-δ}	973	7.1	1.8	-143.8	176.6	0.20	—	—	—	[617]
	323	—	7.9	-853.2	—	—	—	—	—	
Zn _{0.98} Al _{0.02} O	1123	12.6	2.7	-300.0	62.9	0.24	0.4	—	9.6	[618]
	300	107.7	40.2	-97.1	831.2	0.007	73.5	—	0.7	
Ca-doped (ZnO) _{3.5} In ₂ O ₃	1273	16.3	5.3	-179.4	396.8	0.30	—	—	—	[619]
	545	9.7	2.9	-86.0	215.1	0.03	—	—	—	
Zn _{0.96} Al _{0.02} Ga _{0.02} O	1053	8.0	2.2	-168.4	166.7	0.23	—	—	—	[620]
	305	139.3	13.1	-135.3	672.7	0.03	—	—	—	
Zn _{0.96} Ga _{0.04} O _{1.02}	1073	38.0	4.8	-236.0	371.1	0.52	—	—	—	[621]
	350	9.6	8.1	-88.8	105.3	0.003	6.5	—	1.0	
Ni-coated In ₂ O ₃ (ZnO) ₅	1000	5.7	3.6	-174.5	102.6	0.09	—	—	—	[622]
	373	7.7	1.8	-89.0	—	—	24.3	—	0.1	
In ₂ O ₃ (ZnO) ₃	973	7.7	1.3	-172.0	136.0	0.39	—	—	—	[623]
	330	34.5	3.2	-64.1	503.8	0.02	—	—	—	
Sr _{0.61} Ba _{0.39} Nb ₂ O _{5.95} F _{0.05}	973	12.9	2.6	-133.8	361.5	0.24	—	—	—	[624]
	323	3.1	—	-152.9	13.1	0.006	—	—	—	
Sr _{0.50} La _{0.20} Ba _{0.30} Nb ₂ O _{6-δ}	1073	6.7	2.0	-204.3	94.4	0.21	—	—	—	[625]
	323	4.7	1.4	-140.2	23.5	0.01	—	—	—	
Ba _{5.19} Nd _{8.54} Ti ₁₈ O ₅₄	1073	7.1	2.1	-180.9	131.6	0.22	—	—	—	[626]
	350	14.2	—	-110.0	115.8	—	—	—	—	
Ba ₆ Ti ₂ Nb ₈ O ₃₀	1000	5.0	1.5	-210.0	60.0	0.16	—	—	—	[627]
	350	5.9	1.8	-102.1	54.0	0.01	0.4	—	14.5	
Ti ₈ (O,N) ₁₅	873	6.4	1.7	-176.6	90.9	0.14	—	—	—	[628]
	300	13.0	1.6	-125.5	69.2	0.02	—	—	—	

(Continued.)

Table 9. (Continued.)

Material	T (K)	μ_w ($\text{cm}^2 \text{V}^{-1} \text{s}^{-1}$)	κ ($\text{W m}^{-1} \text{K}^{-1}$)	S ($\mu\text{V K}^{-1}$)	σ ($\Omega^{-1} \text{cm}^{-1}$)	zT	μ_{H} ($\text{cm}^2 \text{V}^{-1} \text{s}^{-1}$) ^a	m_s^* (m_e)	n (10^{20}cm^{-3})	References
Ti _{0.83} Nb _{0.17} (O,N) _{2±δ}	550	13.8	1.8	-131.9	167.7	0.09	—	—	—	
	323	46.3	2.0	-230.0	80.0	0.08	—	—	—	[629]
	973	8.8	2.6	-198.4	115.0	0.35	—	—	—	
TiO _{1.76}	323	19.2	2.3	-85.3	195.4	0.02	—	—	—	[630]
	973	14.9	2.1	-148.3	350.0	0.35	—	—	—	
Ti ₉ O ₁₇	305	22.1	—	-178.1	64.2	0.16	0.2	12.6	18.3	[631]
	764	8.6	2.6	-168.8	110.0	0.01	—	—	—	[632]
TiAl _{0.02} O _{1.78}	320	37.4	2.7	-33.9	1007.5	0.20	—	—	—	
	973	14.0	2.6	-87.6	721.6	—	—	—	—	
<i>p-Type oxides</i>										
Ca _{2.7} Y _{0.3}	373	16.6	1.8	137.1	106.2	0.03	—	—	—	[633]
Co ₄ O _{9+δ}	973	6.6	1.5	171.7	117.2	0.22	—	—	—	
Ba _{0.1} Ag _{0.1} Ca _{2.8}	373	14.2	1.9	143.3	84.3	0.04	—	—	—	[634]
Co ₄ O ₉	973	7.8	1.4	172.0	138.9	0.29	—	—	—	
Ca _{2.8} Lu _{0.2}	300	19.4	1.5	155.1	72.0	0.04	—	—	—	[635]
Co ₄ O _{9+δ}	1073	6.6	1.2	194.0	105.0	0.36	—	—	—	
Ca _{2.97} Sr _{0.03} Co ₄ O ₉	1000	5.9	1.8	172.0	110.0	0.23	—	—	—	[636]
Ca ₃	323	16.2	3.4	155.4	67.0	0.02	—	—	—	[637]
Co _{3.9} Cr _{0.1} O _{9+δ}	1073	6.0	2.0	194.1	94.6	0.19	—	—	—	[638]
Ca _{2.9} Cd _{0.1}	323	19.4	2.1	141.2	94.9	0.03	—	—	—	
Co ₄ O ₉	1000	10.0	1.5	207.9	121.9	0.36	—	—	—	
Ca _{2.7} Gd _{0.3}	373	10.9	1.7	145.1	63.2	0.03	—	—	—	[639]
Co ₄ O _{9+δ}	973	7.6	1.4	179.2	124.5	0.24	—	—	—	
Ca _{2.8} Ba _{0.2}	300	30.3	1.7	139.6	135.3	0.05	—	—	—	[640]
Co ₄ O ₉	973	14.7	1.9	181.5	233.6	0.43	—	—	—	
Ca _{2.8} Ba _{0.2}	370	91.2	2.1	142.9	537.0	0.15	—	—	—	[641]
Co ₄ O ₉	1073	12.4	1.9	192.1	201.4	0.43	—	—	—	
Bi _{0.15} Ca _{2.85}	323	28.1	2.1	152.8	119.9	0.04	—	—	—	[642]
Co ₄ O ₉	973	9.1	1.8	181.3	144.6	0.25	—	—	—	
Ca _{2.5} Tb _{0.5}	300	8.0	1.3	132.6	39.2	0.01	—	—	—	[643]
Co ₄ O ₉	800	48.2	1.2	321.7	112.0	0.74	—	—	—	

(Continued.)

Table 9. (Continued.)

Material	T (K)	μ_w ($\text{cm}^2 \text{V}^{-1} \text{s}^{-1}$)	κ ($\text{W m}^{-1} \text{K}^{-1}$)	S ($\mu\text{V K}^{-1}$)	σ ($\Omega^{-1} \text{cm}^{-1}$)	zT	μ_H ($\text{cm}^2 \text{V}^{-1} \text{s}^{-1}$) ^a	m_s^* (m_e)	n (10^{20}cm^{-3})	References
$\text{Ca}_{2.95}\text{Sr}_{0.05}\text{Co}_4\text{O}_9$	367	19.1	2.2	156.8	94.0	0.04	—	—	—	[644]
$\text{Ca}_3\text{Co}_4\text{O}_9$	957	9.2	1.2	180.5	143.6	0.38	—	—	—	[645]
	367	12.6	1.9	144.9	71.6	0.03	—	—	—	[645]
	773	6.5	1.3	162.0	92.0	0.14	—	—	—	[646]
$\text{Bi}_2\text{Sr}_{1.8}\text{Co}_2\text{O}_x$	800	2.9	0.9	105.0	87.0	0.09	—	—	—	[646]
$\text{Bi}_2\text{Sr}_2\text{Co}_2\text{O}_y$	380	9.8	0.8	109.0	91.6	0.07	—	—	—	[647]
(Ag ₂ O powder 3 wt%)	973	3.7	0.9	167.1	68.7	0.26	—	—	—	[648]
$\text{Bi}_2\text{Sr}_{1.96}\text{La}_{0.04}\text{Co}_2\text{O}_9$	300	9.3	1.0	110.6	59.7	0.03	—	—	—	[648]
	737	4.2	1.3	177.9	46.2	0.15	—	—	—	[649]
$\text{Bi}_2\text{Sr}_2\text{Co}_2\text{O}_x$	300	28.5	0.9	111.7	181.1	0.07	—	—	—	[649]
	1000	5.7	1.2	162.4	118.1	0.27	—	—	—	[650]
$\text{Bi}_2\text{Sr}_2\text{Co}_2\text{O}_x$	300	27.9	0.9	112.1	176.2	0.07	—	—	—	[650]
	1000	5.8	1.2	163.5	119.0	0.27	—	—	—	[650]
$\text{La}_{0.95}\text{Sr}_{0.05}\text{Ni}_{0.2}\text{Co}_{0.8}\text{O}_3$	300	37.3	1.6	31.0	1000.0	0.006	—	—	—	[651]
$\text{NaCo}_{1.9}\text{Pd}_{0.1}\text{O}_4$	323	13.9	3.2	74.2	166.7	0.01	—	—	—	[652]
	723	4.6	2.9	108.7	113.6	0.05	—	—	—	[652]
$\text{Na}_x\text{Co}_2\text{O}_4$	300	0.8	3.7	67.5	9.6	0.001	—	—	—	[653]
	973	8.0	2.2	210.7	90.9	0.11	—	—	—	[653]
$\text{NaCo}_{0.9}\text{Ni}_{0.1}\text{O}_2$	373	17.7	2.3	116.6	145.9	0.01	—	—	—	[654]
	773	9.6	2.2	154.3	149.2	0.13	—	—	—	[654]
$\text{Na}_x\text{Co}_2\text{O}_4$	500	53.0	2.0	155.0	424.3	0.29	—	—	—	[655]
+ 10 wt% Ag	900	39.2	1.9	223.1	373.7	0.92	—	—	—	[655]
BiCuSeO	300	2.9	0.6	349.0	1.1	0.01	22.0	—	0.01	[656]
	923	16.0	0.4	425.0	13.9	0.50	—	—	—	[656]
$\text{Bi}_{0.875}\text{Ba}_{0.125}\text{CuSeO}$	300	49.4	0.7	84.9	452.8	0.12	3.0	—	11.0	[657]
	923	13.1	0.5	184.0	186.8	1.11	—	—	—	[657]
$\text{Bi}_{0.94}\text{Pb}_{0.06}\text{CuSeO}$	323	84.2	0.7	159.0	333.3	0.47	7.5	—	3.4	[658]
	823	17.3	0.5	221.0	135.0	1.14	—	—	—	[658]

(Continued.)

Table 9. (Continued.)

Material	T (K)	μ_{Av} ($\text{cm}^2 \text{V}^{-1} \text{s}^{-1}$)	κ ($\text{W m}^{-1} \text{K}^{-1}$)	S ($\mu\text{V K}^{-1}$)	σ ($\Omega^{-1} \text{cm}^{-1}$)	zT	μ_{H} ($\text{cm}^2 \text{V}^{-1} \text{s}^{-1}$) ^a	m_s^* (m_e)	n (10^{20}cm^{-3})	References
$\text{Bi}_{0.985}\text{Na}_{0.015}\text{CuSeO}$	300	108.2	0.8	255.2	125.0	0.31	9.9	—	0.6	[659]
	923	15.7	0.5	317.7	47.5	0.91	—	—	—	
$\text{Bi}_{0.94}\text{Pb}_{0.06}\text{CuSeO}$	300	106.6	1.0	135.7	500.0	0.30	—	—	7.8	[660]
	923	17.3	0.6	223.6	155.6	1.18	—	—	—	
$\text{Bi}_{0.96}\text{Pb}_{0.04}\text{CuSe}_{0.95}\text{Te}_{0.05}\text{O}$	323	73.5	0.8	171.9	250.0	0.28	8.6	2.8	1.8	[661]
	873	15.4	0.4	245.0	99.5	1.20	—	—	—	
$\text{Bi}_{0.875}\text{Ba}_{0.125}\text{Cu}_{0.85}\text{Ni}_{0.15}\text{SeO}$	315	61.5	1.1	358.0	23.2	0.08	4.0	—	0.3	[662]
	923	30.4	0.5	402.0	34.5	0.97	—	—	—	
$\text{Bi}_{0.88}\text{Mg}_{0.06}\text{Pb}_{0.06}\text{CuSeO}$	300	181.6	1.1	100.0	1346.9	0.24	—	—	2.5	[663]
	750	51.6	0.7	183.1	544.7	1.19	—	—	—	
$\text{Bi}_{0.94}\text{Pb}_{0.06}\text{Cu}_{0.99}\text{Fe}_{0.01}\text{SeO}$	310	124.1	0.8	169.8	406.7	0.47	11.5	—	2.2	[664]
	873	23.1	0.5	237.7	162.1	1.46	—	—	—	
$\text{Bi}_{0.90}\text{Ba}_{0.10}\text{CuSe}_{0.90}\text{Te}_{0.10}\text{O}$	300	69.7	1.2	110.2	451.1	0.47	4.9	—	6.9	[665]
	873	71.4	0.8	295.2	257.5	1.17	—	—	—	
$\text{Bi}_{0.94}\text{Y}_{0.06}\text{CuSeO}$	300	14.5	0.7	91.2	121.7	0.04	—	—	—	[666]
	873	12.0	0.5	161.8	204.5	0.93	—	—	—	
$\text{Bi}_{0.92}\text{Pb}_{0.08}\text{CuSeO}$	300	116.4	0.8	120.1	662.8	0.36	1.2	3.1	3.8	[667]
+ 8% SiC	873	19.2	0.6	187.2	243.2	1.32	—	—	—	
$\text{Bi}_{0.88}\text{Li}_{0.06}\text{Ca}_{0.06}\text{CuSeO}$	300	103.6	1.4	192.3	248.7	0.17	4.0	—	10.0	[668]
	873	20.5	0.7	289.0	79.5	0.87	—	—	—	

^a All data in the μ_{H} column are for Hall mobility, except for: SPB = intrinsic mobility—single parabolic band model.

3.10. Sulfides and selenides

Sulfide and selenide thermoelectrics

Anthony V Powell, Shriparna Mukherjee, Sahil Tippireddy and Paz Vaquero

Department of Chemistry, University of Reading, RG6 6DX Reading, United Kingdom

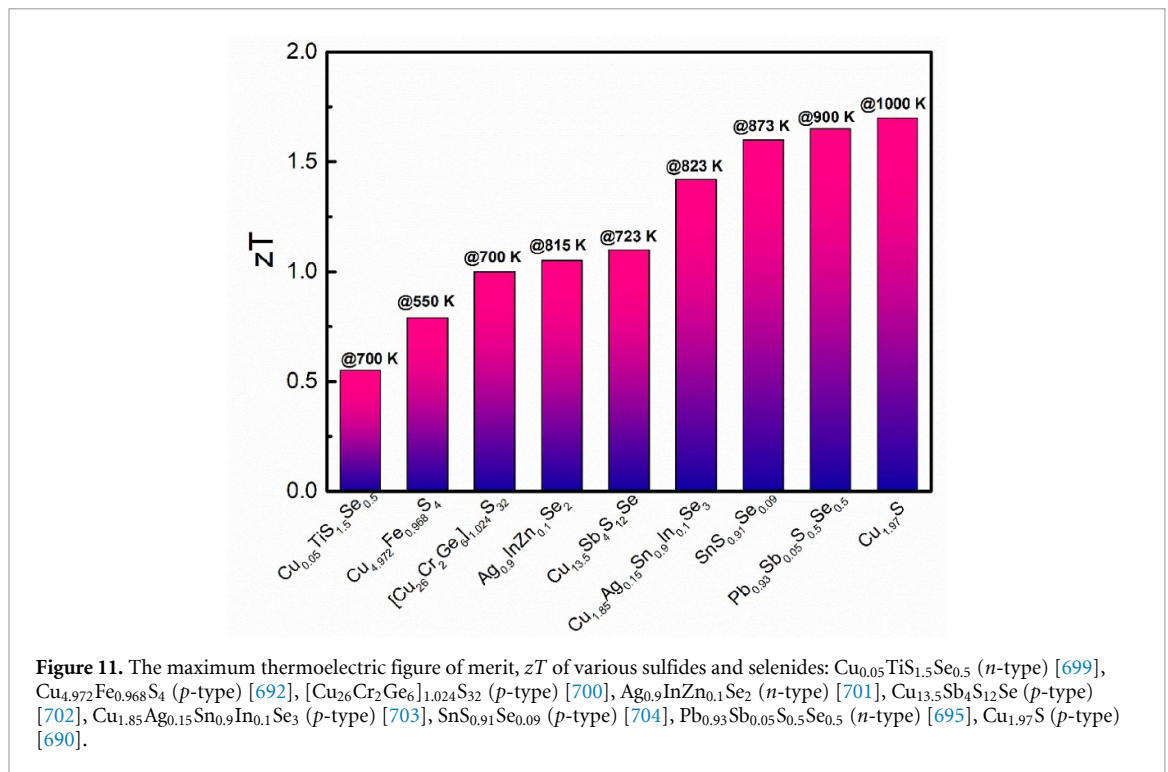
The terrestrial abundance of both sulfur (3.5×10^5 ppb) and selenium (50 ppb) exceeds that of tellurium (1 ppb), making metal sulfides and selenides attractive candidates for large-scale thermoelectric applications. While the higher vibrational frequencies associated with the lighter chalcogens are expected to result in a higher thermal conductivity than in the tellurides, a number of materials-design strategies [678] have been applied to generate high-performance materials. The decrease in electronegativity on progressing down the chalcogen group raises the energy of the anion valence orbitals, thus reducing the bandgap (E_g) between the predominantly anion-based orbitals of the valence band and the cation-derived conduction band. The reduced separation between anion- and cation-derived orbitals leads to more effective orbital overlap and broadening of the bands. This is exploited in partial substitution of sulfur by selenium to fine-tune the electronic structure through band broadening, thereby reducing the carrier effective mass (m^*) and increasing the mobility (μ). Sulfide and selenide thermoelectrics are not without challenges. In particular, volatilization of the chalcogen during preparation or processing may occur, producing compositional changes and the formation of inclusions of secondary phases. In favorable cases, the resulting interfaces may increase phonon scattering and reduce thermal conductivity. The majority of metal sulfide and selenide thermoelectrics are *p*-type semiconductors; *n*-type conduction generally occurring in low-dimensional structures and amongst chalcopyrite-related phases.

In seeking to translate the high-performance of metal tellurides into the more abundant sulfides and selenides, attention has focused on the lighter congeners of tellurides of proven thermoelectric performance. This includes the rocksalt-structured phases PbQ (Q = S, Se) for which both *n*- and *p*-type derivatives can be created through appropriate doping, and figures of merit, $zT \geq 1$. Increasing concerns over the toxicological and environmental impact of lead has prompted investigation of the analogous tin and germanium sulfides and selenides, the layered structures of which arise from distortion of the rocksalt structure. The figure of merit, $zT > 2.4$, achieved in single crystalline SnSe [679], has motivated a wider investigation of tin chalcogenides. Although the corresponding sulfide, SnS, adopts a similar structure, the maximum figure of merit is somewhat lower at $zT = 0.8$ at 873 K [680]. While conventional doping of GeSe leads to modest improvements in performance, alloying with AgSbSe₂ results in a *p*-type material with a figure of merit, $zT = 0.9$ at 710 K [681] while alloying with AgBiSe₂ produces an *n*-type variant which exhibits a maximum figure of merit, $zT = 0.44$ at 677 K [682].

The more structured DOS associated with a low-dimensional structure has stimulated efforts to increase the Seebeck coefficient by tuning the Fermi level to sharp discontinuities in the DOS [683], although reductions in thermal conductivity due to interface scattering of phonons appears to play a more dominant role. One-dimensional chain structures [684] and two-dimensional structures, including intercalates of dichalcogenides, A_xTiS₂ (A = Co, Cu, Ag) [685–687] and a variety of pavonite-related materials [688, 689], have been investigated, together with materials possessing low-dimensional structural motifs within a 3D structure, as exemplified by the derivatives of shandite, Co₃Sn₂S₂.

The high polarizability of the sulfide and selenide anions favors cation diffusion, which at high temperatures can induce the cation sub-lattice to enter a liquid-like state. The term phonon-liquid electron-crystal (PLEC) has been applied to such phases. The PLEC-type phases Cu_{1.97}S and Cu_{2-x}Se exhibit an exceptional thermoelectric performance, with figures of merit reaching $zT = 1.7$ [690] and $zT = 1.5$ [691] respectively (figure 11). The cation mobility that promotes PLEC behavior introduces an instability into the materials, due to copper migration and deposition, resulting in compositional changes that cause cracking and mechanical degradation. Efforts to overcome stability problems have motivated investigation of alternative structure types, in which a proportion of the tetrahedral sites are occupied by other cations. A wide range of cation-ordered derivatives of zinc blende, including chalcopyrite, kesterite and stannite, has been investigated, along with structurally more complex phases such as bornite, in which antiferro- and zinc-blende-type sub-cells alternate. A combination of hole doping and the creation of cation vacancies in bornite, leads to a figure of merit, $zT \approx 0.8$ [692], at 550 K, with no significant degradation in performance on thermal cycling.

The beneficial effect of increasing structural complexity is exemplified by tetrahedrite, the structure of which may be considered as a defective derivative of zinc-blende containing transition-metal cations in both tetrahedral and trigonal-planar sites. The parent sulfide Cu₁₂Sb₄S₁₃ is a *p*-type metal, with a low thermal conductivity, associated with anharmonic localized vibrational modes. Reduction of the hole carrier



concentration through chemical substitution of copper, increases the figure of merit to $zT \approx 1.0$ at relatively modest temperatures ($575 \leq T/\text{K} \leq 725$). Tuning the electronic structure through the partial replacement of sulfide with selenium decreases the resistivity, without a significant impact on the Seebeck coefficient. This appears to have the greatest impact on performance at temperatures close to ambient.

The structure of colusite ($\text{Cu}_{26}\text{V}_2\text{Ge}_6\text{S}_{32}$) may also be considered to be derived from an ordered variant of zinc blende. The complex structure and large unit cell contribute to a low thermal conductivity, $\kappa \approx 0.5 \text{ W m}^{-1} \text{ K}^{-1}$. Substitution of copper in colusite and its congeners, with dipositive transition-metal cations, decreases the hole carrier concentration and improves the Seebeck coefficient, leading to figures of merit at elevated temperatures in the range $0.6 \leq zT \leq 0.9$. Colusite provides a striking example of the impact of consolidation conditions on thermoelectric properties [693]. Hot pressing (HP 1023 K) $\text{Cu}_{26}\text{V}_2\text{Sn}_6\text{S}_{32}$ results in sulfur loss and the formation of intergrowths that help reduce the thermal conductivity to $\kappa \approx 0.66 \text{ W m}^{-1} \text{ K}^{-1}$, increasing the figure of merit by a factor of three ($zT = 0.93$ at 675 K [693]) over that of the same material subjected to spark plasma sintering (SPS 873 K) at a lower temperature.

As illustrated in table 10, there has been considerable progress in the discovery of sulfides and selenides for thermoelectric applications. There are now several families of *p*-type sulfides containing Earth-abundant elements, with figures of merit approaching or exceeding unity at moderate temperatures, including tetrahedrites and colusites. Among *p*-type selenides, Cu_2Se and SnSe , with maximum figures of merit of $zT = 1.54$ and $zT = 2.6$ at 1000 and 923 K respectively, stand out [679, 691]. Furthermore, it has been demonstrated very recently that exceptional thermoelectric performance ($zT = 3.1$ at 783 K [694]) can be achieved in polycrystalline SnSe when feedstock reagents are purified to remove all traces of oxides. By contrast, it is evident from table 10 that there are few examples of *n*-type sulfides and selenides with comparable performances. The few exceptions including $\text{Pb}_{0.93}\text{Sb}_{0.05}\text{S}_{0.5}\text{Se}_{0.5}$, with a maximum figure of merit of $zT = 1.65$ at 900 K [695] and Ag_2Se , with $zT = 1.2$ near room temperature [696]. The discovery of environmentally friendly *n*-type sulfides, containing abundant elements and with good thermoelectric performance, remains a challenge to be addressed.

As noted above, stability problems, due to cation migration, are a concern for PLEC-type phases such as Cu_2Se and Ag_2Se . In a thermoelectric device, electromigration of the mobile cations occurs when an electrical current flows through the PLEC material. This results in a compositional gradient along the thermoelectric leg, together with cracking and loss of performance [697]. Possible approaches to minimize degradation due to ionic diffusion, which need to be fully investigated, include the introduction of additional cations to block the migration path of the mobile cations, or tuning the geometry of the thermoelectric legs to ensure that the voltage applied to the PLEC material remains below a critical threshold [698].

In the case of sulfides or selenides, volatilization of the chalcogen at the elevated temperatures at which a device operates, may result in materials degradation and hence deterioration of the thermoelectric

performance. Development of protective coatings may be required to address this issue. Device construction will also require the identification of suitable diffusion-barrier materials and solders, for these new families of materials. Matching the coefficients of thermal expansion of the different device components will be also essential, to avoid the possible fracture of the thermoelectric device during operation. To achieve progress in the implementation of thermoelectric technology, the research efforts that have led to the discovery of new sulfides and selenides should be followed by work that addresses the device level challenges.

Acknowledgments

We thank the UK Engineering and Physical Sciences Research Council (EP/T020040) and the Leverhulme Trust (RPG-2019-288) for financial support.

Table 10. Sulfide and selenide thermoelectric properties.

Material	T (K)	μ_w ($\text{cm}^2 \text{V}^{-1} \text{s}^{-1}$)	κ_L ($\text{W m}^{-1} \text{K}^{-1}$)	κ ($\text{W m}^{-1} \text{K}^{-1}$)	S ($\mu\text{V K}^{-1}$)	σ ($\Omega^{-1} \text{cm}^{-1}$)	zT	E_g (eV)	μ_{H} ($\text{cm}^2 \text{V}^{-1} \text{s}^{-1}$)	m_s^* (m_e)	ϵ_r or ϵ (ϵ_0)	n_{H} (cm^{-3})	References
Binary phases													
Cu_2Se (p)	420	40.6	0.6	1	100	500	0.2	1.23 ^a	—	4.2	—	3.2×10^{20}	[691, 705]
Cu_2Se (p)	1000	29.8	0.5	0.75	300	125	1.54	1.23 ^a	—	—	—	—	[691]
$\text{Cu}_{1.94}\text{Se}_{0.5}\text{S}_{0.5}$ (p -type)	300	37.7	0.45	0.7	100	280	0.1	—	—	4.2	—	1.0×10^{21}	[706]
$\text{Cu}_{1.94}\text{Se}_{0.5}\text{S}_{0.5}$ (p -type)	1000	27.3	0.2	0.6	220	290	2.3	—	—	—	—	—	[706]
$\text{Cu}_{1.97}\text{S}$ (p -type)	300	10.8	0.55	0.6	100	80	0.04	—	—	—	—	7.27×10^{20}	[690]
$\text{Cu}_{1.97}\text{S}$ (p -type)	1000	22.6	0.35	0.5	300	95	1.7	—	—	5.7	—	—	[690]
Cu_2S (p -type)	300	14.5	0.35	0.39	300	10	0.07	—	—	—	—	0.48×10^{19}	[690]
Cu_2S (p -type)	1000	13.5	0.32	0.35	450	10	0.65	—	—	—	—	—	[690]
$\text{Cu}_2\text{Se}_{0.92}\text{S}_{0.08}$ (p -type)	300	134.6	0.28	0.75	100	1000	0.4	—	—	2.3	—	2.8×10^{20}	[707]
$\text{Cu}_2\text{Se}_{0.92}\text{S}_{0.08}$ (p -type)	1000	23.7	0.37	0.5	275	133	2	—	—	—	—	—	[707]
$\text{Cu}_{1.98}\text{Ag}_{0.2}\text{Se}$ (p -type)	300	24.1	0.6	0.8	40	500	0.03	—	300^e	—	—	—	[111]
$\text{Cu}_{1.98}\text{Ag}_{0.2}\text{Se}$ (p -type)	900	4.4	0.25	0.4	260	25	0.4	0.45	3.16^e	—	—	—	[111]
PbSe (p -type)	300	414.6	—	1.8	320	227	0.38	0.26	—	0.11	210	9.0×10^{17}	[708–710]
PbSe (n -type)	900	5.4	—	1.6	—150	110	0.13	—	—	—	—	—	[710]
$\text{Pb}_{0.975}\text{Cu}_{0.005}\text{Na}_{0.02}\text{Te}_{0.1}\text{Se}_{0.9}$ (p -type)	300	121.3	0.95	2.5	50	2000	0.06	—	—	—	—	1.5×10^{20}	[710]
$\text{Pb}_{0.975}\text{Cu}_{0.005}\text{Na}_{0.02}\text{Te}_{0.1}\text{Se}_{0.9}$ (p -type)	860	50.1	0.7	0.89	294	180	1.5	—	—	—	—	—	[710]
$\text{Te}_{0.1}\text{Se}_{0.9}$ (p -type)	300	102.2	2	3.8	34	2500	0.02	—	—	—	—	0.93×10^{20}	[711]
$\text{Pb}_{0.993}\text{Na}_{0.007}\text{Se}$ (p -type)	850	37.2	0.6	1.1	200	390	1.2	—	—	—	—	—	[711]
$\text{Pb}_{0.993}\text{Na}_{0.007}\text{Se}$ (p -type)	300	83.6	1.59	3.68	24	2901	0.01	—	—	—	—	1.6×10^{20}	[712]
$\text{Pb}_{0.98}\text{Sr}_{0.02}\text{Se}$ 1% Na (p -type)	923	38.5	0.73	1.14	246	268	1.3	—	—	—	—	—	[712]
$\text{Pb}_{0.98}\text{Sr}_{0.02}\text{Se}$ 1% Na (p -type)	300	33.3	—	2.5	300	23	0.02	0.37	—	0.16	169	—	[708, 709, 695]
PbS (p -type)	900	2.0	—	1.25	—200	23	0.066	—	—	—	—	—	[695]
PbS (n -type)	300	78.3	1.1	1.6	—70	900	0.08	—	—	—	—	—	[695]
$\text{Pb}_{0.93}\text{Sb}_{0.05}\text{S}_{0.5}\text{Se}_{0.5}$ (n -type)	900	32.0	0.3	0.8	—188	421	1.65	—	—	—	—	—	[695]
$\text{Pb}_{0.93}\text{Sb}_{0.05}\text{S}_{0.5}\text{Se}_{0.5}$ (n -type)	300	242.2	—	3	—100	1800	0.18	—	—	—	—	1.5×10^{19}	[713]
$\text{Pb}_{0.985}\text{Ga}_{0.0125}\text{In}_{0.001}\text{S}$ (n -type)	920	34.6	—	1	—283	156	1.1	—	—	—	—	—	[713]
$\text{Pb}_{0.985}\text{Ga}_{0.0125}\text{In}_{0.001}\text{S}$ (n -type)	300	5.7	—	1	175	16.67	0.02	0.4^a	630^e	0.35	—	1.67×10^{19}	[714]
$\text{Sn}_{0.98}\text{Na}_{0.02}\text{S}$ (p -type)	850	13.2	—	0.45	325	32.5	0.65	—	—	1.2	—	—	[714]
$\text{Sn}_{0.98}\text{Na}_{0.02}\text{S}$ (p -type)	300	0.0	—	1	250	0.005	9.3×10^{-6}	—	—	—	—	2.0×10^{19}	[715]
SnS (p -type)	848	8.7	—	0.3	400	9	0.41	1.12 ^a	—	—	—	—	[715]
SnS (p -type)	300	113.4	—	1	—875	0.1	2.30×10^{-3}	—	—	—	—	1.0×10^{17}	[716]
$\text{Sn}_{0.98}\text{Br}_{0.02}$ (n -type)	823	44.4	—	0.6	—627	3.15	0.17	—	—	—	—	—	[716]

(Continued.)

Table 10. (Continued.)

Material	T (K)	μ_w ($\text{cm}^2 \text{V}^{-1} \text{s}^{-1}$)	κ_L ($\text{W m}^{-1} \text{K}^{-1}$)	κ ($\text{W m}^{-1} \text{K}^{-1}$)	S ($\mu\text{V K}^{-1}$)	σ ($\Omega^{-1} \text{cm}^{-1}$)	zT	E_g (eV)	μ_{H} ($\text{cm}^2 \text{V}^{-1} \text{s}^{-1}$)	m_e^* (m_e)	ϵ_r or ϵ (ϵ_0)	n_{H} (cm^{-3})	References
$\text{SnS}_{0.9}\text{Se}_{0.09}$ (p-type)	300	568.0	1.7	2.4	200	1250	0.6	—	—	—	—	—	[704]
$\text{SnS}_{0.91}\text{Se}_{0.09}$ (p-type)	873	53.9	0.5	0.61	370	82	1.6	—	—	—	—	—	[704]
SnS (p-type)	300	0.0	—	1.3	400	0.008	2.90×10^{-5}	1.21 ^a	5 ^c	—	—	1.37×10^{14}	[717]
SnS (p-type)	820	14.8	—	0.5	516	3.78	0.16	—	—	—	—	—	[717]
SnS-0.5\%Ag (p-type)	300	10.3	—	0.88	350	4	0.02	1.18 ^a	3.5 ^c	1.42	—	2.72×10^{18}	[717]
SnS-0.5\%Ag (p-type)	870	15.1	—	0.42	377	21.1	0.6	—	—	—	—	—	[717]
SnSe (p-type)	300	147.0	0.68	0.7	500	10	0.1	0.86	—	—	—	3×10^{17}	[679]
SnSe (p-type)	923	38.3	0.25	0.35	350	80	2.6	—	—	—	—	1.0×10^{19}	[679]
$\text{Sn}_{0.85}\text{Se}$ (p-type)	325	4.9	0.95	0.95	217	10	0.02	—	—	—	—	7×10^{19}	[680]
$\text{Sn}_{0.85}\text{Se}$ (p-type)	873	20.9	0.44	0.46	375	30	0.8	—	—	—	—	—	[680]
$\text{Sn}_{0.98}\text{N}_{0.016}\text{Ag}_{0.004}\text{Se}$ (p-type)	300	55.6	—	1.3	150	220	0.1	~ 0.86	—	—	—	6.23×10^{19}	[718]
$\text{Sn}_{0.98}\text{N}_{0.016}\text{Ag}_{0.004}\text{Se}$ (p-type)	785	21.1	—	0.45	250	110	1.2	—	—	—	—	—	[718]
$\text{Ag}_{1.96}\text{S}$ (n-type)	300	424.4	—	0.47	—850	0.5	0.02	0.9 ^a	—	—	—	—	[719]
$\text{Ag}_2\text{Se}_{1.06}$ (n-type)	560	21.9	—	0.45	—143	240	0.62	—	—	—	—	1.2×10^{19}	[719]
Ag_2Se (n-type)	300	338.0	—	1.08	—153	1290	0.84	0.21	—	—	—	5.59×10^{18}	[720]
Ag_2Se (n-type)	300	409.1	—	1.1	—133	1988	0.96	0.16	—	—	—	1.07×10^{18}	[721]
Ag_2Se (n-type)	300	256.2	—	0.6	—170	800	1.2	—	—	—	—	6.63×10^{18}	[696]
Bi_2S_3 (n-type)	300	5.2	1.31	1.31	—351	2	0.01	—	—	—	—	3.7×10^{16}	[684]
Bi_2S_3 (n-type)	625	2.5	0.86	0.86	—323	4	0.03	—	—	—	—	—	[684]
$\text{Bi}_2\text{S}_3 + 0.5 \text{ mol\% BiCl}_3$ (n-type)	300	86.7	1.02	1.37	—103	619	0.15	—	—	—	—	2.6×10^{19}	[684]
$\text{Bi}_2\text{S}_3 + 0.5 \text{ mol\% BiCl}_3$ (n-type)	772	17.3	0.63	0.76	—234	106	0.57	—	—	—	—	—	[684]
$\text{Bi}_2\text{S}_{2.7}\text{Se}_{0.3} + 0.5 \text{ mol\% BiCl}_3$ (n-type)	300	58.7	1.18	1.38	—130	296	0.11	—	—	—	—	—	[684]
$\text{Bi}_2\text{S}_{2.7}\text{Se}_{0.3} + 0.5 \text{ mol\% BiCl}_3$ (n-type)	710	15.2	0.68	0.77	—257	63	0.39	—	—	—	—	—	[684]
Bi_2Se_3 (n-type)	300	97.6	—	2.42	—35	2320	0.04	—	—	—	—	—	[74]
Bi_2Se_3 (n-type)	523	33.6	—	2.08	—48	1329	0.08	—	—	—	—	—	[74]
$\text{Bi}_2\text{Se}_2\text{S}_1$ (n-type)	300	9.2	—	0.7	—193	22	0.03	—	—	—	—	—	[74]
$\text{Bi}_2\text{Se}_2\text{S}_1$ (n-type)	523	17.2	—	0.5	—295	29	0.23	—	—	—	—	—	[74]
$\text{Bi}_2\text{Se}_1\text{S}_2$ (n-type)	300	53.6	—	0.71	—195	125	0.2	—	—	—	—	—	[74]
$\text{Bi}_2\text{Se}_1\text{S}_2$ (n-type)	523	23.7	—	0.65	—224	91	0.37	—	—	—	—	—	[74]
$\text{Cu}_{0.01}\text{Bi}_2\text{Se}_3$ (n-type)	300	89.7	0.64	0.74	—171	277	0.33	—	—	—	—	—	[722]
$\text{Cu}_{0.01}\text{Bi}_2\text{Se}_3$ (n-type)	590	34.3	0.31	0.78	—104	666	0.54	—	—	—	—	—	[722]
$\text{Bi}_2\text{Se}_{1.5}\text{Te}_{1.5}$ (n-type)	300	126.3	0.6	0.83	—159	449	0.41	—	—	—	—	—	[723]

(Continued.)

Table 10. (Continued.)

Material	T (K)	μ_{av} ($\text{cm}^2 \text{V}^{-1} \text{s}^{-1}$)	κ_L ($\text{W m}^{-1} \text{K}^{-1}$)	κ ($\text{W m}^{-1} \text{K}^{-1}$)	S ($\mu\text{V K}^{-1}$)	σ ($\Omega^{-1} \text{cm}^{-1}$)	zT	E_g (eV)	μ_{HI} ($\text{cm}^2 \text{V}^{-1} \text{s}^{-1}$)	m_s^* (m_e)	ϵ_r or ϵ (ϵ_0)	η_{HI} (cm^{-3})	References
Bi_2Se_3 (n -type)	600	32.5	0.44	0.85	-171	284	0.59	—	—	—	—	—	[723]
$(\text{PbSe})_{0.5}\text{Bi}_2\text{Se}_3$ (n -type)	300	5.2	0.59	0.61	-90	44	0.02	—	—	—	—	—	[724]
$(\text{PbSe})_{0.5}\text{Bi}_2\text{Se}_3$ (n -type)	700	8.7	0.34	0.39	-229	49	0.48	—	—	—	—	—	[724]
$(\text{PbSe})_{0.5}(\text{Bi}_2\text{Se}_3)_2$ (n -type)	300	5.0	0.63	0.72	-30	139	0.01	—	—	—	—	—	[724]
$(\text{PbSe})_{0.5}(\text{Bi}_2\text{Se}_3)_2$ (n -type)	700	6.8	0.41	0.57	-128	125	0.25	—	—	—	—	—	[724]
GeSe (p -type)	300	29.2	2.9	2.90	628	0.45	0.001	—	—	—	—	—	[725]
GeSe (p -type)	700	25.8	0.87	0.87	590	2.2	0.05	—	—	—	—	—	[725]
$\text{GeSe}(\text{AgSbTe}_2)_{0.2}$ (p -type)	300	58.0	0.63	0.71	177	167	0.22	—	—	—	—	—	[725]
$\text{GeSe}(\text{AgSbTe}_2)_{0.2}$ (p -type)	750	39.4	0.74	0.90	230	242	0.96	—	—	—	—	—	[725]
$\text{Ge}_{0.97}\text{Ag}_{0.03}\text{Se}$ (p -type)	300	1.1	1.16	1.16	350	0.44	0.002	—	—	—	—	—	[726]
$\text{Ge}_{0.97}\text{Ag}_{0.03}\text{Se}$ (p -type)	650	20.4	0.43	0.45	515	3.71	0.18	—	—	—	—	—	[726]
$\text{Ge}_{0.79}\text{Ag}_{0.01}\text{Sn}_{0.2}\text{Se}$ (n -type)	300	5.3	0.74	0.74	309	3.3	0.01	—	—	—	—	—	[726]
$\text{Ge}_{0.79}\text{Ag}_{0.01}\text{Sn}_{0.2}\text{Se}$ (n -type)	650	15.5	0.4	0.40	475	4.5	0.2	—	—	—	—	—	[726]
$(\text{GeSe})_{0.50}(\text{AgBiSe}_2)_{0.50}$ (n -type)	300	16.0	0.43	0.47	-208	32	0.09	0.4	—	—	—	3.29×10^{18}	[682]
$(\text{GeSe})_{0.50}(\text{AgBiSe}_2)_{0.50}$ (n -type)	677	11.9	0.48	0.61	-175	119	0.44	—	—	—	—	—	[682]
$\text{GeSe}(\text{AgSbSe}_2)_{0.2}$ (p -type)	300	23.1	0.85	0.88	153	88	0.07	—	—	—	—	—	[681]
$\text{GeSe}(\text{AgSbSe}_2)_{0.2}$ (p -type)	710	40.9	0.74	0.9	263	158	0.86	—	—	—	—	—	[681]
Chalcopyrites, tetrahedrites and bornites													
CuFeS_2 (n -type)	300	157.5	8.42	8.46	-362	53	0.02	0.7 ^b	—	1.8	—	3.2×10^{19}	[727, 728]
CuFeS_2 (n -type)	630	41.6	2.35	2.35	-384	33	0.13	—	—	—	—	—	[727]
$\text{Cu}_{0.95}\text{Zn}_{0.05}\text{FeS}_2$ (n -type)	300	94.5	5.3	5.4	-187	242	0.04	—	—	4.9	—	39.6×10^{19}	[727]
$\text{Cu}_{0.92}\text{Zn}_{0.08}\text{FeS}_2$ (n -type)	630	37.8	1.92	2	-263	122	0.26	—	—	—	—	—	[727]
$\text{Cu}_{0.95}\text{Cd}_{0.05}\text{FeS}_2$ (n -type)	300	111.4	3.91	3.98	-230	173.1	0.077	—	4.08 ^c	9	—	3.18×10^{20}	[729]
$\text{Cu}_{0.92}\text{Cd}_{0.08}\text{FeS}_2$ (n -type)	723	26.1	1.2	1.32	-265	101	0.39	—	—	—	—	—	[729]
AgInSe_2 (n -type)	370	164.9	0.71	0.72	-692	1.66	0.04	0.9 ^a	—	—	—	2.04×10^{17} ^c	[701]
AgInSe_2 (n -type)	800	10.3	0.33	0.35	-417	8	0.35	—	—	—	—	—	[701]
$\text{Ag}_{0.95}\text{In}_{0.05}\text{Zn}_{0.1}\text{Se}_2$ (n -type)	300	98.1	0.68	0.7	-436	14	0.1	0.9 ^a	—	—	—	6.68×10^{17}	[701]
$\text{Ag}_{0.95}\text{In}_{0.05}\text{Zn}_{0.1}\text{Se}_2$ (n -type)	815	16.6	0.28	0.37	-306	48	0.95	—	—	—	—	—	[701]
$\text{Ag}_{0.9}\text{InZn}_{0.1}\text{Se}_2$ (n -type)	300	16.7	0.38	0.42	-170	52	0.12	0.97 ^a	—	—	—	4.96×10^{18}	[701]
$\text{Ag}_{0.9}\text{InZn}_{0.1}\text{Se}_2$ (n -type)	815	10.7	0.11	0.34	-195	112	1.05	—	—	—	—	—	[701]
CuIn_3Se_5 (n -type)	300	14.1	1.1	1.12	-600	0.3	0.003	0.75 ^d	—	0.007	—	3×10^{16}	[730]
CuIn_3Se_5 (n -type)	930	2.9	0.64	0.68	-270	15.3	0.15	—	—	—	—	—	[730]

(Continued.)

Table 10. (Continued.)

Material	T (K)	μ_w ($\text{cm}^2 \text{V}^{-1} \text{s}^{-1}$)	κ_L ($\text{W m}^{-1} \text{K}^{-1}$)	κ ($\text{W m}^{-1} \text{K}^{-1}$)	S ($\mu\text{V K}^{-1}$)	σ ($\Omega^{-1} \text{cm}^{-1}$)	zT	E_g (eV)	μ_H ($\text{cm}^2 \text{V}^{-1} \text{s}^{-1}$)	m_s^* (m_e)	ϵ_r or ϵ (ϵ_0)	n_H (cm^{-3})	References
$\text{CuIn}_3\text{Se}_9\text{Te}_{0.1}$ (<i>n</i> -type)	300	1447.9	0.58	0.59	-1000	0.3	0.01	1.05 ^d	—	0.34	—	6×10^{17}	[730]
$\text{CuIn}_3\text{Se}_9\text{Te}_{0.1}$ (<i>n</i> -type)	930	5.0	0.4	0.42	-292	20.5	0.4	—	—	—	—	—	[730]
CuInSe_2 (<i>n</i> -type)	323	0.4	3.98	4	-100	3.5	0.01	0.894 ^a	32.6 ^{c,e}	—	—	9×10^{17} ^c	[731, 732]
CuInSe_2 (<i>n</i> -type)	773	0.2	0.9	0.92	-152	2.8	0.08	—	—	—	—	—	[731]
$\text{CuIn}_{0.98}\text{Zn}_{0.02}\text{Se}_2$ (<i>p</i> -type)	323	47.1	3.7	3.72	400	11.4	0.02	—	10.7 ^{c,e}	0.7 ^c	—	6.6×10^{18} ^c	[731]
$\text{CuIn}_{0.98}\text{Zn}_{0.02}\text{Se}_2$ (<i>p</i> -type)	773	15.8	0.9	0.92	448	8.1	0.18	—	—	—	—	—	[731]
$\text{Cu}_{0.99}\text{InSe}_{2.05}$ (<i>p</i> -type)	323	1.8	—	1.52	300	1.4	0.002	0.892 ^a	—	—	—	—	[732]
$\text{Cu}_{0.99}\text{InSe}_{2.05}$ (<i>p</i> -type)	620	33.3	—	0.38	510	6	0.31	—	—	—	—	—	[732]
Cu_3FeS_4 (<i>p</i> -type)	300	12.7	0.45	0.48	156	46.7	0.04	1.25 ^a	0.16 ^c	—	—	1.9×10^{21}	[733, 734]
$\text{Cu}_3\text{FeS}_3\text{Se}_{0.2}$ (<i>p</i> -type)	540	17.4	0.25	0.4	174	125	0.47	—	—	—	—	—	[733]
$\text{Cu}_3\text{FeS}_3\text{Se}_{0.2}$ (<i>p</i> -type)	300	24.0	0.38	0.47	120	137	0.1	—	1.15 ^c	2.42	—	6.24×10^{20}	[733]
$\text{Cu}_2\text{FeS}_3\text{Se}_{0.2}$ (<i>p</i> -type)	540	18.6	0.24	0.46	150	178	0.5	—	—	—	—	—	[733]
$\text{Cu}_{4.972}\text{Fe}_{0.968}\text{S}_4$ (<i>p</i> -type)	320	5.8	0.44	0.47	138	29.4	0.04	—	—	—	—	—	[692]
$\text{Cu}_{4.972}\text{Fe}_{0.968}\text{S}_4$ (<i>p</i> -type)	550	25.0	0.18	0.3	236	90	0.79	—	—	—	—	—	[692]
$\text{Cu}_{0.96}\text{Co}_{0.04}\text{Fe}_{0.96}\text{Zn}_{0.04}\text{S}_4$ (<i>p</i> -type)	323	5.9	0.33	0.36	106	45.5	0.05	—	—	—	—	—	[735]
$\text{Cu}_{0.96}\text{Co}_{0.04}\text{Fe}_{0.96}\text{Zn}_{0.04}\text{S}_4$ (<i>p</i> -type)	590	14.7	0.23	0.36	171	125	0.6	—	—	—	—	5.8×10^{19}	[735]
CuCrSe_2 (<i>p</i> -type)	300	54.5	—	1.12	95	434	0.1	—	—	—	—	—	[736]
CuCrSe_2 (<i>p</i> -type)	673	16.6	—	0.82	172	170	0.44	—	—	—	—	—	[736]
$\text{CuCr}_{0.99}\text{In}_{0.01}\text{Se}_2$ (<i>p</i> -type)	300	53.7	—	1.11	97	416	0.1	—	—	—	—	5.18×10^{19}	[736]
$\text{CuCr}_{0.99}\text{In}_{0.01}\text{Se}_2$ (<i>p</i> -type)	673	24.3	—	0.73	210	160	0.65	—	—	—	—	—	[736]
$\text{Cu}_{12}\text{Sb}_4\text{S}_{13}$ (<i>p</i> -type)	300	115.7	0.49	1.25	90	987	0.2	1.7 ^a	—	—	—	—	[737, 738]
$\text{Cu}_{12}\text{Sb}_4\text{S}_{13}$ (<i>p</i> -type)	723	41.2	0.5	1.41	131	767	0.65	—	—	—	—	—	[737]
$\text{Cu}_{0.5}\text{Ni}_j\text{Zn}_{0.5}\text{Sb}_4\text{S}_{13}$ (<i>p</i> -type)	300	38.8	0.42	0.5	156	143	0.2	—	—	—	—	—	[739]
$\text{Cu}_{0.5}\text{Ni}_j\text{Zn}_{0.5}\text{Sb}_4\text{S}_{13}$ (<i>p</i> -type)	723	28.9	0.4	0.58	215	200	1.03	—	—	—	—	—	[739]
$\text{Cu}_{13.5}\text{Sb}_4\text{S}_{12}\text{Se}$ (<i>p</i> -type)	300	17.7	0.42	0.46	150	70	0.1	—	—	—	—	—	[702]
$\text{Cu}_{13.5}\text{Sb}_4\text{S}_{12}\text{Se}$ (<i>p</i> -type)	723	35.0	0.25	0.78	174	390	1.1	—	—	—	—	—	[702]
Tetrahedral based structures													
$\text{Cu}_2\text{Sb}_{0.9}\text{Zn}_{0.1}\text{S}_3$ (<i>p</i> -type)	323	42.0	1.50	1.90	70	540	0.05	—	—	—	—	—	[740]
$\text{Cu}_2\text{Sb}_{0.9}\text{Zn}_{0.1}\text{S}_3$ (<i>p</i> -type)	723	19.6	0.43	0.80	150	290	0.58	—	—	—	—	—	[740]
$\text{Cu}_2\text{Sb}_{0.85}\text{Mn}_{0.15}\text{S}_3$ (<i>p</i> -type)	323	70.3	1.50	2.20	65	980	0.06	—	1.5 ^c	8	6×10^{21}	[741]	

(Continued.)

Table 10. (Continued.)

Material	T (K)	μ_{sw} ($\text{cm}^2 \text{V}^{-1} \text{s}^{-1}$)	κ^L ($\text{W m}^{-1} \text{K}^{-1}$)	κ ($\text{W m}^{-1} \text{K}^{-1}$)	S ($\mu\text{V K}^{-1}$)	σ ($\Omega^{-1} \text{cm}^{-1}$)	zT	E_g (eV)	μ_{H} ($\text{cm}^2 \text{V}^{-1} \text{s}^{-1}$)	m_s^* (m_e)	ϵ_r or ϵ (ϵ_0)	n_{H} (cm^{-3})	References
$\text{Cu}_2\text{Sn}_{0.85}\text{Mn}_{0.15}\text{S}_4$ (p-type)	723	28.2	0.32	1.00	135	500	0.68	—	—	—	—	—	[741]
$\text{Cu}_2\text{Sn}_{0.8}\text{Co}_{0.2}\text{S}_4$ (p-type)	323	51.9	0.95	1.40	67	700	0.07	—	1.01 ^c	7	—	4.35×10^{21}	[742]
$\text{Cu}_2\text{Sn}_{0.8}\text{Co}_{0.2}\text{S}_4$ (p-type)	723	29.4	0.33	0.80	155	410	0.85	—	—	—	—	—	[742]
Cu_2SnSe_3 single crystal (p-type)	300	—	—	—	—	—	—	0.843 ^a	4 ^c	1.2	13	1.5×10^{19}	[743]
$\text{Cu}_2\text{Sn}_{0.9}\text{In}_{0.1}\text{Se}_3$ (p-type)	300	64.7	2.66	3.20	57	930	0.03	—	—	—	—	8.3×10^{20}	[744]
$\text{Cu}_2\text{Sn}_{0.9}\text{In}_{0.1}\text{Se}_3$ (p-type)	850	28.9	0.48	0.93	210	270	1.14	—	—	—	—	—	[744]
$\text{Cu}_{1.85}\text{Ag}_{0.15}\text{Sn}_{0.9}\text{In}_{0.1}\text{Se}_3$ (p-type)	323	48.2	—	1.60	73	590	0.07	—	—	—	—	3.43×10^{20}	[703]
$\text{Cu}_{1.85}\text{Ag}_{0.15}\text{Sn}_{0.9}\text{In}_{0.1}\text{Se}_3$ (p-type)	823	27.0	—	0.56	240	170	1.42	—	—	—	—	—	[703]
$\text{Cu}_{1.875}\text{SnSe}_3$ (p-type)	300	11.0	1.43	1.46	145	46	0.02	—	0.2 ^f	—	—	7×10^{20}	[745]
$\text{Cu}_{1.875}\text{SnSe}_3$ (p-type)	800	10.4	0.18	0.26	290	35	0.95	—	—	—	—	—	[745]
$\text{Cu}_2\text{Ga}_{0.07}\text{Ge}_{0.93}\text{Se}_3$ (p-type)	300	49.8	—	2.20	54	758	0.03	—	4.37 ^c	—	—	10.8×10^{20}	[746]
$\text{Cu}_2\text{Ga}_{0.07}\text{Ge}_{0.93}\text{Se}_3$ (p-type)	745	24.1	—	1.33	140	420	0.5	—	—	—	—	—	[746]
$\text{Cu}_3\text{Sb}_{0.85}\text{Sn}_{0.15}\text{S}_4$ (p-type)	300	32.7	2.80	3.00	71	370	0.02	0.9 ^d	—	3	—	7.8×10^{20}	[747]
$\text{Cu}_3\text{Sb}_{0.85}\text{Sn}_{0.15}\text{S}_4$ (p-type)	573	21.2	2.10	2.30	125	300	0.12	—	—	—	—	—	[747]
$\text{Cu}_3\text{Sb}_{0.9}\text{Ge}_{0.1}\text{S}_4$ (p-type)	300	71.6	1.90	2.10	151	280	0.09	—	5.22 ^c	—	—	3.07×10^{20}	[748]
$\text{Cu}_3\text{Sb}_{0.9}\text{Ge}_{0.1}\text{S}_4$ (p-type)	623	38.8	0.76	0.92	243	155	0.63	—	—	—	—	—	[748]
$\text{Cu}_3\text{Sb}_{0.97}\text{Ge}_{0.03}\text{Se}_{2.8}\text{S}_{1.2}$ (p-type)	300	91.7	1.54	1.88	127	480	0.11	—	14.8 ^c	2.33	—	2.03×10^{20}	[749]
$\text{Cu}_3\text{Sb}_{0.97}\text{Ge}_{0.03}\text{Se}_{2.8}\text{S}_{1.2}$ (p-type)	650	47.0	0.52	0.89	235	220	0.89	—	—	—	—	—	[749]
$\text{Cu}_2\text{Cd}_{0.9}\text{GeSe}_4$ (p-type)	336	4.2	1.57	1.59	121	28	0.01	—	—	—	—	—	[750]
$\text{Cu}_2\text{Cd}_{0.9}\text{GeSe}_4$ (p-type)	723	11.8	0.56	0.64	226	72	0.42	—	—	—	—	—	[750]
$\text{Cu}_2\text{Cd}_{0.9}\text{SnSe}_4$ (p-type)	300	39.8	1.92	2.04	129	203	0.05	0.95 ^d	—	—	—	—	[751]
$\text{Cu}_2\text{Cd}_{0.9}\text{SnSe}_4$ (p-type)	700	14.5	0.23	0.49	156	190	0.65	—	—	—	—	—	[751]
$\text{Cu}_{2.075}\text{Co}_{0.925}\text{GeS}_4$ (p-type)	300	6.7	2.00	2.01	123	37	0.01	—	—	—	—	—	[752]
$\text{Cu}_{2.075}\text{Co}_{0.925}\text{GeS}_4$ (p-type)	723	17.2	0.90	1.01	239	90	0.37	—	—	—	—	—	[752]
$\text{Cu}_2\text{CoSnS}_4$ (p-type) nanocrystals	300	8.2	—	0.51	243	11	0.04	—	—	—	—	—	[753]
$\text{Cu}_2\text{CoSnS}_4$ (p-type) nanocrystals	700	11.3	—	0.37	283	34	0.51	—	—	—	—	—	[753]
$\text{Cu}_{2.15}\text{Co}_{0.8}\text{Mn}_{0.05}\text{SnS}_4$ (p-type)	300	35.7	1.98	2.25	69	417	0.03	—	—	—	—	—	[754]
$\text{Cu}_{2.15}\text{Co}_{0.8}\text{Mn}_{0.05}\text{SnS}_4$ (p-type)	800	24.4	0.64	0.98	185	278	0.77	—	—	—	—	—	[754]
$\text{Cu}_2\text{CoSnSe}_4$ (p-type)	300	29.8	—	1.74	104	210	0.03	—	—	1.7	—	1.9×10^{20}	[755]

(Continued.)

Table 10. (Continued.)

Material	T (K)	μ_w ($\text{cm}^2 \text{V}^{-1} \text{s}^{-1}$)	κ_L ($\text{W m}^{-1} \text{K}^{-1}$)	κ ($\text{W m}^{-1} \text{K}^{-1}$)	S ($\mu\text{V K}^{-1}$)	σ ($\Omega^{-1} \text{cm}^{-1}$)	zT	E_g (eV)	μ_H ($\text{cm}^2 \text{V}^{-1} \text{s}^{-1}$)	m_k^* (m_e)	ϵ_r or ϵ (ϵ_0)	n_H (cm^{-3})	References
$\text{Cu}_2\text{CoSnSe}_4$ (p-type)	850	16.9	0.60	0.80	225	133	0.74	—	—	—	—	—	[755]
$\text{Cu}_2\text{FeSnS}_4$ (p-type) nanocrystals	300	6.6	—	0.60	232	10	0.03	—	—	—	—	—	[753]
$\text{Cu}_2\text{FeSnS}_4$ (p-type) nanocrystals	700	7.5	—	0.44	270	26	0.31	—	—	—	—	—	[753]
$\text{Cu}_2\text{FeSnS}_4$ (p-type)	300	24.9	—	2.90	227	40	0.01	—	—	3.5	—	0.9×10^{20}	[755]
$\text{Cu}_2\text{FeSnSe}_4$ (p-type)	850	8.6	0.65	0.73	234	61	0.4	—	—	—	—	—	[755]
$\text{Cu}_{2.1}\text{Fe}_{0.9}\text{SnSe}_4$ (p-type)	300	48.6	2.62	2.72	151	190	0.05	—	—	3.2	—	2.3×10^{20}	[756]
$\text{Cu}_{2.1}\text{Fe}_{0.9}\text{SnSe}_4$ (p-type)	800	14.9	—	0.91	180	180	0.52	—	—	—	—	—	[756]
$\text{Cu}_2\text{MnSnS}_4$ (p-type) nanocrystals	300	2.2	—	0.70	234	3.3	0.01	—	—	—	—	—	[753]
$\text{Cu}_2\text{MnSnS}_4$ (p-type) nanocrystals	700	4.1	—	0.53	265	15	0.14	—	—	—	—	—	[753]
$\text{Cu}_2\text{MnSnSe}_4$ (p-type)	300	12.0	—	2.60	189	30	0.01	—	—	1.2	—	0.3×10^{20}	[755]
$\text{Cu}_2\text{MnSnSe}_4$ (p-type)	850	10.3	0.49	0.57	268	49	0.53	—	—	—	—	—	[755]
$\text{Cu}_{2.1}(\text{Fe}_{0.5}\text{Mn}_{0.5})_{0.9}\text{SnSe}_4$ (p-type)	300	23.5	—	2.40	150	93	0.01	—	—	1.5	—	0.6×10^{20}	[757]
$\text{Cu}_{2.1}(\text{Fe}_{0.5}\text{Mn}_{0.5})_{0.9}\text{SnSe}_4$ (p-type)	800	16.4	—	0.84	204	150	0.6	—	—	—	—	—	[757]
$\text{Cu}_{2.1}\text{Mn}_{0.9}\text{SnSe}_4$ (p-type)	300	20.6	2.55	2.71	67	249	0.01	—	—	1.44	—	2.89×10^{20}	[758]
$\text{Cu}_{2.1}\text{Mn}_{0.9}\text{SnSe}_4$ (p-type)	800	18.2	0.67	0.91	186	205	0.6	—	—	—	—	—	[758]
$\text{Cu}_2\text{ZnGeS}_4$ (p-type)	300	—	3.80	3.80	187	—	—	2.0 ^a	—	—	—	—	[759]
$\text{Cu}_2\text{ZnGeS}_4$ (p-type)	670	2.6	—	1.00	409	1.7	—	—	—	—	—	—	[759]
$\text{Cu}_2\text{ZnGeS}_4$ (p-type)	300	2.0	3.20	3.20	320	1.1	—	1.4 ^a	—	—	—	—	[759]
$\text{Cu}_2\text{ZnGeSe}_4$ (p-type)	670	7.0	—	0.83	325	12	—	—	—	—	—	—	[759]
$\text{Cu}_{2.075}\text{Zn}_{0.925}\text{GeSe}_4$ (p-type)	300	5.5	2.45	2.50	83	52	0.005	—	—	—	1.0×10^{20}	[760]	
$\text{Cu}_{2.075}\text{Zn}_{0.925}\text{GeSe}_4$ (p-type)	670	19.3	0.66	0.86	195	150	0.45	—	—	—	—	—	[760]
$\text{Cu}_{1.8}\text{Zn}_{1.05}\text{Sn}_{0.95}\text{S}_4$ (p-type) single crystal	300	43.6	—	2.90	420	7.5	0.04	—	80.8 ^e	—	—	5.8×10^{17}	[761]
$\text{Cu}_{1.8}\text{Zn}_{1.05}\text{Sn}_{0.95}\text{S}_4$ (p-type) single crystal	400	563.1	—	2.40	506	55	0.2	—	—	—	—	—	[761]
$\text{Cu}_{2.125}\text{Zn}_{0.875}\text{SnS}_4$ (p-type) Hot forged	300	5.5	1.16	1.20	40	115	0.005	—	—	—	—	—	[762]
$\text{Cu}_{2.125}\text{Zn}_{0.875}\text{SnS}_4$ (p-type) Hot forged	725	14.3	0.07	0.33	155	200	1.1	—	—	—	—	—	[762]
$\text{Cu}_2\text{ZnSnSe}_4$ (p-type) single crystal	300	117.5	—	3.90	420	20.2	0.06	—	141.2 ^e	—	—	8.8×10^{17}	[763]
$\text{Cu}_2\text{ZnSnSe}_4$ (p-type) single crystal	400	738.8	—	2.80	505	73	0.32	—	—	—	—	—	[763]

(Continued.)

Table 10. (Continued.)

Material	T (K)	μ_w ($\text{cm}^2 \text{V}^{-1} \text{s}^{-1}$)	κ_L ($\text{W m}^{-1} \text{K}^{-1}$)	κ ($\text{W m}^{-1} \text{K}^{-1}$)	S ($\mu\text{V K}^{-1}$)	σ ($\Omega^{-1} \text{cm}^{-1}$)	zT	E_g (eV)	μ_H ($\text{cm}^2 \text{V}^{-1} \text{s}^{-1}$)	m_e^* (m_e)	ϵ_r or ϵ (ϵ_0)	η_H (cm^{-3})	References
Cu ₂₁ Zn _{0.5} SnSe ₄ (p-type) coated	300	57.6	—	3.66	55	860	0.02	1.4 ^a	—	—	—	—	[764]
Cu ₂₁ Zn _{0.5} SnSe ₄ (p-type) coated	860	31.9	—	1.28	206	318	0.91	—	—	—	—	—	[764]
Cu ₂ ZnSn _{0.90} In _{0.10} Se ₄ (p-type) coated	300	34.5	3.2	3.3	93	282	0.015	—	—	—	—	—	[765]
Cu ₂ ZnSn _{0.90} In _{0.10} Se ₄ (p-type) coated	850	30.4	—	0.82	300	100	0.95	—	—	—	—	—	[765]
Colusites													
Cu ₂₆ V ₂ Ge ₆ S ₃₂ (p-type)	350	41.0	0.41	0.63	125	277	0.26	—	—	—	—	—	[766]
Cu ₂₆ V ₂ Ge ₆ S ₃₂ (p-type)	663	23.0	0.5	0.57	215	140	0.73	—	—	—	—	—	[766]
Cu ₂₄ Ni ₂ V ₂ Ge ₆ S ₃₂ (p-type)	300	38.0	0.88	1.2	79	380	0.06	—	—	—	—	—	[767]
Cu ₂₄ Ni ₂ V ₂ Ge ₆ S ₃₂ (p-type)	690	19.2	0.36	0.8	145	281	0.5	—	—	—	—	—	[767]
Cu ₂₄ Co ₂ V ₂ Ge ₆ S ₃₂ (p-type)	300	19.2	0.68	0.7	179	54	0.07	—	—	—	—	—	[767]
Cu ₂₄ Co ₂ V ₂ Ge ₆ S ₃₂ (p-type)	690	13.3	0.45	0.5	265	48	0.4	—	—	—	—	—	[767]
Cu ₂₆ Nb ₂ Ge ₆ S ₃₂ (p-type)	310	47.0	0.53	0.79	125	265	0.16	—	—	—	—	1.2 × 10 ²¹	[768]
Cu ₂₆ Nb ₂ Ge ₆ S ₃₂ (p-type)	673	18.1	0.34	0.58	202	131	0.65	—	—	—	—	—	[768]
Cu ₂₆ Nb ₂ Ge _{5.5} S ₃₂ (p-type)	300	48.4	0.4	0.53	132	238	0.24	—	—	—	—	—	[769]
Cu ₂₆ Nb ₂ Ge _{5.5} S ₃₂ (p-type)	670	20.1	0.41	0.53	220	117	0.73	—	—	—	—	—	[769]
Cu _{26.5} Nb ₂ Ge _{5.5} S ₃₂ (p-type)	330	70.1	0.51	0.72	125	434	0.29	—	—	—	—	2.1 × 10 ²¹	[770]
Cu _{26.5} Nb ₂ Ge _{5.5} S ₃₂ (p-type)	670	28.4	0.45	0.67	199	211	0.84	—	—	—	—	—	[770]
Cu _{26.5} Nb ₂ Ge _{5.5} S ₃₂ (p-type)	310	51.0	0.56	0.82	135	254	0.22	—	—	—	—	1.8 × 10 ²¹	[768]
Cu ₂₆ Nb ₂ Ge ₆ Co _{0.5} S ₃₂ (p-type)	673	20.7	0.41	0.55	210	136	0.71	—	—	—	—	—	[768]
Cu ₂₆ Nb ₂ Ge ₆ Co _{0.5} S ₃₂ (p-type)	310	47.8	0.68	0.83	120	287	0.15	—	—	—	—	1.2 × 10 ²¹	[768]
Cu ₂₆ Nb ₂ Ge ₆ Ni _{0.5} S ₃₂ (p-type)	673	20.1	0.45	0.60	194	159	0.66	—	—	—	—	—	[768]
Cu ₂₆ Nb ₂ Ge ₆ Ni _{0.5} S ₃₂ (p-type)	310	33.2	0.77	0.82	166	114	0.12	—	—	—	—	9.0 × 10 ²⁰	[768]
Cu ₂₆ Nb ₂ Ge ₆ Fe _{0.5} S ₃₂ (p-type)	673	16.5	0.44	0.55	212	106	0.57	—	—	—	—	—	[768]
Cu ₂₆ Nb ₂ Ge ₆ Fe _{0.5} S ₃₂ (p-type)	300	38.4	0.56	0.65	143	165	0.15	—	—	—	—	—	[769]
Cu ₂₆ Ta ₂ Ge ₆ S ₃₂ (p-type)	670	18.1	0.4	0.49	229	95	0.66	—	—	—	—	—	[769]

(Continued.)

Table 10. (Continued.)

Material	T (K)	μ_w ($\text{cm}^2 \text{V}^{-1} \text{s}^{-1}$)	κ_L ($\text{W m}^{-1} \text{K}^{-1}$)	κ ($\text{W m}^{-1} \text{K}^{-1}$)	S ($\mu\text{V K}^{-1}$)	σ ($\Omega^{-1} \text{cm}^{-1}$)	zT	E_g (eV)	μ_{H} ($\text{cm}^2 \text{V}^{-1} \text{s}^{-1}$)	m_n^* (m_e)	ϵ_r or ϵ (ϵ_0)	n_{H} (cm^{-3})	References
Cu ₃₆ Ta ₂ Ge ₅ S ₃₂ (p-type)	300	45.3	0.46	0.57	136	212	0.22	—	—	—	—	—	[769]
Cu ₂₆ Ta ₂ Ge _{5.5} S ₃₂ (p-type)	670	20.0	0.36	0.48	222	114	0.79	—	—	—	—	—	[769]
Cu ₃₆ V ₂ Sn ₆ S ₃₂ (p-type)	300	49.9	0.6	0.76	116	300	0.16	—	—	3.2	—	4.2×10^{20}	[771]
Cu ₂₆ V ₂ Sn ₆ S ₃₂ (p-type)	670	20.2	0.47	0.64	194	159	0.64	—	—	—	—	—	[771]
Cu ₃₆ V ₂ Sn ₆ S ₃₂ (SPS 873) (p-type)	300	55.5	1.4	2.08	45	1020	0.03	—	—	—	—	—	[693]
Cu ₂₆ V ₂ Sn ₆ S ₃₂ (SPS 873) (p-type)	675	27.3	0.58	1.45	102	667	0.33	—	—	—	—	—	[693]
Cu ₃₆ V ₂ Sn ₆ S ₃₂ (HP 1023) (p-type)	300	63.1	0.35	0.66	91	531	0.19	—	—	—	—	—	[693]
Cu ₃₆ V ₂ Sn ₆ S ₃₂ (HP 1023) (p-type)	675	25.2	0.21	0.57	162	292	0.93	—	—	—	—	—	[693]
Cu ₂₆ V ₂ Sn _{5.5} S ₃₂ (p-type)	300	30.1	—	0.66	130	152	0.18	—	—	—	—	—	[772]
Cu ₂₆ V ₂ Sn _{5.5} S ₃₂ (p-type)	673	20.9	—	0.60	205	146	0.63	—	—	—	—	—	[772]
Cu ₂₄ Zn ₂ V ₂ Sn ₆ S ₃₂ (p-type)	300	58.2	1.53	1.96	66	714	0.05	—	—	—	—	—	[773]
Cu ₃₄ Zn ₂ V ₂ Sn ₆ S ₃₂ (p-type)	700	20.6	0.71	1.1	143	316	0.44	—	—	—	—	—	[773]
Cu ₂₆ Nb ₂ Sn ₆ S ₃₂ (p-type)	300	44.4	0.51	0.65	116	267	0.18	—	—	3.6	—	4.7×10^{20}	[771]
Cu ₂₆ Nb ₂ Sn ₆ S ₃₂ (p-type)	670	19.3	0.43	0.57	203	137	0.66	—	—	—	—	—	[771]
Cu ₂₆ Nb ₂ Sn _{5.5} S ₃₂ (p-type)	300	59.1	0.55	0.76	117	351	0.2	—	—	—	—	—	[769]
Cu ₂₆ Nb ₂ Sn _{5.5} S ₃₂ (p-type)	670	25.0	0.44	0.62	194	197	0.76	—	—	—	—	—	[769]
Cu ₂₆ Ta ₂ Sn ₆ S ₃₂ (p-type)	300	63.5	0.47	0.69	116	382	0.23	—	—	4.3	—	6.6×10^{20}	[771]
Cu ₂₆ Ta ₂ Sn ₆ S ₃₂ (p-type)	670	23.3	0.4	0.59	198	175	0.78	—	—	—	—	—	[771]
Cu ₂₆ Ta ₂ Sn _{5.5} S ₃₂ (p-type)	300	68.4	0.41	0.64	115	417	0.27	—	—	—	—	—	[769]
Cu ₂₆ Ta ₂ Sn _{5.5} S ₃₂ (p-type)	670	27.3	0.35	0.55	206	187	0.96	—	—	—	—	—	[769]
Cu ₃₆ Cr ₂ Ge ₆ S ₃₂ (p-type)	300	231.9	1.59	2.93	83	2188	0.15	—	—	—	—	—	[774]
Cu ₂₆ Cr ₂ Ge ₆ S ₃₂ (p-type)	700	62.1	0.49	1.56	150	875	0.86	—	—	—	—	—	[774]
Cu ₂₆ Cr ₂ Ge ₆ S ₃₂ (p-type)	300	232.8	1.52	2.84	84	2164	0.16	—	2.93 ^f	—	—	—	[775]
Cu ₂₆ Cr ₂ Ge ₆ S ₃₂ (p-type)	700	60.3	0.46	1.52	149	860	0.89	—	—	—	—	—	[775]
[Cu ₂₆ Cr ₂ Ge ₆] _{1.024} S ₃₂ (p-type)	300	66.6	1.35	1.58	114	411	0.1	—	0.66 ^f	—	—	—	[700]
[Cu ₂₆ Cr ₂ Ge ₆] _{1.024} S ₃₂ (p-type)	700	50.3	0.52	1.14	178	510	1	—	—	—	—	—	[700]
Cu ₂₅ ZnCr ₂ Ge ₆ S ₃₂ (p-type)	300	128.9	1.79	2.26	110	838	0.12	—	—	—	—	—	[774]
Cu ₂₅ ZnCr ₂ Ge ₆ S ₃₂ (p-type)	700	35.8	0.75	1.20	176	371	0.67	—	—	—	—	—	[774]
Cu ₂₆ Cr ₁ MoGe ₆ S ₃₂ (p-type)	300	93.0	1.44	1.94	87	828	0.1	—	1.39 ^f	—	—	—	[775]
Cu ₂₆ Cr ₁ MoGe ₆ S ₃₂ (p-type)	700	46.0	0.49	1.24	154	619	0.83	—	—	—	—	—	[775]
Cu ₂₆ Cr ₁ WGe ₆ S ₃₂ (p-type)	300	112.3	1.09	1.74	81	1091	0.13	—	1.56 ^f	—	—	—	[775]
Cu ₂₆ Cr ₁ WGe ₆ S ₃₂ (p-type)	700	47.9	0.37	1.20	151	668	0.9	—	—	—	—	—	[775]

(Continued.)

Table 10. (Continued.)

Material	T (K)	μ_{av} ($\text{cm}^2 \text{V}^{-1} \text{s}^{-1}$)	κ_L ($\text{W m}^{-1} \text{K}^{-1}$)	κ ($\text{W m}^{-1} \text{K}^{-1}$)	S ($\mu\text{V K}^{-1}$)	σ ($\Omega^{-1} \text{cm}^{-1}$)	zT	E_g (eV)	μ_{H} ($\text{cm}^2 \text{V}^{-1} \text{s}^{-1}$)	m_s^* (m_e)	ϵ_r or ϵ (ϵ_0)	n_{H} (cm^{-3})	References
Low Dimensional Materials													
TiS ₂ (<i>n</i> -type)	300	167.6	4.22	4.5	-277	151	0.08	—	—	—	—	0.11×10^{21}	[776]
TiS ₂ (<i>n</i> -type)	700	42.7	2.3	2.43	-390	37	0.16	—	—	—	—	—	[776]
Ti _{1.025} S ₂ (<i>n</i> -type)	300	144.8	1.54	2.3	-103	1033	0.14	—	—	—	—	1.11×10^{21}	[776]
Ti _{1.025} S ₂ (<i>n</i> -type)	700	33.8	1.08	1.58	-192	291	0.48	—	—	—	—	—	[776]
Cu _{0.10} TiS ₂ (<i>n</i> -type)	300	227.1	1.68	3.89	-50	3745	0.05	—	—	—	—	3.67×10^{21}	[685]
Cu _{0.10} TiS ₂ (<i>n</i> -type)	800	27.6	0.77	1.8	-142	524	0.47	—	—	—	—	—	[685]
Ag _{0.1} TiS ₂ (<i>n</i> -type)	300	111.8	1.63	3.5	-62	1469	0.05	—	—	—	—	—	[686]
Ag _{0.1} TiS ₂ (<i>n</i> -type)	700	35.1	0.85	1.72	-153	478	0.46	—	—	—	—	—	[686]
Co _{0.04} TiS ₂ (<i>n</i> -type)	321	81.4	—	2.76	-112	571	0.08	—	—	—	—	—	[687]
Co _{0.04} TiS ₂ (<i>n</i> -type)	573	47.7	—	1.98	-200	277	0.3	—	—	—	—	—	[687]
TiS _{1.5} Se _{0.5} (<i>n</i> -type)	300	150.2	2.2	2.6	-141	662	0.15	—	—	—	—	3.5×10^{21}	[699]
TiS _{1.5} Se _{0.5} (<i>n</i> -type)	700	29.8	1.58	1.48	-232	161	0.33	—	—	—	—	—	[699]
Cu _{0.05} TiS _{1.5} Se _{0.5} (<i>n</i> -type)	300	179.5	1.54	2.92	-77	1851	0.1	—	—	—	—	7×10^{21}	[699]
Cu _{0.05} TiS _{1.5} Se _{0.5} (<i>n</i> -type)	700	39.8	0.92	1.61	-167	459	0.55	—	—	—	—	—	[699]
Co ₃ Sn ₂ S ₂ (<i>n</i> -type)	310	215.6	1.9	4.56	-52	3584	0.07	—	—	—	—	—	[777]
Co ₃ Sn ₂ S ₂ (<i>n</i> -type)	677	80.7	0.59	4.74	-85	2506	0.26	—	—	—	—	—	[777]
Co ₃ Sn _{1.6} In _{0.4} S ₂ (<i>n</i> -type)	310	201.2	1.7	3.15	-79	2115	0.13	—	—	—	—	—	[777]
Co ₃ Sn _{1.6} In _{0.4} S ₂ (<i>n</i> -type)	677	65.9	1.06	3.62	-104	1574	0.32	—	—	—	—	—	[777]
Co _{2.6} Fe _{0.4} Sn ₂ S ₂ (<i>n</i> -type)	300	178.0	2.38	3.97	-70	2046	0.08	—	—	—	—	—	[778]
Co _{2.6} Fe _{0.4} Sn ₂ S ₂ (<i>n</i> -type)	575	81.6	1.39	4.08	-88	1901	0.2	—	—	—	—	—	[778]
Co _{2.6} Fe _{0.33} Sn _{1.6} In _{0.4} S ₂ (<i>n</i> -type)	300	219.8	2.12	3.47	-102	1590	0.14	—	—	—	—	—	[779]
Co _{2.667} Fe _{0.333} Sn _{1.6} In _{0.4} S ₂ (<i>n</i> -type)	575	88.1	1.12	3.45	-103	1669	0.29	—	—	—	—	—	[779]
MnBi ₄ S ₇ (<i>n</i> -type)	300	21.0	0.89	1	-87	187	0.04	—	—	—	—	—	[688]
MnBi ₄ S ₇ (<i>n</i> -type)	700	6.6	0.61	0.67	-200	52	0.21	—	—	—	—	—	[688]
FeBi ₄ S ₇ (<i>n</i> -type)	300	17.0	0.74	0.82	-93	139	0.05	—	—	—	—	—	[688]
FeBi ₄ S ₇ (<i>n</i> -type)	700	6.1	0.75	0.81	-191	53	0.17	—	—	—	—	—	[688]
CdPb ₂ Bi ₄ S ₉ (<i>n</i> -type)	300	5.7	0.73	0.78	-59	79	0.02	—	—	—	—	1.6×10^{18}	[689]
CdPb ₂ Bi ₄ S ₉ (<i>n</i> -type)	775	7.5	0.49	0.52	-253	37	0.53	—	—	—	—	—	[689]
CdAg ₂ Bi ₆ Se ₁₁ (<i>n</i> -type)	300	18.7	0.36	0.54	-57	269	0.05	—	—	—	—	1.8×10^{19}	[689]
CdAg ₂ Bi ₆ Se ₁₁ (<i>n</i> -type)	775	14.0	0.13	0.43	-149	232	0.95	—	—	—	—	—	[689]

(Continued.)

Table 10. (Continued.)

Material	T (K)	μ_{av}^w ($\text{cm}^2 \text{V}^{-1} \text{s}^{-1}$)	κ_L ($\text{W m}^{-1} \text{K}^{-1}$)	κ ($\text{W m}^{-1} \text{K}^{-1}$)	S ($\mu\text{V K}^{-1}$)	σ ($\Omega^{-1} \text{cm}^{-1}$)	zT	E_g (eV)	μ_{HI} ($\text{cm}^2 \text{V}^{-1} \text{s}^{-1}$)	m_s^* (m_e)	ϵ_r or ϵ (ϵ_0)	n_{H} (cm^{-3})	References
Pb ₃ Bi ₆ Se ₁₄ (n-type)	300	17.9	0.48	0.58	-88	157	0.06	—	—	—	—	4.8×10^{19}	[780]
Pb ₃ Bi ₆ Se ₁₄ (n-type)	705	9.7	0.34	0.46	-211	68	0.46	—	—	—	—	—	[780]
Pb ₃ Bi ₂ S ₆ (n-type)	300	13.7	0.79	0.94	-58	193	0.02	—	—	—	—	1.2×10^{20}	[780]
Pb ₃ Bi ₂ S ₆ (n-type)	715	7.5	0.56	0.68	-197	63	0.26	—	—	—	—	—	[780]
PbBi ₂ S ₄ (n-type)	300	19.2	0.63	0.64	-136	90	0.08	—	—	—	—	4.6×10^{19}	[780]
PbBi ₂ S ₄ (n-type)	710	10.3	0.53	0.57	-269	37	0.33	—	—	—	—	—	[780]
CdPbBi ₄ Se ₈ (n-type)	325	7.3	0.43	0.45	-125	44	0.05	—	15.2 ^c	—	—	3.21×10^{19}	[781]
CdPbBi ₄ Se ₈ (n-type)	850	6.1	0.27	0.32	-254	34	0.63	—	—	—	—	—	[781]
CdSnBi ₄ Se ₈ (n-type)	325	19.9	0.61	0.72	-109	148	0.08	—	32.9 ^c	—	—	2.85×10^{19}	[781]
CdSnBi ₄ Se ₈ (n-type)	850	7.1	0.44	0.64	-151	132	0.4	—	—	—	—	—	[781]
Cu _{1.62} Bi _{4.61} S ₈ (n-type)	300	10.6	0.57	0.58	-222	18	0.05	—	—	—	—	—	[782]
Cu _{1.62} Bi _{4.61} S ₈ (n-type)	660	7.4	0.49	0.55	-231	37	0.21	—	—	—	—	—	[782]
Cu _{1.595} Zn _{0.025} Bi _{4.61} S ₈ (n-type)	300	13.9	0.46	0.58	-66	170	0.04	—	—	—	—	—	[782]
Cu _{1.595} Zn _{0.025} Bi _{4.61} S ₈ (n-type)	660	7.7	0.35	0.54	-137	116	0.26	—	—	—	—	—	[782]

^a Band gap determined by optical spectroscopy.

^b Band gap determined by x-ray photoelectron spectroscopy.

^c Measured at room temperature.

^d Bandgap measured from Seebeck coefficient (S) using $E_g = 2S_{\text{max}}eT$.

^e Mobility data based on Hall measurements.

^f Technique of measuring mobility not defined explicitly.

3.11. Silicides

Silicide thermoelectrics

Franck Gascoin¹ and Theodora Kyratsi²

¹ Laboratoire CRISMAT UMR 6508 CNRS ENSICAEN, 14050 Caen Cedex 04, France

² Department of Mechanical and Manufacturing Engineering, University of Cyprus, Nicosia 2109, Cyprus

Since the 1960s, a multitude of silicides based thermoelectric materials have been studied for their potential or promising thermoelectric properties. Indeed, their combination with virtually any other metal provides an ideal playground for thermoelectricians [783]. The alloys Si–Ge certainly stand out from the crowd as they have been used in the fabrication of radio-isotope thermoelectric generators and thus utilized by NASA for powering a large number of space missions. Their stability over time is undeniable and that makes up for their high cost and rather poor efficiency. If Si–Ge could be seen as a model compound for high temperature applications, other silicides are now scrutinized against them.

Amongst the different class of silicides, present and probable future investigations focus on the cheap and non-toxic Mg₂Si and MnSi_x based materials. Evidently, cost and environmentally friendly materials are today crucial parameters as they largely compete with efficiency. Moreover, silicides are often low-density materials, another key aspect of their potential for industrial applications. Therefore, combining the *n*-type Mg₂Si and *p*-type MnSi_x into a thermoelectric module is indeed very appealing and would represent a major achievement. All these positive arguments have resulted in a myriad of investigations that focused first on the improvement of the thermoelectric figure of merit of these two materials.

Magnesium silicide Mg₂Si and the related solid solutions Mg₂(Si_xGe_{1-x}) and Mg₂(Si_xSn_{1-x}) were first identified as promising by Nicolau during the first international congress on thermoelectric energy conversion in 1976 [784] and these predictions were quickly confirmed by the experimental results of different groups in the early 1990s [785–787]. Since then, efforts have been devoted to optimize materials in terms of synthesis, performance, and stability over time. The best results are obtained using multiple substitutions on both the magnesium and the silicon sites. These have led to materials with *zT* often exceeding 1.3 at 700 K with a record high *zT* of 1.7 for Mg_{1.98}Cr_{0.02}(Si_{0.3}Sn_{0.7})_{0.98}Bi_{0.02} at 680 K [788], although the stability, at the operating temperature, of the silico-stannides still being under investigation.

Higher manganese silicides (HMS) have been considered as promising *p*-type thermoelectric materials because they are ecologically benign but also because they possess high mechanical strength and they are stable in air up to 1023 K. HMS exist as several incommensurate phases with chemical formulae of Mn₄Si₇, Mn₁₁Si₁₉, Mn₁₅Si₂₆, and Mn₂₇Si₄₇, all crystallizing in the Nowotny chimney-ladder structures. These structures are constructed by the two Mn and Si sublattices, where the Mn atoms form the chimneys in which the Si atoms spiral as ladders. The tetragonal unit cells of different HMS compounds have similar *a* parameter, and different *c* parameter, depending on the *c*Si/*c*Mn ratio of the two sublattices.

Despite all the efforts undertaken to improve the thermoelectric efficiency, most of the HMS have relatively mediocre *zT*, typically between 0.4 and 0.5 at the most, which is detrimental to a module hypothetically made of an *n*-type Mg₂Si counter leg. Only recently, via addition of rhenium or introduction of high density dislocation, *zT*s reaching the unity value at 825 K have been found [789, 790].

Only a few investigation and projects have tried to tackle the design and construction of an all silicide thermoelectric module. Not surprisingly, the major issue is the difference between the coefficients of thermal expansion of HMS and Mg₂Si, which often leads to violent breakage of the module upon cycling over the operating temperature range. This inescapable problem might necessitate the use of buffer layers or other engineering tactics that remain to be proven efficient but also triggered efforts toward discovering an efficient *p*-type Mg₂Si that could therefore advantageously replace HMS [791, 792]

A summary of the best *zT* values as a function of temperature for magnesium silicides and manganese silicides is presented in figure 12 (*p*-type) and figure 13 (*n*-type).

Acknowledgments

Theodora Kyratsi acknowledges support from the THERMOSS Project funded by EU network M-ERA.NET (KOINA/M-ERA.NET/0316/03).

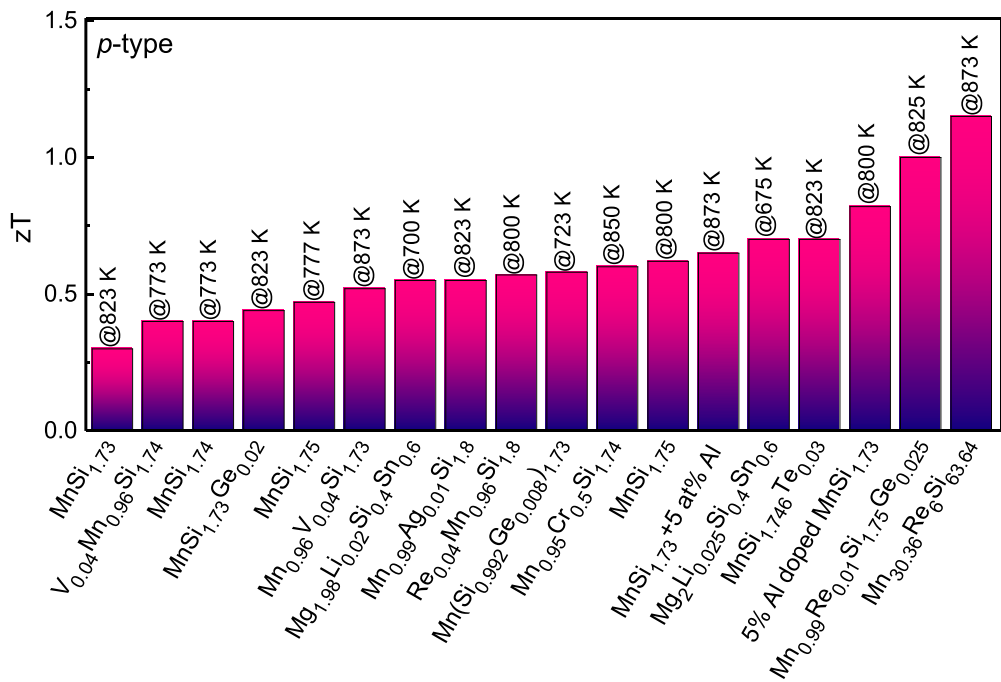


Figure 12. The maximum thermoelectric figure of merit, zT , of selected p -type magnesium silicides and manganese silicides: MnSi_{1.73} [793], V_{0.04}Mn_{0.96}Si_{1.74} [794], MnSi_{1.74} [794], MnSi_{1.73}Ge_{0.02} [795], MnSi_{1.75} [796], Mn_{0.96}V_{0.04}Si_{1.73} [797], Mg_{1.98}Li_{0.02}Si_{0.4}Sn_{0.6} [791], Mn_{0.99}Ag_{0.01}Si_{1.8} [798], Re_{0.04}Mn_{0.96}Si_{1.8} [799], Mn(Si_{0.992}Ge_{0.008})_{1.73} [800], Mn_{0.95}Cr_{0.5}Si_{1.74} [801], MnSi_{1.75} [802], MnSi_{1.73} + 5 at% Al [803], Mg₂Li_{0.025}Si_{0.4}Sn_{0.6} [792], MnSi_{1.746}Te_{0.03} [804], 5% Al doped MnSi_{1.73} [805], Mn_{0.99}Re_{0.01}Si_{1.75}Ge_{0.025} [789], Mn_{30.36}Re₆Si_{63.64} [790].

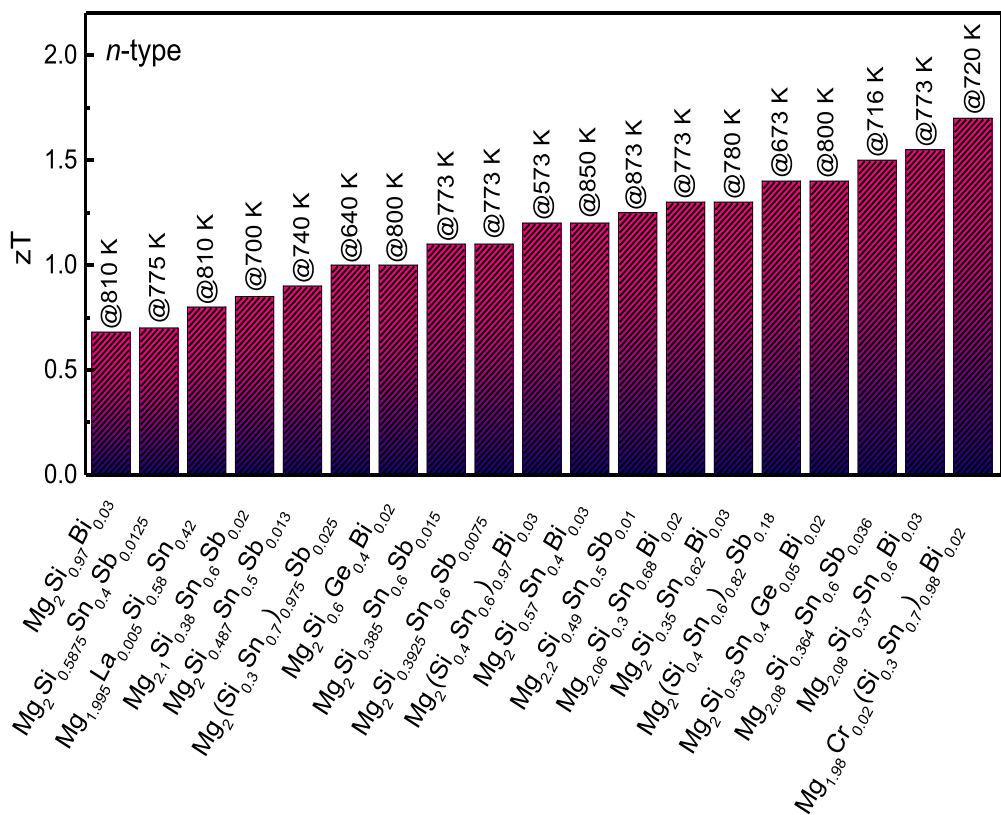


Figure 13. The maximum thermoelectric figure of merit, zT , of selected n -type magnesium silicides: Mg₂Si_{0.97}Bi_{0.03} [806], Mg₂Si_{0.5875}Sn_{0.4125}Sb_{0.0125} [807], Mg_{1.995}La_{0.005}Si_{0.58}Sn_{0.42} [808], Mg_{2.10}Si_{0.38}Sn_{0.62}Sb_{0.02} [809], Mg₂Si_{0.487}Sn_{0.513}Sb_{0.013} [810], Mg₂(Si_{0.3}Sn_{0.7})_{0.975}Sb_{0.025} [811], Mg₂Si_{0.6}Ge_{0.4}Bi_{0.02} [812], Mg₂Si_{0.385}Sn_{0.615}Sb_{0.015} [813], Mg₂Si_{0.3925}Sn_{0.6075}Sb_{0.0075} [814], Mg₂(Si_{0.4}Sn_{0.6})_{0.97}Bi_{0.03} [815], Mg₂Si_{0.57}Sn_{0.43}Bi_{0.03} [816], Mg_{2.2}Si_{0.49}Sn_{0.51}Sb_{0.01} [817], (Mg_{2.06}Si_{0.3}Sn_{0.68}Bi_{0.02} [818], Mg₂Si_{0.35}Sn_{0.65}Bi_{0.03} [819], Mg₂(Si_{0.4}Sn_{0.6})_{0.82}Sb_{0.18} [820], Mg₂Si_{0.53}Sn_{0.47}Ge_{0.05}Bi_{0.02} [821], Mg_{2.08}Si_{0.364}Sn_{0.636}Sb_{0.036} [789], Mg_{2.08}Si_{0.37}Sn_{0.63}Bi_{0.03} [822], Mg_{1.98}Cr_{0.02}(Si_{0.3}Sn_{0.7})_{0.98}Bi_{0.02} [788].

Table 11. Silicides thermoelectric properties.

Material	T (K)	μ_{av} (cm ² V ⁻¹ s ⁻¹)	κ_L (W m ⁻¹ K ⁻¹)	S (μ V K ⁻¹)	σ (Ω^{-1} cm ⁻¹)	zT	k (W m ⁻¹ K ⁻¹)	References
Magnesium silicides								
<i>n</i> -type								
Mg _{1.98} Cr _{0.02} (Si _{0.3} Sn _{0.7}) _{0.98} Bi _{0.02}	300	421.0	1.55	-129	2149	0.4	2.7	[788]
	680	213.1	1.08	-230	1130	1.7	2.3	
Mg _{2.08} Si _{0.4-x} Sn _{0.6} Bi _x , x = 0.030	300	452.2	—	-130	2280	0.44	2.7	[822]
	773	121.7	—	-205	1045	1.55	2.2	
Mg _{2.08} Si _{0.364} Sn _{0.6} Sb _{0.036}	300	455.4	1.38	-121	2570	0.45	2.7	[789]
	716	149.0	1.03	-207	1115	1.5	2.04	
Mg ₂ Si _{0.3} Sn _{0.67} Bi _{0.03} /3.0 wt % SiC	323	370.3	1.97	-133	2010	—	3.14	[823]
	773	130.9	1.3	-230	841	—	2.4	
Mg ₂ (Si _{0.3} Ge _y Sn _{0.7-y}) _{0.98} Sb _{0.02} , y = 0.05	300	383.9	2	-125	2060	0.3	3.16	[824]
	800	118.5	1.25	-220	900	1.45	2.4	
Mg ₂ Si _{0.55-x} Sn _{0.4} Ge _{0.05} Sb _x , x = 0.0125	300	221.7	2.5	-107	1500	0.15	3.4	[825]
	800	87.5	1.3	-220	665	1.2	2.15	
Mg ₂ Si _{0.55-x} Sn _{0.4} Ge _{0.05} Bi _x , x = 0.02	300	212.4	1.6	-94.5	1702	0.15	2.96	[821]
	800	93.1	1	-216	741	1.4	2	
Mg _{2.16} (Si _{0.4} Sn _{0.6}) _{0.97} Bi _{0.03}	300	361.5	1.64	-121	2040	0.3	2.78	[826]
	800	111.8	1	-215	900	1.4	2.3	
Mg ₂ (Si _{0.4} Sn _{0.6})Sb _x , x = 0.18	300	—	—	—	—	—	—	[820]
	673	135.3	0.66	-232	690	1.4	1.85	
Mg ₂ Si _{0.3} Sn _{0.665} Bi _{0.035}	300	—	—	—	—	—	—	[827]
	323	349.6	1.75	-115	2380	0.35	2.9	
	773	118.8	1	-205	1020	1.4	2.4	
Mg ₂ Si _{0.5875} Sn _{0.4} Sb _{0.0125}	300	328.2	—	-115	2000	0.3	2.8	[828]
	883	91.0	—	-210	900	1.4	2.2	

(Continued.)

Table 11. (Continued.)

Material	T (K)	μ_{AV} ($\text{cm}^2 \text{V}^{-1} \text{s}^{-1}$)	κ_L ($\text{W m}^{-1} \text{K}^{-1}$)	S ($\mu\text{V K}^{-1}$)	σ ($\Omega^{-1} \text{cm}^{-1}$)	zT	k ($\text{W m}^{-1} \text{K}^{-1}$)	References
$\text{Mg}_2\text{Si}_{0.35}\text{Sn}_{0.65-x}\text{Bi}_x$, x = 0.03	300	426.9	1.95	-120	2440	0.3	3.3	[819]
	780	116.9	1.3	-210	960	1.3	2.5	
$\text{Mg}_{2.16}(\text{Si}_{0.4}\text{Sn}_{0.6})_{0.985}\text{Sb}_{0.015}$	300	317.3	1.7	-130	1600	0.3	2.54	[829]
	740	107.3	1.1	-220	725	1.3	2	
$\text{Mg}_{2.16}(\text{Si}_{0.3}\text{Sn}_{0.7})_{0.98}\text{Sb}_{0.02}$	300	482.5	2.2	-115	2940	0.3	3.85	[830]
	—	—	1.4	-205	1180	1.3	2.8	
$\text{Mg}_{2.15}(\text{Si}_{0.3}\text{Sn}_{0.7})_{0.99}\text{Sb}_{0.01}$	300	483.7	1.45	-158	1740	0.45	2.75	[831]
	700	156.9	0.95	-235	820	1.3	2.3	
$\text{Mg}_2(\text{Si}_{0.3}\text{Sn}_{0.7})_{1-y}\text{Bi}_y$, y = 0.15	300	412.5	1.75	-130	2080	0.35	2.9	[832]
	700	136.0	1.3	-210	950	1.3	2.45	
$(\text{Mg}_{2.06}\text{Si}_{0.3}\text{Sn}_{0.68}\text{Bi}_{0.02})$	300	—	—	—	—	0.22	3.6	[818]
	773	—	—	—	—	1.3	2.5	
$\text{Mg}_2\text{Si}_{0.6-x}\text{Sn}_{0.4}\text{Bi}_x$, x = 0.03	300	218.5	—	-93.3	1780	0.16	3.21	[816]
	850	88.1	1.5	-213	795	1.2	2.51	
$\text{Mg}_2\text{Si}_{0.55-x}\text{Sn}_{0.4}\text{Ge}_{0.05}\text{Sb}_x$, x = 0.0125	300	221.7	2.5	-107	1500	0.15	3.4	[833]
	800	87.5	1.3	-220	665	1.2	2.15	
$\text{Mg}_{2.16}(\text{Si}_{0.3}\text{Sn}_{0.7})_{0.98}\text{Sb}_{0.02}$	300	437.9	—	-125	2350	0.31	—	[834]
	800	114.3	—	-215	920	1.3	—	
$\text{Mg}_2(\text{Si}_{0.4}\text{Sn}_{0.6})\text{Bi}_x$, x = 0.03	373	618.3	0.85	-205	1780	0.6	1.28	[815]
	573	—	0.95	-275	—	1.2	1.33	
$\text{Mg}_{2.16}(\text{Si}_{0.30}\text{Sn}_{0.70})_{0.98}\text{Sb}_{0.02}$	300	370.9	2.2	-130	1870	0.3	3.4	[835]
	750	118.9	1.5	-220	820	1.2	2.5	
$\text{Mg}_{2.2}\text{Si}_{0.49}\text{Sn}_{0.5}\text{Sb}_{0.01}$	300	253.7	1.9	-120	1450	0.25	2.7	[817]
	873	73.9	1.2	-230	570	1.25	2.1	

(Continued.)

Table 11. (Continued.)

Material	T (K)	μ_w ($\text{cm}^2 \text{V}^{-1} \text{s}^{-1}$)	κ_L ($\text{W m}^{-1} \text{K}^{-1}$)	S ($\mu\text{V K}^{-1}$)	σ ($\Omega^{-1} \text{cm}^{-1}$)	zT	k ($\text{W m}^{-1} \text{K}^{-1}$)	References
$\text{Mg}_{2.08}\text{Si}_{0.8}\text{Sn}_{0.2}/3\%\text{Bi}$	300	133.3	2.45	-145	560	0.06	2.8	[836]
	850	91.7	0.75	-260	480	1.17	1.8	
$\text{Mg}_2\text{Si}_{0.4-x}\text{Sn}_{0.6}\text{Sb}_x$, x = 0.0075	300	—	—	—	—	0.3	2.85	[814]
	773	—	—	—	—	1.1	2.35	
$\text{Mg}_2\text{Si}_{0.4}\text{Sn}_{0.6-x}\text{Sb}_x$, x = 0.1, 2 at% Zn	300	—	—	—	—	0.2	—	[837]
	750	—	—	—	—	1.1	—	
$\text{Mg}_2\text{Si}_{0.4}\text{Sn}_{0.6-y}\text{Ge}_y$, y = 0.1	300	249.0	2	-100	1850	0.17	3.15	[838]
	800	96.1	1.2	-210	820	1.1	2.6	
$\text{Mg}_2\text{Si}_{0.6-y}\text{Sn}_{0.4}\text{Sb}_y$, y = 0.0125	300	217.3	1.65	-95	1729	0.15	2.9	[839]
	860	80.1	1	-225	640	1.11	2.4	
$\text{Mg}_{2.2}\text{Si}_{0.392}\text{As}_{0.008}\text{Sn}_{0.5925}\text{Sb}_{0.0075}/2\%$ TiO ₂ nanoparticles	300	303.8	—	-125	1630	—	3.2	[839]
	823	76.6	—	-235	510	1.1	3.1	
$\text{Mg}_{2.2}\text{Si}_{0.392}\text{As}_{0.008}\text{Sn}_{0.5925}\text{Sb}_{0.0075}/5\%$ TiO ₂ nanoparticles	300	293.5	—	-130	1480	—	3	[840]
	823	74.8	—	-240	470	1.1	3	
$\text{Mg}_2\text{Si}_{0.4-x}\text{Sn}_{0.6}\text{Sb}_x$, x = 0.015	300	275.5	1.5	-150	1090	0.3	2.8	[813]
	773	102.0	1.4	-250	520	1.1	2.35	
$\text{Mg}_{2(1+x)}\text{Si}_{0.45}\text{Sn}_{0.537}\text{Sb}_{0.013}$, x = 0.08	300	297.5	2	-130	1500	0.3	2.9	[841]
	725	96.8	1.55	-200	800	1	2.5	
$\text{Mg}_2\text{Si}_{0.6}\text{Ge}_{0.4}\text{Bi}_{0.02}$	300	109.1	—	-85	1000	0.05	3	[812]
	800	41.8	—	-190	450	1	1.8	
$\text{Mg}_2(\text{Si}_{0.3}\text{Sn}_{0.7})_{0.975}\text{Sb}_{0.025}$	300	380.3	2.1	-175	1120	0.35	2.9	[811]
	640	156.5	1.4	-260	535	1	2.25	
$\text{Mg}_{1.96}\text{Al}_{0.04}\text{Si}_{0.97}\text{Bi}_{0.03}$	300	243.0	3.1	-89.91	2076	0.15	4.75	[842]
	873	—	1	—	900	1	3	

(Continued.)

Table 11. (Continued.)

Material	T (K)	μ_w ($\text{cm}^2 \text{V}^{-1} \text{s}^{-1}$)	κ_L ($\text{W m}^{-1} \text{K}^{-1}$)	S ($\mu\text{V K}^{-1}$)	σ ($\Omega^{-1} \text{cm}^{-1}$)	zT	k ($\text{W m}^{-1} \text{K}^{-1}$)	References
$\text{Mg}_{2.2}\text{Si}_{0.5925}\text{Sn}_{0.4}\text{Sb}_{0.0075}$	300	179.7	—	−95	1430	0.12	3	[843]
	673	93.3	—	−200	690	1	1.95	
$\text{Mg}_2\text{Si}_{0.785}\text{Sn}_{0.2}\text{Sb}_{0.015}$	340	123.9	2	−85	1370	0.2	3.25	[844]
	740	74.1	1.2	−190	710	0.95	2	
$\text{Mg}_2\text{Si}_{0.5-x}\text{Sn}_{0.5}\text{Sb}_x$, x = 0.013	300	188.6	2	−105.6	1300	0.17	2.8	[810]
	740	86.8	1.35	−200	740	0.9	2.3	
$\text{Mg}_2\text{Si:Bi} = 1-x$, x = 2 at %	300	156.8	5.5	−100	1165	0.05	6.3	[845]
	850	89.9	2.4	−245	560	0.86	3.5	
$\text{Mg}_{2.10}\text{Si}_{0.38}\text{Sn}_{0.6}\text{Sb}_{0.02}$	300	218.4	2.2	−103.9	1540	0.2	3.12	[809]
	700	87.3	—	−215	575	0.85	2.3	
$\text{Mg}_{2-x}\text{La}_x\text{Si}_{0.58}\text{Sn}_{0.42}$, x = 0.005	300	82.0	—	−105	570	0.05	3.1	[808]
	810	48.8	—	−205	450	0.8	2.3	
$\text{Mg}_2\text{Si} + 2$ at% Bi	300	229.2	—	−85	2100	0.05	6.2	[846]
	840	74.7	—	−200	770	0.74	3.8	
$\text{Mg}_2\text{Si} + 2$ at% Bi	300	15.8	4.8	−105	110	0.05	4.9	[847]
	823	57.0	1.8	−200	570	0.7	2.9	
$\text{Mg}_2\text{Si} + 0.15$ at% Bi	300	168.2	6	−100	1250	0.05	6.8	[848]
	775	81.4	2.4	−230	525	0.7	3	
$\text{Mg}_2\text{Si}_{0.5875}\text{Sn}_{0.4}\text{Sb}_{0.0125}$	300	84.4	—	−135	400	0.1	2.5	[807]
	775	55.0	—	−235	335	0.7	2	
$\text{Mg}_2\text{Si}_{0.970}\text{Bi}_{0.030}$	300	222.9	5.1	−89	1929	0.07	6.61	[806]
	810	73.1	1.8	−187	830	0.68	3.5	
$\text{Mg}_2\text{Si}_{0.6-y}\text{Sb}_y\text{Sn}_{0.4}$, y = 0.005	300	70.7	2.35	−110	460	0.07	2.7	[849]
	724	49.7	1.3	−220	325	0.68	1.8	
$\text{Mg}_2\text{Si} + 2$ at% Al	300	122.4	—	−180	340	0.05	9.2	[850]
	970	—	—	—	−225	460	0.66	
p-type	—	—	—	—	—	—	—	

(Continued.)

Table 11. (Continued.)

Material	T (K)	μ_{av} ($\text{cm}^2 \text{V}^{-1} \text{s}^{-1}$)	κ_L ($\text{W m}^{-1} \text{K}^{-1}$)	S ($\mu\text{V K}^{-1}$)	σ ($\Omega^{-1} \text{cm}^{-1}$)	zT	k ($\text{W m}^{-1} \text{K}^{-1}$)	References
$\text{Mg}_{1.98}\text{Li}_{0.02}\text{Si}_{0.4}\text{Sn}_{0.6}$	300	101.2	1.6	135	480	0.15	2	[791]
	700	41.9	1.25	205	310	0.55	1.6	
$\text{Mg}_2\text{Li}_{0.025}\text{Si}_{0.4}\text{Sn}_{0.6}$	300	99.7	—	125	535	0.13	1.9	[792]
	675	52.2	—	210	345	0.7	1.3	
Manganese silicides								
$\text{MnSi}_{1.73}$	823	29.7	2.5	234	200	0.3	—	[793]
$\text{Mn}_{0.99}\text{Re}_{0.01}\text{Si}_{1.75}\text{Ge}_{0.025}$	825	70.6	1.5	230	500	1	—	[789]
$\text{Mn}_{0.95}\text{Cr}_{0.05}\text{Si}_{1.74} + 2\% \text{mol V}_{17}\text{Ge}_{31}$	900	46.1	2.2	180	666	0.7	—	[851]
$\text{Mn}(\text{Si}_{0.992}\text{Ge}_{0.008})_{1.73}$	723	73.1	—	225	450	0.58	2.8	[800]
$\text{MnSi}_{1.73}$ with 5% Al doping	800	42.9	—	252	225	0.82	—	[805]
$\text{MnSi}_{1.73}\text{Ge}_{0.02}$	823	31.5	—	220	250	0.44	2.8	[795]
$(\text{Mn}_{15}\text{Si}_{26})_{99}(\text{MnS})$	800	40.8	—	220	310	0.59	—	[852]
$\text{Re}_{0.04}\text{Mn}_{0.96}\text{Si}_{1.8}$	800	38.4	1.8	230	260	0.57	—	[799]
$\text{Mn}(\text{Si}_{0.992}\text{Ge}_{0.008})_{1.73}$	833	35.9	2	220	290	0.6	—	[853]
$\text{MnSi}_{1.75}$	800	46.1	1.4	220	350	0.62	—	[802]
$\text{Mn}_{0.95}\text{Cr}_{0.05}\text{Si}_{1.74}$	850	53.5	2.3	210	500	0.6	—	[801]
$\text{Mn}_{0.99}\text{Ag}_{0.01}\text{Si}_{1.8}$	823	42.1	2.0	210	375	0.55	—	[798]
$\text{MnSi}_{1.8} + 1.5\% \text{Ag/Pt QDs}$	823	49.0	1.92	234	330	0.64	—	[798]
$\text{Mn}_{0.96}\text{V}_{0.04}\text{Si}_{1.73}$	873	40.3	—	170	625	0.52	3.1	[797]
$\text{MnSi}_{1.75}$	777	35.5	—	230	230	0.47	2.7	[796]
$\text{MnSi}_{1.787}\text{Al}_{0.01} + 0.6\% \text{Fe NPs}$	773	45.7	1.9	220	330	0.53	—	[854]
$\text{MnSi}_{1.74}$	773	38.9	2	230	250	0.4	—	[794]
$\text{V}_{0.04}\text{Mn}_{+}\text{Al}_{120}\text{Si}_{1.74}$	773	36.4	2	210	295	0.4	—	[794]
$\text{Mn}_{30.36}\text{Re}_6\text{Si}_{63.64}$	873	57.2	1.27	235	416	1.15	—	[790]
$\text{MnSi}_{1.746}\text{Te}_{0.03}$	823	43.9	1.5	230	310	0.7	—	[804]
$\text{MnSi}_{1.73} + 5 \text{ at}\% \text{Al}$	873	30.8	1.1	210	300	0.65	—	[803]
$\text{MnSi}_{1.733}$	850	0.2	2	240	330	0.55	—	[855]

3.12. Borides and carbides

Boride and carbide thermoelectrics

Philipp Sauerschnig^{1,2} and Takao Mori^{1,3}

¹ International Center for Materials Nanoarchitectonics (WPI-MANA), National Institute for Materials Science (NIMS), Tsukuba, Ibaraki 305-0044, Japan

² Global Zero Emission Research Center, National Institute of Advanced Industrial Science and Technology (AIST), Tsukuba, Ibaraki 305-8569, Japan

³ Graduate School of Pure and Applied Science, University of Tsukuba, Tsukuba, Ibaraki 305-8671, Japan

A couple of notable application directions for thermoelectric materials are: thermal energy harvesting, to power innumerable sensors and mobile devices expected to be utilized in future society [856–859], and high temperature waste heat thermoelectric conversion for energy saving and carbon reduction [860, 861]. For the latter to be serviceable, the thermoelectric materials themselves need to be high temperature stable refractory materials such as oxides [601, 862–864], silicides [865–868], nitrides [869, 870], borides and carbides. The latter two classes of materials are gathered in this section. Thermoelectric properties of boride and carbide compounds collected from the literature are shown in table 12.

In general, borides have excellent mechanical properties including high temperature stability, chemical stability, and low compressibility due to the strong covalent bonding of boron. It is a particularly refractory class of materials with borides like RB_{66} typically having melting points above 2400 K. In addition, boron cluster compounds, formed with the boron icosahedron as a structural unit, have been found to exhibit intrinsic low thermal conductivity, which is advantageous for thermoelectrics, despite the compounds possessing strong bonding and generally high speed of sound. Many of the compounds exhibit large Seebeck coefficients, and electrical conductivities that increase with an increase in temperature due to hopping conduction. Therefore, despite their relatively low zT at lower temperatures, they are considered a promising system as ultra-high temperature thermoelectric materials [871–879].

We first briefly cover the very boron-rich compounds, namely, those which possess the B_{12} icosahedron as main building block of the boron cluster atomic network. The thermoelectric properties of the most common form of elemental boron, beta-boron, have been extensively studied through modification of properties via TM doping [880–887]. As the excellent properties of p -type boron carbide became clear [888–890], effort was focussed on the search for a viable n -type counterpart. We mention here that because of the electron deficient nature of the boron atomic network as reviewed previously [871, 873], the boron icosahedral borides are predominantly p -type. The n -type characteristics, in even a limited range of temperature, in boron cluster compounds were first found by Werheit with Fe doping [881] and Slack with V doping [884]. Later both p -type and n -type characteristics with very large absolute values of Seebeck coefficients were found for Zr doped beta-boron with variation of the Zr content [887]. Boron carbide has been reported with the highest performance of $zT \sim 1$ for boron carbide and TiB_2 composites [891, 892]. In addition to the wide range of compositions of boron carbide [888–890], there has also been extensive work investigating the thermoelectric properties of boron carbide in different forms like single crystals, thin films, nanowires, and various composites [893–901]. Boron carbide belongs to the alpha-boron rhombohedral structure type, and various compounds of this family such as boron phosphide, boron arsenide, boron oxide, boron sulfide, in addition to alpha-boron itself, have been investigated [882, 902–908]. Amongst the boron cluster compounds, Si doped B_{12}P_2 has been reported to have high mobility because of the hole carriers [903], although mobility has not been measured for many of these borides, presumably due to low mobility. Amorphous boron also has been measured with low electrical conductivity as would be expected [880]. The RB_{66} compounds are found to have amorphous-like behavior of thermal conductivity; relatively high thermoelectric performance has been observed for some rare earths like SmB_{66} and compounds with relatively high metal content [882, 909–915]. The $\text{RB}_{44}\text{Si}_2$ compounds have also been investigated and shown to have moderate thermoelectric performance [528, 910, 916–920], behavior of general interest, the possibility to control morphology through addition of volatile element [919], anisotropic properties related to interesting crystal structure channels [920], and insight into the importance of disorder as the origin of amorphous-like behavior of thermal conductivity in such crystalline compounds [917]. It should be mentioned that for most of the boron icosahedral compounds, the measurements with conventional facilities were typically limited to a maximum of 1100 K, but thermoelectric performance of compounds like RB_{66} and $\text{RB}_{44}\text{Si}_2$ were showing steep increases in thermoelectric properties toward higher temperatures, with melting points of these compounds above 2400 K and 2300 K, respectively,

In the aluminoborides [882, 921, 922], a striking discovery was made for $\text{Al}_x\text{YB}_{14}$, in that, unusually, it was found to be possible to vary the Al content in a relatively wide range and as a result, both p -type and

n-type characteristics could be obtained with relatively high performance for a boride [923]. Liquid phase sintering was also recently discovered for this important compound, simplifying processing and reducing synthesis time [924]. The $\text{RB}_{22}\text{C}_2\text{N}$ and homologous series of compounds has also attracted interest with its structural similarities and as the *n*-type counterpart compounds to boron carbide [925–928]. The synthesis process for this compound has also been radically improved by using a gaseous reaction which may also be useful for the synthesis of nitride compounds [929].

Silicon boride compounds have also been investigated as potential high temperature thermoelectric materials [882, 930, 931]. For a SiB_n ($n = 15\text{--}49$)/ SiB_6 composite prepared by SPS a remarkably high Seebeck coefficient close to $900 \mu\text{V K}^{-1}$ and a zT approaching 0.2 at 1100 K with an upwards trend with increasing temperature have been reported [931]. Unlike the boron-rich compounds discussed so far, diboride, tetraboride and hexaboride compounds are not built from B_{12} icosahedra and generally show *n*-type behavior [577, 894, 921, 932–937]. TM diborides, e.g. TiB_2 [894] and ZrB_2 [932] show metallic behavior and while $\text{PF}_s > 1 \text{ mW m}^{-1} \text{ K}^{-2}$ have been observed in $\text{ZrB}_2\text{--SiC}$ composite materials [932], very high thermal conductivity values limit the overall thermoelectric performance. Layered REMB_4 compounds ($\text{RE} = \text{rare earth element}$, $\text{M} = \text{transition metal}$) have been studied by applying the *mno* electron counting rule to find semiconducting compounds. REMB_4 ($\text{RE} = \text{Y, Gd, Ho}$; $\text{M} = \text{Cr, Mo, W}$) compounds of the YCrB_4 -type were found to be *n*-type semiconducting materials [577]. TM hexaborides MB_6 ($\text{M} = \text{Ca, Sr, Ba}$) are among the best performing boride thermoelectric materials with zT values of 0.3 around 1000 K [934, 935]. To reduce thermal conductivity of these compounds thin films have been deposited for YbB_6 and SrB_6 [936, 937].

Besides borides, another group of materials which has been investigated for the use as high temperature thermoelectric applications due to their good thermal stability are carbides [938–951]. Efforts have been focused on the compound SiC which exists in several different modifications, the most prominent being the hexagonal 6-H α -SiC [938, 939, 947] and the cubic 3-C β -SiC [938, 939, 944–946, 948–950]. Depending on the synthesis conditions both *p*-type and *n*-type behavior have been reported. Strategies for improving the thermoelectric properties have included the addition of secondary phases for the fabrication of composite materials, e.g. B_4C [947], C [945, 947], Al_2O_3 [947], Si_3N_4 [944], Si [948] and Si/Au/polysilastyrene [948]. Thermoelectric properties of carbide materials in addition to SiC have been reported for layered Mo-based MXene carbides [951], $\text{TiC}_{0.7}\text{C}_{0.3}$ [940], flexible WC/poly(lactic acid) composites [941], $\text{VC/Cr}_{23-x}\text{Fe}_x\text{C}_6$ containing Fe-2.3C-Si-5Mn-7V-8Cr alloy [942] and $\text{Zr}_2[\text{Al}_{3.56}\text{Si}_{0.44}]\text{C}_5$ [943].

Boride and carbide thermoelectric materials have great structural and chemical variety and have been studied thoroughly from a fundamental point of view. Their thermoelectric performance compared to the established thermoelectrics is however relatively low. Many of the borides have very large Seebeck coefficients and relatively low electrical conductivities. Compositing partial metallic networks has been shown to largely enhance the performance for several cases, like $\text{YB}_{22}\text{C}_2\text{N}$ [952] and boron carbide [891, 892], and this should also be attempted in future with other borides with relatively high performance. Besides necessary improvements in the thermoelectric performance, in order to exploit the advantages of this class of thermoelectrics, i.e. high thermal and chemical stability and generally increasing performance with increasing temperature, appropriate evaluation and application systems need to be established; these are currently limited to fairly moderate temperature ranges. For example, most commercial thermoelectric facilities used to measure Seebeck coefficients and electrical conductivity typically have a maximum measuring temperature of $800 \text{ }^\circ\text{C}$ or $1000 \text{ }^\circ\text{C}$ at most. Whereas, for example, most of the borides presented in this work have zT values showing a large increasing trend at these temperatures and possess melting points above $2000 \text{ }^\circ\text{C}$. Thereby, for ultra-high temperature applications in the range $1000 \text{ }^\circ\text{C}\text{--}2000 \text{ }^\circ\text{C}$, such as occurring in jet engine exhausts, topping cycle for fusion power generation, etc, borides are one of the few thermoelectric materials which are actually stable at these temperatures and may potentially possess higher zT values than has been given so far in the literature. As two prominent refractory thermoelectric material systems, consideration and investigations of these two materials should continue.

Acknowledgments

Support from JSPS JP16H06441 and JST Mirai Program JPMJMI19A1 are acknowledged.

Table 12. Borides and carbides thermoelectric properties.

Material	μ_w ($\text{cm}^2 \text{V}^{-1} \text{s}^{-1}$)	κ ($\text{W m}^{-1} \text{K}^{-1}$)	S ($\mu\text{V K}^{-1}$)	σ ($\Omega^{-1} \text{cm}^{-1}$)	zT	E_g (eV)	μ_{HF} ($\text{cm}^2 \text{V}^{-1} \text{s}^{-1}$)	Power factor ($\text{mW m}^{-1} \text{K}^{-2}$)	T (K)	References
β -rhombohedral B (C doping) (p -type)	3.6	9.7	401	4.7	0.0078	—	—	0.076	1000	[880]
β -rhombohedral B (Fe doping) (n -type) AM	0.02	—	-17.5	4.6	—	—	—	0.00014	750	[881]
β -rhombohedral B (p -type) SC	3.1	240 (262 K)	396	4.5	—	—	—	0.071	1030	[882] ^a
β -rhombohedral B	—	—	—	—	—	1.32(1)/1.50(1) for E c , 1.29(1)/1.46(1) eV for E \perp c	—	—	300	[883]
β -rhombohedral B (0.5 at.%V doping) (n -type) SC	—	—	-399	—	—	—	—	—	300	[884]
β -rhombohedral B (1.23 at.%V doping) SC	—	—	—	42.4	—	—	—	—	300	[884]
β -rhombohedral B (2 at.%Hf doping) SC	—	2.9	—	—	—	—	—	—	963	[884]
β -rhombohedral B (2.5 at.%Fe doping) (p -type) SC	1.7	—	89	146	—	—	—	0.12	1400	[884]
β -rhombohedral B (1 at.%Zr doping) (p -type) SC	6.6	—	271	71.6	—	—	—	0.53	1500	[884]
β -rhombohedral B (1 at.%Zr doping) (p -type) SC	0.2	4.7	589	0.00799	2.9×10^{-5}	—	—	0.00028	500	[884]
β -rhombohedral B (5 at.%Si doping) (p -type) SC	8.9	—	262	118	—	—	—	0.81	1600	[884]
β -rhombohedral B (4.8 at.%Si doping) SC	—	18.5	—	—	—	—	—	—	500	[884]
β -rhombohedral B ₀₅ V _{1.5} (n -type) HP	0.5	4.1	342	1.4	0.0042	—	—	0.016	1040	[885]
β -rhombohedral B ₀₅ V _{1.5} (n -type) HP	0.4	2.1	-104	15.7	0.0078	—	—	0.017	963	[885]
β -rhombohedral B ₀₅ Co _{1.5} (p -type) HP	0.3	4.1	188	4.3	0.0039	—	—	0.015	1040	[885]
β -rhombohedral B ₀₅ Cu ₅ (p -type) SPS	0.8	2.3	208	9.8	0.018	—	—	0.042	973	[886]
β -rhombohedral B _{88.12} Zr _{1.88} (p -type) SPS	0.1	—	332	0.13	—	—	—	0.0014	850	[887]
β -rhombohedral B _{97.20} Zr _{2.74} (n -type) SPS	0.02	—	-516	0.0053	—	—	—	0.00014	850	[887]
B ₄ C (p -type) HP	2.8	—	223	40.8	—	—	1.1	0.20	1273	[888]
B ₄ 7C (p -type) HP	7.7	—	219	119	—	—	—	0.57	1273	[888]
B _{6.7} C (p -type) HP	16.5	—	221	249	—	—	—	1.2	1273	[888]
B ₄ C HP	—	6.3	—	—	—	—	—	—	1700	[889]
B _{6.5} C HP	—	5.5	—	—	—	—	—	—	1700	[889]
B _{7.5} C HP	—	5.4	—	—	—	—	—	—	1700	[889]
B ₄ C (p -type) HP	3.4	15.7	235	32.4	0.012	—	—	0.18	1053	[890]
B _{7.13} C ^b (p -type) HP	26.6	3.2	240	272	0.47	—	—	1.4	1053	[890]
B _{7.70} C (p -type) HP	8.6	3.9	247	72.2	0.12	—	—	0.44	1053	[890]
B ₄ C + 2 mol.% TiB ₂ (p -type) AM	59.0	8.7	304	273	0.32	—	—	2.5	1100	[891]
B ₄ C + 6 mol.% TiB ₂ (p -type) AM	161.9	10.6	355	415	0.54	—	—	5.2	1100	[891]
B ₃ C-SiB ₁₄ -Si (B ₈₀ C ₁₆ Si ₂) (p -type) AM	54.5	11.0	341	156.5	0.18	—	—	1.8	1065	[892]
B ₄ C-SiB ₁₄ -Si (B ₈₀ C ₅ Si ₁₃) (p -type) AM	73.8	5.6	412	93.1	0.30	—	—	1.6	1065	[892]
B ₅ C (62.4% rel.density) (p -type) HP	0.6	3.8	283	3.9	0.0096	—	—	0.031	1173	[893]

(Continued.)

Table 12. (Continued.)

Material	μ_w ($\text{cm}^2 \text{V}^{-1} \text{s}^{-1}$)	κ ($\text{W m}^{-1} \text{K}^{-1}$)	S ($\mu\text{V K}^{-1}$)	σ ($\Omega^{-1} \text{cm}^{-1}$)	zT	E_g (eV)	μ_{H1} ($\text{cm}^2 \text{V}^{-1} \text{s}^{-1}$)	Power factor ($\text{mW m}^{-1} \text{K}^{-2}$)	T (K)	References
B ₄ C (0.2 at.% Si) (78.3% rel. density) (p-type) HP	2.6	6.5	230	30.8	0.029	—	—	0.16	1173	[893]
B ₄ C (2 wt.% W ₂ B ₅) (p-type) HP	1.5	7.5	216	21.9	0.016	—	—	0.10	1173	[893]
B ₄ C—2 mol.%TiB ₂ (parallel) (p-type) FZ	7.5	—	222	80.6	—	—	2.3	0.40	1023	[894]
B ₄ C—2 mol.%TiB ₂ (perpendicular) (p-type) FZ	9.5	—	219	105.8	—	—	2.3	0.51	1023	[894]
B ₄ C (p-type) FZ SC	11.2	16.3	248	85.7	0.032	—	1	0.53	1000	[895]
B _{4.3} C:SC (parallel C) (p-type) FZ SC	0.03	—	160	0.11	—	—	—	0.00028	300	[896]
B _{4.3} C:SC (perpendicular C) (p-type) FZ SC	0.01	—	160	0.05	—	—	—	0.00013	300	[896]
B _{6.5} C (p-type) IBE thin film	12.0	—	238	111	—	—	—	0.63	1050	[897]
B ₄ C	—	—	—	—	—	2.09	—	—	300	[898]
B ₄ C (p-type) nanowires	23.9	—	295	30	—	—	—	0.26	430	[899]
B ₁₃ C ₂ (10 wt.% HfB ₂) ^c (p-type) SPS	18.6	5.1	157	41.4	0.20	—	—	1.0	1003	[900]
B ₄ C (p-type) SPS	9.0	13	271	50.8	0.028	—	—	0.37	973	[901]
B ₆ P	—	—	—	—	—	3.35	—	—	300	[902]
B ₆ As	—	—	—	—	—	3.48	—	—	300	[902]
B ₁₂ P ₂ CVD (Si doped) (p-type) CVD	0.1	3.6	738	0.0015	2.2×10^{-5}	—	$31.7 (\text{Si}(100))/10.8 (\text{Si}(111))$ at 300 K	8.2×10^{-5}	963	[903]
B ₆ O (p-type) HP	4.5	5.5	545	1.1	0.0059	—	1.2	0.033	993	[904]
B ₁₂ As ₂	—	—	—	—	—	—	80	—	300	[905]
B ₁₂ As ₂ CVD (p-type) CVD thin film	0.2	—	107	1.4	—	—	18.8	0.0016	300	[906]
B ₁₂ As ₂ CVD thin film	—	15.3/27.0	—	—	—	—	—	—	300	[906]
B ₁₂ As ₂ (p-type) SC (solution growth)	0.7	—	471	0.23	—	3.47	20 (300 K)	0.0051	663	[907]
B ₆ S (p-type) (sintering)	0.02	—	211	0.15	—	—	—	0.00067	800	[908]
α -rhombohedral B (p-type) polycrystalline	0.6	—	501	0.38	—	—	20 (680 K)	0.0095	1400	[882] ^a
amorphous B (p-type)	0.04	—	332	0.092	—	—	—	0.0010	853	[880]
SrB ₆ (p-type) (zone melting)	0.001	—	100	0.01	—	0.8	15	0.00001	300	[909]
GdB ₆ (p-type) (zone melting)	0.008	—	390	0.002	—	0.87	15	3.0×10^{-5}	300	[909]
YbB ₆ (p-type) (zone melting)	0.006	—	270	0.006	—	1.27	5	4.4×10^{-5}	300	[909]
YB ₆ (p-type) (zone melting)	0.007	—	340	0.003	—	1	—	3.5×10^{-5}	300	[882] ^a
DyB ₆ (p-type) (zone melting)	0.002	—	140	0.007	—	0.72	—	1.4×10^{-5}	300	[882] ^a
ErB ₆ (p-type) FZ SC	0.1	—	225	1.2	—	—	—	0.0061	1035	[910]
YB ₆ (p-type) FZ SC	0.2	—	206	3	—	—	—	0.013	1035	[911]
YB ₄₈ (p-type) FZ SC	4.6	2.5	202	59.7	0.096	—	—	0.24	990	[912]
SrB ₆ (p-type) FZ SC	5.4	2.7	210	69.1	0.12	—	—	0.30	1050	[913]
YbB ₆ (p-type) FZ SC	5.2	2.6	241	41.7	0.091	—	—	0.24	973	[914]
HoB ₆ (p-type) SPS	5.2	2.6	235	44.4	0.092	—	—	0.25	973	[528]
TmB ₆ (p-type) SPS	5.0	2.6	235	42.9	0.089	—	—	0.24	973	[528]
YB ₄₁ Si ₁₂ (p-type) FZ SC	0.6	—	184	1.4	—	—	<0.1	0.0047	290	[915]
YbB ₄₄ Si ₂ (p-type) FZ SC	0.8	—	209	10	—	—	—	0.044	1023	[910]
ErB ₄₄ Si ₂ (p-type) FZ SC	1.1	2.7 (300 K)	222	12	—	—	—	0.059	1023	[910]
TbB ₄₄ Si ₂ (p-type) FZ SC	0.8	—	185	14	—	—	—	0.048	1023	[910]
ErB ₄₄ Si ₂ FZ SC	—	—	—	—	—	—	—	—	873	[916]
YbB ₄₄ Si ₂ FZ SC	—	1.6	—	—	—	—	—	—	300	[917]
	—	3.3	—	—	—	—	—	—	—	—

(Continued.)

Table 12. (Continued.)

Material	μ_{sw} ($\text{cm}^2 \text{V}^{-1} \text{s}^{-1}$)	κ ($\text{W m}^{-1} \text{K}^{-1}$)	S ($\mu\text{V K}^{-1}$)	σ ($\Omega^{-1} \text{cm}^{-1}$)	zT	E_g (eV)	μ_H ($\text{cm}^2 \text{V}^{-1} \text{s}^{-1}$)	Power factor ($\text{mW m}^{-1} \text{K}^{-2}$)	T (K)	References
Tb _{0.48} Si ₂ (<i>p</i> -type) sintering	0.04	—	242	0.35	—	—	—	0.0020	1023	[918]
Tb _{0.9} Lu _{0.1} B _{0.4} Si ₂ (<i>p</i> -type) sintering	0.05	—	258	0.32	—	—	—	0.0021	1023	[918]
Tb _{0.8} Lu _{0.2} B _{0.4} Si ₂ (<i>p</i> -type) sintering	0.05	—	299	0.21	—	—	—	0.0019	1023	[918]
YB _{0.4} Si ₂ (Zn doping) (<i>p</i> -type) AM	2.0	—	190	32.4	—	—	—	0.12	1040	[919]
YB _{0.1} Si _{1.3} ([110] direction) (<i>p</i> -type) FZ SC	2.7	4.2	225	27	0.033	—	—	0.14	1000	[920]
YB _{0.1} Si _{1.3} ([012] direction) (<i>p</i> -type) FZ SC	1.0	—	301	4.1	—	—	—	0.037	1000	[920]
α -AlB ₁₂ (<i>p</i> -type)	19.8	—	398	59	—	—	—	0.93	1693	[882] ^a
MgAlB ₁₄ (Ni doping) (<i>p</i> -type)	0.3	—	144	17.4	—	—	—	0.036	1553	[882] ^a
AlMgB ₁₄ (<i>p</i> -type) SPS	1.6	—	338	4.5	—	—	—	0.051	1030	[921]
Al _{0.55} Y _{0.58} B _{1.4} (Al added) (<i>n</i> -type) SPS	9.5	4.5	-12.3	304	0.099	—	—	0.46	973	[922]
Y _{1-x} B _{0.85} C _{0.4} (<i>n</i> -type) sintering	1.0	2.1	387	1.5	0.010	—	—	0.022	973	[922]
LuB _{2.2} C ₂ N (<i>n</i> -type) HP	0.005	—	-58	0.47	—	—	—	0.00034	673	[925]
YB ₂₂ C ₂ N (<i>n</i> -type) HP	0.0001	—	-35	0.015	—	—	—	0.00016	1040	[926]
YB ₂₂ C ₂ N (<i>n</i> -type) SPS	0.004	4.5	-33	0.57	—	—	—	1.8×10^{-6}	973	[927]
HoB ₁₇ CN (<i>n</i> -type) SPS	0.0006	—	-36	0.0081	—	—	—	6.2×10^{-5}	973	[927]
ErB ₂₂ C ₂ N (<i>n</i> -type) HP	0.0004	—	-21	0.0092	—	—	—	1.0×10^{-6}	973	[927]
YB ₂₂ C ₂ N (12% VB ₂) (<i>n</i> -type) sintering	0.1	1.8	-57	5.4	—	—	—	4.1×10^{-7}	973	[927]
YB ₂₂ C ₂ N (16% VB ₂) (<i>n</i> -type) sintering	0.03	0.9	-29	5.1	—	—	—	0.0018	1040	[928]
B ₁₄ Si (<i>p</i> -type)	23.2	—	443	27.6	—	—	—	0.54	1300	[882] ^a
SiB ₆ ^d (<i>p</i> - <i>n</i> transition) sintering	0.3	2.5	140	11	—	—	—	0.022	1273	[930]
SiB _n (<i>n</i> = 15–49, 90 at.% B) (<i>p</i> -type) SPS	1958.9	5.2	897	9.4	0.011	—	—	0.76	1100	[931]
YCrB ₄ (<i>n</i> -type) AM	36.5	—	-110	510.4	—	—	—	0.62	500	[933]
YMoB ₄ (<i>n</i> -type) AM	2.6	—	-85	130.8	—	—	—	0.095	923	[933]
YWB ₄ (<i>n</i> -type) AM	2.2	—	-70	123.9	—	—	—	0.061	873	[933]
YMo _{0.8} Fe _{0.2} B ₄ (<i>n</i> -type) AM	6.9	—	-72	447.3	—	—	—	0.23	973	[933]
GdCrB ₄ (<i>n</i> -type) AM	31.2	—	-116	403.5	—	—	—	0.54	500	[933]
HoCrB ₄ (<i>n</i> -type) AM	25.9	—	-79	556.8	—	—	—	0.35	500	[933]
TiB ₂ (<i>n</i> -type) SPS	60.0	—	-14	17 675	—	—	—	0.35	873	[894]
ZrB ₂ -SiC (20 vol.% (n-type) HP)	201.1	67.0	-23.8	29 126	0.019	—	—	1.6	773	[932]
ZrB ₂ -SiC (20 vol.%-WC (5 vol.% (n-type) HP)	91.1	47.0	-20.3	15 457	0.010	—	—	0.64	773	[932]
CaB ₆ (<i>n</i> -type) SPS	25.9	—	-273	160	—	—	—	1.2	1050	[921]
SrB ₆ (<i>n</i> -type) SPS	48.5	—	-145	1335	—	—	—	2.8	1050	[921]
YbB ₆ (<i>n</i> -type) SPS	24.6	—	-111	1033	—	—	—	1.3	1050	[921]
CeB ₆ (<i>p</i> -type) SPS	5.1	—	2	12 617	—	—	—	0.0050	1050	[921]
SrB ₆ (<i>p</i> -type) SPS	3.1	—	3	5211	—	—	—	0.0047	1050	[921]
CaB ₆ (<i>n</i> -type) SPS	44.3	—	992	992	0.19	—	—	2.7	1073	[934]
SrB ₆ (<i>n</i> -type) SPS	47.9	15.2	-165	756	0.026	—	—	2.9	1073	[934]
Ca _{0.5} Sr _{0.5} B ₆ (<i>n</i> -type) SPS	45.7	8.6	-169	976	0.035	—	—	2.8	1073	[934]
CaB ₆ (<i>n</i> -type) SPS	53.7	11.7	-162	1181	0.027	—	—	3.1	1035	[935]
SrB ₆ (<i>n</i> -type) SPS	16.9	9.1	-246	140	0.096	—	—	0.85	1035	[935]
BaB ₆ (<i>n</i> -type) SPS	31.7	10.7	-209	403	0.17	—	—	1.8	1035	[935]
SrB ₆ (<i>n</i> -type) CVD thin film	4.0	—	-74	140	—	—	—	0.077	660	[936]

(Continued.)

Table 12. (Continued.)

Material	μ_w ($\text{cm}^2 \text{V}^{-1} \text{s}^{-1}$)	κ ($\text{W m}^{-1} \text{K}^{-1}$)	S ($\mu\text{V K}^{-1}$)	σ ($\Omega^{-1} \text{cm}^{-1}$)	zT	E_g (eV)	μ_H ($\text{cm}^2 \text{V}^{-1} \text{s}^{-1}$)	Power factor ($\text{mW m}^{-1} \text{K}^{-2}$)	T (K)	References
YB ₆ (<i>n</i> -type) HPCVD thin film	16.1	2.54 (at 296 K)	-60	563	—	0.44	—	0.20	563	[937]
UB ₄ (<i>p</i> -type) AM	23.2	—	40	2300	—	—	—	0.37	850	[577]
α -SiC (<i>n</i> -type) sintering (N ₂ atmosphere)	0.001	1.4	-76	0.073	3.2×10^{-5}	—	—	0.000 042	1065	[938]
α -SiC (<i>p</i> -type) sintering (Ar atmosphere)	0.2	0.5	301	0.7	0.014	—	—	0.0063	1065	[938]
α -SiC <i>n</i> -type (monocrystalline)	—	—	-29 to -108	—	—	—	20–100	—	300	[943]
α -SiC (0.5 wt.% B ₄ C, 2.5 wt.% C) (<i>p</i> -type) sintering	70.0	—	615	8.5	—	—	—	0.32	1073	[947]
α -SiC (0.5 wt.% B ₄ C, 2.5 wt.% C, 3 wt.% Al ₂ O ₃) (<i>p</i> -type) sintering	81.7	—	500	37.6	—	—	—	0.94	1073	[947]
β -SiC (<i>n</i> -type) sintering (N ₂ atmosphere)	0.6	1.2	-65	49.8	0.019	—	—	0.021	1065	[938]
β -SiC (<i>n</i> -type) sintering (Ar atmosphere)	0.7	3.5	-121	25.6	0.011	—	—	0.037	1065	[938]
β -SiC (<i>n</i> -type) (polycrystalline film)	—	—	-9 to -28	—	—	—	0.1–3	—	300	[943]
β -SiC + 7 wt.% Si ₃ N ₄ (<i>n</i> -type) SPS	4.3	—	-76	265	—	—	—	0.15	973	[944]
β -SiC/C composite (<i>p</i> -type) SPS	0.5	4.1	15.8	56.6	0.000 16	—	—	0.0014	473	[945]
β -SiC (B _N -doped) (<i>p</i> -type) vapor phase growth	12.5	32	89	730	0.019	—	—	0.58	1072	[946]
β -SiC/Si/Au polysilastyrene composite (<i>p</i> -type) sintering	36.1	52.4	92.4	298	0.0015	—	5.74	0.25	300	[948]
β -SiC (<i>n</i> -type) CVD (He atmosphere)	0.02	4.6	-67	1.1	0.0001	—	—	0.000 49	950	[949]
β -SiC (<i>n</i> -type) nanowire	6.5	6	-67	107	0.0030	—	—	0.048	370	[950]
Mo ₂ C _{1-x} (<i>n</i> -type, annealed) solution synthesis	9.7	—	-31	1132	—	—	0.016 (pristine) ^d , 1.86 (annealed) ^d	0.11	800	[939]
Mo ₂ TiC ₂ T _x (<i>n</i> -type) solution synthesis	18.2	—	-47	1392	—	—	0.323 (pristine) ^d , 2.85 (annealed) ^d	0.31	800	[939]
Mo ₂ Ti ₃ C ₃ T _x (<i>n</i> -type) solution synthesis	5.8	—	-28	754	—	—	0.451 (pristine) ^d , 2.05 (annealed) ^d	0.059	800	[939]
TiC _{0.7} N _{0.3} (<i>n</i> -type) sintering	24.3	18.0	-18	5587	0.0088	—	—	0.18	873	[940]
WC/Polylactic Acid composite (<i>n</i> -type) additive manufacturing	0.6	28.0	-12	42	6.5×10^{-6}	—	—	0.000 60	300	[941]
Fe-2.3C-Si-5Mn-7 V-8Cr (VC/Cr _{23-x} Fe _x C ₆) (<i>n</i> -type) induction melting	70.0	21.6	-25	10 155	0.024	—	—	0.63	800	[942]
Zr ₂ [Al _{3.56} Si _{0.44}]C ₅ (<i>n</i> -type) SPS	12.3	—	-13	4427	—	—	—	0.075	953	[952]

^a And references therein.

^b κ of sample composition B_{6.81}C.

^c κ of sample calculated from zT , resistivity and Seebeck coefficient.

^d Data from [953].

AM = arc melting; CVD = chemical vapor deposition; FZ = floating zone; HP = hot press; HPCVD = hybrid physical chemical vapor deposition; IBE = intense pulsed-ion beam evaporation; SC = single crystal; SPS = spark plasma sintering.

4. Challenges and future perspectives

In this compilation we have sought to provide an overview of the thermoelectric properties of a wide range of inorganic materials. These include current state-of-the-art thermoelectric materials but also a number of more 'exotic' materials which could become important in the coming years or provide insights into routes to improve the more established materials. Whilst many publications in the field perhaps give undue attention to the maximum figure of merit, zT_{\max} , as the critical parameter, we have tried to stress the importance of the average zT , particularly over the intended temperature range for the application, and indeed the other important thermoelectric parameters (documented here) which indicate the strengths and potential limitations of the material.

With the advances in modeling and experimental instrumentation over the past decade there are considerable opportunities in the development and discovery of new materials and understanding the structures and mechanisms controlling properties from the atomic to the macroscopic level. Materials discovery through data mining, machine learning or high throughput calculations can point the way in the selection of potential new materials with high thermoelectric performance, enabling candidates to be screened theoretically, and the most promising evaluated experimentally. A further constraint here is that the work should target Earth-abundant, non-toxic starting materials to minimize cost and environmental impact. Atomistic and Density of States calculations along with band structure engineering can be used to define the most effective additives for enhancing electrical conductivity or reducing thermal conductivity and ways to induce band convergence, thus improving the PF.

Whatever new materials appear in the coming years there are many important challenges that will need to be addressed if the thermoelectrics are to reach their full potential at the material and device level and be fully exploited in a growing range of applications. For maximum output from a thermoelectric module the n -type and p -type materials should exhibit comparable performance. Many of the existing materials have significant imbalance between their best n -type and p -type candidates; for example, for Tellurides and Zintlts the p -type performance is much better than the n -type, whilst for Skutterudites it is the reverse. Work is necessary to develop more, better matched thermoelectric materials in the different systems, but also to extend the temperature range of operation through enhancing performance away from the peak temperature. In many cases this is particularly desirable at lower temperatures, even down to room temperature; for example with HHs, skutterudites and oxides, a reduction in thermal conductivity is highly desirable to help improve the average zT .

Looking beyond zT and PF performance, another very important challenge to be addressed is the mechanical properties and stability of the materials. To avoid serious mechanical stresses in the modules, the p -type and n -type materials should have similar coefficients of thermal expansion, but greater attention also needs to be paid to a variety of mechanical properties including brittleness and mechanical strength at elevated temperatures. This is especially true of the metal-based thermoelectrics. A closely related, more general challenge is that of controlling degradation at elevated temperature, or as a result of thermal cycling. Materials that contain volatile species (e.g. Na, Sb, S, Pb) tend to degrade via the physical loss of material or via electromigration when a current flows. The former can be addressed by some form of coating or encapsulation, and the latter by cation doping to block migration pathways, but greater understanding of corrosion and degradation mechanisms are essential if viable, long-lasting solutions are to be achieved.

As the construction of thermoelectric modules involves multiple interfaces, between dissimilar materials in many cases, greater understanding of these interfaces and transport processes across them is essential to avoid physical degradation and unnecessary power losses in device operation. Identification of most suitable diffusion-barrier materials and solders, for the various families of materials will be important.

In order to ensure that thermoelectrics become more competitive in the market place, a detailed analysis of processing costs at each step in module production, and the development of cheaper material-processing and manufacturing routes are critical. The availability of cost-effective thermoelectrics, with increased conversion efficiencies, covering wider temperature ranges would open up new markets from the room temperature IoT to ultra-high temperature engineering systems.

Acknowledgments

Robert Freer gratefully acknowledges support of the UK Engineering and Physical Sciences Research Council for the provision of funding through EP/L014068/1, EP/L017695/1 and EP/T020040/1.

Disclaimer and declaration

The information presented in this review was selected in good faith by all the authors. We accept that it is impossible to include all the available data. However, errors and omissions will be corrected in the subsequent editions of the tables. Corrections and more complete information from the scientific community are most welcome in order to improve the value and scope of the data presented in the tables.

Conflict of interest

The authors declare that they have no known competing financial interests or personal relationships that could have appeared to influence the work reported in this paper.

ORCID iDs

Robert Freer  <https://orcid.org/0000-0003-1100-8975>
Dursun Ekren  <https://orcid.org/0000-0002-9080-9094>
Tanmoy Ghosh  <https://orcid.org/0000-0002-4078-7093>
Kanishka Biswas  <https://orcid.org/0000-0001-9119-2455>
Shen Han  <https://orcid.org/0000-0003-0426-8453>
Chenguang Fu  <https://orcid.org/0000-0002-9545-3277>
Tiejun Zhu  <https://orcid.org/0000-0002-3868-0633>
Kazuki Imasato  <https://orcid.org/0000-0001-7294-1780>
G. Jeffrey Snyder  <https://orcid.org/0000-0003-1414-8682>
Melis Ozen  <https://orcid.org/0000-0003-3498-3941>
Kivanc Saglik  <https://orcid.org/0000-0001-7910-8652>
Umut Aydemir  <https://orcid.org/0000-0003-1164-1973>
Raúl Cardoso-Gil  <https://orcid.org/0000-0003-1706-1910>
E Svanidze  <https://orcid.org/0000-0003-2893-1379>
Shriparna Mukherjee  <https://orcid.org/0000-0002-1941-5551>
Sahil Tippireddy  <https://orcid.org/0000-0002-5383-6966>
Paz Vaqueiro  <https://orcid.org/0000-0001-7545-6262>

References

- [1] Wang W and Bai S 2021 Chapter 3.4. Measurement techniques of thermoelectric devices and modules *Thermoelectric Energy Conversion: Theories and Mechanisms, Materials, Devices, and Applications* 1st edn, ed E R Funahashi (Woodhead Publishing/Elsevier) pp 521–37
- [2] Koumoto K, Funahashi R, Guilmeau E, Miyazaki Y, Weidenkaff A, Wang Y, Wan C L and Zhou X-D 2013 Thermoelectric ceramics for energy harvesting *J. Am. Ceram. Soc.* **96** 1–23
- [3] Franz R and Wiedemann G 1853 Ueber die Wärme-Leitungsfähigkeit der Metalle *Ann. Phys.* **165** 497–531
- [4] Funahashi R (ed) 2021 *Thermoelectric Energy Conversion: Theories and Mechanisms, Materials, Devices, and Applications* 1st edn (Cambridge: Woodhead Publishing/Elsevier)
- [5] May A F and Snyder G J 2012 Chapter 11. Introduction to modeling thermoelectric transport at high temperatures *Thermoelectrics and its Energy Harvesting* vol 1, ed D M Rowe (Boca Raton, FL: CRC Press) pp K1–18
- [6] Pei Y, Wang H and Snyder G J 2012 Band engineering of thermoelectric materials *Adv. Mater.* **24** 6125–35
- [7] Witkoske E, Wang X, Maassen J and Lundstrom M 2019 Universal behavior of the thermoelectric figure of merit, zT , vs. quality factor *Mater. Today Phys.* **8** 43–48
- [8] Mahan G D 1998 Good thermoelectrics *Solid State Physics* vol 51, ed H Ehrenreich and F Spaepen (San Diego: Academic) p 81
- [9] Snyder G J, Snyder A H, Wood M, Gurunathan R, Snyder B H and Niu C 2020 Weighted mobility *Adv. Mater.* **35** 2001537
- [10] Tsai Y-F et al 2021 *Adv. Mater.* **33** 2005612
- [11] Wu Y, Chen Z, Nan P, Xiong F, Lin S, Zhang X, Chen Y, Chen L, Ge B and Pei Y 2019 *Joule* **3** 1276
- [12] Li W, Zheng L, Ge B, Lin S, Zhang X, Chen Z, Chang Y and Pei Y 2017 *Adv. Mater.* **29** 1605887
- [13] Banik A, Ghosh T, Arora R, Dutta M, Pandey J, Acharya S, Soni A, Waghmare U V and Biswas K 2019 *Energy Environ. Sci.* **12** 589
- [14] Heremans J P, Jovovic V, Toberer E S, Saramat A, Kurosaki K, Charoenphakdee A, Yamanaka S and Snyder G J 2008 *Science* **321** 554
- [15] Pei Y, Shi X, LaLonde A, Wang H, Chen L and Snyder G J 2011 *Nature* **473** 66
- [16] Zhang Q, Liao B, Lan Y, Lukas K, Liu W, Esfarjani K, Opeil C, Broido D, Chen G and Ren Z 2013 *Proc. Natl Acad. Sci.* **110** 13261
- [17] Wu L, Li X, Wang S, Zhang T, Yang J, Zhang W, Chen L and Yang J 2017 *NPG Asia Mater.* **9** e343
- [18] Perumal S, Bellare P, Shenoy U S, Waghmare U V and Biswas K 2017 *Chem. Mater.* **29** 10426
- [19] Zheng Z et al 2018 *J. Am. Chem. Soc.* **140** 2673
- [20] Hong M, Wang Y, Feng T, Sun Q, Xu S, Matsumura S, Pantelides S T, Zou J and Chen Z-G 2019 *J. Am. Chem. Soc.* **141** 1742
- [21] Hong M, Wang Y, Liu W, Matsumura S, Wang H, Zou J and Chen Z-G 2018 *Adv. Energy Mater.* **8** 1801837
- [22] Wu H et al 2015 *Energy Environ. Sci.* **8** 3298
- [23] Banik A, Shenoy U S, Anand S, Waghmare U V and Biswas K 2015 *Chem. Mater.* **27** 581
- [24] Tan G, Zhao L-D, Shi F, Doak J W, Lo S-H, Sun H, Wolverton C, Dravid V P, Uher C and Kanatzidis M G 2014 *J. Am. Chem. Soc.* **136** 7006

- [25] Tan G, Shi F, Doak J W, Sun H, Zhao L-D, Wang P, Uher C, Wolverton C, Dravid V P and Kanatzidis M G 2014 *Energy Environ. Sci.* **8** 267
- [26] Tan G, Shi F, Hao S, Chi H, Zhao L-D, Uher C, Wolverton C, Dravid V P and Kanatzidis M G 2015 *J. Am. Chem. Soc.* **137** 5100
- [27] Banik A, Shenoy U S, Saha S, Waghmare U V and Biswas K 2016 *J. Am. Chem. Soc.* **138** 13068
- [28] Biswas K, He J, Blum I D, Wu C-I, Hogan T P, Seidman D N, Dravid V P and Kanatzidis M G 2012 *Nature* **489** 414
- [29] Perumal S, Samanta M, Ghosh T, Shenoy U S, Bohra A K, Bhattacharya S, Singh A, Waghmare U V and Biswas K 2019 *Joule* **3** 2565
- [30] Sarkar D, Ghosh T, Banik A, Roychowdhury S, Sanyal D and Biswas K 2020 *Angew. Chem., Int. Ed.* **59** 11115
- [31] Wu D et al 2014 *J. Am. Chem. Soc.* **136** 11412
- [32] Hong M, Chen Z-G, Yang L, Zou Y-C, Dargusch M S, Wang H and Zou J 2018 *Adv. Mater.* **30** 1705942
- [33] Liu Z et al 2018 *Proc. Natl Acad. Sci.* **115** 5332
- [34] Li J et al 2018 *Joule* **2** 976
- [35] Hong M, Lyv W, Li M, Xu S, Sun Q, Zou J and Chen Z-G 2020 *Joule* **4** 2030
- [36] Samanta M, Ghosh T, Arora R, Waghmare U V and Biswas K 2019 *J. Am. Chem. Soc.* **141** 19505
- [37] Zhang Q et al 2018 *Energy Environ. Sci.* **11** 933
- [38] Luo Z-Z et al 2019 *J. Am. Chem. Soc.* **141** 16169
- [39] Xiao Y, Wu H, Cui J, Wang D, Fu L, Zhang Y, Chen Y, He J, Pennycook S J and Zhao L-D 2018 *Energy Environ. Sci.* **11** 2486
- [40] Zhang J, Wu D, He D, Feng D, Yin M, Qin X and He J 2017 *Adv. Mater.* **29** 1703148
- [41] Goldsmid H J and Douglas R W 1954 *Br. J. Appl. Phys.* **5** 386
- [42] Poudel B et al 2008 *Science* **320** 634
- [43] Deng R et al 2018 *Energy Environ. Sci.* **11** 1520
- [44] Pan Y et al 2018 *Adv. Mater.* **30** 1802016
- [45] Kim S I et al 2015 *Science* **348** 109
- [46] Zhu B, Liu X, Wang Q, Qiu Y, Shu Z, Guo Z, Tong Y, Cui J, Gu M and He J 2020 *Energy Environ. Sci.* **13** 2106
- [47] Hong M, Chasapis T C, Chen Z-G, Yang L, Kanatzidis M G, Snyder G J and Zou J 2016 *ACS Nano* **10** 4719
- [48] Park K et al 2016 *J. Am. Chem. Soc.* **138** 14458
- [49] Ren Y, Yang J, Jiang Q, Zhang D, Zhou Z, Li X, Xin J and He X 2017 *J. Mater. Chem. C* **5** 5076
- [50] Deng H et al 2021 *Nano Energy* **81** 105649
- [51] Zheng Y et al 2019 *Sci. Adv.* **5** eaat9461
- [52] Roychowdhury S, Jana M K, Pan J, Guin S N, Sanyal D, Waghmare U V and Biswas K 2018 *Angew. Chem., Int. Ed.* **57** 4043
- [53] Qiu Y, Liu Y, Ye J, Li J and Lian L 2018 *J. Mater. Chem. A* **6** 18928
- [54] He Y, Lu P, Shi X, Xu F, Zhang T, Snyder G J, Uher C and Chen L 2015 *Adv. Mater.* **27** 3639
- [55] Pei Y, Heinz N A and Snyder G J 2011 *J. Mater. Chem.* **21** 18256
- [56] Zhu T, Bai H, Zhang J, Tan G, Yan Y, Liu W, Su X, Wu J, Zhang Q and Tang X 2020 *ACS Appl. Mater. Interfaces* **12** 39425
- [57] Cao Y, Su X, Meng F, Bailey T P, Zhao J, Xie H, He J, Uher C and Tang X 2020 *Adv. Funct. Mater.* **30** 2005861
- [58] Su X et al 2019 *Adv. Funct. Mater.* **29** 1806534
- [59] Zhang J, Qin X, Li D, Xin H, Song C, Li L, Zhu X, Wang Z, Guo G and Wang L 2014 *J. Mater. Chem. A* **2** 2891
- [60] Luo Y, Jiang Q, Yang J, Li W, Zhang D, Zhou Z, Cheng Y, Ren Y, He X and Li X 2017 *Nano Energy* **32** 80
- [61] Luo Y, Yang J, Jiang Q, Li W, Zhang D, Zhou Z, Cheng Y, Ren Y and He X 2016 *Adv. Energy Mater.* **6** 1600007
- [62] Xie H, Hao S, Cai S, Bailey T P, Uher C, Wolverton C, Dravid V P and Kanatzidis M G 2020 *Energy Environ. Sci.* **13** 3693
- [63] Zhang J et al 2019 *Adv. Mater.* **31** 1905210
- [64] Roychowdhury S, Ghosh T, Arora R, Samanta M, Xie L, Singh N K, Soni A, He J, Waghmare U V and Biswas K 2021 *Science* **371** 722
- [65] Cheikh D, Hogan B E, Vo T, von Allmen P, Lee K, Smiadak D M, Zevalkink A, Dunn B S, Fleurial J-P and Bux S K 2018 *Joule* **2** 698–709
- [66] Samanta M, Pal K, Waghmare U V and Biswas K 2020 *Angew. Chem., Int. Ed.* **59** 4822
- [67] Chang H-C, Chen T-H, Sankar R, Yang Y-J, Chen L-C and Chen K-H 2020 *Mater. Today Phys.* **15** 100248
- [68] May A F, Fleurial J-P and Snyder G J 2010 *Chem. Mater.* **22** 2995
- [69] Xu Z, Wu H, Zhu T, Fu C, Liu X, Hu L, He J, He J and Zhao X 2016 *NPG Asia Mater.* **8** e302
- [70] Hao F et al 2016 *Energy Environ. Sci.* **9** 3120
- [71] Deng R, Su X, Zheng Z, Liu W, Yan Y, Zhang Q, Dravid V P, Uher C, Kanatzidis M G and Tang X 2018 *Sci. Adv.* **4** eaar5606
- [72] Pan Y et al 2019 *Energy Environ. Sci.* **12** 624
- [73] Yan X, Poudel B, Ma Y, Liu W S, Joshi G, Wang H, Lan Y, Wang D, Chen G and Ren Z F 2010 *Nano Lett.* **10** 3373
- [74] Liu W, Lukas K C, McEnaney K, Lee S, Zhang Q, Opeil C P, Chen G and Ren Z 2013 *Energy Environ. Sci.* **6** 552–60
- [75] Perumal S, Roychowdhury S, Negi D S, Datta R and Biswas K 2015 *Chem. Mater.* **27** 7171
- [76] Gelbstein Y, Davidow J, Girard S N, Chung D Y and Kanatzidis M 2013 *Adv. Energy Mater.* **3** 815
- [77] Gelbstein Y and Davidow J 2014 *Phys. Chem. Chem. Phys.* **16** 20120
- [78] Fahrnbauer F, Souchay D, Wagner G and Oeckler O 2015 *J. Am. Chem. Soc.* **137** 12633
- [79] Perumal S, Roychowdhury S and Biswas K 2016 *Inorg. Chem. Front.* **3** 125
- [80] Samanta M and Biswas K 2017 *J. Am. Chem. Soc.* **139** 9382
- [81] Acharyya P, Roychowdhury S, Samanta M and Biswas K 2020 *J. Am. Chem. Soc.* **142** 20502
- [82] Banik A, Vishal B, Perumal S, Datta R and Biswas K 2016 *Energy Environ. Sci.* **9** 2011
- [83] Banik A and Biswas K 2014 *J. Mater. Chem. A* **2** 9620
- [84] Al Rahal Al Orabi R, Mecholsky N A, Hwang J, Kim W, Rhyee J-S, Wee D and Fornari M 2016 *Chem. Mater.* **28** 376
- [85] Zhao L-D et al 2016 *J. Am. Chem. Soc.* **138** 2366
- [86] Zhang X, Wang D, Wu H, Yin M, Pei Y, Gong S, Huang L, Pennycook S J, He J and Zhao L-D 2017 *Energy Environ. Sci.* **10** 2420
- [87] Wang L, Tan X, Liu G, Xu J, Shao H, Yu B, Jiang H, Yue S and Jiang J 2017 *ACS Energy Lett.* **2** 1203
- [88] Zheng L, Li W, Lin S, Li J, Chen Z and Pei Y 2017 *ACS Energy Lett.* **2** 563
- [89] Xu X, Cui J, Yu Y, Zhu B, Huang Y, Xie L, Wu D and He J 2020 *Energy Environ. Sci.* **13** 5135
- [90] Roychowdhury S, Biswas R K, Dutta M, Pati S K and Biswas K 2019 *ACS Energy Lett.* **4** 1658
- [91] Poudeu P F P, d'Angelo J, Downey A D, Short J L, Hogan T P and Kanatzidis M G 2006 *Angew. Chem., Int. Ed.* **45** 3835
- [92] Girard S N, He J, Zhou X, Shoemaker D, Jaworski C M, Uher C, Dravid V P, Heremans J P and Kanatzidis M G 2011 *J. Am. Chem. Soc.* **133** 16588
- [93] Biswas K, He J, Wang G, Lo S-H, Uher C, Dravid V P and Kanatzidis M G 2011 *Energy Environ. Sci.* **4** 4675

- [94] Pei Y, LaLonde A D, Heinz N A, Shi X, Iwanaga S, Wang H, Chen L and Snyder G J 2011 *Adv. Mater.* **23** 5674
- [95] Pei Y, LaLonde A, Iwanaga S and Snyder G J 2011 *Energy Environ. Sci.* **4** 2085
- [96] Pei Y, Wang H, Gibbs Z M, LaLonde A D and Snyder G J 2012 *NPG Asia Mater.* **4** e28
- [97] Zhang Q, Cao F, Liu W, Lukas K, Yu B, Chen S, Opeil C, Broido D, Chen G and Ren Z 2012 *J. Am. Chem. Soc.* **134** 10031
- [98] Ohta M, Biswas K, Lo S-H, He J, Chung D Y, Dravid V P and Kanatzidis M G 2012 *Adv. Energy Mater.* **2** 1117
- [99] Zhao L D et al 2013 *Energy Environ. Sci.* **6** 3346
- [100] Wu H J, Zhao L-D, Zheng F S, Wu D, Pei Y L, Tong X, Kanatzidis M G and He J Q 2014 *Nat. Commun.* **5** 1
- [101] Korkosz R J et al 2014 *J. Am. Chem. Soc.* **136** 3225
- [102] Tan G, Shi F, Hao S, Zhao L-D, Chi H, Zhang X, Uher C, Wolverton C, Dravid V P and Kanatzidis M G 2016 *Nat. Commun.* **7** 12167
- [103] Jood P, Ohta M, Yamamoto A and Kanatzidis M G 2018 *Joule* **2** 1339
- [104] Ahn K, Han M-K, He J, Androulakis J, Ballikaya S, Uher C, Dravid V P and Kanatzidis M G 2010 *J. Am. Chem. Soc.* **132** 5227
- [105] LaLonde A D, Pei Y and Snyder G J 2011 *Energy Environ. Sci.* **4** 2090
- [106] Pei Y, LaLonde A D, Wang H and Snyder G J 2012 *Energy Environ. Sci.* **5** 7963
- [107] Xiao Y, Wang D, Qin B, Wang J, Wang G and Zhao L-D 2018 *J. Am. Chem. Soc.* **140** 13097
- [108] Roychowdhury S, Panigrahi R, Perumal S and Biswas K 2017 *ACS Energy Lett.* **2** 349
- [109] Hong M, Chen Z-G, Yang L, Liao Z-M, Zou Y-C, Chen Y-H, Matsumura S and Zou J 2018 *Adv. Energy Mater.* **8** 1702333
- [110] Xu Y, Li W, Wang C, Li J, Chen Z, Lin S, Chen Y and Pei Y 2017 *J. Mater. Chem. A* **5** 19143
- [111] Ballikaya S, Chi H, Salvador J R and Uher C 2013 *J. Mater. Chem. A* **1** 12478–84
- [112] Zhao K et al 2019 *Adv. Mater.* **31** 1903480
- [113] Niu Y, Li S, Mao J, Yang C, Zhang Q, Zhang Q, Jiang J, Wang C and Ren Z 2020 *Nano Energy* **77** 105297
- [114] Yusufu A, Kurosaki K, Kosuga A, Sugahara T, Ohishi Y, Muta H and Yamanaka S 2011 *Appl. Phys. Lett.* **99** 061902
- [115] Plirdpring T et al 2012 *Adv. Mater.* **24** 3622
- [116] Li Y, Meng Q, Deng Y, Zhou H, Gao Y, Li Y, Yang J and Cui J 2012 *Appl. Phys. Lett.* **100** 231903
- [117] Cui J, Li Y, Du Z, Meng Q and Zhou H 2012 *J. Mater. Chem. A* **1** 677
- [118] Liu R, Xi L, Liu H, Shi X, Zhang W and Chen L 2012 *Chem. Commun.* **48** 3818
- [119] Kosuga A, Plirdpring T, Higashine R, Matsuzawa M, Kurosaki K and Yamanaka S 2012 *Appl. Phys. Lett.* **100** 042108
- [120] Zhang J, Liu R, Cheng N, Zhang Y, Yang J, Uher C, Shi X, Chen L and Zhang W 2014 *Adv. Mater.* **26** 3848
- [121] Vaquero P, Guélou G, Stec M, Guilmeau E and V Powell A 2013 *J. Mater. Chem. A* **1** 520
- [122] May A F, Fleurial J-P and Snyder G J 2008 *Phys. Rev. B* **78** 125205
- [123] Nolas G S, Morelli D T and Tritt T M 1999 *Annu. Rev. Mater. Sci.* **29** 89–116
- [124] Zhu T, Liu Y, Fu C, Heremans J P, Snyder J G and Zhao X 2017 *Adv. Mater.* **29** 1605884
- [125] Xi L, Zhang W, Chen L and Yang J 2010 *J. Korean Ceram. Soc.* **47** 54–60.
- [126] Slack G 1995 *CRC Handbook of Thermoelectrics* ed D M Rowe (Boca Raton, FL: CRC Press) ch 34 pp 401–13
- [127] Sales B C, Mandrus D, Chakoumakos B C, Keppens V and Thompson J R 1997 *Phys. Rev. B* **56** 15081–9
- [128] Pei Y Z, Chen L D, Zhang W, Shi X, Bai S Q, Zhao X Y, Mei Z G and Li X Y 2006 *Appl. Phys. Lett.* **89** 221107
- [129] Pei Y Z, Yang J, Chen L D, Zhang W, Salvador J R and Yang J 2009 *Appl. Phys. Lett.* **95** 042101
- [130] Chen L D, Kawahara T, Tang X E, Goto T, Hirai T, Dyck J S, Chen W and Uher C 2001 *J. Appl. Phys.* **90** 1864–8
- [131] Zhao X Y, Shi X, Chen L D, Zhang W Q, Zhang W B and Pei Y Z 2006 *J. Appl. Phys.* **99** 053711
- [132] Qiu Y et al 2013 *Adv. Funct. Mater.* **23** 3194–203
- [133] Tang Y, Qiu Y, Xi L, Shi X, Zhang W, Chen L, Tseng S, Chen S and Snyder G J 2014 *Energy Environ. Sci.* **7** 812–9
- [134] Caillat T, Borshchevsky A and Fleurial J-P 1996 *J. Appl. Phys.* **80** 4442–9
- [135] Li X Y, Chen L D, Fan J F, Zhang W B, Kawahara T and Hirai T 2005 *J. Appl. Phys.* **98** 083702
- [136] Alleno E, Zehani E and Rouleau O 2013 *J. Alloys Compd.* **572** 43–48
- [137] Nolas G S, Kaeser M, Littleton R T I and Tritt T M 2000 *Appl. Phys. Lett.* **77** 1855–7
- [138] Yang J et al 2009 *Phys. Rev. B* **80** 115329
- [139] Pei Y, Bai S, Zhao X, Zhang W and Chen L 2008 *Solid State Sci.* **10** 1422–8
- [140] Tang Y, Hanus R, Chen S and Snyder G J 2015 *Nat. Commun.* **6** 7584
- [141] Li Y, Qiu P, Duan H, Chen J, Snyder G J, Shi X, Iversen B B and Chen L 2016 *J. Mater. Chem. C* **4** 4374–9
- [142] Shi X, Kong H, Li C-P, Uher C, Yang J, Salvador J R, Wang H, Chen L and Zhang W 2008 *Appl. Phys. Lett.* **92** 182101
- [143] Zhao W, Wei P, Zhang Q, Dong C, Liu L and Tang X 2009 *J. Am. Chem. Soc.* **131** 3713–20
- [144] Shi X, Yang J, Salvador J R, Chi M, Cho J Y, Wang H, Bai S, Yang J, Zhang W and Chen L 2011 *J. Am. Chem. Soc.* **133** 7837–46
- [145] Duan B et al 2016 *Energy Environ. Sci.* **9** 2090–8
- [146] Wan S, Huang X, Qiu P, Shi X and Chen L 2017 *ACS Appl. Mater. Interfaces* **9** 22713–24
- [147] Wan S, Qiu P, Huang X, Song Q, Bai S, Shi X and Chen L 2018 *ACS Appl. Mater. Interfaces* **10** 625–34
- [148] Sales B C, Mandrus D and Williams R K 1996 *Science* **272** 1325–8
- [149] Rogl G, Grytsiv A, Rogl P, Peranio N, Bauer E, Zehetbauer M and Eibl O 2014 *Acta Mater.* **63** 30–43
- [150] Yang J, Xi L, Zhang W, Chen L and Yang J 2009 *J. Electron. Mater.* **38** 1397–401
- [151] Qiu P, Yang J, Liu R, Shi X, Huang X, Snyder G, Zhang W and Chen L 2011 *J. Appl. Phys.* **109** 063713
- [152] Liu R, Qiu P, Chen X, Huang X and Chen L 2011 *J. Mater. Res.* **26** 1813–9
- [153] Liu R, Yang J, Chen X, Shi X, Chen L and Uher C 2011 *Intermetallics* **19** 1747–51
- [154] Rogl G, Grytsiv A, Bauer E, Rogl P and Zehetbauer M 2010 *Intermetallics* **18** 57–64
- [155] Rogl G, Grytsiv A, Rogl P, Bauer E and Zehetbauer M 2011 *Intermetallics* **19** 546–55
- [156] KIM I-H, Park K-H, Ur S-C, Choi S and Seo W 2010 *J. Korean Phys. Soc.* **57** 1000–4
- [157] Rogl G, Grytsiv A, Rogl P, Bauer E, Hoehenhofer M, Anbalagan R, Mallik R C and Schafner E 2014 *Acta Mater.* **76** 434–48
- [158] Witting I, Chasapis T, Ricci F, Peters M, Heinz N, Hautier G and Snyder G J 2019 *Adv. Electron. Mater.* **5** 1800904
- [159] Hachemaoui M, Khenata R, Bouhemadou A, Reshak A H, Rached D and Semari F 2009 *Curr. Opin. Solid State Mater. Sci.* **13** 105–11
- [160] Ghosez P and Veithen M 2007 *J. Phys.: Condens. Matter.* **19** 096002
- [161] Kliche G and Lutz H D 1984 *Infrared Phys.* **24** 171–7
- [162] Dordevic S V, Dille N R, Bauer E D, Basov D N, Maple M B and Degiorgi L 1999 *Phys. Rev. B* **60** 11321–8
- [163] Ögüt S and Rabe K M 1995 *Phys. Rev. B* **51** 10443–53
- [164] Schwall M and Balke B 2013 *Phys. Chem. Chem. Phys.* **15** 1868–72

- [165] Sekimoto T, Kurosaki K, Muta H and Yamanaka S 2007 *Jpn. J. Appl. Phys.* **2** 46 L673–75
- [166] Culp S R, Simonson J W, Poon S J, Ponnambalam V, Edwards J and Tritt T M 2008 *Appl. Phys. Lett.* **93** 022105
- [167] Yan X et al 2011 *Nano Lett.* **11** 556–60
- [168] Rausch E, Balke B, Stahlhofen J M, Ouardi S, Burkhardt U and Felser C 2015 *J. Mater. Chem. C* **3** 10409–14
- [169] He R, Zhu H, Sun J, Mao J, Reith H, Chen S, Schierning G, Nielsch K and Ren Z 2017 *Mater. Today Phys.* **1** 24–30
- [170] Liu Y, Fu C, Xia K, Yu J, Zhao X, Pan H, Felser C and Zhu T 2018 *Adv. Mater.* **30** 1800881
- [171] Qiu Q, Liu Y, Xia K, Fang T, Yu J, Zhao X and Zhu T 2019 *Adv. Energy Mater.* **9** 1803447
- [172] Young D P, Khalifah P, Cava R J and Ramirez A P 2000 *J. Appl. Phys.* **87** 317–21
- [173] Fu C, Zhu T, Pei Y, Xie H, Wang H, Snyder G J, Liu Y, Liu Y and Zhao X 2014 *Adv. Energy Mater.* **4** 1400600
- [174] Fu C, Zhu T, Liu Y, Xie H and Zhao X 2015 *Energy Environ. Sci.* **8** 216–20
- [175] Fu C, Bai S, Liu Y, Tang Y, Chen L, Zhao X and Zhu T 2015 *Nat. Commun.* **6** 8144
- [176] He R et al 2016 *Proc. Natl Acad. Sci.* **113** 13576–81
- [177] Yu J, Fu C, Liu Y, Xia K, Aydemir U, Chasapis T C, Snyder G J, Zhao X and Zhu T 2018 *Adv. Energy Mater.* **8** 1701313
- [178] Shen J, Fan L, Hu C, Zhu T, Xin J, Fu T, Zhao D and Zhao X 2019 *Mater. Today Phys.* **8** 62–70
- [179] Zhu H et al 2019 *Nat. Commun.* **10** 270
- [180] Huang L, He R, Chen S, Zhang H, Dahal K, Zhou H, Wang H, Zhang Q and Ren Z 2015 *Mater. Res. Bull.* **70** 773–8
- [181] Xia K, Liu Y, Anand S, Snyder G J, Xin J, Yu J, Zhao X and Zhu T 2018 *Adv. Funct. Mater.* **28** 1705845
- [182] Xia K, Nan P, Tan S, Wang Y, Ge B, Zhang W, Anand S, Zhao X, Snyder G J and Zhu T 2019 *Energy Environ. Sci.* **12** 1568–74
- [183] Li S et al 2020 *Ann. Phys.* **525** 1900440
- [184] Fang T, Xia K, Nan P, Ge B, Zhao X and Zhu T 2020 *Mater. Today Phys.* **13** 100200
- [185] Zhu H et al 2018 *Nat. Commun.* **9** 2497
- [186] Zhu H, Mao J, Feng Z, Sun J, Zhu Q, Liu Z, Singh D J, Wang Y and Ren Z 2019 *Sci. Adv.* **5** eaav5813
- [187] He R, Huang L, Wang Y, Samsonidze G, Kozinsky B, Zhang Q and Ren Z 2016 *APL Mater.* **4** 104804
- [188] Xie H, Wang H, Fu C, Liu Y, Snyder G J, Zhao X and Zhu T 2014 *Sci. Rep.* **4** 6888
- [189] Serrano-Sánchez F et al 2020 *J. Mater. Chem. A* **8** 14822–8
- [190] Sekimoto T, Kurosaki K, Muta H and Yamanaka S 2006 *J. Appl. Phys.* **99** 103701
- [191] Ciesielski K, Synoradzki K, Veremchuk I, Skokowski P, Szymański D, Grin Y and Kaczorowski D 2020 *Phys. Rev. Appl.* **14** 054046
- [192] Shen Q, Chen L, Goto T, Hirai T, Yang J, Meisner G P and Uher C 2001 *Appl. Phys. Lett.* **79** 4165–7
- [193] Culp S R, Poon S J, Hickman N, Tritt T M and Blumm J 2006 *Appl. Phys. Lett.* **88** 1–3
- [194] Kim S W, Kimura Y and Mishima Y 2004 *Sci. Technol. Adv. Mater.* **5** 485–9
- [195] Sakurada S and Shutoh N 2005 *Appl. Phys. Lett.* **86** 1–3
- [196] Yu C, Zhu T-J, Xiao K, Shen J-J, Yang S-H and Zhao X-B 2010 *J. Electron. Mater.* **39** 2008–12
- [197] Kimura Y, Tanoguchi T and Kita T 2010 *Acta Mater.* **58** 4354–61
- [198] Joshi G, Yan X, Wang H, Liu W, Chen G and Ren Z 2011 *Adv. Energy Mater.* **1** 643–7
- [199] Birkel C S et al 2012 *Chem. Mater.* **24** 2558–65
- [200] Xie H, Wang H, Pei Y, Fu C, Liu X, Snyder G J, Zhao X and Zhu T 2013 *Adv. Funct. Mater.* **23** 5123–30
- [201] Chen S, Lukas K C, Liu W, Opeil C P, Chen G and Ren Z 2013 *Adv. Energy Mater.* **3** 1210–4
- [202] Misra D K, Bhardwaj A and Singh S 2014 *J. Mater. Chem. A* **2** 11913–21
- [203] Liu Y, Xie H, Fu C, Snyder G J, Zhao X and Zhu T 2015 *J. Mater. Chem. A* **3** 22716–22
- [204] Zhang H, Wang Y, Dahal K, Mao J, Huang L, Zhang Q and Ren Z 2016 *Acta Mater.* **113** 41–47
- [205] Lkhagvasuren E, Fu C, Fecher G H, Auffermann G, Kreiner G, Schnelle W and Felser C 2017 *J. Phys. D: Appl. Phys.* **50** 425502
- [206] Mao J, Zhou J, Zhu H, Liu Z, Zhang H, He R, Chen G and Ren Z 2017 *Chem. Mater.* **29** 867–72
- [207] Barczak S A, Halpin J E, Buckman J, Decourt R, Pollet M, Smith R I, Maclaren D A and Bos J-W G 2018 *ACS Appl. Mater. Interfaces* **10** 4786–93
- [208] Mallick M M, Rajput K and Vitta S 2019 *J. Mater. Sci.: Mater. Electron.* **30** 6139–47
- [209] Kang H B, Poudel B, Li W, Lee H, Saparamadu U, Nozariasbmarz A, Kang M G, Gupta A, Heremans J J and Priya S 2020 *Mater. Today* **36** 63–72
- [210] Zhou M, Feng C, Chen L and Huang X 2005 *J. Alloys Compd.* **391** 194–7
- [211] Xie W, Jin Q and Tang X 2008 *J. Appl. Phys.* **103** 043711
- [212] Qiu P, Huang X, Chen X and Chen L 2009 *J. Appl. Phys.* **106** 103703
- [213] Poon S J, Wu D, Zhu S, Xie W, Tritt T M, Thomas P and Venkatasubramanian R 2011 *J. Mater. Res.* **26** 2795–802
- [214] Yan X, Liu W, Wang H, Chen S, Shiomi J, Esfarjani K, Wang H, Wang D, Chen G and Ren Z 2012 *Energy Environ. Sci.* **5** 7543–8
- [215] Yan X, Liu W, Chen S, Wang H, Zhang Q, Chen G and Ren Z 2013 *Adv. Energy Mater.* **3** 1195–200
- [216] Rausch E, Balke B, Ouardi S and Felser C 2014 *Phys. Chem. Chem. Phys.* **16** 25258–62
- [217] Chauhan N S, Bhardwaj A, Senguttuvan T D, Pant R P, Mallik R C and Misra D K 2016 *J. Mater. Chem. C* **4** 5766–78
- [218] Hu C, Xia K, Chen X, Zhao X and Zhu T 2018 *Mater. Today Phys.* **7** 69–76
- [219] Zou M, Li J-F, Guo P and Kita T 2010 *J. Phys. D: Appl. Phys.* **43** 415403
- [220] Fu C, Liu Y, Xie H, Liu X, Zhao X, Jeffrey Snyder G, Xie J and Zhu T 2013 *J. Appl. Phys.* **114** 134905
- [221] Zou M, Li J-F and Kita T 2013 *J. Solid State Chem.* **198** 125–30
- [222] Fu C, Xie H, Liu Y, Zhu T J, Xie J and Zhao X B 2013 *Intermetallics* **32** 39–43
- [223] Joshi G et al 2014 *Energy Environ. Sci.* **7** 4070–6
- [224] Fu C, Wu H, Liu Y, He J, Zhao X and Zhu T 2016 *Adv. Sci.* **3** 1600035
- [225] Shen J, Fu C, Liu Y, Zhao X and Zhu T 2018 *Energy Storage Mater.* **10** 69–74
- [226] Huang L, Wang Y, Shuai J, Zhang H, Yang S, Zhang Q and Ren Z 2015 *RSC Adv.* **5** 102469–76
- [227] Zhang H, Wang Y, Huang L, Chen S, Dahal H, Wang D and Ren Z 2016 *J. Alloys Compd.* **654** 321–6
- [228] Ono Y, Inayama S, Adachi H and Kajitani T 2006 *Jpn. J. Appl. Phys.* **1** 45 8740–3
- [229] Kimura Y, Tamura Y and Kita T 2008 *Appl. Phys. Lett.* **92** 2–5
- [230] Zhao D, Zuo M, Bo L and Wang Y 2018 *Materials* **11** 728
- [231] Aliev F G, Brandt N B, Moshchalkov V V, Kozyrkov V V, Skolozdra R V and Belogorokhov A I 1989 *Z. Phys. B* **75** 167–71
- [232] Cook B A, Meisner G P, Yang J and Uher C 1999 *Int. Conf. Thermoelectrics ICT, Proc.* pp 64–67
- [233] Yu C, Zhu T-J, Shi R-Z, Zhang Y, Zhao X-B and He J 2009 *Acta Mater.* **57** 2757–64
- [234] Yu J et al 2020 *Adv. Energy Mater.* **10** 2000888
- [235] Xing Y, Liu R, Liao J, Wang C, Zhang Q, Song Q, Xia X, Zhu T, Bai S and Chen L 2020 *Joule* **4** 2475–83

- [236] Zeier W G, Anand S, Huang L, He R, Zhang H, Ren Z, Wolverton C and Snyder G J 2017 *Chem. Mater.* **29** 1210–7
- [237] Yang J, Li H, Wu T, Zhang W, Chen L and Yang J 2008 *Adv. Funct. Mater.* **18** 2880–8
- [238] Lee M-S, Poudeu F P and Mahanti S D 2011 *Phys. Rev. B* **83** 085204
- [239] Ioffe A F 1957 *Semiconductor Thermoelements and Thermoelectric Cooling* (London: Infosearch Ltd)
- [240] Pei Y, Gibbs Z M, Gloskovskii A, Balke B, Zeier W G and Snyder G J 2014 *Adv. Energy Mater.* **4** 1400486
- [241] Larson P, Mahanti S D and Kanatzidis M G 2000 *Phys. Rev. B* **62** 12754–62
- [242] Zeeshan M, Nautiyal T, van den Brink J and Kandpal H C 2018 *Phys. Rev. Mater.* **2** 065407
- [243] Tobola J, Pierre J, Kaprzyk S, Skolozdra R V and Kouacou M A 1998 *J. Phys.: Condens. Matter.* **10** 1013–32
- [244] Fu C et al 2020 *Adv. Sci.* **7** 1902409
- [245] Snyder G J, Snyder A H, Wood M, Gurunathan R, Snyder B H and Niu C 2020 *Adv. Mater.* **32** 2001537
- [246] Cahill D G, Watson S K and Pohl R O 1992 *Phys. Rev. B* **46** 6131–40
- [247] Adams M J, Verosky M, Zebarjadi M and Heremans J P 2019 *Phys. Rev. Appl.* **11** 054008
- [248] Roy A, Bennett J W, Rabe K M and Vanderbilt D 2012 *Phys. Rev. Lett.* **109** 037602
- [249] Zhou J et al 2018 *Nat. Commun.* **9** 1721
- [250] Graziosi P, Kumarasinghe C and Neophytou N 2020 *ACS Appl. Energy Mater.* **3** 5913–26
- [251] Joshi H, Rai D P, Hnamte L, Laref A and Thapa R K 2019 *Heliyon* **5** e01155
- [252] Shen J, Wang Z, Chu J, Bai S, Zhao X, Chen L and Zhu T 2019 *ACS Appl. Mater. Interfaces* **11** 14182–90
- [253] Toberer E S, Cox C A, Brown S R, Ikeda T, May A F, Kauzlarich S M and Jeffrey Snyder G 2008 *Adv. Funct. Mater.* **18** 2795–800
- [254] Kim H-S, Gibbs Z M, Tang Y, Wang H and Snyder G J 2015 *APL Mater.* **3** 41506
- [255] Zhang J, Song L, Madsen G K H, Fischer K F F, Zhang W, Shi X and Iversen B B 2016 *Nat. Commun.* **7** 1–7
- [256] Hu Y, Lee K and Kauzlarich S M 2018 *Crystals* **8** 211
- [257] Tan W-J, Liu Y-T, Zhu M, Zhu T-J, Zhao X-B, Tao X-T and Xia S-Q 2017 *Inorg. Chem.* **56** 1646–54
- [258] Hu Y, Wang J, Kawamura A, Kovnir K and Kauzlarich S M 2015 *Chem. Mater.* **27** 343–51
- [259] Justl A P, Cerretti G, Bux S K and Kauzlarich S M 2019 *J. Appl. Phys.* **126** 165106
- [260] Tan W, Wu Z, Zhu M, Shen J, Zhu T, Zhao X, Huang B, Tao X-T and Xia S-Q 2017 *Inorg. Chem.* **56** 10576–83
- [261] Gascoin F, Ottensmahn S, Stark D, Haile S M and Snyder G J 2005 *Adv. Funct. Mater.* **15** 1860–4
- [262] Sun J and Singh D J 2017 *J. Mater. Chem. A* **5** 8499–509
- [263] Zhang Z et al 2020 *Adv. Energy Mater.* **10** 2001229
- [264] Bhardwaj A and Misra D K 2014 *RSC Adv.* **4** 34552–60
- [265] Kim S, Kim C, Hong Y-K, Onimaru T, Suekuni K, Takabatake T and Jung M-H 2014 *J. Mater. Chem. A* **2** 12311–6
- [266] Wood M, Aydemir U, Ohno S and Snyder G J 2018 *J. Mater. Chem. A* **6** 9437–44
- [267] Zheng L, Li W, Wang X and Pei Y 2019 *J. Mater. Chem. A* **7** 12773–8
- [268] Wang X, Li W, Zhou B, Sun C, Zheng L, Tang J, Shi X and Pei Y 2019 *Mater. Today Phys.* **8** 123–7
- [269] Wang X J, Tang M B, Chen H H, Yang X X, Zhao J T, Burkhardt U and Grin Y 2009 *Appl. Phys. Lett.* **94** 2007–10
- [270] Shuai J, Geng H, Lan Y, Zhu Z, Wang C, Liu Z, Bao J, Chu C-W, Sui J and Ren Z 2016 *Proc. Natl Acad. Sci. USA* **113** E4125–32
- [271] Shuai J, Liu Z, Kim H S, Wang Y, Mao J, He R, Sui J and Ren Z 2016 *J. Mater. Chem. A* **4** 4312–20
- [272] Aydemir U, Zevalkink A, Ormeci A, Bux S and Snyder G J 2016 *J. Mater. Chem. A* **4** 1867–75
- [273] Bux S K, Zevalkink A, Janka O, Uhl D, Kauzlarich S, Snyder J G and Fleurial J-P 2014 *J. Mater. Chem. A* **2** 215–20
- [274] Kazem N, Zaikina J V, Ohno S, Snyder G J and Kauzlarich S M 2015 *Chem. Mater.* **27** 7508–19
- [275] Ohno S, Aydemir U, Amsler M, Pöhls J-H, Chanakian S, Zevalkink A, White M A, Bux S K, Wolverton C and Snyder G J 2017 *Adv. Funct. Mater.* **27** 1606361
- [276] Kazem N, Xie W, Ohno S, Zevalkink A, Miller G J, Snyder G J and Kauzlarich S M 2014 *Chem. Mater.* **26** 1393–403
- [277] Kazem N, Hurtado A, Sui F, Ohno S, Zevalkink A, Snyder J G and Kauzlarich S M 2015 *Chem. Mater.* **27** 4413–21
- [278] Zevalkink A, Swallow J, Ohno S, Aydemir U, Bux S and Snyder G J 2014 *Dalton Trans.* **43** 15872–8
- [279] Zevalkink A, Pomrehn G S, Johnson S, Swallow J, Gibbs Z M and Snyder G J 2012 *Chem. Mater.* **24** 2091–8
- [280] Johnson S I, Zevalkink A and Snyder G J 2013 *J. Mater. Chem. A* **1** 4244–9
- [281] Zevalkink A, Swallow J and Snyder G J 2013 *J. Chem. Soc., Dalton Trans.* **42** 9713–9
- [282] Chanakian S, Zevalkink A, Aydemir U, Gibbs Z M, Pomrehn G, Fleurial J-P, Bux S and Snyder G J 2015 *J. Mater. Chem. A* **3** 10289–95
- [283] Chanakian S, Aydemir U, Zevalkink A, Gibbs Z M, Fleurial J-P, Bux S and Jeffrey Snyder G 2015 *J. Mater. Chem. C* **3** 10518–24
- [284] Zevalkink A, Toberer E S, Zeier W G, Flage-Larsen E and Snyder G J 2011 *Energy Environ. Sci.* **4** 510–8
- [285] Zevalkink A, Pomrehn G, Takagiwa Y, Swallow J and Snyder G J 2013 *ChemSusChem* **6** 2316–21
- [286] Zevalkink A, Zeier W G, Pomrehn G, Schechtel E, Tremel W and Snyder G J 2012 *Energy Environ. Sci.* **5** 9121–8
- [287] Ortiz B R, Gorai P, Krishna L, Mow R, Lopez A, McKinney R, Stevanović V and Toberer E S 2017 *J. Mater. Chem. A* **5** 4036–46
- [288] Ortiz B R, Gorai P, Stevanović V and Toberer E S 2017 *Chem. Mater.* **29** 4523–34
- [289] He A, Bux S K, Hu Y, Uhl D, Li L, Donadio D and Kauzlarich S M 2019 *Chem. Mater.* **31** 8076–86
- [290] Toberer E S, May A F, Scanlon C J and Snyder G J 2009 *J. Appl. Phys.* **105** 063701
- [291] Wang J, Liu X-C, Xia S-Q and Tao X-T 2013 *J. Am. Chem. Soc.* **135** 11840–8
- [292] Li X, Zhu M, Wu Z, Guo J, Tao X-T and Xia S-Q 2017 *Chem. Mater.* **29** 3324–33
- [293] Zhenga Y, Liua C, Miao L, Li C, Huang R, Gao J, Wang X, Chen J, Zhoud Y and Nishibori E 2019 *Nano Energy* **59** 311–20
- [294] Zou T, Qin X, Zhang Y, Li X, Zeng Z, Li D, Zhang J, Xin H, Xie W and Weidenkaff A 2015 *Sci. Rep.* **5** 1–9
- [295] Tamaki H, Sato H K and Kanno T 2016 *Adv. Mater.* **28** 10182–7
- [296] Zhang J, Song L, Pedersen S H, Yin H, Hung L T and Iversen B B 2017 *Nat. Commun.* **8** 13901
- [297] Ohno S, Imasato K, Anand S, Tamaki H, Kang S D, Gorai P, Sato H K, Toberer E S, Kanno T and Snyder G J 2018 *Joule* **2** 141–54
- [298] Mao J, Wu Y, Song S, Zhu Q, Shuai J, Liu Z, Pei Y and Ren Z 2017 *ACS Energy Lett.* **2** 2245–50
- [299] Singh D J and Parker D 2013 *J. Appl. Phys.* **114** 143703
- [300] Peng W, Petretto G, Rignanese G, Hautier G and Zevalkink A 2018 *Joule* **19** 1879–93
- [301] Imasato K, Kang S D, Ohno S and Snyder G J 2018 *Mater. Horiz.* **5** 59–64
- [302] Shu R et al 2019 *Adv. Funct. Mater.* **29** 1807235
- [303] Imasato K, Kang S D and Snyder G J 2019 *Energy Environ. Sci.* **12** 965–71
- [304] Wang Y, Zhang X, Wang Y, Liu H and Zhang J 2019 *Phys. Status Solidi a* **216** 1800811
- [305] Tani J-I and Ishikawa H 2019 *Mater. Lett.* **262** 127056
- [306] Imasato K, Wood M, Kuo J J and Snyder G J 2018 *J. Mater. Chem. A* **6** 19941–6

- [307] Tani J-I and Ishikawa H 2020 *Physica B* **588** 412173
- [308] Shi X, Zhao T, Zhang X, Sun C, Chen Z, Lin S, Li W, Gu H and Pei Y 2019 *Adv. Mater.* **31** 1903387
- [309] Shi X, Sun C, Zhang X, Chen Z, Lin S, Li W and Pei Y 2019 *Chem. Mater.* **31** 8987–94
- [310] Song S W et al 2019 *Mater. Today Phys.* **8** 25–33
- [311] Kuo J J, Kang S D, Imasato K, Tamaki H, Ohno S, Kanno T and Snyder G J 2018 *Energy Environ. Sci.* **11** 429–34
- [312] Wang Y, Zhang X, Liu Y-Q, Zhang J-X J-X and Yue M 2020 *Chin. Phys. B* **29** 067201
- [313] Wood M, Kuo J J, Imasato K and Snyder G J 2019 *Adv. Mater.* **13** 1902337
- [314] Ozen M, Yahyaoglu M, Candolfi C, Veremchuk I, Kaiser F, Burkhardt U, Snyder G J, Grin Y and Aydemir U 2021 *J. Mater. Chem. A* **9** 1733–42
- [315] Wood M, Imasato K, Anand S, Yang J and Snyder G J 2020 *J. Mater. Chem. A* **8** 2033–8
- [316] Shang H, Liang Z, Xu C, Song S, Huang D, Gu H, Mao J, Ren Z and Ding F 2020 *Acta Mater.* **201** 572–9
- [317] Shuai J et al 2017 *Energy Environ. Sci.* **10** 799–807
- [318] Mao J, Wu Y, Song S, Shuai J, Liu Z, Pei Y and Ren Z 2017 *Mater. Today Phys.* **3** 1–6
- [319] Zhang J, Song L, Mamakhel A, Jørgensen M R V and Iversen B B 2017 *Chem. Mater.* **29** 5371–83
- [320] Zhang J, Song L, Borup K A, Jørgensen M R V and Iversen B B 2018 *Adv. Energy Mater.* **8** 1702776
- [321] Zhang J, Song L and Iversen B B 2020 *Chem. Eng. Sci.* **17** 955
- [322] Kihou K, Kunioka H, Nishiata H and Lee C H 2020 *J. Mater. Res. Technol.* **10** 438–44
- [323] Zhang J, Song L and Iversen B B 2020 *Adv. sci.* **7** 2002867
- [324] Gorai P, Ortiz B R, Toberer E S and stevanović V 2018 *J. Mater. Chem. A* **6** 13806–15
- [325] Gurunathan R, Hanus R and Snyder G J 2020 *Mater. Horiz.* **7** 1452–6
- [326] Zhang J and Iversen B B 2019 *J. Appl. Phys.* **126** 085104
- [327] Mao J, Zhu H, Ding Z, Liu Z, Gamage G A, Chen G and Ren Z 2019 *Science* **365** 495–8
- [328] Han Z, Gui Z, Zhu Y B, Qin P, Zhang B-P, Zhang W, Huang L and Liu W 2020 *Research* **2** 1672051
- [329] Shi X, Sun C, Bu Z, Zhang X, Wu Y, Lin S, Li W, Faghaninia A, Jain A and Pei Y 2019 *Adv. Sci.* **6** 1802286
- [330] Mao J, Chen G and Ren Z 2021 *Nat. Mater.* **20** 454–61
- [331] Wang H et al 2015 *J. Electron. Mater.* **44** 4482–91
- [332] Imasato K, Anand S, gurunathan R and Snyder G J 2021 *Dalton Trans.* **50** 9376–82
- [333] Kanno T, Tamaki H, Sato H K, Kang S D, Ohno S, Imasato K, Kuo J J, Snyder G J and Miyazaki Y 2018 *Appl. Phys. Lett.* **112** 033903
- [334] Chen X et al 2018 *Nano Energy* **52** 246–55
- [335] Kuo J J, Wood M, Slade T, Kanatzidis M G and Snyder G J 2020 *Energy Environ. Sci.* **13** 1250–8
- [336] Imasato K, Fu C, Pan Y, Wood M, Kuo J J, Felser C and Snyder G J 2020 *Adv. Mater.* **32** 1908218
- [337] Pan Y et al 2020 *Energy Environ. Sci.* **13** 1717–24
- [338] Slade T J, Grovogui J A, Kuo J J, Anand S, Bailey T P, Wood M, Uher C, Snyder G J, Dravid V P and Kanatzidis M G 2020 *Energy Environ. Sci.* **13** 1509–18
- [339] Liang Z, Xua C, Shang H, Zhu Q, Ding F, Mao J and Ren Z 2021 *Mater. Today Phys.* **19** 100413
- [340] Liu Z et al 2021 *Joule* **5** 1196–208
- [341] Li Y, Zhang S, Jia F, Zheng S, Shi X, Jiang D, Wang S, Lu G, Wu L and Chen Z G 2020 *Mater. Today Phys.* **15** 100269
- [342] Tani J-I, Takahashi M and Kido H 2010 *Physica B* **405** 4219–25
- [343] Chen X, Zhu J, Qin D, Qu N, Xue W, Wang Y, Zhang Q, Cai W, Guo F and Sui J 2021 *Sci. China Mater.* **64** 1761–9
- [344] Nolas G S 2014 *The Physics and Chemistry of Inorganic Clathrates* (Berlin: Springer)
- [345] Dolyniuk J-A, Owens-Baird B, Wang J, Zaikina J V and Kovnir K 2016 *Mater. Sci. Eng. R* **108** 1–46
- [346] Kauzlarich S M 1996 *Chemistry, Structure, and Bonding of Zintl Phases and Ions: Selected Topics and Recent Advances* (New York: Wiley)
- [347] Schäfer H, Eisenmann B and Müller W 1973 *Angew. Chem., Int. Ed. Engl.* **12** 694–712
- [348] Rowe D M 1995 *CRC Handbook of Thermoelectrics* 1st edn (Boca Raton, FL: CRC Press)
- [349] Lory P-F et al 2017 *Nat. Commun.* **8** 1–10
- [350] Euchner H, Pailhès S, Nguyen L T K, Assmus W, Ritter F, Haghighirad A, Grin Y, Paschen S and de Boissieu M 2012 *Phys. Rev. B* **86** 224303
- [351] Aydemir U, Candolfi C, Ormeci A, Baitinger M, Oeschler N, Steglich F and Grin Y 2014 *J. Phys.: Condens. Matter.* **26** 485801
- [352] Candolfi C, Aydemir U, Baitinger M, Oeschler N, Steglich F and Grin Y 2012 *J. Appl. Phys.* **111** 043706
- [353] Bohme B, Bobnar M, Ormeci A, Peters S, Schnelle W, Baitinger M and Grin Y 2016 *Z. Kristallogr. Cryst. Mater.* **232** 223–33
- [354] Feng X-J, Bobnar M, Lerch S, Biller H, Schmidt B M, Baitinger M, Strassner T, Grin Y and Böhme B 2021 *Chem. Eur. J.* **27** 12776
- [355] Zhuang H, Pei J, Cai B, Dong J, Hu H, Sun F, Pan Y, Snyder J and Li J 2021 *Adv. Funct. Mater.* **31** 2009681
- [356] German R M, Suri P and Park S J 2009 *J. Mater. Sci.* **44** 1–39
- [357] Gan Y, Wang G, Sun Z and Zhou J 2021 *npj Comput. Mater.* **7** 176
- [358] Chen W et al 2016 *J. Mater. Chem. C* **4** 4414
- [359] de Pablo J J et al 2019 *npj Comput. Mater.* **5** 4
- [360] Gorai P, Stevanović V and Toberer E S 2017 *Nat. Rev. Mater.* **2** 17053
- [361] Liu B, Ma H, Huo D, Liu H, Liu B and Jia X 2018 *Mater. Chem. Phys.* **205** 84–89
- [362] Sun B et al 2020 *J. Phys. Chem. C* **124** 9082–8
- [363] Sun B, Jia X, Huo D, Sun H, Zhang Y, Liu B, Liu H, Kong L, Liu B and Ma H 2016 *J. Alloys Compd.* **681** 374–8
- [364] Sun B, Jia X, Huo D, Sun H, Zhang Y, Liu B, Liu H, Kong L and Ma H 2016 *Mod. Phys. Lett. B* **30** 1650087
- [365] Troppenz M, Rigamonti S and Draxl C 2017 *Chem. Mater.* **29** 2414–24
- [366] Liu B, Jia X, Sun H, Sun B, Zhang Y, Liu H, Kong L, Huo D and Ma H 2016 *J. Solid State Chem.* **233** 363–7
- [367] Tsujii N, Roudebush J H, Zevalkink A, Cox-Uvarov C A, Snyder G J and Kauzlarich S M 2011 *J. Solid State Chem.* **184** 1293–303
- [368] Rajput K and Vitta S 2019 *ACS Appl. Energy Mater.* **2** 4255–63
- [369] Roudebush J H, Toberer E S, Hope H, Snyder G J and Kauzlarich S M 2011 *J. Solid State Chem.* **184** 1176–85
- [370] Condrón C L, Kauzlarich S M, Gascoin F and Snyder G J 2006 *Chem. Mater.* **18** 4939–45
- [371] Tomeš P, Himmelbauer T, Sidorenko A, Yan X, Prokofiev A and Paschen S 2017 *Acta Mater.* **129** 521–31
- [372] Aydemir U, Candolfi C, Ormeci A, Oztan Y, Baitinger M, Oeschler N, Steglich F and Grin Y 2011 *Phys. Rev. B* **84** 195137
- [373] Prokofiev A, Sidorenko A, Hradil K, Ikeda M, Svagera R, Waas M, Winkler H, Neumaier K and Paschen S 2013 *Nat. Mater.* **12** 1096–101
- [374] Dong Y, Ding X, Yan X, Zhang L, Tang Z, Chen W, Rogl P and Paschen S 2018 *Materials* **11** 946

- [375] Falmbigl M, Chen M X, Grytsiv A, Rogl P, Royanian E, Michor H, Bauer E, Podloucky R and Giester G 2012 *Dalton Trans.* **41** 8839–49
- [376] Aydemir U, Candolfi C, Ormeci A, Borrmann H, Burkhardt U, Oztan Y, Oeschler N, Baitinger M, Steglich F and Grin Y 2012 *Inorg. Chem.* **51** 4730–41
- [377] Sun B, Jia X, Huo D, Sun H, Zhang Y, Liu B, Liu H, Kong L and Ma H 2016 *J. Alloys Compd.* **658** 19–22
- [378] Sui F and Kauzlarich S M 2016 *Chem. Mater.* **28** 3099–107
- [379] Singh S K, Isoda Y and Imai M 2017 *Intermetallics* **82** 93–100
- [380] Anno H, Yamada H, Nakabayashi T, Hokazono M and Shirataki R 2012 *J. Solid State Chem.* **193** 94–104
- [381] Dong Y, Ding X, Yan X, Zhang L, Ju T, Liu C, Rogl P and Paschen S 2019 *Materials* **12** 27
- [382] Gao Y, Zhang X, Zhou Y and Hu M 2017 *J. Mater. Chem. C* **5** 10578–88
- [383] Kume T, Ohashi F and Nonomura S 2017 *Jpn. J. Appl. Phys.* **56** 05DA05
- [384] Yang J-Y, Cheng L and Hu M 2017 *Appl. Phys. Lett.* **111** 242101
- [385] Stefanoski S, Malliakas C D, Kanatzidis M G and Nolas G S 2012 *Inorg. Chem.* **51** 8686–92
- [386] Sui F, He H, Bobev S, Zhao J, Osterloh F E and Kauzlarich S M 2015 *Chem. Mater.* **27** 2812–20
- [387] Baran V, Senyshyn A, Karttunen A J, Fischer A, Scherer W, Raudaschl-Sieber G and Fässler T F 2014 *Chem. Eur. J.* **20** 15077–88
- [388] Wei K, Dong Y and Nolas G S 2016 *J. Solid State Chem.* **237** 81–85
- [389] Zhang H, Peng W, Mu G, Hu T, Huang F and Xie X 2017 *Chem. Eur. J.* **23** 9505–16
- [390] Anno H, Ueda T and Okamoto K 2017 *J. Electron. Mater.* **46** 1730–9
- [391] Aydemir U et al 2010 *Dalton Trans.* **39** 1078–88
- [392] Falmbigl M, Grytsiv A, Rogl P, Yan X, Royanian E and Bauer E 2013 *Dalton Trans.* **42** 2913–20
- [393] Zhang H, Borrmann H, Oeschler N, Candolfi C, Schnelle W, Schmidt M, Burkhardt U, Baitinger M, Zhao J and Grin Y 2011 *Inorg. Chem.* **50** 1250–7
- [394] Fu J, Su X, Yan Y, Liu W, Zhang Z, She X, Uher C and Tang X 2017 *J. Solid State Chem.* **253** 414–20
- [395] Xu J, Wu J, Shao H, Heguri S, Tanabe Y, Liu Y, Liu G, Jiang J, Jiang H and Tanigaki K 2015 *J. Mater. Chem. A* **3** 19100–6
- [396] Sato H K, Tamaki H and Kanno T 2020 *Appl. Phys. Lett.* **116** 253901
- [397] Wu C et al 2020 *Mod. Phys. Lett. B* **34** 2050357
- [398] Suekuni K, Avila M A, Umeo K, Fukuoka H, Yamanaka S, Nakagawa T and Takabatake T 2008 *Phys. Rev. B* **77** 235119
- [399] Yan X, Bauer E, Rogl P and Paschen S 2013 *Phys. Rev. B* **87** 115206
- [400] Liu B, Jia X, Huo D, Sun H, Zhang Y, Sun B, Liu H, Kong L and Ma H 2016 *J. Alloys Compd.* **666** 93–97
- [401] Yan X, Prokofiev A, Bauer E, Rogl P, Bernardi J and Paschen S 2017 *J. Alloys Compd.* **725** 783–91
- [402] Wu J, Xu J and Tanigaki K 2020 *Mater. Adv.* **1** 2953–63
- [403] Nguyen L T K et al 2010 *Dalton Trans.* **39** 1071–7
- [404] Hou Y-H and Chang L-S 2018 *J. Alloys Compd.* **736** 108–14
- [405] Liu B, Ma H, Huo D, Liu H, Liu B, Chen J and Jia X 2018 *J. Materiomics* **4** 68–74
- [406] Sun B, Jia X, Huo D, Sun H, Zhang Y, Liu B, Liu H, Kong L, Liu B and Ma H 2016 *J. Phys. Chem. C* **120** 10104–10
- [407] González-Romero R L and Antonelli A 2017 *Phys. Chem. Chem. Phys.* **19** 3010–8
- [408] Zhang Y, Brorsson J, Qiu R and Palmqvist A E 2020 *Adv. Electron. Mater.* **7** 2000782
- [409] Deng S-K, Tang X-F, Yang P-Z and Li M 2009 *J. Mater. Sci.* **44** 939–44
- [410] Deng S, Tang X and Zhang Q 2007 *J. Appl. Phys.* **102** 043702
- [411] Cederkrantz D, Nygren M and Palmqvist A E C 2010 *J. Appl. Phys.* **108** 113711
- [412] Deng S, Tang X, Li P and Zhang Q 2008 *J. Appl. Phys.* **103** 073503
- [413] Leszczynski J, Kozłowski A and Wojciechowski K T 2012 *J. Solid State Chem.* **193** 114–21
- [414] Toberer E S, Christensen M, Iversen B B and Snyder G J 2008 *Phys. Rev. B* **77** 075203
- [415] Wang L-H and Chang L-S 2017 *J. Alloys Compd.* **722** 644–50
- [416] Tang X, Li P, Deng S and Zhang Q 2008 *J. Appl. Phys.* **104** 013706
- [417] Shi X, Yang J, Bai S, Yang J, Wang H, Chi M, Salvador J R, Zhang W, Chen L and Wong-Ng W 2010 *Adv. Funct. Mater.* **20** 755–63
- [418] Chen C, Zhang L, Dong J and Xu B 2017 *J. Electron. Mater.* **46** 2860–6
- [419] Yan Y, Tang X, Li P and Zhang Q 2009 *J. Electron. Mater.* **38** 1278–81
- [420] Martin J, Nolas G S, Wang H and Yang J 2007 *J. Appl. Phys.* **102** 103719
- [421] Takeshita R, Kishimoto K, Asada H and Akai K 2021 *J. Solid State Chem.* **294** 121911
- [422] Perez C J, Bates V J and Kauzlarich S M 2018 *Inorg. Chem.* **58** 1442–50
- [423] Zhang H, Baitinger M, Fanga L, Schnelle W, Borrmann H, Burkhardt U, Ormeci A, Zhao J T and Grin Y 2013 *Inorg. Chem.* **52** 9720–6
- [424] Kishimoto K, Utsunomiya S, Akai K, Asada H and Koyanagi T 2017 *J. Alloys Compd.* **695** 1610–6
- [425] Deng S, Liu H, Li D, Wang J, Cheng F, Shen L and Deng S 2017 *J. Electron. Mater.* **46** 2662–7
- [426] Shen L, Li D, Deng S, Tang Y, Chen Z, Liu Z, Yang P and Deng S 2018 *Cryst. Res. Technol.* **53** 1700150
- [427] Saiga Y, Suekuni K, Deng S K, Yamamoto T, Kono Y, Ohya N and Takabatake T 2010 *J. Alloys Compd.* **507** 1–5
- [428] Saiga Y, Du B, Deng S K, Kajisa K and Takabatake T 2012 *J. Alloys Compd.* **537** 303–7
- [429] Chen Y, Du B, Kajisa K and Takabatake T 2014 *J. Electron. Mater.* **43** 1916–21
- [430] Deng S-K, Li D-C, Shen L-X, Hao R-T and Takabatake T 2012 *Chin. Phys. B* **21** 017401
- [431] Cheng F, Shen L, Li D, Liu H, Wang J and Deng S 2016 *J. Mater. Eng. Perform.* **25** 2180–4
- [432] Du B, Saiga Y, Kajisa K and Takabatake T 2012 *J. Appl. Phys.* **111** 3–8
- [433] Deng S-P, Cheng F, Li D-C, Tang Y, Chen Z, Shen L-X, Liu H-X, Yang P-Z and Deng S-K 2017 *Chin. Phys. Lett.* **34** 047401
- [434] Deng S K, Saiga Y, Suekuni K and Takabatake T 2011 *J. Electron. Mater.* **40** 1124–8
- [435] Kawasaki K, Kishimoto K, Asada H and Akai K 2020 *J. Solid State Chem.* **290** 121540
- [436] Kishimoto K and Akai K 2019 *Jpn. J. Appl. Phys.* **58** 101002
- [437] Wei K, Zeng X, Tritt T M, Khabibullin A R, Woods L M and Nolas G S 2016 *Materials* **9** 732
- [438] Koda S, Kishimoto K, Akai K, Asada H and Koyanagi T 2014 *J. Appl. Phys.* **116** 023710
- [439] Utsunomiya S, Kishimoto K, Koda S, Akai K, Fujita R, Asada H and Koyanagi T 2017 *J. Alloys Compd.* **693** 1039–44
- [440] Mano S, Onimaru T, Yamanaka S and Takabatake T 2011 *Phys. Rev. B* **84** 214101
- [441] Kaltzoglou A, Fässler T, Christensen M, Johnsen S, Iversen B, Presniakov I, Sobolev A and Shevelkov A 2008 *J. Mater. Chem.* **18** 5630–7
- [442] Nolas G S, Cohn J L, Dyck J S, Uher C and Yang J 2002 *Phys. Rev. B* **65** 165201–6

- [443] Christensen M, Johnsen S and Iversen B B 2010 *Dalton Trans.* **39** 978–92
- [444] Tanaka T, Onimaru T, Suekuni K, Mano S, Fukuoka H, Yamanaka S and Takabatake T 2010 *Phys. Rev. B* **81** 1–6
- [445] Hayashi M, Kishimoto K, Akai K, Asada H, Kishio K and Koyanagi T 2012 *J. Phys. D: Appl. Phys.* **45** 455308
- [446] Baran V, Fischer A, Scherer W and Fässler T F 2013 *Z. Anorg. Allg. Chem.* **639** 2125–8
- [447] Kanno M, Yamada T, Ikeda T, Nagai H and Yamane H 2017 *Chem. Mater.* **29** 859–66
- [448] Wang J, He Y, Mordvinova N E, Lebedev O I and Kovnir K 2018 *Chem* **4** 1465–75
- [449] Wang J, Lebedev O I, Lee K, Dolyniuk J-A, Klavins P, Bux S and Kovnir K 2017 *Chem. Sci.* **8** 8030–8
- [450] Dolyniuk J, Whitfield P S, Lee K, Lebedev O I and Kovnir K 2017 *Chem. Sci.* **8** 3650–9
- [451] Dolyniuk J-A, Wang J, Marple M A T, Sen S, Cheng Y, Ramirez-Cuesta A J and Kovnir K 2018 *Chem. Mater.* **30** 3419–28
- [452] Wang J, Voyles J, Grzybowski S and Kovnir K 2020 *J. Appl. Phys.* **127** 055104
- [453] Fulmer J, Lebedev O I, Roddatis V V, Kaseman D C, Sen S, Dolyniuk J-A, Lee K, Olenev A V and Kovnir K 2013 *J. Am. Chem. Soc.* **135** 12313–23
- [454] Plokhikh I V, Khan N, Tsirlin A A, Kuznetsov A N, Charkin D O, Shevelkov A V and Pfitzner A 2020 *Inorg. Chem. Front.* **7** 1115–26
- [455] Wang J et al 2020 *Chem. Mater.* **32** 7932–40
- [456] Dolyniuk J-A, Wang J, Lee K and Kovnir K 2015 *Chem. Mater.* **27** 4476–84
- [457] Dolyniuk J-A, Zaikina J V, Kaseman D C, Sen S and Kovnir K 2017 *Angew. Chem., Int. Ed.* **56** 2418–22
- [458] Cox T, Gvozdzetskiy V, Bertolami M, Lee S, Shipley K, Lebedev O I and Zaikina J V 2021 *Angew. Chem.* **133** 419–27
- [459] Owens-Baird B, Wang J, Wang S G, Chen Y-S, Lee S, Donadio D and Kovnir K 2020 *J. Am. Chem. Soc.* **142** 2031–41
- [460] Owens-Baird B, Yox P, Lee S, Carroll X B, Wang S G, Chen Y-S, Lebedev O I and Kovnir K 2020 *Chem. Sci.* **11** 10255–64
- [461] Abramchuk N S, Carrillo-Cabrera W, Veremchuk I, Oeschler N, Olenev A V, Prots Y, Burkhardt U, Dikarev E V, Grin J and Shevelkov A V 2012 *Inorg. Chem.* **51** 11396–405
- [462] Kishimoto K, Akai K, Muraoka N, Koyanagi T and Matsuura M 2006 *Appl. Phys. Lett.* **89** 6–9
- [463] Zaikina J V, Mori T, Kovnir K, Teschner D, Senyshyn A, Schwarz U, Grin Y and Shevelkov A V 2010 *Chem. Eur. J.* **16** 12582–9
- [464] Kishimoto K, Arimura S and Koyanagi T 2006 *Appl. Phys. Lett.* **88** 10–222115
- [465] Häussermann U, Boström M, Viklund P, Rapp Ö and Björnängen T 2002 *J. Solid State Chem.* **165** 94
- [466] Wagner F R, Cardoso-Gil R, Boucher B, Wagner-Reetz M, Sichelschmidt J, Gille P, Baenitz M and Grin Y 2018 *Inorg. Chem.* **57** 12908
- [467] Grin Y 2019 *J. Solid State Chem.* **274** 329–36
- [468] Wagner M, Cardoso-Gil R, Oeschler N, Rosner H and Grin Y 2011 *J. Mater. Res.* **26** 1886
- [469] Takagiwa Y, Kitahara K, Matsubayashi Y and Kimura K 2012 *J. Appl. Phys.* **111** 123707
- [470] Kasinathan D, Wagner M, Koepernik K, Cardoso-Gil R, Grin Y and Rosner H 2012 *Phys. Rev. B* **85** 035207
- [471] Amagai Y, Yamamoto A, Iida T and Takanashi Y 2004 *J. Appl. Phys.* **96** 5644
- [472] Haldolaarachchige N, Phelan W A, Xiong Y M, Jin R, Chan J Y, Stadler S and Young D P 2013 *J. Appl. Phys.* **113** 083709
- [473] Haldolaarachchige N, Karki A B, Phelan W A, Xiong Y M, Jin R, Chan J Y, Stadler S and Young D P 2011 *J. Appl. Phys.* **109** 103712
- [474] Likhonov M S, Verchenko V Y, Gippius A A, Zhurenko S V, Tkachev A V, Wei Z, Dikarev E V, Kuznetsov A N and Shevelkov A V 2020 *Inorg. Chem.* **59** 12748
- [475] Likhonov M S and Shevelkov A V 2020 *Russ. Chem. Bull., Int. Ed.* **69** 2231
- [476] Boucher B, Al Rahal Al Orabi R, Fontaine B, Grin Y, Gautier R and Halet J-F 2017 *Inorg. Chem.* **56** 4229–37
- [477] Imai Y and Watanabe A 2006 *Intermetallics* **14** 722
- [478] Tsujii N et al 2008 *J. Phys. Soc. Japan* **77** 024705
- [479] Arita M, Shimada K, Utsumi Y, Morimoto O, Sato H, Namatame H, Taniguchi M, Hadano Y and Takabatake T 2011 *Phys. Rev. B* **83** 245116
- [480] Lue C, Lai W and Kuo Y-K 2005 *J. Alloys Compd.* **392** 72
- [481] Hadano Y, Narazu S, Avila M A, Onimaru T and Takabatake T 2009 *J. Phys. Soc. Japan* **78** 013702
- [482] Schnurr S, Wiedwald U, Ziemann P, Verchenko V Y and Shevelkov A V 2013 *Beilstein J. Nanotechnol.* **4** 461
- [483] Wagner-Reetz M, Kasinathan D, Schnelle W, Cardoso-Gil R, Rosner H, Grin Y and Gille P 2014 *Phys. Rev. B* **90** 195206
- [484] Wagner-Reetz M, Cardoso-Gil R and Grin Y 2014 *J. Electron. Mater.* **43** 1857
- [485] Ramachandran B, Syu K Z, Kuo Y K, Gippius A A, Shevelkov A V, Verchenko V Y and Lue C S 2014 *J. Alloys Compd.* **608** 229
- [486] Takagiwa Y, Matsuura Y and Kimura K 2014 *J. Electron. Mater.* **43** 2206
- [487] Gamza M, Tomczak J M, Brown C, Puri A, Kotliar G and Aronson M C 2014 *Phys. Rev. B* **89** 195102
- [488] Ponnambalam V and Morelli D T 2015 *J. Appl. Phys.* **118** 245101
- [489] Likhonov M S, Verchenko V Y, Bykov M A, Tsirlin A A, Gippius A A, Berthebaud D, Maignan A and Shevelkov A V 2016 *J. Solid State Chem.* **236** 166
- [490] Mondal D, Kamal C, Banik S, Bhakar A, Kak A, Das G, Reddy V R, Chakrabarti A and Ganguli T 2016 *J. Appl. Phys.* **120** 1565102
- [491] Likhonov M S, Zhupanov V O, Verchenko V Y, Gippius A A, Zhurenko S V, Tkachev A V, Fazlizhanova D I, Berthebaud D and Shevelkov A V 2019 *J. Alloys Compd.* **804** 331
- [492] Wagner-Reetz M, Cardoso-Gil R, Prots Y, Schnelle W and Grin Y 2014 *Solid State Sci.* **32** 56
- [493] Bogdanov D, Winzer K, Nekrasov I A and Pruschke T 2007 *J. Phys.: Condens. Matter.* **19** 232202
- [494] Wagner-Reetz M, Cardoso-Gil R, Schmidt M and Grin Y 2014 *J. Solid State Chem.* **215** 260
- [495] Cheikh D, Lee K, Peng W, Zevalkink A, Fleurial J-P and Bux S 2019 *Materials* **12** 734
- [496] Samsonov G V, Veinstein E I and Paderno Y B 1962 *Fiz. Met. Metalloved.* **13** 744
- [497] Kong H 2008 *PhD Dissertation* University of Michigan
- [498] Giannò K, Sologubenko A V, Chernikov M A, Ott H R, Fisher I R and Canfield P C 2000 *Mater. Sci. Eng. A* **294–296** 715–8
- [499] Takagiwa Y, Kimura K, Sawama K, Hiroto T, Nishio K and Tamura R 2015 *J. Alloys Compd.* **652** 139–44
- [500] Pope A L, Tritt T M, Gagnon R and Strom-Olsen J 2001 *Appl. Phys. Lett.* **79** 2345–7
- [501] Lallement R and Veysie J J 1968 *Monocarbures Et Mononitrides Des Terres Rares* (Berlin: Springer) vol 3
- [502] Samsonov G V, Neshpor V S and Paderno Y B 1963 *Redk. Elem.* **22** 22
- [503] Zhuze V P, Golubkov A V, Goncharov E V and Sergeeva V M 1964 *Fiz. Tverd. Tela* **6** 257
- [504] Danielson L R, Raag V and Wood C 1986 *Proc. 6th Int. Conf. Thermoelectric Energy Conversion* vol 60 p 66
- [505] Danielson L R, Matsuda S and Raag V 1984 *Proc. 5th Int. Conf. Thermoelectric Energy Conversion* vol 60 p 41
- [506] Katsuyama S, Tokuno S, Ito M, Majima K and Nagai H 2001 *J. Alloys Compd.* **320** 126–32
- [507] Samsonov G V and Paderno Y B 1959 *Akad. Nauk Ukr. SSR, Inst. Met.* **11** 102
- [508] Obolonchik V A and Lashkarev G V 1964 *Nauk* **71** 166

- [509] Mularz W L and Wolnik S J 1964 *Rare Earth Res.* **60** 473
- [510] Yarembash E I, Vigileva E S, Eliseev A A and Kalitin V I 1964 *Izv. Akad. Nauk SSSR Ser. Fiz.* **28** 1306
- [511] Wood C 1984 *Energy Convers. Manage.* **24** 331–43
- [512] Jonker G H 1969 *Philips Res. Rep.* **24** 1–14
- [513] Falkowski M, Krychowski D and Strydom A M 2016 *J. Appl. Phys.* **120** 195106
- [514] Fess K, Kaefer W, Thurner C, Friemelt K, Kloc C and Bucher E 1998 *J. Appl. Phys.* **83** 2568–73
- [515] Raag V and Garvey L P 1979 *Proc. Intersociety Energy Conversion Engineering Conf.* vol 2 pp 1811–5
- [516] Rhyee J-S, Cho E, Lee K H, Lee S M, Kim H-S and Kwon Y S 2010 *J. Appl. Phys.* **107** 053705
- [517] Samsonov G V, Paderno Y B and Vainstein E I 1964 *Izv. Sib. Otd. Akad. Nauk SSSR* **503** 78
- [518] Reid F J, Matson L K, Miller J F and Himes R C 1964 *J. Electrochem. Soc.* **111** 943
- [519] Carter F L, Miller R C and Ryan F M 1961 *Adv. Energy Convers.* **1** 165–75
- [520] Bando Y, Suemitsu T, Takagi K, Tokushima H, Echizen Y, Katoh K, Umeo K, Maeda Y and Takabatake T 2000 *J. Alloys Compd.* **313** 1–6
- [521] Gottwick U, Held R, Sparr G, Steglich F, Vey K, Assmus W, Rietchel H, Stewart G R and Giorgi A L 1987 *Anomalous Rare Earths Actinides* (Amsterdam: North Holland) vol 64 pp 341–3
- [522] Thomas P, Cook B, Stokes D, Krueger G and Venkatasubramanian R 2012 *Energy Harvesting and Storage: Materials, Devices, and Applications III* vol 8377 (SPIE) pp 83770H–7
- [523] Marchenko V I and Samsonov G V 1963 Properties of rare earth monosulfides *Z. Neorg. Chim.* **8** 2053
- [524] Hashimoto H, Kusunose T and Sekino T 2009 *J. Alloys Compd.* **484** 246–8
- [525] Gomez S J, Cheikh D, Vo T, von Allmen P, Lee K, Wood M, Snyder G J, Dunn B S, Fleurial J-P and Bux S K 2019 *Chem. Mater.* **31** 38
- [526] Yamanaka S, Kobayashi H and Kurosaki K 2003 *J. Alloys Compd.* **349** 321–4
- [527] Henkie Z and Cichorek T 1993 *J. Alloys Compd.* **196** L3–L5
- [528] Sauerschnig P, Vaney J B, Michiue Y, Kouzu K, Yamasaki T, Okada S, Yoshikawa A, Shishido T and Mori T 2020 *J. Eur. Ceram. Soc.* **40** 3585–91
- [529] Alleno E, Lamquembe N, Cardoso-Gil R, Ikeda M, Widder F, Rouleau O, Godart C, Grin Y and Paschen S 2014 *Phys. Status Solidi a* **211** 1293–300
- [530] Kazem N, Cooley J, Burks E C, Liu K and Kauzlarich S M 2016 *Inorg. Chem.* **55** 12230–7
- [531] Paderno Y B, Yupko V L, Rud B M, Kvas O F and Makarenko G H 1967 *Izv. Akad. Nauk SSSR Neorg. Mater.* **3** 395
- [532] Dudnikov V A, Orlov Y S, Kazak N V, Fedorov A S, Solov'yov L A, Vereshchagin S N, Burkov A T, Novikov S V, Gavrilkin S Y and Ovchinnikov S G 2018 *Ceram. Int.* **44** 10299–305
- [533] Gebresenbut G H, Tamura R, Eklöf D and Gómez C P 2013 *J. Phys.: Condens. Matter.* **25** 135402
- [534] Gofryk K, Kaczorowski D, Leithe-Jasper A and Grin Y 2005 *Int. Conf. on Thermoelectrics, ICT, Proc.* vol 2005 pp 383–6
- [535] Han C, Li Z and Dou S 2014 *Chin. Sci. Bull.* **59** 2073–91
- [536] Zhu H et al 2015 *J. Mater. Chem. C* **3** 10554
- [537] He T, Calvarese T G, Chen J Z, Rosenfeld H D, Small R J, Krajewski J J and Subramanian M A 2005 *Int. Conf. Thermoelectrics ICT, Proc.* vol 2005 pp 437–42
- [538] Muro Y, Sasakawa T, Suemitsu T, Takabatake T, Tamura R and Takeuchi S 2002 *Jpn. J. Appl. Phys.* **41** 3787–90
- [539] Paderno Y B, Yupko V L, Rud B M and Makarenko G H 1966 *Izv. Akad. Nauk SSSR Neorg. Mater.* **504** 626
- [540] Kuo Y K, Lai J R, Huang C H, Ku W C, Lue C S and Lin S T 2004 *J. Appl. Phys.* **95** 1900–5
- [541] Kunz Wille E, Grewal N, Bux S and Kauzlarich S 2019 *Materials* **12** 731
- [542] Brown S R, Toberer E S, Ikeda T, Cox C A, Gascoin F, Kauzlarich S M and Snyder G J 2008 *Chem. Mater.* **20** 3412–9
- [543] Chamoire A, Gascoin F, Estournès C, Caillat T and Tédénac J-C 2010 *J. Electron. Mater.* **39** 1579–82
- [544] Chamoire A, Gascoin F, Estournès C, Caillat T and Tédénac J-C 2010 *Dalton Trans.* **39** 1118–23
- [545] Jazbec S, Vrtnik S, Jagličić Z, Kashimoto S, Ivkov J, Popčević P, Smontara A, Kim H J, Kim J G and Dolinšek J 2014 *J. Alloys Compd.* **586** 343–8
- [546] Paschen S, Bentien A, Budnyk S, Strydom A M, Grin Y and Steglich F 2006 *Int. Conf. on Thermoelectrics, ICT, Proc.* pp 168–71
- [547] Makarenko G H, Pustovoi L T, Yupko V L and Rud B M 1965 *Izv. Akad. Nauk SSSR Neorg. Mater.* **5010** 1787
- [548] Vickery R C and Muir H M 1961 *Adv. Energy Convers.* **1** 179–86
- [549] Samsonov G V, Paderno Y B and Rud B M 1968 *Rev. Int. Hautes Temp. Refract.* **2** 105–10
- [550] Tritt T M 1998 Thermoelectric materials 1998—the next generation materials for small-scale refrigeration and power generation applications *MRS Symp. Boston, USA 1998, MRS Proc.* vol 545, ed T M Tritt, M G Kanatzidis, G D Mahan and H B Lyon Jr
- [551] Lee J A and Meaden G T 1963 *Proc. Int. Conf. Low Temp. Phys.* **3** 262
- [552] Vedernikov M V 1969 *Adv. Phys.* **18** 337–70
- [553] Trzebiatowski W, Henkie Z and Misiuk A 1972 *Proc., Int. Conf. Physics of Semiconductors, 11th* vol 2 pp 1287–93
- [554] Price C E and Warren I H 1965 *J. Electrochem. Soc.* **112** 510
- [555] Henkie Z and Markowski P 1978 *J. Phys. Chem. Solids* **39** 39–43
- [556] Gnida D, Henkie Z, Wojakowski A and Cichorek T 2006 *Physica B* **378–380** 974–5
- [557] Santini P, Lémanski R and Erdős P 1999 *Adv. Phys.* **48** 537
- [558] Wawryk R, Wojakowski A, Marucha C, Cichorek T and Henkie Z 2001 *Acta Phys. Pol. B* **32** 3487–91
- [559] Wawryk R, Wojakowski A, Pietraszko A and Henkie Z 2005 *Solid State Commun.* **133** 295–300
- [560] Sportouch S and Kanatzidis M G 2001 *J. Solid State Chem.* **162** 158–67
- [561] Pillai C G S and Raj P 2000 *J. Nucl. Mater.* **277** 116–9
- [562] Costa P and Lallement R 1964 *J. Phys. Chem. Solids* **25** 559–65
- [563] Auskern A B and Aronson S 1967 *J. Appl. Phys.* **38** 3508–14
- [564] Auskern A B and Aronson S 1967 *J. Phys. Chem. Solids* **28** 1069–71
- [565] Tetenbaum M 1964 *J. Appl. Phys.* **35** 2468–72
- [566] Aliev F G, Andreev A V, Brandt N B, Kovacic V and Moshchalkov V V 1987 *Fiz. Tverd. Tela* **29** 2181
- [567] Auskern A B and Aronson S 1968 *J. Chem. Phys.* **49** 253–7
- [568] Warren I H and Price C E 1964 *Adv. Energy Convers.* **4** 169–78
- [569] Warren I 1963 *Can. Min. Met. Bull.* **56** 147
- [570] Shlyk L and Troc R 1999 *Physica B* **262** 90
- [571] Shrestha K, Yao T, Lian J, Antonio D, Sessim M, Tonks M R and Gofryk K 2019 *J. Appl. Phys.* **126** 125116

- [572] Yamamoto E, Honma T, Haga Y, Inada Y, Aoki D, Suzuki N, Settai R, Sugawara H, Sato H and Onuki Y 1999 *J. Phys. Soc. Japan* **68** 972–5
- [573] Warren J H and Price C E 1964 *Can. Metall. Q.* **3** 183–96
- [574] Didchenko R and Gortsema F P 1963 *Inorg. Chem.* **2** 1079–80
- [575] Henkie Z and Wiśniewski P 1995 *Acta Phys. Pol. A* **88** 1103–12
- [576] Nishi Y, Arita Y, Terao K, Matsui T and Nagasaki T 2001 *J. Nucl. Mater.* **294** 209–11
- [577] Nishi Y, Arita Y, Matsui T, Iwasaki K and Nagasaki T 2005 *J. Phys. Chem. Solids* **66** 652–4
- [578] Nozariasbmarz A et al 2017 *Jpn. J. Appl. Phys.* **56** 1–27
- [579] Arita Y, Terao K, Mitsuda S, Nishi Y, Matsui T and Nagasaki T 2001 *J. Nucl. Mater.* **294** 206–8
- [580] Sechovsky V and Havela L 1998 *Handb. Magn. Mater.* **11** 1–289
- [581] Wawryk R, Henkie Z, Cichorek T, Geibel C and Steglich F 2002 *Phys. Status Solidi b* **232** 7–9
- [582] Svanidze E, Veremchuk I, Leithe-Jasper A and Grin Y 2019 *Appl. Phys. Lett.* **115** 1–8
- [583] Berthebaud D, Lopes E B, Tougait O, Gonçalves A P, Potel M and Noël H 2007 *J. Alloys Compd.* **442** 348–50
- [584] Brixner L H, Hills B and To A 1963 *Patent* 3208947
- [585] Kurosaki K, Matsuda T, Uno M, Kobayashi S and Yamanaka S 2001 *J. Alloys Compd.* **319** 271–75
- [586] Arita Y, Ogawa T, Kobayashi H, Iwasaki K, Matsui T and Nagasaki T 2005 *J. Nucl. Mater.* **344** 79–83
- [587] Strydom A M, du Plessis P D V and Gridin V V 1995 *Solid State Commun.* **95** 867–71
- [588] Paschen S, Baenitz M, Tran V H, Rabis A, Steglich F, Carrillo-Cabrera W, Grin Y, Strydom A M and du Plessis P D V 2002 *J. Phys. Chem. Solids* **63** 1183–8
- [589] Tran V H and Bauer E 2006 *J. Phys.: Condens. Matter.* **18** 4677
- [590] Ortega L H, Blamer B, Stern K M, Vollmer J and McDevitt S M 2020 *J. Nucl. Mater.* **531** 151982
- [591] Arajs S and Colvin R V 1964 *J. Less-Common Met.* **7** 54–66
- [592] Hu Y, Long Z, Liu K and Liu J 2016 *Mater. Lett.* **178** 124–7
- [593] Whiting C E, Vasquez E S and Barklay C D 2018 *IEEE Aerospace Conf. Proc. (March 2018)* (IEEE) pp 1–9
- [594] Matson L K, Moody J W and Himes R C 1963 *J. Inorg. Nucl. Chem.* **25** 795–800
- [595] Stewart G R 1984 *Rev. Mod. Phys.* **56** 755–87
- [596] Ohta S, Nomura T, Ohta H, Hirano M, Hosono H and Koumoto K 2005 *Appl. Phys. Lett.* **87** 97–100
- [597] Kikuchi A, Okinaka N and Akiyama T 2010 *Scr. Mater.* **63** 407–10
- [598] Wang H C C et al 2010 *Mater. Res. Bull.* **45** 809–12
- [599] Dehkordi A M, Bhattacharya S, He J, Alshareef H N and Tritt T M 2014 *Appl. Phys. Lett.* **104** 193902
- [600] Lin Y, Norman C, Srivastava D, Azough F, Wang L, Robbins M, Simpson K, Freer R and Kinloch I A 2015 *ACS Appl. Mater. Interfaces* **7** 15898–908
- [601] Srivastava D, Norman C, Azough F, Schäfer M C, Guilmeau E, Kepaptsoglou D, Ramasse Q M, Nicotra G and Freer R 2016 *Phys. Chem. Chem. Phys.* **18** 26475–86
- [602] Wang J et al 2017 *Nano Energy* **35** 387–95
- [603] Srivastava D, Norman C, Azough F, Schäfer M C, Guilmeau E and Freer R 2018 *J. Alloys Compd.* **731** 723–30
- [604] Ekren D, Azough F, Gholinia A, Day S J, Hernandez-Maldonado D, Kepaptsoglou D M, Ramasse Q M and Freer R 2018 *J. Mater. Chem. A* **6** 24928–39
- [605] Srivastava D, Norman C, Azough F, Ekren D, Chen K, Reece M J, Kinloch I A and Freer R 2019 *J. Mater. Chem. A* **7** 24602–13
- [606] Rahman J U, Van D N, Nam W H, Shin W H, Lee K H, Seo W S, Kim M H and Lee S 2019 *Sci. Rep.* **9** 1–12
- [607] Okhay O, Zlotnik S, Xie W, Orłinski K, Hortiguera Gallo M J, Otero-Irurueta G, Fernandes A J S, Pawlak D A, Weidenkaff A and Tkach A 2019 *Carbon* **143** 215–22
- [608] Qin M, Lou Z, Zhang P, Shi Z, Xu J, Chen Y and Gao F 2020 *ACS Appl. Mater. Interfaces* **12** 53899–909
- [609] Dey P, Jana S S, Anjum F, Bhattacharya T and Maiti T 2020 *Appl. Mater. Today* **21** 100869
- [610] Huang J, Yan P, Liu Y, Xing J, Gu H, Fan Y and Jiang W 2020 *ACS Appl. Mater. Interfaces* **12** 52721–30
- [611] Hirata S, Ohtaki M and Watanabe K 2020 *Ceram. Int.* **46** 25964–9
- [612] Cao J, Ekren D, Peng Y, Azough F, Kinloch I A and Freer R 2021 *ACS Appl. Mater. Interfaces* **13** 11879–90
- [613] Bocher L, Aguirre M H, Logvinovich D, Shkabko A, Robert R, Trottmann M and Weidenkaff A 2008 *Inorg. Chem.* **47** 8077–85
- [614] Li C, Chen Q and Yan Y 2018 *Materials* **11** 1–13
- [615] Song X, Paredes Navia S A, Liang L, Boyle C, Romo-De-La-Cruz C-O, Jackson B, Hinerman A, Wilt M, Prucz J and Chen Y 2018 *ACS Appl. Mater. Interfaces* **10** 39018–24
- [616] Liu K K, Liu Z Y, Zhang F P, Zhang J X, Yang X Y, Zhang J W, Shi J L, Ren G, He T W and Duan J J 2019 *J. Alloys Compd.* **808** 151476
- [617] Xiao X et al 2017 *Phys. Chem. Chem. Phys.* **19** 13469–80
- [618] Tsubota T, Ohtaki M, Eguchi K and Arai H 1997 *J. Mater. Chem.* **7** 85–90
- [619] Kaga H, Asahi R and Tani T 2004 *Jpn. J. Appl. Phys.* **43** 3540–3
- [620] Ohtaki M, Araki K and Yamamoto K 2009 *J. Electron. Mater.* **38** 1234–8
- [621] Guilmeau E, Diaz-Chao P, Lebedev O I, Rečnik A, Schäfer M C, Delorme F, Giovannelli F, Košir M and Bernik S 2017 *Compd. Inorg. Chem.* **56** 480–7
- [622] Guo J, Qin P, Ma Z, Yang Q-L, Feng J and Ge Z-H 2019 *Scr. Mater.* **164** 71–75
- [623] Li S, Zhou Y, Cui L, Ge Z and Feng J 2019 *J. Electron. Mater.* **48** 7068–75
- [624] Li Y, Liu J, Wang Z, Zhou Y C, Wang C, Li J, Zhu Y, Li M and Mei L 2015 *Phys. Scr.* **90** 025801
- [625] Li Y, Liu J, Zhang Y, Zhou Y, Li J, Su W, Zhai J, Wang H and Wang C 2016 *Ceram. Int.* **42** 1128–32
- [626] Azough F et al 2016 *J. Electron. Mater.* **45** 1894–9
- [627] Jiang D, Ekren D, Azough F, Day S J, Chen K, Mahajan A, Kepaptsoglou D M, Ramasse Q M, Reece M J and Freer R 2019 *J. Appl. Phys.* **126** 125115
- [628] Mikami M and Ozaki K 2012 *J. Phys.: Conf. Ser.* **379** 012006
- [629] Liu C, Miao L, Zhou J, Huang R, Fisher C A J and Tanemura S 2013 *J. Phys. Chem. C* **117** 11487–97
- [630] Liu H, Ma H, Wang C, Wang F, Liu B, Chen J, Ji G, Zhang Y and Jia X 2018 *Ceram. Int.* **44** 19859–65
- [631] Fan Y, Feng X, Zhou W, Murakami S, Kikuchi K, Nomura N, Wang L, Jiang W and Kawasaki A 2018 *J. Eur. Ceram. Soc.* **38** 507–13
- [632] Ji G et al 2020 *Ceram. Int.* **46** 6878–81
- [633] Liu H Q, Song Y, Zhang S N, Zhao X B and Wang F P 2009 *J. Phys. Chem. Solids* **70** 600–3
- [634] Zhang F P, Lu Q M and Zhang J X 2009 *J. Alloys Compd.* **484** 550–4

- [635] Nong N V, Liu C-J and Ohtaki M 2011 *J. Alloys Compd.* **509** 977–81
- [636] Delorme F, Fernandez Martin C, Marudhachalam P, Ovono Ovono D and Guzman G 2011 *J. Alloys Compd.* **509** 2311–5
- [637] Prasoetsopha N, Pinitsoontorn S, Kamwanna T, Amornkitbamrung V, Kurosaki K, Ohishi Y, Muta H and Yamanaka S 2014 *J. Alloys Compd.* **588** 199–205
- [638] Butt S, Xu W, He W Q, Tan Q, Ren G K, Lin Y and Nan C-W 2014 *J. Mater. Chem. A* **2** 19479–87
- [639] Liu H Q, Zhao X B, Liu F, Song Y, Sun Q, Zhu T J and Wang F P 2008 *J. Mater. Sci.* **43** 6933–7
- [640] Lu Q M, Zhang J X, Zhang Q Y, Liu Y Q and Liu D M 2006 *Proc. Int. Conf. Thermoelectrics IEEE* pp 66–69
- [641] Boyle C, Carvillo P, Chen Y, Barbero E J, McIntyre D and Song X 2016 *J. Eur. Ceram. Soc.* **36** 601–7
- [642] Liu Y, Lin Y, Jiang L, Nan C-W and Shen Z 2008 *J. Electroceramics* **21** 748–51
- [643] Saini S, Yaddanapudi H S, Tian K, Yin Y, Maggini D and Tiwari A 2017 *Mater. Sci. Rep.* **7** 44621
- [644] Zhang L et al 2020 *J. Adv. Ceram.* **9** 769–81
- [645] Nag A and Shubha V 2014 *J. Electron. Mater.* **43** 962–77
- [646] Funahashi R, Matsubara I and Sodeoka S 2000 *Appl. Phys. Lett.* **76** 2385–7
- [647] Wang S, Bai Z, Wang H, Lü Q, Wang J and Fu G 2013 *J. Alloys Compd.* **554** 254–7
- [648] Shen J J, Liu X X, Zhu T J and Zhao X B 2009 *J. Mater. Sci.* **44** 1889–93
- [649] Combe E, Funahashi R, Azough F and Freer R 2014 *J. Mater. Res.* **29** 1376–82
- [650] Combe E, Funahashi R, Barbier T, Azough F and Freer R 2016 *J. Mater. Res.* **31** 1296–305
- [651] Migiakis P, Androulakis J and Giapintzakis J 2003 *J. Appl. Phys.* **94** 7616
- [652] Kurosaki K, Muta H, Uno M and Yamanaka S 2001 *J. Alloys Compd.* **315** 234–6
- [653] Seetawan T, Amornkitbamrung V, Burinprakhon T, Maensiri S, Tongbai P, Kurosaki K, Muta H, Uno M and Yamanaka S 2006 *J. Alloys Compd.* **416** 291–5
- [654] Wang L, Wang M and Zhao D 2009 *J. Alloys Compd.* **471** 519–23
- [655] Ito M and Furumoto D 2008 *J. Alloys Compd.* **450** 517–20
- [656] Pei Y, He J, Li J, Li F, Liu Q, Pan W, Barreateau C, Berardan D, Dragoe N and Zhao L 2013 *NPG Asia Mater.* **5** e47
- [657] Li J, Sui J, Pei Y, Barreateau C, Berardan D, Dragoe N, Cai W, He J and Zhao L-D *Energy Environ. Sci.* **5** 8543–7 2012
- [658] Lan J-L, Liu Y-C, Zhan B, Lin Y-H, Zhang B, Yuan X, Zhang W, Xu W and Nan C-W 2013 *Adv. Mater.* **25** 5086–90
- [659] Li J, Sui J, Pei Y, Meng X, Berardan D, Dragoe N, Cai W and Zhao L-D 2014 *J. Mater. Chem. A* **2** 4903–6
- [660] Yang D, Su X, Yan Y, Hu T, Xie H, He J, Uher C, Kanatzidis M G and Tang X 2016 *Chem. Mater.* **28** 4628–40
- [661] Ren G-K, Wang S-Y, Zhu Y-C, Ventura K J, Tan X, Xu W, Lin Y-H, Yang J and Nan C-W 2017 *Energy Environ. Sci.* **10** 1590–9
- [662] Wen Q et al 2017 *J. Mater. Chem. A* **5** 13392–9
- [663] Sun Y, Zhang C, Cao C, Fu J and Peng L 2017 *Ceram. Int.* **43** 17186–93
- [664] Pan L et al 2018 *J. Mater. Chem. A* **6** 13340–9
- [665] Feng B, Li G, Pan Z, Hu X, Liu P, He Z, Li Y and Fan X 2018 *J. Solid State Chem.* **266** 297–303
- [666] Feng B, Li G, Hu X, Liu P, Li R, Zhang Y, Li Y, He Z and Fan X 2020 *J. Mater. Sci.: Mater. Electron.* **31** 4915–23
- [667] Feng B, Li G, Hu X, Liu P, Li R, Zhang Y, Li Y, He Z and Fan X 2020 *J. Alloys Compd.* **818** 152899
- [668] He T, Li X, Tang J, Lou X, Zuo X, Zheng Y, Zhang D and Tang G 2020 *J. Alloys Compd.* **831** 154755
- [669] Urata S, Funahashi R, Mihara T, Kosuga A, Sodeoka S and Tanaka T 2007 *Int. J. Appl. Ceram. Technol.* **4** 535–40
- [670] Wang Y, Sui Y, Fan H, Wang X, Su Y, Su W and Liu X 2009 *Chem. Mater.* **21** 4653–60
- [671] Dylla M T, Kuo J J, Witting I and Snyder G J 2019 *Adv. Mater. Interfaces* **6** 1900222
- [672] Zhao L-D, He J, Berardan D, Lin Y, Li J-F, Nan C-W and Dragoe N 2014 *Energy Environ. Sci.* **7** 2900–24
- [673] Li F, Wei T-R, Kang F and Li J-F 2013 *J. Mater. Chem. A* **1** 11942–9
- [674] Prashun G, Vladan S and Eric S T 2017 *Nat. Rev. Mater.* **2** 1–16
- [675] Gaultois M W, Oliynyk A O, Mar A, Sparks T D, Mulholland G J and Meredig B 2016 *APL Mater.* **4** 053213
- [676] Gibson Q D et al 2021 *Science* **373** 1017–22
- [677] Lin Y, Dylla M T, Kuo J J, Male J P, Kinloch I A, Freer R and Snyder G J 2020 *Adv. Funct. Mater.* **30** 1910079
- [678] Powell A V and Vaquero P 2017 *Thermoelectric Materials and Devices* ed I Nandhakumar, N M White and S Beeby (Cambridge: Royal Society of Chemistry) ch 2 pp 27–59
- [679] Zhao L-D, Lo S-H, Zhang Y, Sun H, Tan G, Uher C, Wolverton C, Dravid V P and Kanatzidis M G 2014 *Nature* **508** 373–7
- [680] Yang H Q, Wang X Y, Wu H, Zhang B, Xie D D, Chen Y J, Lu X, Han X D, Miao L and Zhou X Y 2019 *J. Mater. Chem. C* **7** 3359
- [681] Huang Z et al 2017 *Angew. Chem., Int. Ed.* **56** 14113–8
- [682] Roychowdhury S, Ghosh T, Arora R, Waghmare U V and Biswas K 2018 *Angew. Chem., Int. Ed.* **57** 15167–71
- [683] Hicks L D and Dresselhaus M S 1993 *Phys. Rev. B* **47** 16631–4
- [684] Biswas K, Zhao L-D and Kanatzidis M G 2012 *Adv. Energy Mater.* **2** 634–8
- [685] Guilmeau E, Bréard Y and Maignan A 2011 *Appl. Phys. Lett.* **99** 052107
- [686] Barbier T, Lebedev O I, Roddatis V, Bréard Y, Maignan A and Guilmeau E 2015 *Dalton Trans.* **44** 7887–95
- [687] Guélou G, Vaquero P, Prado-Gonjal J, Barbier T, Hébert S, Guilmeau E, Kockelmann W and Powell A V 2016 *J. Mater. Chem. C* **4** 1871–80
- [688] Labégorre J-B et al 2019 *Adv. Funct. Mater.* **29** 1904112
- [689] Zhao J, Hao S, Islam S M, Chen H, Tan G, Ma S, Wolverton C and Kanatzidis M G 2019 *Chem. Mater.* **31** 3430–9
- [690] He Y, Day T, Zhang T, Liu H, Shi X, Chen L and Snyder G J 2014 *Adv. Mater.* **26** 3974–8
- [691] Liu H, Shi X, Xu F, Zhang L, Zhang W, Chen L, Li Q, Uher C, Day T and Snyder G J 2012 *Nat. Mater.* **11** 422–5
- [692] Long S O J, Powell A V, Vaquero P and Hull S 2018 *Chem. Mater.* **30** 456–64
- [693] Bourgès C et al 2018 *J. Am. Chem. Soc.* **140** 2186–95
- [694] Zhou C et al 2021 *Nat. Mater.* **20** 1378–84
- [695] Jiang B et al 2020 *Energy Environ. Sci.* **13** 579–91
- [696] Perez-Taborda J A, Caballero-Calero O, Vera-Londono L, Briones F and Martin-Gonzalez M 2018 *Adv. Energy Mater.* **8** 1702024
- [697] Dennler G, Chmielowski R, Jacob S, Capet F, Roussel P, Zastrow S, Nielsch K, Opahle I and Madsen G K H 2014 *Adv. Energy Mater.* **4** 1301581
- [698] Qiu P et al 2019 *Joule* **3** 1538–48
- [699] Nunna R, Gascoin F and Guilmeau E 2015 *J. Alloys Compd.* **634** 32–36
- [700] Guélou G et al 2020 *ACS Appl. Energy Mater.* **3** 4180–5
- [701] Wang L, Ying P, Deng Y, Zhou H, Dub Z and Cui J 2014 *RSC Adv.* **4** 33897–906
- [702] Yana Y, Wua H, Wang G, Lua X and Zhou X 2018 *Energy Storage Mater.* **13** 127–33

- [703] Li Y, Liu G, Cao T, Liu L, Li J, Chen K, Li L, Han Y and Zhou M 2016 *Adv. Funct. Mater.* **26** 6025–32
- [704] He W et al 2019 *Science* **365** 1418–24
- [705] Sorokin G P, Papshev Y M and Oush P T 1966 *Sov. Phys. Solid State* **7** 1810–1
- [706] Zhao K, Qiu P, Song Q, Blichfeld A B, Eikeland E Z, Ren D, Ge B, Iversen B B, Shi X and Chen L 2017 *Mater. Today Phys.* **1** 14–23
- [707] Zhao K et al 2017 *Chem. Mater.* **29** 6367–77
- [708] Wang H, Pei Y, LaLonde A D and Snyder G J 2013 *Thermoelectric Nanomaterials* ed T Koumoto and K Mori (Berlin: Springer) pp 3–32
- [709] Madelung O and Rössler U 1998 *Non-Tetrahedrally Bonded Elements and Binary Compounds I* ed M Schulz (Berlin: Springer) pp 1–8
- [710] Huang Z, Zhang Y, Wu H, Pennycook S J and Zhao L D 2019 *ACS Appl. Energy Mater.* **2** 8236–43
- [711] Wang H, Pei Y, LaLonde A D and Snyder G J 2011 *Adv. Mater.* **23** 1366–70
- [712] Lee Y, Lo S-H, Androulakis J, Wu C-I, Zhao L-D, Chung D-Y, Hogan T P, Dravid V P and Kanatzidis M G 2013 *J. Am. Chem. Soc.* **135** 5152–60
- [713] Luo Z-Z et al 2019 *J. Am. Chem. Soc.* **141** 6403–12
- [714] Zhou B, Li S, Li W, Li J, Zhang X, Lin S, Chen Z and Pei Y 2017 *ACS Appl. Mater. Interfaces* **9** 34033–41
- [715] Wang C, Chen Y, Jiang J, Zhang R, Niu Y, Zhou T, Xia J, Tian H, Hu J and Yang P 2017 *RSC Adv.* **7** 16795–800
- [716] Hu X, He W, Wang D, Yuan B, Huang Z and Zhao L-D 2019 *Scr. Mater.* **170** 99–105
- [717] Tan Q, Zhao L-D, Li J-F, Wu C-F, Wei T-R, Xing Z-B and Kanatzidis M G 2014 *J. Mater. Chem. A* **4** 1610–18
- [718] Li C, Wu H, Zhang B, Zhu H, Fan Y, Lu X, Sun X, Zhang X, Wang G and Zhou X 2020 *ACS Appl. Mater. Interfaces* **12** 8446–55
- [719] Wang H, Ma H, Duan B, Geng H, Zhou L, Li J, Zhang X, Yang H, Li G and Zhai P 2021 *ACS Appl. Energy Mater.* **4** 1610–8
- [720] Mi W, Qiu P, Zhang T, Lv Y, Shi X and Chen L 2014 *Appl. Phys. Lett.* **104** 133903
- [721] Ferhat M and Nagao J 2000 *J. Appl. Phys.* **88** 813
- [722] Sun G, Qin X, Li D, Zhang J, Ren B, Zou T, Xin H, Paschen S B and Yan X 2015 *J. Alloys Compd.* **639** 9–14
- [723] Liu R, Tan X, Ren G, Liu Y, Zhou Z, Liu C, Lin Y and Nan C 2017 *Crystals* **7** 257
- [724] Sassi S, Candolfi C, Delaizir G, Migot S, Ghanbaja J, Gendarme C, Dauscher A, Malaman B and Lenoir B 2018 *Inorg. Chem.* **57** 422–34
- [725] Yan M, Tan X, Huang Z, Liu G, Jiang P and Bao X 2018 *J. Mater. Chem. A* **6** 8215–20
- [726] Zhang X, Shen J, Lin S, Li J, Chen Z, Li W and Pei Y 2016 *J. Materiomics* **2** 331–7
- [727] Xie H, Su X, Zheng G, Zhu T, Yin K, Yan Y, Uher C, Kanatzidis M G and Tang X 2017 *Adv. Energy Mater.* **7** 1601299
- [728] Fujisawa M, Suga S, Mizokawa T, Fujimori A and Sato K 1994 *Phys. Rev. B* **49** 7155–64
- [729] Ge B, Hu J, Shi Z, Wang H, Xia H and Qiao G 2019 *Nanoscale* **11** 17340
- [730] Lu Y, Chen S, Wu W, Du Z, Chao Y and Cui J 2017 *Sci. Rep.* **7** 40224
- [731] Yang N, Chen C, Pan L, Zhao Y and Wang Y 2020 *J. Alloys Compd.* **847** 156410
- [732] Wang K, Qin P, Ge Z and Feng J 2018 *Scr. Mater.* **149** 88–92
- [733] Kumar V P, Barbier T, Lemoine P, Raveau B, Nassif V and Guilmeau E 2017 *Dalton Trans.* **46** 2174
- [734] Wiltout A M, Freymeyer N J, Machani T, Rossi D P and Plass K E 2011 *J. Mater. Chem.* **21** 19286–92
- [735] Moghaddam A O, Shokuhfar A, Guardia P, Zhang Y and Cabot A 2019 *J. Alloys Compd.* **773** 1064–74
- [736] Cheng Y, Yang J, Jiang Q, Fu L, Xiao Y, Luo Y, Zhang D, Zhang M and White M A 2015 *Am. Ceram. Soc.* **98** 3975–80
- [737] Chetty R, d. S. P K, Rogl G, Rogl P, Bauer E, Michor H, Suwas S, Puchegger S, Giester G and Mallik R C 2015 *Phys. Chem. Chem. Phys.* **17** 1716
- [738] Embden J, Latham K, Duffy N W and Tachibana Y 2013 *J. Am. Chem. Soc.* **135** 11562–71
- [739] Lu X, Morelli D T, Xia Y and Ozolins V 2015 *Chem. Mater.* **27** 408–13
- [740] Shen Y, Li C, Huang R, Tian R, Ye Y, Pan L, Koumoto K, Zhang R, Wan C and Wang Y 2016 *Sci. Rep.* **6** 32501
- [741] Zhang Z, Zhao H, Wang Y, Hu X, Lyu Y, Cheng C, Pan L and Lu C 2019 *J. Alloys Compd.* **780** 618–25
- [742] Zhao H et al 2017 *J. Mater. Chem. A* **5** 23267–75
- [743] Marcano G, Rincón C, de Chalbaud L M, Bracho D B and Pérez G S 2001 *J. Appl. Phys.* **90** 1847–53
- [744] Shi X, Xi L, Fan J, Zhang W and Chen L 2010 *Chem. Mater.* **22** 6029–31
- [745] Cheng X, Li Z, You Y, Zhu T, Yan Y, Su X and Tang X 2019 *ACS Appl. Mater. Interfaces* **11** 24212–20
- [746] Cho J Y, Shi X, Salvador J R, Meisner G P, Yang J, Wang H, Wereszczak A A, Zhou X and Uher C 2011 *Phys. Rev. B* **84** 085207
- [747] Goto Y, Sakai Y, Kamihara Y and Matoba M 2015 *J. Phys. Soc. Japan* **84** 044706
- [748] Chen K, Du B, Bonini N, Weber C, Yan H and Reece M J 2016 *J. Phys. Chem. C* **120** 27135–40
- [749] Skoug E J, Cain J D and Morelli D T 2011 *Appl. Phys. Lett.* **98** 261911
- [750] Chetty R, Dadda J, de Boor J, Müller E and Mallik R C 2015 *Intermetallics* **57** 156–62
- [751] Liu M-L, Chen I-W, Huang F-Q and Chen L-D 2009 *Adv. Mater.* **21** 3808–12
- [752] Bourges C, Al Orabi R A R and Miyazaki Y 2020 *J. Alloys Compd.* **826** 154240
- [753] Xiao C, Li K, Zhang J, Tong W, Liu Y, Li Z, Huang P, Pan B, Su H and Xie Y 2014 *Mater. Horiz.* **1** 81
- [754] Zhang D, Yang J, Jiang Q, Zhou Z, Li X, Xin J, Basit A, Ren Y and He X 2017 *Nano Energy* **36** 156–65
- [755] Song Q, Qiu P, Hao F, Zhao K, Zhang T, Ren D, Shi X and Chen L 2016 *Adv. Electron. Mater.* **2** 1600312
- [756] Song Q et al 2018 *Mater. Today Phys.* **7** 45–53
- [757] Song Q, Qiu P, Zhao K, Deng T, Shi X and Chen L 2020 *ACS Appl. Energy Mater.* **3** 2137–46
- [758] Song Q, Qiu P, Chen H, Zhao K, Ren D, Shi X and Chen L 2018 *ACS Appl. Mater. Interfaces* **10** 10123–31
- [759] Heinrich C P, Day T W, Zeier W G, Snyder G J and Tremel W 2014 *J. Am. Chem. Soc.* **136** 442–8
- [760] Zeier W G, LaLonde A, Gibbs Z M, Heinrich C P, Panthöfer M, Snyder G J and Tremel W 2012 *J. Am. Chem. Soc.* **134** 7147–54
- [761] Nagaoka A, Masuda T, Yasui S, Taniyama T and Nose Y 2018 *Appl. Phys. Express* **11** 051203
- [762] Jiang Q, Yan H, Lin Y, Shen Y, Yang J and Reece M J 2020 *J. Mater. Chem. A* **8** 10909
- [763] Nagaoka A, Masuda T, Yasui S, Taniyama T and Nose Y 2018 *Jpn. J. Appl. Phys.* **57** 101201
- [764] Liu M-L, Huang F-Q, Chen L-D and Chen I-W 2009 *Appl. Phys. Lett.* **94** 202103
- [765] Shi X Y, Huang F Q, Liu M L and Chen L D 2009 *Appl. Phys. Lett.* **94** 122103
- [766] Suekuni K, Kim F S, Nishiate H, Ohta M, Tanaka H I and Takabatake T 2014 *Appl. Phys. Lett.* **105** 132107
- [767] Bouyrie Y, Ohorodniichuk V, Sassi S, Masschelein P, Dauscher A, Candolfi C and Lenoir B 2017 *J. Electron. Mater.* **46** 2684–90
- [768] Bouyrie Y, Ohta M, Suekuni K, Jood P and Takabatake T J 2018 *J. Alloys Compd.* **735** 1838–45
- [769] Bouyrie Y, Ohta M, Suekuni K, Kikuchi Y, Jood P, Yamamoto A and Takabatake T 2017 *J. Mater. Chem. C* **5** 4174–84
- [770] Bouyrie Y, Chetty R, Suekuni K, Saitou N, Jood P, Yoshizawa N, Takabatake T and Ohta M 2020 *J. Mater. Chem. C* **8** 6442–9

- [771] Kikuchi Y, Bouyrie Y, Ohta M, Suekuni K, Aihara M and Takabatake T 2016 *J. Mater. Chem. A* **4** 15207–14
- [772] Kim F S, Suekuni K, Nishiata H, Ohta M, Tanaka H I and Takabatake T 2016 *J. Appl. Phys.* **119** 175105
- [773] Bourges C, Gilmas M, Lemoine P, Mordvinova N E, Lebedev O I, Hug E, Nassif V, Malaman B, Daou R and Guilmeau E 2016 *J. Mater. Chem. C* **4** 7455–63
- [774] Kumar V P, Mitra S, Guélou G, Supka A R, Lemoine P, Raveau B, Al Orabi R A R, Fornari M, Suekuni K and Guilmeau E 2020 *Appl. Phys. Lett.* **117** 173902
- [775] Kumar V P, Guélou G, Lemoine P, Raveau B, Supka A R, Al Orabi R A R, Fornari M, Suekuni K and Guilmeau E 2019 *Angew. Chem., Int. Ed.* **58** 15455–63
- [776] Beaumale M, Barbier T, Bréard Y, Guelou G, Powell A V, Vaqueiro P and Guilmeau E 2014 *Acta Mater.* **78** 86–92
- [777] Corps J, Vaqueiro P, Aziz A, Grau-Crespo R, Kockelmann W, Jumas J and Powell A V 2015 *Chem. Mater.* **27** 3946–56
- [778] Mangels P, Vaqueiro P, Jumas J-C, da Silva I, Smith R I and Powell A V 2017 *J. Solid State Chem.* **251** 204–10
- [779] Mangels P, Vaqueiro P and Powell A V 2020 *ACS Appl. Energy Mater.* **3** 2168–74
- [780] Ohta M, Chung D Y, Kuniib M and Kanatzidis M G 2014 *J. Mater. Chem. A* **2** 20048–58
- [781] Zhao J, Islam S M, Hao S, Tan G, Su X, Chen H, Lin W, Li R, Wolverson C and Kanatzidis M G 2017 *Chem. Mater.* **29** 8494–503
- [782] Hwang J-Y, Ahn J Y, Lee K H and Kim S W 2017 *J. Alloys Compd.* **704** 282–8
- [783] Cronin B V 1995 Chapter 23 *CRC Handbook of Thermoelectrics* ed M Rowe (Boca Raton, FL: CRC Press) pp 277–85
- [784] Nicolaou M C 1976 *Proc. 1st Int. Congress on Thermoelectric Energy Conversion* ed K Rao (Arlington, TX: University of Texas) p 59
- [785] Kajikawa T, Shida K, Shiraiishi K, Ito T, Omori M and Hirai T 1998 *Proc. 17th Int. Conf. on Thermoelectrics* pp 362–9
- [786] Marchuck N D, Zaitsev V K, Fedorov M I and Kaliazin A E 1989 *Proc. 8th Int. Conf. Thermoelectric Energy Conversion* ed H Scherrer and S Scherrer (Nancy: Institute National Polytechnique de Lorraine) p 210
- [787] Noda Y, Kon H, Furukawa Y, Otsuka N, Nishida I A and Masumoto K 1992 *Mater. Trans.* **33** 845
- [788] Goyal G K, Mukherjee S, Mallik R C, Vitta S, Samajdar I and Dasgupta T 2019 *ACS Appl. Energy Mater.* **2** 2129–37
- [789] Gao P, Berkun I, Schmidt R D, Luzenski M F, Lu X, Bordon Sarac B, Case E D and Hogan T P 2014 *J. Electron. Mater.* **43** 1790–803
- [790] Ghodke S, Yamamoto A, Hu H-C, Nishino S, Matsunaga T, Byeon D, Ikuta H and Takeuchi T 2019 *ACS Appl. Mater. Interfaces* **11** 31169–75
- [791] Gao Z et al 2019 *J. Mater. Chem. A* **7** 3384
- [792] de Boor J, Saparamadu U, Mao J, Dahal K, Müller E and Ren Z F 2016 *Acta Mater.* **120** 273–80
- [793] Liu L, Oda H, Onda T, Yodoshi N, Wada T and Chen Z-C 2020 *Mater. Chem. Phys.* **249** 122990
- [794] le Tonquesse S, Dorcet V, Joanny L, Demange V, Prestipino C, Guo Q, Berthebaud D, Mori T and Pasturel M 2020 *J. Alloys Compd.* **816** 152577
- [795] Park S-B, Lee I-J and Kim I-H 2018 *Korean J. Met. Mater.* **56** 693–8
- [796] Teknetzi A, Tarani E, Symeou E, Karfaridis D, Stathokostopoulos D, Pavlidou E, Kyratsi T, Hatzikraniotis E, Chrissafis K and Vourlias G 2021 *Ceram. Int.* **47** 243–51
- [797] Pichon P-Y et al 2020 *J. Alloys Compd.* **832** 154602
- [798] Wang Q, Song S, Yang X, Liu Z, Ma Y, San X, Wang J, Zhang D, Wang S-F and Li Z 2021 *J. Materiomics* **7** 377–87
- [799] Chen X, Girard S N, Meng F, Lara-Curzio E, Jin S, Goodenough J B, Zhou J and Shi L 2014 *Adv. Energy Mater.* **4** 1400452
- [800] Vives S, Navone C, Gaudin E and Gorsse S 2017 *J. Mater. Sci.* **52** 12826–33
- [801] Ponnambalam V, Morelli D T, Bhattacharya S and Tritt T M 2013 *J. Alloys Compd.* **580** 598–603
- [802] Luo W, Li H, Yan Y, Lin Z, Tang X, Zhang Q and Uher C 2011 *Intermetallics* **19** 404–8
- [803] Muthiah S, Singh R C, Pathak B D and Dhar A 2016 *Scr. Mater.* **119** 60–64
- [804] Li Z, Dong J-F, Sun F-H, Hirono S and Li J-F 2017 *Chem. Mater.* **29** 7378–89
- [805] Muthiah S, Singh R C, Pathak B D, Avasthi P K, Kumar R, Kumar A, Srivastava A K and Dhar A 2018 *Nanoscale* **10** 1970
- [806] Ioannou M, Polymeris G S, Hatzikraniotis E, Paraskevopoulos K M and Kyratsi T 2014 *J. Phys. Chem. Solids* **75** 984–91
- [807] Berthebaud D and Gascoin F 2013 *J. Solid State Chem.* **202** 61–64
- [808] Zhang Q, He J, Zhao X B, Zhang S N, Zhu T J, Yin H and Tritt T M 2008 *J. Phys. D: Appl. Phys.* **41** 185103
- [809] Du Z, Zhu T, Chen Y, He J, Gao H, Jiang G, Tritt T M and Zhao X B 2012 *J. Mater. Chem.* **22** 6838–44
- [810] Gao H, Zhu T, Liu X, Chena L and Zhao X B 2011 *J. Mater. Chem.* **21** 5933–7
- [811] Liu W, Zhang Q, Tang X, Li H and Sharp J 2011 *J. Electron. Mater.* **40** 1062–6
- [812] Mars K, Ihou-Mouko H, Pont G, Tobola J and Scherrer H 2009 *J. Electron. Mater.* **38** 1360–4
- [813] Zhang Q, He J, Zhu T J, Zhang S N, Zhao X B and Tritt T M 2008 *Appl. Phys. Lett.* **93** 102109
- [814] Zhu T-J, Cao Y, Zhang Q and Zhao X-B 2010 *J. Electron. Mater.* **39** 1990–5
- [815] zhang X, Liu H, Lu Q, Zhang J and Zhang F 2013 *Appl. Phys. Lett.* **103** 063901
- [816] Polymeris G S, Vlachos N, Symeou E and Kyratsi T 2018 *Phys. Status Solidi a* **215** 1800136
- [817] Liu W, Tang X, Li H, Sharp J, Zhou X and Uher C 2011 *Chem. Mater.* **23** 5256–63
- [818] Dasgupta T, Stiewe C, de Boor J and Müller E 2014 *Phys. Status Solidi a* **211** 1250–4
- [819] Macario L R, Cheng X, Ramirez D, Mori T and Kleinke H 2018 *ACS Appl. Mater. Interfaces* **10** 40585–91
- [820] Zheng L, Zhang X, Liu H, Li S, Zhou Z, Lu Q, Zhang J and Zhang F 2016 *J. Alloys Compd.* **671** 452–7
- [821] Khan A U, Vlachos N, Hatzikraniotis E, Polymeris G S, Lioutas C B, Stefanaki E C, Paraskevopoulos K M, Giapintzakis I and Kyratsi T 2014 *Acta Mater.* **77** 43–53
- [822] Gao P, Davis J D, Poltavets V V and Hogan T P 2016 *J. Mater. Chem. C* **4** 929
- [823] Macario L R, Shi Y, Jafarzadeh P, Zou T, Kycia J B and Kleinke H 2019 *ACS Appl. Mater. Interfaces* **11** 45629–35
- [824] Yin K, Su X, Yan Y, You Y, Zhang Q, Uher C, Kanatzidis M G and Tang X 2016 *Chem. Mater.* **28** 5538–48
- [825] Khan A U, Vlachos N and Kyratsi T 2013 *Scr. Mater.* **69** 606–9
- [826] Liu W, Zhang Q, Yin K, Chi H, Zhou X, Tang X and Uher C 2013 *J. Solid State Chem.* **203** 333–9
- [827] Farahi N, Prabhudev S, Botton G A, Salvador J R and Kleinke H 2016 *ACS Appl. Mater. Interfaces* **8** 34431–7
- [828] Bernard-Granger G, Navone C, Leforestier J, Boidot M, Romanjek K, Carrete J and Simon J 2015 *Acta Mater.* **96** 437–51
- [829] Liu W, Tang X, Li H, Yin K, Sharp J, Zhou X and Uher C 2012 *J. Mater. Chem.* **22** 13653
- [830] Zhang Q, Zheng Y, Su X, Yin K, Tang X and Uher C 2015 *Scr. Mater.* **96** 1–4
- [831] Liu W, Tan X, Yin K, Liu H, Tang X, Shi J, Zhang Q and Uher C 2012 *Phys. Rev. Lett.* **108** 166601
- [832] Liu W, Chi H, Sun H, Zhang Q, Yin K, Tang X, Zhang Q and Uher C 2014 *Phys. Chem. Chem. Phys.* **16** 6893
- [833] Vlachos N et al 2017 *J. Alloys Compd.* **714** 502–13
- [834] Yin K, Zhang Q, Zheng Y, Su X, Tang X and Uher C 2015 *J. Mater. Chem. C* **3** 10381
- [835] Yin K, Su X, Yan Y, Uher C and Tang X 2016 *RSC Adv.* **6** 16824

- [836] Luo W, Yang M, Chen F, Shen Q, Jiang H and Zhang L 2010 *Mater. Trans.* **51** 288–91
- [837] Jiang G, He J, Zhu T J, Fu C, Liu X, Hu L and Zhao X B 2014 *Adv. Funct. Mater.* **24** 3776–81
- [838] Zhang L, Xiao P, Shi L, Henkelman G, Goodenough J B and Zhou J 2015 *J. Appl. Phys.* **117** 155103
- [839] Liu W, Tang X and Sharp J 2010 *J. Phys. D: Appl. Phys.* **43** 085406
- [840] Tazebay A S, Yi S, Lee J, Kim H, Bahk J-H, Kim S L, Park S-D, Lee H S, Shakouri A and Yu C 2016 *ACS Appl. Mater. Interfaces* **8** 7003–12
- [841] Liu X, Zhu T, Wang H, Hu L, Xie H, Jiang G, Snyder G J and Zhao X B 2013 *Adv. Energy Mater.* **3** 1238–44
- [842] Kim G, Lee H, Kim J, Roh J, Lyo I, Kim B-W, Lee K H and Lee W 2017 *Scr. Mater.* **128** 53–56
- [843] Søndergaard M, Christensen M, Borup K A, Yin H and Iversen B B 2012 *Acta Mater.* **60** 5745–51
- [844] de Boor J, Gupta S, Kolb H, Dasgupta T and Müller E 2015 *J. Mater. Chem. C* **3** 10467–75
- [845] Tani J-I and Kido H 2005 *Physica B* **364** 218–24
- [846] Choi S-M, Kim K-H, Kim I-H, Kim S-U and Seo W-S 2011 *Curr. Appl. Phys.* **11** S388–91
- [847] You S-W and Kim I-H 2011 *Curr. Appl. Phys.* **11** S392–5
- [848] Bux S K, Yeung M T, Toberer E S, Snyder G J, Kaner R B and Fleurial J-P 2011 *J. Mater. Chem.* **21** 12259–66
- [849] Zhang Q, Yin H, Zhao X B, He J, Ji X H, Zhu T J and Tritt T M 2008 *Phys. Status Solidi a* **205** 1657–61
- [850] Satyala N T, Krasinski J S and Vashaee D 2012 *IEEE Conf. Proc.*
- [851] Ponnambalam V and Morelli D T 2019 *Mater. Res. Express* **6** 025507
- [852] Li Z, Dong J-F, Sun F-H, Asfandiyar Pan A, Pan Y, Wang S-F, Wang Q, Zhang D, Zhao L and Li J-F 2018 *Adv. Sci.* **5** 1800626
- [853] Zhou A J, Zhu T J, Zhao X B, Yang S H, Dasgupta T, Stiewe C, Hassdorf R and Mueller E 2010 *J. Electron. Mater.* **39** 2002–7
- [854] Kim G, Kim H-S, Lee H S, Kim J, Lee K H, Roh J W and Lee W 2020 *Nano Energy* **72** 104698
- [855] Truong D Y-N, Kleinke H and Gascoin F 2015 *Intermetallics* **66** 127–32
- [856] Mori T and Priya S 2018 *MRS Bull.* **43** 176–80
- [857] Petsagkourakis I, Tybrandt K, Crispin X, Ohkubo I, Satoh N and Mori T 2018 *Sci. Technol. Adv. Mater.* **19** 836–62
- [858] Soleimani Z, Zoras S, Ceranic B, Shahzad S and Cui Y 2020 *Sustain. Energy Technol. Assess.* **37** 100604
- [859] Nandihalli N, Liu C J and Mori T 2020 *Nano Energy* **78** 105186
- [860] Bell L E 2008 *Science* **321** 1457–61
- [861] Mori T 2016 *JOM* **68** 2673–9
- [862] Koumoto K, Wang Y, Zhang R, Kosuga A and Funahashi R 2010 *Annu. Rev. Mater. Res.* **40** 363–94
- [863] Ohtaki M, Tsubota T, Eguchi K and Arai H 1996 *J. Appl. Phys.* **79** 1816–8
- [864] Virtudazo R V R, Srinivasan B, Guo Q, Wu R, Takei T, Shimasaki Y, Wada H, Kuroda K, Bernik S and Mori T 2020 *Inorg. Chem. Front.* **7** 4118–32
- [865] Tani J and Kido H 2008 *Intermetallics* **16** 418–23
- [866] Ning H, Mastrorillo G D, Grasso S, Du B, Mori T, Hu C, Xu Y, Simpson K, Maizza G and Reece M J 2015 *J. Mater. Chem. A* **3** 17426–32
- [867] Miyazaki Y, Igarashi D, Hayashi K, Kajitani T and Yubuta K 2008 *Phys. Rev. B* **78** 214104
- [868] Le Tonquesse S, Joanny L, Guo Q, Elkaim E, Demange V, Berthebaud D, Mori T, Pasturel M and Prestipino C 2020 *Chem. Mater.* **32** 10601–9
- [869] Ohkubo I and Mori T 2015 *Chem. Mater.* **27** 7265–75
- [870] Ohkubo I and Mori T 2014 *Chem. Mater.* **26** 2532–6
- [871] Mori T 2020 *Handbook on the Physics and Chemistry of Rare Earths* vol 58 (Amsterdam: Elsevier B.V.) pp 39–154
- [872] Aselage T L and Emin D 2003 *Chemistry, Physics and Materials Science of Thermoelectric Materials—Beyond Bismuth Telluride* (Berlin: Springer) pp 55–70
- [873] Mori T 2019 *J. Solid State Chem.* **275** 70–82
- [874] Slack G A and Morgan K E 2014 *J. Phys. Chem. Solids* **75** 1054–74
- [875] Werheit H 2009 *J. Phys.: Conf. Ser.* **176** 012019
- [876] Mori T 2012 *Modules, Systems, and Applications in Thermoelectrics* (Boca Raton, FL: CRC Press) pp 14–1–18
- [877] Mori T 2016 *Materials Aspect of Thermoelectricity* ed C Uher (Boca Raton, FL: CRC Press) pp 455–72
- [878] Werheit H 2006 *2006 25th Int. Conf. Thermoelectrics* pp 159–63
- [879] Mori T 2008 *Handbook on the Physics and Chemistry of Rare Earths* vol 38 (Amsterdam: Elsevier) pp 105–73
- [880] Berezin A A, Golikova O A, Kazanin M M, Khomidov T, Mirlin D N, Petrov A V, Umarov A S and Zaitsev V K 1974 *J. Non-Cryst. Solids* **16** 237–46
- [881] Werheit H, de Groot K, Malkemper W and Lundström T 1981 *J. Less-Common Met.* **82** 163–8
- [882] Golikova O A 1987 *Phys. Status Solidi* **101** 277–314
- [883] Werheit H, Laux M and Kuhlmann U 1993 *Phys. Status Solidi* **176** 415–32
- [884] Slack G A, Rosolowski J H, Hejna C, Garbaskas M and Kasper J S 1987 *9th Int. Symp. Boron, Borides Related Compounds* pp 132–41
- [885] Kim H K, Nakayama T, Shimizu J and Kimura K 2008 *Mater. Trans.* **49** 593–9
- [886] Takagiwa Y, Kuroda N, Imai E, Kanazawa I, Hyodo H, Soga K and Kimura K 2016 *Mater. Trans.* **57** 1066–9
- [887] Sologub O, Salamakha L, Stöger B, Michiue Y and Mori T 2017 *Acta Mater.* **122** 378–85
- [888] Wood C and Emin D 1984 *Phys. Rev. B* **29** 4582–7
- [889] Wood C, Emin D and Gray P E 1985 *Phys. Rev. B* **31** 6811–4
- [890] Bouchacourt M and Thevenot F 1985 *J. Mater. Sci.* **20** 1237–47
- [891] Goto T, Li J and Hirai T 1997 *J. Japan Soc. Powder Powder Metall.* **44** 60–64
- [892] Li J, Goto T and Hirai T 1998 *J. Ceram. Soc. Japan* **106** 194–7
- [893] Cai K F and Nan C-W 2000 *Ceram. Int.* **26** 523–7
- [894] Gunjishima I, Akashi T and Goto T 2000 *J. Japan Soc. Powder Powder Metall.* **47** 1184–8
- [895] Gunjishima I, Akashi T and Goto T 2001 *Mater. Trans.* **42** 1445–50
- [896] Werheit H, Leithe-Jasper A, Tanaka T, Rotter H W and Schwetz K A 2004 *J. Solid State Chem.* **177** 575–9
- [897] Sasaki S, Takeda M, Yokoyama K, Miura T, Suzuki T, Suematsu H, Jiang W and Yatsui K 2005 *Sci. Technol. Adv. Mater.* **6** 181–4
- [898] Werheit H, Rotter H W, Shalamberidze S, Leithe-Jasper A and Tanaka T 2011 *Phys. Status Solidi* **248** 1275–9
- [899] Kirihara K, Mukaida M and Shimizu Y 2017 *Nanotechnology* **28** 145404
- [900] Innocent J-L, Portehault D, Gouget G, Maruyama S, Ohkubo I and Mori T 2017 *Mater. Renew. Sustain. Energy* **6** 1–7
- [901] Sauerschnig P, Watts J L, Vaney J B, Talbot P C, Alarco J A, Mackinnon I D R and Mori T 2020 *Adv. Appl. Ceram.* **119** 97–106

- [902] Slack G A, McNelly T F and Taft E A 1983 *J. Phys. Chem. Solids* **44** 1009–13
- [903] Kumashiro Y, Yokoyama T, Sato K, Ando Y, Nagatani S and Kajiyama K 2000 *J. Solid State Chem.* **154** 33–38
- [904] Akashi T, Itoh T, Gunjishima I, Masumoto H and Goto T 2002 *Mater. Trans.* **43** 1719–23
- [905] Nagarajan R, Xu Z, Edgar J H, Baig F, Chaudhuri J, Rek Z, Payzant E A, Meyer H M, Pomeroy J and Kuball M 2005 *J. Cryst. Growth* **273** 431–8
- [906] Gong Y, Zhang Y, Dudley M, Zhang Y, Edgar J H, Heard P J and Kuball M 2010 *J. Appl. Phys.* **108** 084906
- [907] Frye C D, Edgar J H, Ohkubo I and Mori T 2013 *J. Phys. Soc. Japan* **82** 095001
- [908] Sologub O, Matsushita Y and Mori T 2013 *Scr. Mater.* **68** 289–92
- [909] Golikova O A and Tadzhiyev A 1981 *J. Less-Common Met.* **82** 169–71
- [910] Mori T 2005 *J. Appl. Phys.* **97** 093703
- [911] Mori T and Tanaka T 2006 *J. Solid State Chem.* **179** 2889–94
- [912] Hossain M A, Tanaka I, Tanaka T, Khan A U and Mori T 2015 *J. Phys. Chem. Solids* **8** 221–7
- [913] Sussardi A, Tanaka T, Khan A U, Schlapbach L and Mori T 2015 *J. Materiomics* **1** 196–204
- [914] Sauerschnig P, Tsuchiya K, Tanaka T, Michiue Y, Sologub O, Yin S, Yoshikawa A, Shishido T and Mori T 2020 *J. Alloys Compd.* **813** 152182
- [915] Ishizawa Y and Tanaka T 2000 *J. Solid State Chem.* **154** 229–31
- [916] Mori T 2006 *Physica B* **383** 120–1
- [917] Mori T, Martin J and Nolas G 2007 *J. Appl. Phys.* **102** 073510
- [918] Mori T, Shishido T and Nakajima K 2009 *J. Electron. Mater.* **38** 1098–103
- [919] Mori T, Berthebaud D, Nishimura T, Nomura A, Shishido T and Nakajima K 2010 *Dalton Trans.* **39** 1027–30
- [920] Hossain M A, Tanaka I, Tanaka T, Khan A U and Mori T 2016 *J. Solid State Chem.* **233** 1–7
- [921] Takeda M, Fukuda T, Domingo F and Miura T 2004 *J. Solid State Chem.* **177** 471–5
- [922] Maruyama S, Prytuliak A, Miyazaki Y, Hayashi K, Kajitani T and Mori T 2014 *J. Appl. Phys.* **115** 123702
- [923] Maruyama S, Miyazaki Y, Hayashi K, Kajitani T and Mori T 2012 *Appl. Phys. Lett.* **101** 152101
- [924] Son H W, Berthebaud D, Yubuta K, Yoshikawa A, Shishido T, Suzuta K and Mori T 2020 *Sci. Rep.* **10** 1–16
- [925] Mori T, Nishimura T, Schnelle W, Burkhardt U and Grin Y 2014 *Dalton Trans.* **43** 15048–54
- [926] Mori T and Nishimura T 2006 *J. Solid State Chem.* **179** 2908–15
- [927] Mori T, Nishimura T, Yamaura K and Takayama-Muromachi E 2007 *J. Appl. Phys.* **101** 093714
- [928] Prytuliak A, Maruyama S and Mori T 2013 *Mater. Res. Bull.* **48** 1972–7
- [929] Son H-W, Sauerschnig P, Berthebaud D and Mori T 2020 *J. Ceram. Soc. Japan* **128** 181–5
- [930] Takashima N, Azuma Y and Matsushita J-I 2000 *Mater. Res. Soc. Symp. Proc.* **604** 233–8
- [931] Chen L, Goto T, Li J and Hirai T 1996 *Mater. Trans. JIM* **37** 1182–5
- [932] Ma H-B, Zou J, Zhu J-T, Lu P, Xu F-F and Zhang G-J 2017 *Acta Mater.* **129** 159–69
- [933] Simonson J W and Poon S J 2010 *J. Alloys Compd.* **504** 265–72
- [934] Takeda M, Terui M, Takahashi N and Ueda N 2006 *J. Solid State Chem.* **179** 2823–6
- [935] Gürsoy M, Takeda M and Albert B 2015 *J. Solid State Chem.* **221** 191–5
- [936] Tynell T, Aizawa T, Ohkubo I, Nakamura K and Mori T 2016 *J. Cryst. Growth* **449** 10–14
- [937] Guélou G et al 2018 *Materialia* **1** 244–8
- [938] Koumoto K, Shimohigoshi M, Takeda S and Yanagida H 1987 *J. Mater. Sci. Lett.* **6** 1453–5
- [939] Kim H, Anasori B, Gogotsi Y and Alshareef H N 2017 *Chem. Mater.* **29** 6472–9
- [940] Kaya P, Gregori G, Yordanov P, Ayas E, Habermeier H-U, Maier J and Turan S 2017 *J. Eur. Ceram. Soc.* **37** 3367–73
- [941] Du Y, Chen J, Liu X, Lu C, Xu J, Paul B and Eklund P 2018 *Coatings* **8** 25
- [942] Wang J, Li Y, Yaer X, Qiqige A, Fang C, Miao L and Liu C 2016 *J. Alloys Compd.* **665** 7–12
- [943] Abu-Geel N, Aslam M, Ager R and Rimai L 2000 *Semicond. Sci. Technol.* **15** 32–33
- [944] Kitagawa H, Kado N and Noda Y 2002 *Mater. Trans.* **43** 3239–41
- [945] Fujisawa M, Hata T, Bronsveld P, Castro V, Tanaka F, Kikuchi H and Imamura Y 2005 *J. Eur. Ceram. Soc.* **25** 2735–8
- [946] Ivanova L M, Aleksandrov P A and Demakov K D 2006 *Inorg. Mater.* **42** 1205–9
- [947] Ohba Y, Shimozaki T and Era H 2008 *Mater. Trans.* **49** 1235–41
- [948] Nakatsugawa H, Nagasawa K, Okamoto Y, Yamaguchi S, Fukuda S and Kitagawa H 2009 *J. Electron. Mater.* **38** 1387–91
- [949] Kim J G, Choi Y Y, Choi D J and Choi S M 2011 *J. Electron. Mater.* **40** 840–4
- [950] Valentín L A, Betancourt J, Fonseca L F, Pettes M T, Shi L, Soszyński M and Huczko A 2013 *J. Appl. Phys.* **114** 184301
- [951] Mori T and Hara T 2016 *Scr. Mater.* **111** 44–48
- [952] Fukuda K, Hisamura M, Iwata T, Tera N and Sato K 2007 *J. Solid State Chem.* **180** 1809–15
- [953] Imam M A and Reddy R G 2019 *High Temp. Mater. Process.* **38** 411–24